



**Tomas Bata University in Zlín**  
**Faculty of Technology**

Doctoral Thesis

**Study on Calcium Reinforced Polymeric Hydrogel  
Scaffolds for Bone Tissue Regeneration**

**Studie polymerních hydrogelových scaffoldů plněných  
vápníkem pro regeneraci kostní tkáně**

Author: **Probal Basu, M.Sc.**

Degree programme: Chemistry and Material Technology

Degree course: Technology of Macromolecular compounds

Supervisor: Assoc. Prof. Nabanita Saha, M.Sc., Ph.D.

Consultant: prof. Ing. Petr Sáha, CSc.

Zlín, September, 2020

© Probal Basu

## *Dedication*

This Ph.D. thesis is dedicated to my adorable parents:  
*Smt. Nabanita Basu*, B.A., my mother, and *Sri Prabir Kumar Basu*,  
B.Sc., my father.

# CONTENTS

<b>ABSTRACT</b> .....	07
<b>ABSTRAKT</b> .....	09
<b>ACKNOWLEDGEMENTS</b> .....	11
<b>TABLES AND FIGURES</b> .....	14
<b>SYMBOLS AND ACRONYMS</b> .....	16
<b>LIST OF PUBLICATIONS</b> .....	17
<b>Chapter 1. BACKGROUND</b>	
1.1 Bone and bone tissue regeneration (BTR).....	20
1.2 Tissue engineering and its principles in BTR.....	24
1.3 History of TE: from past to present .....	30
1.4 Biomaterial & Scaffolds in BTR.....	31
1.5 Polymeric hydrogel used in TE for BTR.....	35
1.6 Bacterial cellulose (BC) and BTR.....	38
1.7 Different polymers for TE scaffold preparation .....	42
1.8 Calcium and its importance in BTR.....	44
1.9 Cell and cell biology in BTR.....	49
1.10 Scaffold and cell interaction in BTR.....	51
<b>Chapter 2. EXPERIMENTATION</b>	
2.1 Materials for calcium reinforced BC based hydrogel preparation.....	54
2.1.a <i>Materials used in the study</i> .....	54
2.1.b <i>Polymers and their purpose of use for the preparation of the hydrogel scaffold</i> .....	56
2.1.c <i>Sources of the utilized materials in this study</i> .....	56
2.2 Methodology of preparation of hydrogel scaffolds.....	58
2.2.1 <i>Synthesis of raw material i.e. Bacterial cellulose</i> .....	58
2.2.2 <i>Preparation of calcium reinforced BC based hydrogel</i> .....	59
2.2.2. a. <i>Calcium phosphate reinforced BC based hydrogel</i> .....	59
2.2.2. b <i>Calcium phosphate and Calcium carbonate reinforced BC based hydrogel</i> .....	61
2.3 Physical characterization.....	63

2.3.1 Swelling study.....	63
2.3.2 Porosity.....	64
2.3.3 Biodegradation.....	65
2.4 Morphological characterization.....	68
2.5 Chemical characterization.....	69
2.6 Thermal characterization.....	70
2.7 Mechanical Property analysis.....	71
2.7.1 Viscoelastic property analysis.....	71
2.7.2 Compression analysis.....	72
2.8 Biological Property analysis.....	72
2.8.1 Antimicrobial study.....	72
2.8.2 Cell biological study.....	73
2.8.2. a Biocompatibility study.....	73
2.8.2. b DNA damage analysis.....	76
2.8.2. c Apoptosis/necrosis analysis .....	77
2.8.2. d Bone marker analysis .....	77
2.8.2. e Cell-biomaterial interaction study.....	78
<b>Chapter 3. MOTIVATION OF THE DOCTORAL STUDY.....</b>	<b>79</b>
<b>Chapter 4. AIM OF THE THESIS AND BRIEF SUMMARY.....</b>	<b>82</b>
<b>Chapter 5. CONCLUDING REMARKS.....</b>	<b>91</b>
5.1 Conclusion.....	91
5.2 Contribution to the society.....	94
5.3 Future plan.....	95
<b>REFERENCES.....</b>	<b>95</b>
<b>PUBLICATION I.....</b>	<b>115</b>
<b>PUBLICATION II.....</b>	<b>116</b>
<b>PUBLICATION III.....</b>	<b>117</b>
<b>PUBLICATION IV.....</b>	<b>118</b>
<b>PUBLICATION V.....</b>	<b>119</b>
<b>PUBLICATION VI.....</b>	<b>120</b>
<b>PUBLICATION VII.....</b>	<b>121</b>
<b>CURRICULUM VITAE.....</b>	<b>122</b>



## ABSTRACT

Treatments for unwanted bone fractures have different limitations like potential infection risks and requirement of secondary surgery. Polymeric tissue engineering scaffold material can be a suitable alternative treatment device for the bone tissue regeneration due to its excellent biocompatibility, mechanical property and degradability.

This thesis reports *the preparation and characterization of novel calcium reinforced bacterial cellulose (BC) based hydrogel scaffolds for its possible application in bone tissue regeneration*. The scaffolds were developed by using a combination of natural polymer, BC and other synthetic polymers like polyvinylpyrrolidone (PVP), polyethylene glycol (PEG). The scaffolds were prepared in two forms. First, *calcium phosphate (CaP) reinforced BC based hydrogel scaffolds were prepared*, where CaP was used in the form of  $\beta$ -tri calcium phosphate ( $\beta$ -TCP) and hydroxyapatite (HA) in different concentrations. Second, *calcium phosphate & calcium carbonate reinforced BC based hydrogel scaffolds* were prepared through template mediated *in vitro* biomineralization of *CaP filled BC based hydrogel scaffolds*.

The *structural properties* (physiochemical, morphological, mechanical and/or viscoelastic characterization) indicated the *CaP reinforced scaffolds* have demonstrated significant swelling ability, suitable porosity and other mechanical and viscoelastic properties.

Furthermore, *functional properties* (involving the biocompatibility, cell viability, cell-biomaterial interaction and bone marker expression) indicated their better efficiency for bone tissue regeneration.

Thus, the *CaP reinforced BC based hydrogel scaffolds (BC-PVP- $\beta$ -TCP/HA\_20:80 and BC-PVP- $\beta$ -TCP/HA\_50:50)* are recommended for further analysis (e.g. *in vivo study*) and application in soft bone tissue (ie. cancellous bone) regeneration.

*Keywords:* Bacterial cellulose, Hydrogel scaffolds, calcium phosphate, bone tissue engineering



## ABSTRAKT

Léčba nežádoucích zlomenin se potýká s celou řadou problémů jako jsou infekce či další následné vynucené chirurgické zákroky. Pro řešení těchto případů se s výhodou dají použít polymerní scaffoldy, které dokáží vylepšit regeneraci kostní tkáně. Polymerní scaffoldy mají totiž vynikající biokompatibilitu, vhodné mechanické vlastnosti a jsou dobře odbouratelné v tkáni.

Tato práce se zabývá *přípravou a charakterizací nových polymerních hydrogelových scaffoldů na bázi bakteriální celulózy (BC) plněné vápníkem, jejichž úkolem je zvýšit regeneraci poškozené kostní tkáně*. Byly připraveny scaffoldové kompozice na bázi BC a syntetických polymerů polyvinylpyrrolidonu (PVP) a polyethynglykolu (PEG) ve dvou kombinacích. V prvním případě byly použity *hydrogelové scaffoldy na bázi BC plněné/vyztužené fosfátem vápenatým (CaP)*, kde CaP byl ve formě beta-tri-fosfátu vápenatého ( $\beta$ -TCP) a hydroxyapatitu (HA) v různých koncentracích. Druhou kombinaci tvořily *hydrogelové scaffoldy na bázi BC plněné fosfátem vápenatým/uhličitanem vápenatým*, které byly připraveny *in vitro* biomineralizací *hydrogelového scaffoldu na bázi BC plněné CaP*.

**Strukturální vlastnosti** (fyzikálně-chemické, morfologické, mechanické a viskoelastické) naznačují, že *scaffoldy plněné CaP* mají značnou schopnost bobtnání, mají vhodnou pórovitost, a další mechanické a viskoelastické vlastnosti.

Kromě toho výsledky testů **funkčních vlastností**, zahrnující biokompatibilitu, životaschopnost buněk, interakci buněk a biomateriálů (prostřednictvím studie SEM) a expresi kostních markerů (pomocí ALP analýzy) ukázaly lepší účinnost při regeneraci kostní tkáně.

Na základě zjištěných poznatků lze hydrogelové scaffoldy na bázi BC vyztužené CaP (BC-PVP- $\beta$ -TCP / HA\_20: 80 a BC-PVP- $\beta$ -TCP / HA\_50: 50) doporučit k další

analýze (např. Studium in vivo) a případně použít navržený scaffold pro regeneraci měkkých (spongiózních) kostí.

*Klíčová slova:* Bakteriální celulóza, hydrogelové scaffoldy, fosforečnan vápenatý, inženýrství kostní tkáň

## ACKNOWLEDGEMENTS

The successful accomplishment of this doctoral thesis has become possible with the sustained support of the dearest ones of my surrounding.

First of all, I would like to express my honest gratitude to my doctoral advisor, *Assoc. Prof. Nabanita Saha* for her continuous support, patience and guidance throughout my doctoral study. I am also thankful to her for her kind and valuable suggestions for my overall development.

I am thankful to my doctoral study consultant, *Prof. Ing. Petr Sáha* for the inspiration throughout my study.

Furthermore, I would like to extend my gratitude to *Tomas Bata University in Zlín* for providing me the necessary infrastructure and financial support in the form of *Ph.D. extraordinary scholarship (2016-2020)* and *IGA project fund (IGA-2016-2019)* for my research, attending different conferences in abroad and my living in Zlín.

Moreover, I would also thank the *COST Action MP1301 (NEWGEN)* for providing financial support for *Training School at Partas, Greece* and *“Short Term Scientific Mission (STSM) fellowship”* for the cell biological research at IEMPAM-BAS, Bulgaria. Additionally, I would also thankful to *COST Action ENBA* for providing me *“ITC Conference Grant”* to attend ESB 2019 conference at Vienna, Austria.

I am also thankful to *Assoc. Prof. Radostina Alexandrova* for giving me the opportunity to access to her laboratory and research facilities at IEMPAM-BAS, Bulgaria, Sofia for cell biological studies.

I would express my gratitude especially to my seniors and peers of center of polymer systems, *doc. Zandraa Oyunchimeg, doc. Haojei Fei, Mr. Hao Trung Nguyễn, doc. Roman Kolařík, doc. Pavel Bažant, Ms. Katarina Filatova, Mr. Thaiskang Jamatia, doc. Martin Cvek, Dr. Raghvendra Singh Yadav, Dr. Sanjoy Dutta, Mrs. Monika Kasálková Primasová* for their kind suggestions and/or help and assistance. Nevertheless, simple thank is also due to other colleagues as well.

I express a sincere gratitude to *Assoc. Prof. Sajal Bhattacharya*, for his sustained support and encouragement since my pre-doctoral phase of life.

Thanks are also due to my late childhood friend, *Mr. Rajesh Singh* for his active encouragement in the pre-doctoral phase of my life.

I would also like to express gratitude towards my adorable and amiable wife, ***Mrs. Poulomi Basu*** for her continuous support and patience throughout my doctoral study period.

Finally, this thesis would not be possible without the unconditional support from my parents, ***Mrs. Nabanita Basu (My mother)*** and ***Sri. Prabir Kumar Basu (My father)***. I would also like to thank my “*inner-self*” which constantly equipped me spiritually for the successful completion of this doctoral work.

Thank you.

A handwritten signature in blue ink that reads "Probal Basu". The signature is written in a cursive style with a long, sweeping underline.

Probal Basu.



## **LIST OF TABLES**

*Table.1. Bone graft substitute materials*

*Table.2. List of bone graft substitutes presently in market*

*Table.3. Natural Biomaterials*

*Table. 4. Artificial Biomaterials*

*Table. 5. Generation of biomaterials*

*Table. 6. Polymeric hydrogels used in BTE application*

*Table. 7. Different components of a BC production*

*Table. 8. BC based scaffolds used in bone tissue engineering*

*Table.9. Cell lines used as in vitro model for BTE*

*Table. 10. Material used in the preparation of hydrogel scaffolds.*

*Table. 11. Polymers and their advantages and specific purpose in this study.*

*Table. 12. Sources of the materials in this study.*

*Table 13. Composition of calcium reinforced BC based hydrogel scaffold.*

*Table 14. Composition of calcium phosphate reinforced BC based hydrogel scaffold.*

## **LIST OF FIGURES**

*Figure 1. Bone and its components*

*Figure 2. Cortical and cancellous bone of human long bone*

*Figure 3. Bone fracture healing and bone regeneration*

*Figure 4. Bone remodeling event*

*Figure 5. Autologous Bone Grafting*

*Figure 6. Allogenic Bone Grafting*

*Figure 7. Tissue engineering triad*

*Figure 8. Tissue engineering construct with cells and scaffolds*

*Figure 9. Application of acellular scaffold for BTR*

*Figure 10. A brief history of tissue engineering applications*

*Figure 11. Hydrogel and the interactions of the polymer chains of hydrogel*

*Figure 12. A brief history of hydrogel application in tissue engineering and bone tissue engineering*

*Figure 13. Property of hydrogel for bone tissue engineering application*

*Figure 14. Biosynthesis of cellulose*

*Figure 15. Stimulus provided by calcium based bone tissue engineering scaffold*

*Figure 16. MAPK/ERK pathway for osteoblast proliferation*

*Figure 17. Integrin mediated signaling and Integrin-Scaffold interaction*

*Figure 18. Scaffold and cell Interaction*

*Figure 19. BC production in H.S. medium*

*Figure 20. Preparation of calcium reinforced BC based hydrogel scaffolds.*

*Figure 21. Interaction of water and polymer chains of a hydrogel during swelling*

*Figure 22. Agar Disc Diffusion method for antibacterial test*

*Figure 23. Hydrogel application for BTR from 2006 to 2020*

*Figure 24. Outline of extracellular calcium stimulation for bone cell growth and development.*

## **SYMBOLS AND ACRONYMS**

BC	Bacterial Cellulose
BTR	Bone Tissue Regeneration
TE	Tissue Engineering
PVP	Polyvinylpyrrolidone
CMC	Carboxymethyl cellulose
PEG	Polyethylene glycol
ECM	Extracellular matrix
CaCO <sub>3</sub>	Calcium carbonate
β-TCP	β tricalcium phosphate
HA	Hydroxyapatite
UV	Ultraviolet
HS	Hestrin and Schramm
NaOH	Sodium Hydroxide
KOH	Potassium Hydroxide
M-CSF	Macrophage Colony-Stimulating factor
MSC	Mesenchymal stem cells
MAPK	Map-Kinase
TGA	Thermogravimetric analysis



## LIST OF PUBLICATIONS

The doctoral work of Mr. Probal Basu, entitled “*Study on Calcium Reinforced Polymeric Hydrogel Scaffolds for Bone Tissue Regeneration*” involves the following articles:

### *Article I*

**Basu P. (50%), Saha N & Saha P. (2019)** “Inorganic calcium filled bacterial cellulose based hydrogel scaffold: novel biomaterial for bone tissue regeneration”, *International Journal of Polymeric Material and Polymeric Biomaterial* (Web of Science indexed, Q2 [Polymer Science], **Jimp: 2.263**), 68:1-3, 134-144. DOI: <https://doi.org/10.1080/00914037.2018.1525733>

### *Article II*

**Basu P. (50%), Saha N, Bandyopadhyay S, Saha P. (2017)** “Rheological Performance of Bacterial Cellulose based non-mineralized and mineralized hydrogel scaffolds”, *AIP Conference Proceedings of Novel Trends in Rheology VII* (Web of Science Indexed; Book Chapter) 1843, 050008-1–050008-7. DOI: <https://doi.org/10.1063/1.4983000>. ISBN: 978-0-7354-1513-3

### *Article III*

**Basu P (50%), Saha N, Alexandrova R, Andonova-Lilova B, Georgieva M, Miloshev G, Saha P. (2018)** “Biocompatibility and Biological Efficiency of Inorganic Calcium Filled Bacterial Cellulose Based Hydrogel Scaffolds for Bone Bioengineering”, *International Journal of Molecular Sciences* (Web of Science Indexed, Q2 [Multidisciplinary, Chemistry, Biochemistry & Molecular Biology], **Jimp: 4.183**) *19* (12): 3980. DOI: 10.3390/ijms19123980

#### *Article IV*

**Basu P (50%), Saha N & Saha P. (2020)** “Swelling and rheological study of calcium phosphate filled bacterial cellulose based hydrogel scaffold”, *Journal of Applied Polymer Science* [Web of Science Indexed, Q2 [Polymer Science], **J<sub>imp</sub>: 2.188**), 137, 48522. DOI: 10.1002/app.48522

#### *Article V*

**Basu P. (50%), Saha N., Saha P. (2020)** “Viscoelastic behaviour of Calcium Phosphate Packed Bacterial Cellulose -Polyvinylpyrrolidone based Hydrogel Scaffolds at Human Fever Temperature”, *AIP conference proceedings of PPS Europe-Africa 2019 Regional Conference* (will be in Web of Science Indexed, Book Chapter), *Accepted for publication*.

#### *Article VI*

**Basu P. (50%), Saha N, Saha P. (2019)** “Calcium Phosphate Incorporated Bacterial Cellulose-Polyvinylpyrrolidone Based Hydrogel Scaffold: Structural Property and Cell Viability Study for Bone Regeneration Application”, *Polymers* [Web of Science Indexed, Q1 [Polymer Science], **J<sub>imp</sub>: 3.164**), 11(11), 1821. DOI:10.3390/polym11111821

#### *Article VII*

**Basu P. (50%), Saha N., Alexandrova R., Andonova-Lilova, B., Saha, P.** “*In vitro* efficiency of calcium phosphate incorporated bacterial cellulose based hydrogel scaffold for bone regeneration”, *Manuscript is in preparation and will be submitted to an Impact Factor Journal*.



# Chapter 1. BACKGROUND

## 1.1. Bone and Bone Tissue Regeneration (BTR)

### 1.1.i. Bone

Bone is one of the most important parts of human musculoskeletal system. It maintains the structural framework of the animal body <sup>1, 2, 3, 4</sup>.

The architecture of animal bone is comprised of various structural attributes (Figure.1). It is comprised of extracellular matrix, which is composed of inorganic matrix that provides the strength to the bone and organic matrix, which facilitates the bone flexibility <sup>5, 6</sup>. The bone structure composed of the following components <sup>1, 7</sup>:

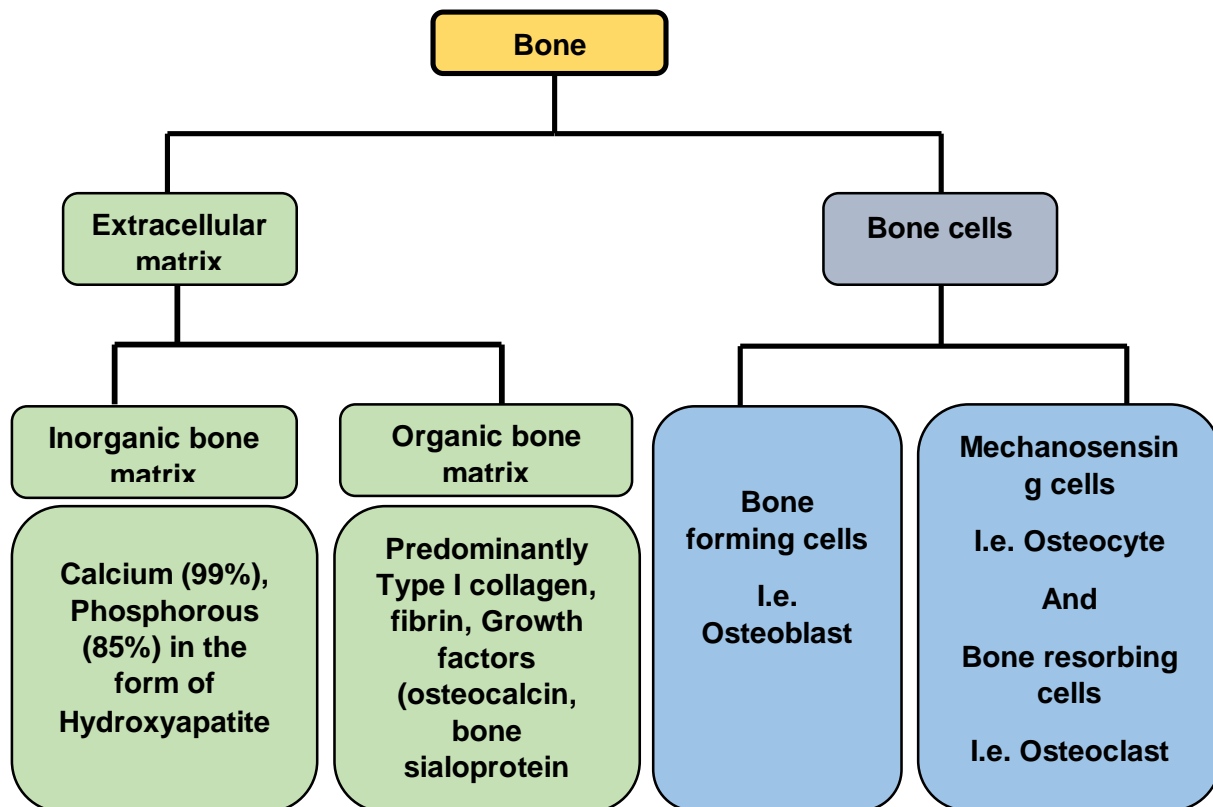


Figure 1. Bone and its components (self-representation)

The adult animal body is comprised of two types of bony structures: cortical bones (80%) and trabecular/ cancellous bones (20%) <sup>8</sup> (Figure. 2). The cortical or compact bones are dense and contain high concentration of inorganic mineral components (like hydroxyapatite); however, it also lacks high number of blood vessels and osteocytes. On the other hand, trabecular bones are composed of porous “honeycomb” like network structures <sup>2,8</sup>. These two types of bones have differential mechanical properties. The mechanical property of trabecular bone has been less compared to the compact bone due to its structural architecture and porosity <sup>2</sup>.

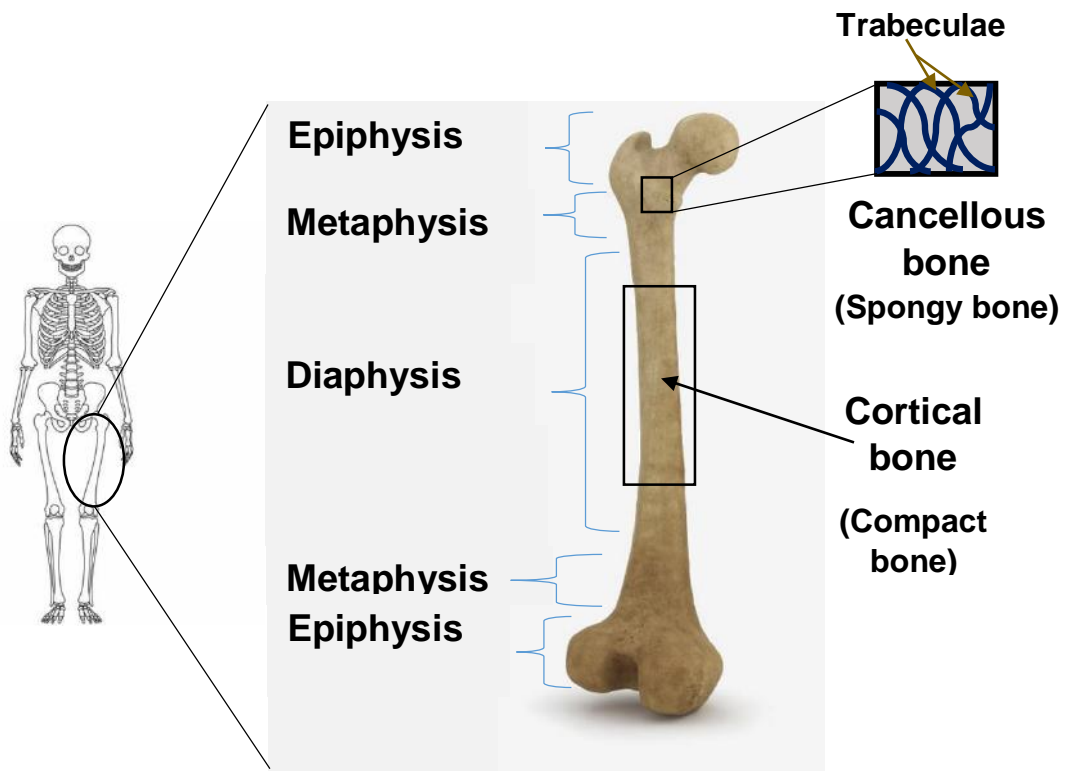


Figure 2. Cortical and cancellous bone of human long bone. (Self-representation)

## 1. 1. ii. Bone regeneration and Bone remodeling

### a. Bone regeneration event

The bone regeneration event is a complex process (Figure. 3). However, the important events of bone fracture healing or bone regeneration are indicated below<sup>9</sup>:

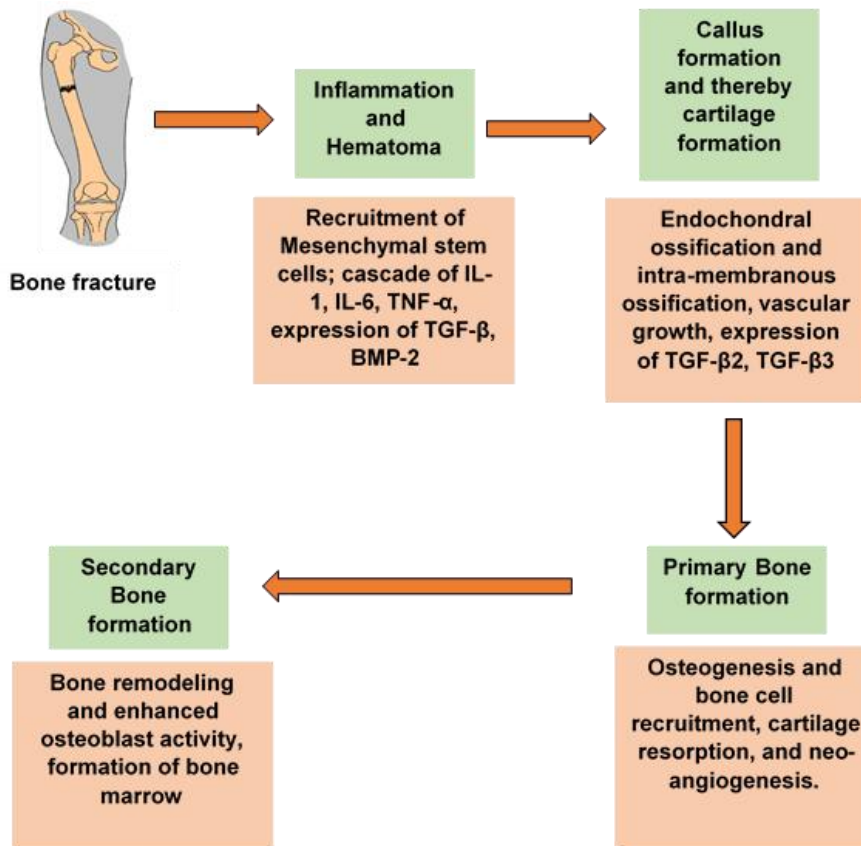
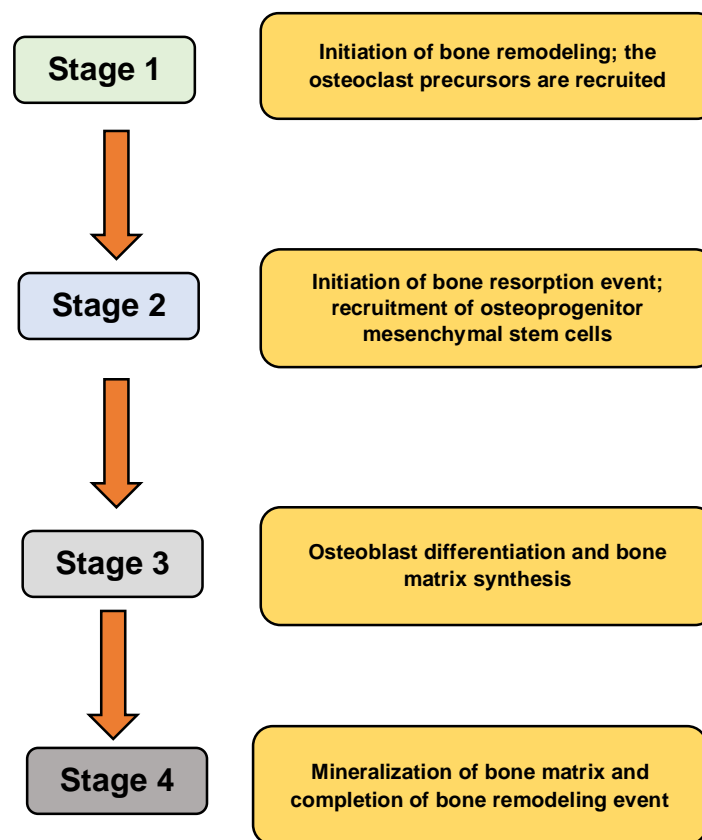


Figure 3. Bone fracture healing and bone regeneration. (Self-representation based on AI-AQI et al., 2008<sup>9</sup>).

## b. Bone remodeling event

Bone remodeling refers to the physiological event in which old/damaged bone is replaced by newly formed bone. In this process, osteoclast removes the damaged bone by bone resorption and new bones are formed by osteoblast. Interestingly, this event is tightly regulated by bone formation and resorption process (Figure. 4) as such that there is no loss of total bone mass occurs after the remodeling event <sup>7</sup>. This process has 4 different stages, which are following:



*Figure 4. Bone remodeling event. (Self-representation based on EI-SAYED et al., 2019 <sup>7</sup>).*

## **1.2 Tissue engineering and its principles in BTR**

### **1.2. i. Tissue Engineering**

“Tissue engineering is an interdisciplinary field that applies the principles of engineering and the life sciences toward the development of biological substitutes that restore, maintain, or improve tissue function”<sup>10</sup>.

Different studies and researches indicated that bone related disorders like osteoporosis caused 8.9 million fracture situations worldwide annually, with a condition where a fracture happens in every 3 seconds<sup>11</sup>. The existing treatment methods include the application of bone grafts<sup>12, 13</sup>. The bone grafts contain the following characteristics in the context of bone tissue engineering application<sup>2, 14, 15</sup>:

#### **I. *Osteoconductivity***

*Osteoconductivity* is the property of the graft/implant material, which elaborates the significant formation and growth of the bone cells on the surface or within the porous structures of the graft material. This finally results in formation of bone. In this case, the mesenchymal stem cells will grow through osteoconductivity of the graft material.

#### **II. *Osteoinductivity***

*Osteoinductivity* is the ability or property of the graft material through which the graft material induces the pluripotent stem cells to differentiate into bone-forming cell lineage.

#### **III. *Osseo-integration***

*Osseo-integration* refers to the direct contact between the bone and the graft material. The characteristics of bone graft materials, implantation site of a specific



graft material can influence the efficient application of the graft and its subsequent contact with bone.

The *bone grafting method* is most popular methods for tissue fracture repair. This method includes two different approaches:

### **a. Autologous bone grafting:**

Autologous bone grafting is considered as a gold standard for the bone defect treatment. In this process, the graft is collected from one site and implanted in another site of the same host (Figure.5). The damage recovery of the patients happens faster. However, different limitations like longer surgical time, potential infection, limited quantity of the graft material are also notable. This type of bone grafts has used for the defects of cancellous, cortical bones, bone marrow etc. <sup>2, 14, 16.</sup>

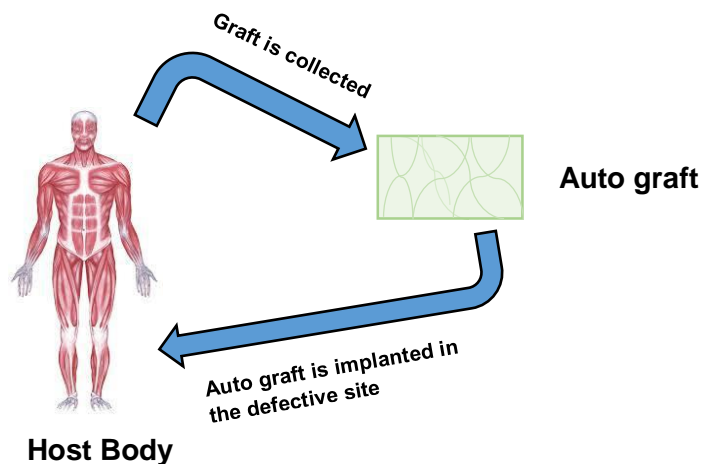


*Figure 5. Autologous Bone Grafting. (Self-representation)*

### **b. Allogenic bone grafting**

Allogenic bone grafting involves the collection of bone graft from another person and implanted into the patient (Figure.6). However, the limitations of this methods are also notable like graft rejection, possible introduction of infection from donor

to host etc. The allogenic grafting is used for cortical bones, cancellous and demineralized bones <sup>16, 17</sup>.

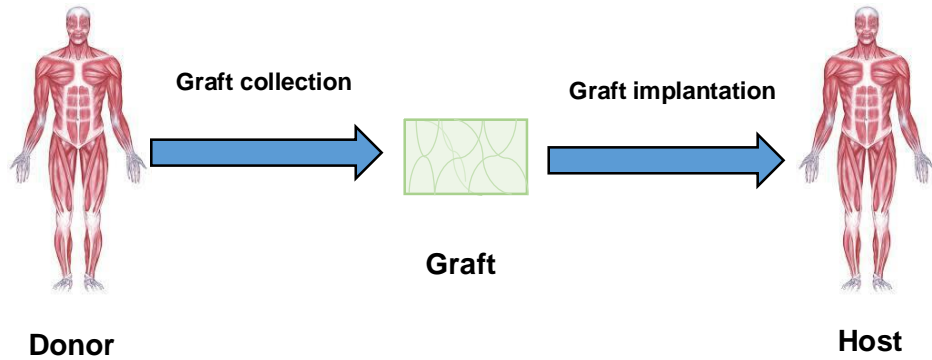


Figure 6. Allogenic Bone Grafting. (Self-representation)

### 1.2. ii Bone graft substitutes

On the other hand, different graft substitutes have been used notably for orthopedic application. The following graft substitute materials have been used currently as shown in **Table 1**.<sup>18, 19</sup>

**Table 1.** Bone graft substitute materials

Type of graft substitute	Osteoconductive	Osteoinductive
<i>Growth factor based substitutes</i>	+++	+++
<i>Cell based substitutes</i>	+++	+++
<i>Ceramic based substitutes</i>	+++	+++
<i>Polymer based substitutes</i>	+++	-

+++ = activity significant

- = no activity

### 1.2. iii. Bone graft substitutes presently in market

Different types of bone graft substitutes are present in the market currently. The list of the bone graft substitutes that are currently available/ in development stage given below in **Table 2**.<sup>20, 21, 22, 23, 24</sup>

**Table 2.** List of the bone graft substitutes that are currently available

<b>Product</b>	<b>Type of scaffold/composition</b>	<b>Intended use</b>	<b>Company, Country</b>
<i>ACI-Maix</i>	Collagen scaffold	Articular cartilage treatment	Matricel, Germany
<i>BioSeed®C</i>	Autologous 3D chondrocyte graft	Knee articular cartilage treatment	Biotissue, Germany
<i>Carticel®</i>	Cell laden construct	Articular cartilage treatment	Genzyme, USA
<i>CaReS®</i>	3D type I collagen matrix gel with cartilage cells	Articular cartilage treatment	Arthro Kinetics GmbH, Germany
<i>CONDUIT® TCP Granules</i>	100% $\beta$ -TCP	Bone Void Filler	DePuy Spine, USA
<i>OpteMxTM</i>	HA/TCP biphasic combination	Bone Void Filler	Exactech Inc., USA
<i>MasterGraft® Matrix</i>	Biphasic calcium phosphate and collagen	Bone Void Filler	Medtronic Spinal & Biologics, USA
<i>MBCP®</i>	Biphasic calcium phosphate synthetic bone graft substitute	Osseus defect filler	Biomatlante Biologic solutions, France
<i>Graftys® Quickset</i>	Calcium Phosphate Cement	Cancellous bone treatment	Graftys, France
<i>Artebone ®</i>	Tri calcium phosphate graft	Tibia and Spine defects	BBS-Bioactive Bone Substitute, Finland
<i>HA TCP Granules ®</i>	HA (60%) and TCP (40%)	Autograft and Allograft	KYERON ®, The Netherlands

### 1.2. iv. Principle of tissue engineering (TE)

The successful implementation of tissue engineering (TE) application involves the significant interaction and functioning of scaffolds, cells, and cell signaling systems. These three components together form a “*Tissue engineering triad*”<sup>25</sup> (Figure 7), which stimulates and facilitates the tissue regeneration event.

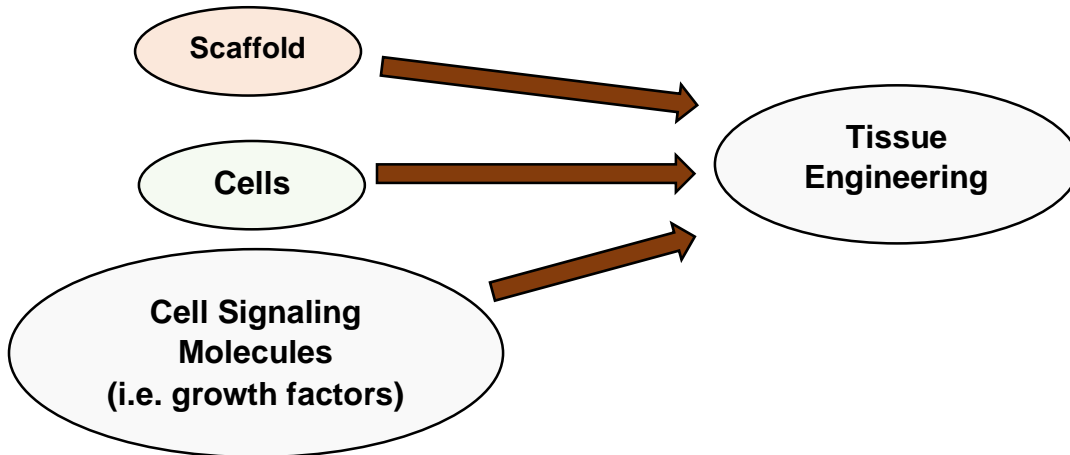


*Figure 7. Tissue engineering triad.  
(Self- representation based on Mathew et al., 2016<sup>25</sup>).*

The tissue engineering strategy involves **TWO** major approaches:

#### **a. TE construct with cell and scaffold**

The cells from allogenic or autologous sources are cultured and proliferated *in vitro*, then these cells are seeded onto a scaffold matrix, which ultimately forms a cell laden structure. The cell laden structure serves as tissue engineering construct (Figure 8) where the cells can proliferate, differentiate and thereby facilitates the formation of a regenerated tissue<sup>25, 26, 27</sup>.

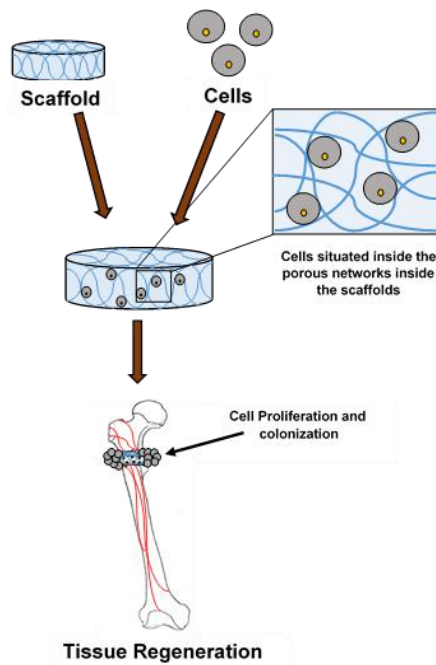


Figure 8. Tissue engineering construct with cells and scaffolds. (Self-representation)

**b. Cellular TE construct that mimics extra cellular matrix:**

Another significant approach of tissue engineering involves the utilization of an acellular biomaterial that essentially mimics the characteristics of extra cellular matrix of living tissue (Figure 9) <sup>25, 28</sup>. In this case, the scaffold will be used as “implant material” which will stimulate the significant proliferation and colonization of cells and thereby facilitate tissue regeneration process <sup>2, 25, 29</sup>.

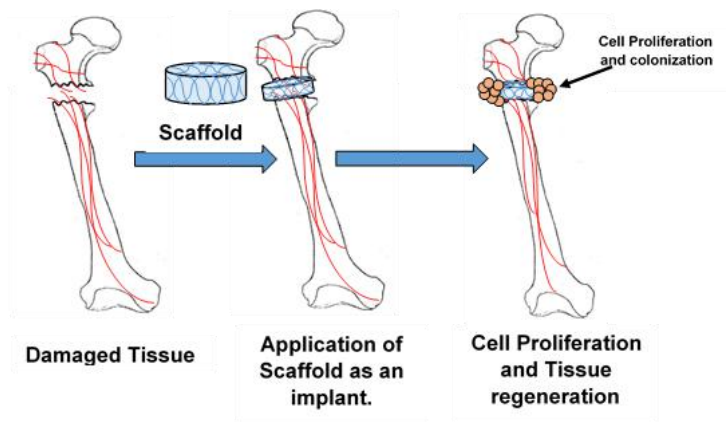


Figure 9. Application of acellular scaffold for BTR. (Self-created)

### 1.3 History of Tissue engineering: from past to present

A brief history of tissue engineering is indicated as follows (Figure 10):

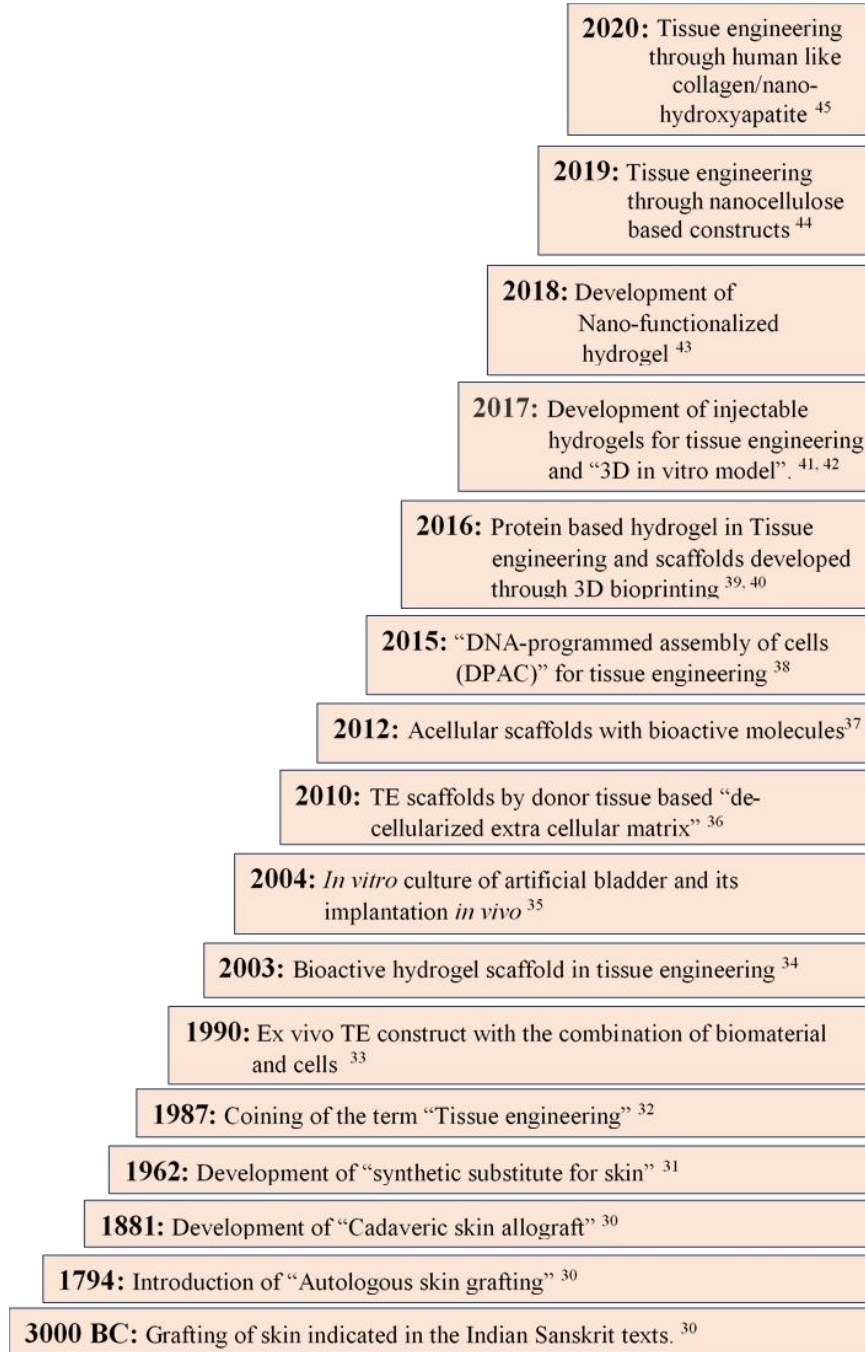


Figure 10. A brief history of tissue engineering applications (Self-representation)

## 1.4 Biomaterial & Scaffolds in BTR

Biomaterials are the natural or synthetic material that has a notable therapeutic usage in the context of repair and restore/replace of biological tissue <sup>46, 47, 48, 49, 50, 51</sup>.

The principle objective of biomaterial includes the stimulation of tissue regeneration phenomenon through delivering a notable signal which are necessary for cell proliferation and growth and thereby facilitate the regeneration of healthy tissue <sup>28</sup>.

### 1.4.1 Biomaterials in TE & Bone regeneration

Different types of biomaterial have been used in tissue engineering <sup>2</sup> are discussed below.

#### a. Natural Biomaterials

The natural biomaterials are the following **Table 3.** <sup>52, 53, 54</sup>

**Table 3.** Natural Biomaterials

Type of natural biomaterial	Example
<i>Protein based biomaterial</i>	Silk
	Collagen
<i>Polysaccharide based biomaterial</i>	Chitosan
	Alginate
	Hyaluronic acid

#### b. Artificial Biomaterials

The artificial biomaterials are the following **Table 4.** <sup>2, 55, 56</sup>

**Table 4.** Artificial Biomaterials

<b>Type of biomaterial</b>	<b>Example</b>
<i>Metals</i>	Titanium, Gold, silver
<i>Ceramics</i>	Calcium phosphate, Calcium carbonate
<i>Polymers</i>	Poly lactic acid (PLA), poly glycolic acid (PGA), poly (caprolactone) [PCL], poly (lactic-co-glycolic) acid [PLGA], poly (L-lactic acid) [PLLA], polyvinyl alcohol (PVA) etc.
<i>Composites</i>	Metal composite, polymer composite

### 1.4.2 Classification of biomaterials on the basis of its generation

The biomaterials and its types can also be classified on the basis of the following generations discussed in **Table 5.** <sup>57, 58, 59, 60</sup>

**Table 5.** Generations of biomaterial

<b>Generation of Biomaterial</b>	<b>Time Line</b>	<b>Characteristics</b>	<b>Example</b>
<i>First generation biomaterials</i>	1960-1970	Non-toxic “bio-inert” composite biomaterial which can replace tissues	Polymeric matrix of polyethylene and dispersed hydroxyapatite (HA) (Commercial name “Hapex”)
<i>Second generation biomaterials</i>	1971-mid-1980	Bioactive resorbable biomaterial	Resorbable fracture fixation plates and screws
		Stimulation of specific cellular	Application of cell-seeded tissue engineering



<i>Third generation biomaterials</i>	1990-2016	response through sustained controlled release of biochemical cues	construct/scaffold and application of scaffolds as extracellular matrix
<i>Fourth generation biomaterials</i>	2016 onwards	Fourth generation biomaterials can be produced by considering the bio-electrical property of a biomaterial and its effect on cell signaling.	Application of scaffolds prepared by conductive polymers like polyaniline and piezoelectric biomaterials for bone tissue engineering.

### 1.4.3 Scaffolds for BTR

Scaffolds are the artificial structures that facilitate the three dimensional (3D) tissue formation <sup>61, 62</sup>.

The scaffolds materials might be used as “acellular systems” or “cell laden structures” for tissue engineering applications <sup>29</sup>.

The following significant characteristics of the scaffold materials are *important* to be considered before its application <sup>63, 64</sup>.

- a. **Extra Cellular Matrix (ECM) mimicking material.** The scaffold material must mimic the natural extra cellular matrix and provide the necessary structural support to the cells. In this way, the scaffold can facilitate the cells to produce and deposit extracellular matrix and thereby accelerate the process of tissue regeneration process.
- b. **Geometry and architecture.** The internal geometry and structural architecture of scaffold material (like interconnected porous structures and pore sizes) ensures high surface density, which in turn provide significant space for cellular attachment for tissue engineering.

- c. **Porosity.** It is an important factor for scaffold material. A significant porous scaffold material will ensure the cell attachment and facilitate significant vascularization inside the scaffold during regeneration.
- d. **Mechanical property.** The stability of the scaffold material depends upon its appropriate mechanical property. The compressive strength of trabecular bone ranges from 0.22 MPa- 10.44 MPa and cortical bone ranges from 130-200 MPa <sup>65</sup>.  
<sup>66</sup>. The cell morphology and the expression of specific cellular proteins are contingent on the proper elastic property of the scaffold matrix.
- e. **Biodegradability.** The gradual and controlled biodegradability is an important aspect of good tissue engineering scaffold material. During tissue regeneration process, the newly formed tissue predominantly replaces the implant scaffold material and the scaffold material will be degraded eventually to its fundamental chemical units that will then be eliminated from body.
- f. **Biocompatibility.** The term biocompatibility can be defined as “the ability of a material to perform with an appropriate host response in a specific application”  
<sup>67</sup>. The scaffold material must augment the cell attachment, proliferation and differentiation process through providing stimulatory signals to the surrounding cells and tissues.

#### **1.4.4 Significant biological characteristics of the tissue engineering scaffold**

The tissue engineering scaffold must be biocompatible and non-toxic <sup>29</sup>. In addition, the cell attachment, colonization, proliferation and differentiation are the key biological requirement of the tissue engineering scaffold <sup>62</sup>. On the other hand, the scaffold material should be accepted by host immune system. The immunologically inert tissue engineering materials has been recently utilized efficiently <sup>68</sup>.

The most important characteristics that should be present in the tissue engineering scaffold is “*Bioactive*” property. In recent years, different bioactive compounds have been introduced in the composition of scaffold materials like bioactive calcium phosphates (hydroxyapatite, tri-calcium phosphate etc.) to enhance the efficiency of the scaffold material/implant<sup>1, 2, 3</sup>. The bioactive tissue engineering scaffold material will efficiently facilitate the cell migration/differentiation, successful integration of the implant within the host, and tissue formation<sup>69, 70</sup>.

## **1.5 Polymeric hydrogel scaffolds**

### **1.5.1 Hydrogel scaffold**

Hydrogels can be defined as a class of bio-inspired and bio-functionalized biomaterials composed of hydrophilic cross-linked polymeric three dimensional networks structure, which can absorb and retain high quantity of water and thus has the similarity with a living tissue<sup>71, 72, 73, 74, 75, 76, 77</sup>.

A hydrogel (Figure. 11) contain following properties<sup>75</sup>:

- Hydrogel is made up of hydrophilic polymeric materials which are cross-linked either by covalent bonds or intra/intermolecular physical interactions (Figure. 11).
- They can swell significantly and can retain notable amount of water without dissolving<sup>78, 79</sup>.
- Hydrogels due to its structural attributes has considered as biocompatible.

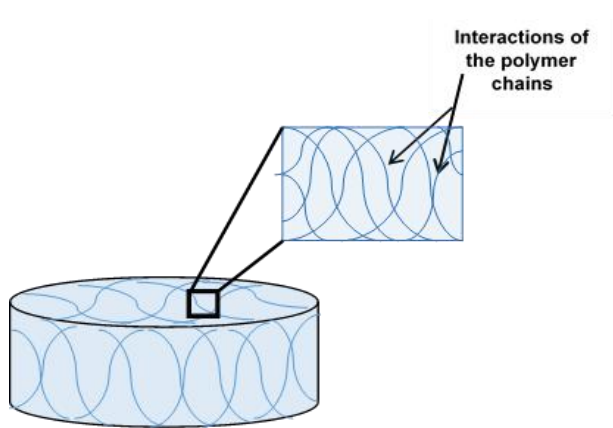


Figure 11. Hydrogel and the interactions of the polymer chains of hydrogel. (Self-representation)

### 1.5.2 Polymeric hydrogels used in tissue engineering application for BTR

The polymeric hydrogels which have been used in bone tissue engineering are listed below in **Table 6.** <sup>80, 81, 82, 83, 84, 85, 86.</sup>

**Table 6.** Polymeric hydrogel in BTE application

Application	Polymeric hydrogel
<i>Bone Tissue Engineering application</i>	Hyaluronic acid
	Alginate
	Collagen
	Chitosan
	Silk Fibroin (SF)
	Poly(lactic acid (PLA)- Polyglycolic acid (PGA) Co-polymer
	Polycaprolactone (PCL)
	Polyvinyl alcohol (PVA)
	Polyethylene glycol (PEG)
	Gelatin-hyaluronic acid
	Poly(lactic-co-glycolic acid) (PLGA)
	Bacterial cellulose (BC)
Gelatin	

### 1.5.3 History of polymeric hydrogel scaffolds in BTR

A brief history/time line of utilization of polymeric tissue engineering hydrogel scaffolds is indicated as follows (Figure 12):

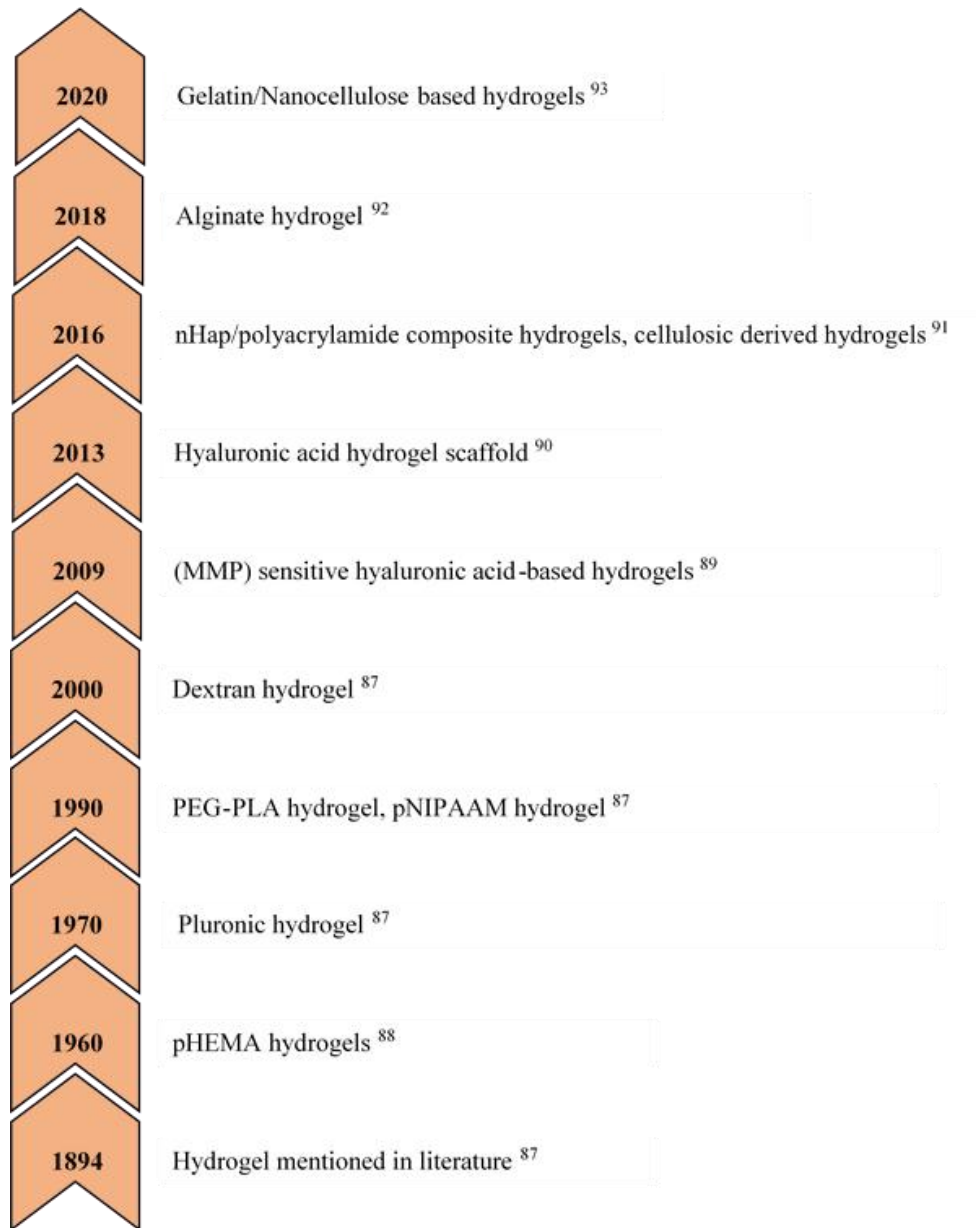


*Figure 12. A brief history of hydrogel application in tissue engineering and bone tissue engineering (Self-representation)*

### 1.5.4 Role of polymeric hydrogel scaffold in BTR

Hydrogel can be significantly use in bone tissue engineering either as a cell entrapped tissue engineering construct or as a scaffold material. Hydrogel in swollen state mimics the living tissue and thus can be able to utilize in tissue engineering application as a scaffold material <sup>3, 7, 94</sup>.

Hydrogel scaffold can efficiently mimic bone extra cellular matrix <sup>3, 14</sup>. In the context of bone tissue engineering, hydrogel as a scaffold material should contain the following characteristics (Figure.13) to promote bone cell colonization/proliferation, tissue growth and thereby facilitate regeneration <sup>94</sup>:

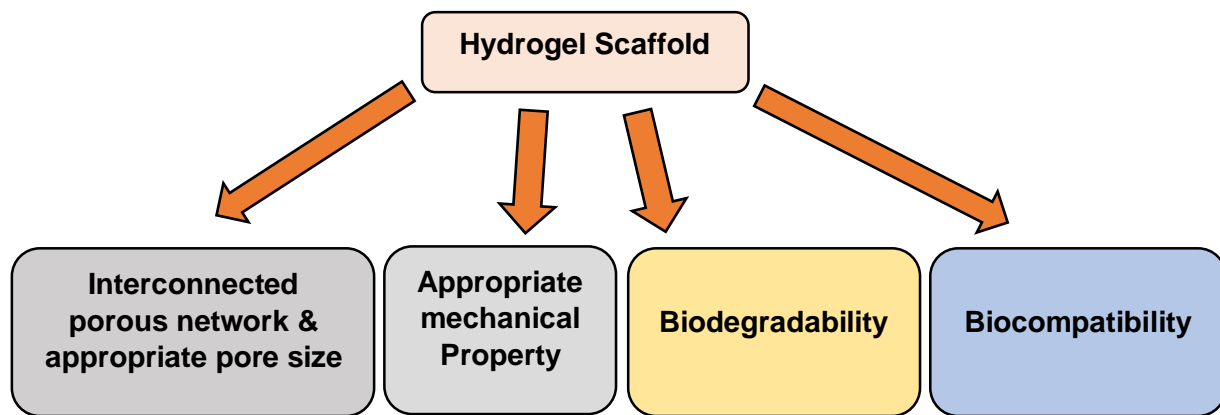


*Figure 13. Property of hydrogel for bone tissue engineering application (Self-representation)*

### 1.6 Bacterial cellulose (BC) and BTR

Cellulose is considered as significant and naturally abundant biopolymer composed of a linear homopolysaccharides developed by  $\beta$ -D-glucopyranose units linked through  $\beta$ -1,4 glycosidic bonds <sup>78</sup>. Cellulose is produced by the green plants as well

as some bacteria. Additionally, cellulose is also synthesized by certain algae and tunicates <sup>95, 96</sup>.

Bacterial cellulose (BC) is cellulose majorly is synthesized by bacteria of the genera, *Gluconobacter* <sup>97, 98</sup>. In 1886, Brown A.J. discovered the development of pellicle structure by bacteria which is similar to plant cellulose <sup>99, 100, 101</sup>. BC is devoid of lignin and hemicellulose and thus differs from the plant cellulose. Additionally, BC has I $\alpha$  and I $\beta$  crystalline domains, where plant cellulose has only I $\beta$  crystalline domain. The properties of BC are indicated below <sup>102</sup>:

- BC has significant crystallinity and biocompatibility.
- The high degree of hydrogen bonding provides high mechanical property to BC.
- BC microfibrils are smaller than the plant cellulose.
- BC has high porosity and notable biodegradability.
- BC microfibrils has high aspect ratio thus provides high surface area which give BC a water retention capacity.

### 1.6.1 Synthesis and production of BC

The BC production is done through fermentation process. The different components of a BC production are indicated below in **Table 7**. <sup>103, 104, 105, 106</sup>

**Table 7.** Different components of a BC production

Components		Description
<i>Bacterial strain</i>	Normal bacteria	<i>Gram –ve Bacteria: Gluconobacter, Achromobacter, Aerobacter, Agrobacterium, Azotobacter, Rhizobium, Gram + ve Bacteria: Sarcina,</i>
	Genetically engineered bacteria	<i>Komagataeibacter rhaeticus</i> iGEM
	Standard media	Hestrin and Schramm (HS) medium (Glucose, peptone, yeast extract as carbon and nitrogen source)

<i>Culture media</i>	Alternate media	Fruit juice, Sugar cane molasses, Brewery waste,
<i>pH</i>	pH of culture medium	pH 4-7
<i>Temperature</i>	Optimum temperature	28-30°C
<i>Mode of production</i>	Static	The method involves the inoculation of culture medium in production trays, which causes the development of BC pellicle. The entrapped CO <sub>2</sub> bubbles produced through bacterial metabolism leads this BC pellicle to the surface and thus the pellicle generally floats on the surface.
	Agitated	In agitated production condition, oxygen is continuously supplied and yield BC is higher. However, in this method, there is a possibility of development of potential mutations in the bacteria and generation of cellulose negative mutants under the influence of high shear stress condition.
<i>Post production treatment of BC</i>	Alkali treatment	The newly synthesized BC is then treated with mild alkaline solution like NaOH or KOH solution
	Drying	According to final application of BC, BC can be freeze dried or super-critically dried.

### 1.6.2 Mechanism of biosynthesis of BC

The BC fibrillar matrix is composed of numerous three dimensional BC nano-fibers that ultimately form a hydrogel sheet like structure with high surface area. *Gluconobacter* is the most commonly used bacterium in BC production. The bacteria under appropriate carbon-nitrogen nutrient condition, and optimum temperature (28-30°C) and pH (pH: 4-7) condition produce ribbon like cellulose I and thermodynamically stable cellulose-II polymers. The glucose units form the bacterial cellulose through cellular biosynthetic pathway (Figure. 14). The bacteria first produce protofibrils (2-4 nm) of glucose chains which are then secreted by



bacterial cell wall and produce microfibrils and then aggregated to form cellulose fiber ribbons (80 nm) <sup>107, 108</sup>.

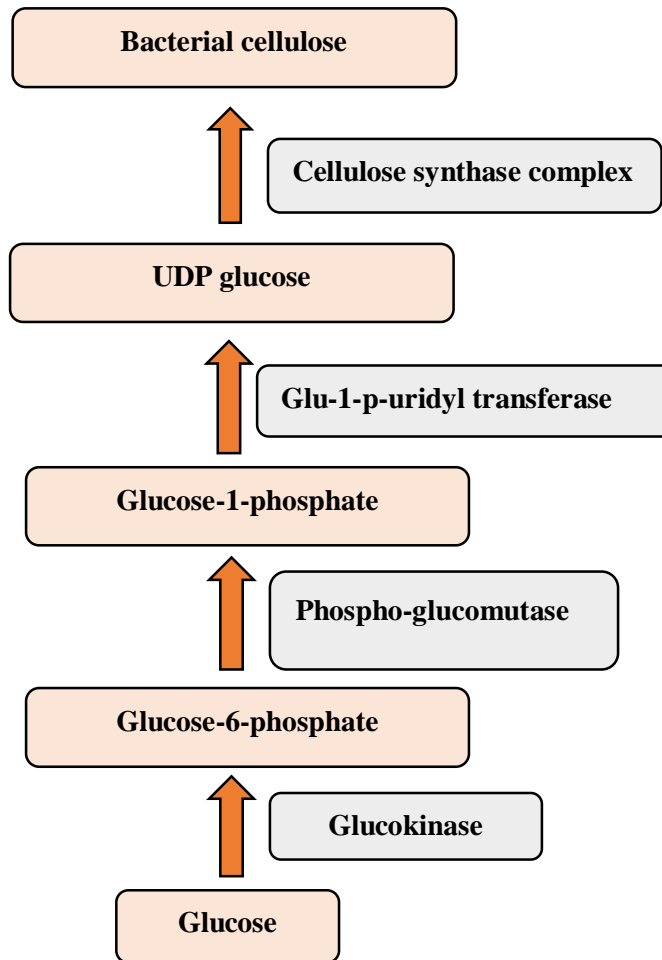


*Figure 14. Biosynthesis of cellulose. (Self-representation)*

### **1.6.3 BC as tissue engineering scaffold**

BC has been extensively used in biomedical application. The advantage of BC over other polymers involves the fact that BC has significant controllable three dimensional fibrous network structure and notable biocompatibility <sup>3, 55, 97, 109</sup>. BC has a notable use as bone tissue engineering scaffold due to its remarkable similarity with bone extra cellular matrix and collagen <sup>110</sup>. Interestingly, it has been reported that collagen and BC nanofibers contain similar diameter i.e. 100 nm and are

developed in the extracellular region from precursor molecule into chains of polymers <sup>97</sup>. The BC based scaffolds used in bone tissue engineering are indicated below in **Table 8.** <sup>55, 97, 103</sup>

**Table 8.** BC based scaffolds used in BTR application

<b>Application</b>	<b>BC based scaffolds or BC based composite</b>
<i>Bone Tissue Engineering</i>	BC/gelatin composite
	BC/chitosan
	BC/starch, BC/Paraffin
	BC/ poly(vinyl alcohol) [PVA]
	BC/poly(methyl methacrylate) [PMMA]
	BC/Hydroxyapatite
	BC/Polyacrylamide

## **1.7 Different polymers for TE scaffold preparation**

Other polymers utilized in hydrogel scaffold preparation for BTR application are following:

### **a. Polyvinylpyrrolidone (PVP)**

PVP is a biocompatible, water soluble synthetic polymer that used successfully as an additive to drugs like blood plasma expander <sup>111, 112, 113</sup>. PVP based hydrogels can notably prepared by physical (by applying heat, pressure etc.) and chemical cross-linking phenomenon. PVP based hydrogels do not dissolve in water <sup>113</sup> and thus consider as an exciting scaffold material for BTR applications.

**b. Polyvinyl alcohol (PVA)**

PVA is an excellent biocompatible synthetic polymer with low biodegradable property <sup>112, 114</sup>. PVA based hydrogel can be prepared through physical/chemical/radiation mediated crosslinking. Due to its notable hydrophilic nature PVA based hydrogels are considered as a significant material for biomedical and/tissue engineering purposes. The significant porous structural attributes of PVP based hydrogels make this hydrogel an excellent tissue engineering implant material <sup>112</sup>.

**c. Carboxymethyl cellulose (CMC)**

CMC is an ether derivative of cellulose. It is a hydrophilic polymer which has considered as biocompatible to animal cells. CMC is generally used in the cosmetics and as a viscosity modifier. Due to its hydrophilic character, it is used largely in the biomedical fields <sup>113, 115</sup>. CMC based hydrogels could exhibit a significant swelling ability and thus can be an excellent polymeric component for bone tissue engineering scaffold.

**d. Agar**

Agar is a natural polymer and mixture of two components: the linear polysaccharide agarose and a heterogeneous mixture of smaller molecules called agaropectin. Agar is generally used as gelling agent <sup>113</sup>. It provides the agar based hydrogels a notable gelling property at room temperature. Furthermore, agar based hydrogels contain porous structures which makes them an excellent material for bone tissue engineering application <sup>116</sup>.

**e. Polyethylene glycol (PEG)**

PEG is a synthetic polymer of ethylene glycol and shows an excellent biocompatibility property. This polymer has been widely used in biomedical

fields like wound dressing application <sup>113</sup>. PEG is a hydrophilic polymer and can easily dissolve in water. PEG based hydrogels can be prepared through introduction of physical/chemical crosslinking. Thus, PEG based hydrogels are feasible to prepare. Moreover, PEG based hydrogels has the ability to lower the cytotoxic effect on the animal cells <sup>3</sup>. Hence, PEG based hydrogels are exciting material for BTR application.

**f. Chitosan (CS)**

CS is a natural cationic polymer which is notably biocompatible. The CS has high similarity with glycosaminoglycan (GAG) and thus could facilitate bone formation <sup>115</sup>. It has an excellent antimicrobial property. Furthermore, it facilitates notable osteoconductivity and *in vivo* neovascularization. Moreover, CS induces osteoblast proliferation and thus considered as excellent material for BTR application <sup>117</sup>.

## **1.8 Calcium and its importance in BTR**

Different calcium based bioactive compounds like calcium phosphate and calcium carbonate <sup>3, 55, 118, 119, 120</sup> have been utilized in bone tissue engineering scaffold material. The primary objective of bioactive compounds is to function as osteo-inductive agents and facilitate bone cell proliferation and differentiation. On the other hand, calcium based compounds are also act as a rigid filler which will provide necessary mechanical property to the bone scaffold.

Calcium (i.e. calcium phosphate) can be incorporated through direct mixing to the polymer solution <sup>3, 55</sup>. On the other hand, calcium mineral in the form of calcium carbonate can be incorporated in the scaffold through *in vitro* bio-mineralization <sup>55, 83</sup>. The calcium based bone tissue engineering scaffold provides two major physiochemical and biochemical stimuli (Figure. 15) to the bone forming cells (i.e. osteoblast) and osteoprogenitor cells (i.e. mesenchymal stem cells [MSC]):

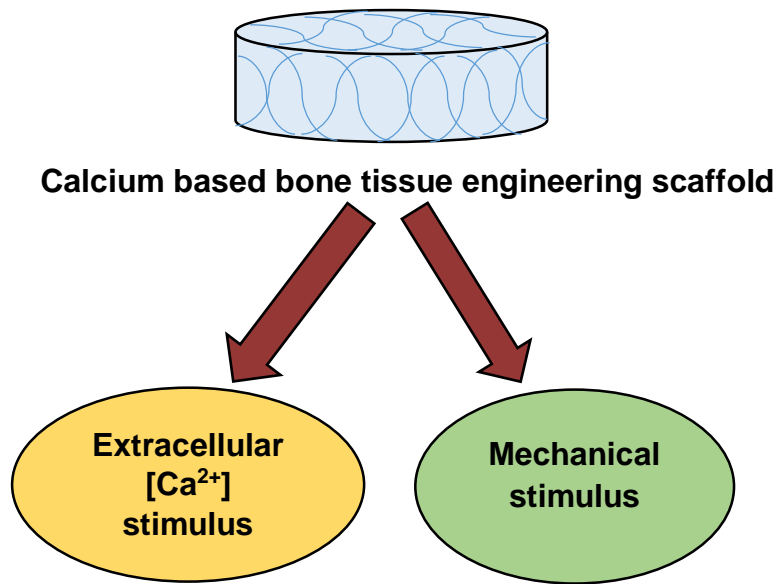


*Figure 15. Stimulus provided by calcium based bone tissue engineering scaffold. (Self-representation)*

### **1.8.1 Extracellular [Ca<sup>2+</sup>] based signaling**

In osteoclast mediated normal bone resorption process, calcium ions (Ca<sup>2+</sup>) are generally moves out from the bone matrix and this causes local increase of Ca<sup>2+</sup> concentration (nearly 40 mM)<sup>121</sup>. On other hand, bone damage can also increase local Ca<sup>2+</sup> concentration significantly (nearly 10 mM)<sup>82</sup>. Bioactive calcium agents like calcium phosphates and calcium carbonate equipped with tissue engineering scaffold can also lead to the development of elevated extracellular calcium concentration<sup>3, 83</sup>. Different macropores and micropores of tissue engineering scaffold facilitate the efficient release of calcium and phosphate for the local increase of concentration of this bioactive mineral<sup>84</sup>. Studies reported that the elevated extracellular Ca<sup>2+</sup> has the ability to stimulate the chemotaxis of osteoblasts and osteoblast precursors and this elevated calcium ion can significantly induce osteoblast proliferation and differentiation<sup>85, 86</sup>. It has been reported that increase in

local  $\text{Ca}^{2+}$  concentration can also stimulate notable intra cellular calcium signaling<sup>82</sup>. Additionally, the high concentration of calcium subsequently initiate MAPK/ERK signaling pathway (Figure. 16) which ultimately causes the gene expression (like *bone morphogenetic protein-2* or *bmp-2* gene) for osteoblast proliferation and migration<sup>122, 123</sup>.

### **1.8.2 Mechanical stimulus and signaling**

Calcium based compounds like calcium carbonate are considered as rigid filler in the filled-in polymer system. The presence of calcium based bioactive agents also enhances the mechanical property of the tissue engineering scaffold. Thus composite material containing polymeric matrix and rigid reinforcing material could also provide mechanobiological signals to the bone cells to proliferate along with biochemical cues<sup>124, 125</sup>. The mechanobiological stimulus provided by extracellular matrix (ECM) and tissue engineering scaffold is at first recognized by a eukaryotic transmembrane cell-ECM receptor, *Integrin*<sup>125</sup>. The binding of ECM/tissue engineering scaffold to Integrin receptor of bone cells<sup>126</sup> initiates a qualitative intracellular biochemical signaling cascade (Figure. 17) which ultimately stimulate the gene expression of the genes (*runx2*, *ocn* etc.) specific for bone cell proliferation<sup>127</sup>. The bone cell cycle progression and bone cell proliferation are dependent on *Integrin-dependent cell signaling pathway* that also depends on the hard and soft matrix properties. However, actin cytoskeletal tension also plays a vital role in cell proliferation event<sup>127</sup>.

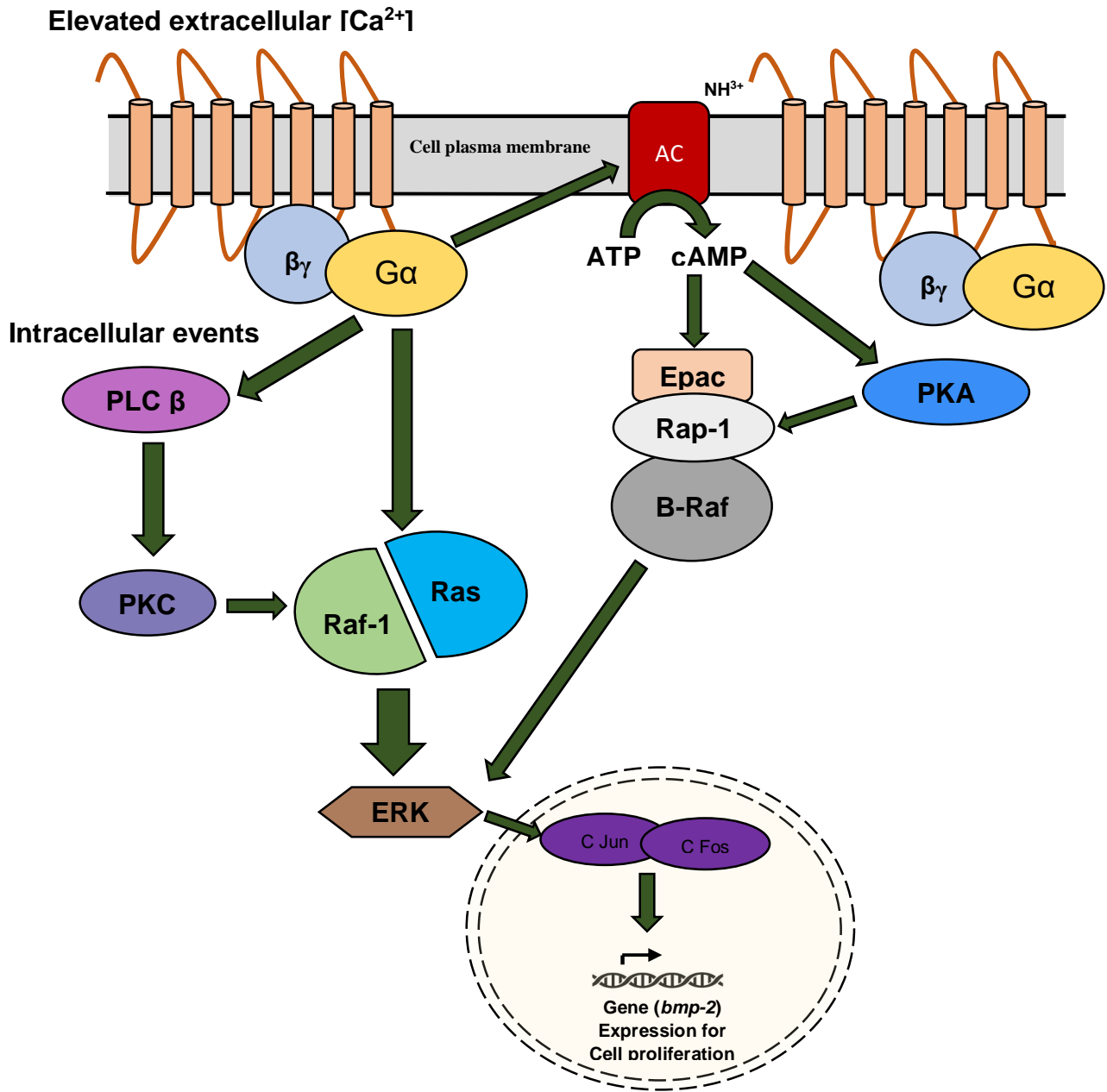


Figure 16. MAPK/ERK pathway for osteoblast proliferation  
(Self-representation based on New and Wong, 2007<sup>123</sup>)

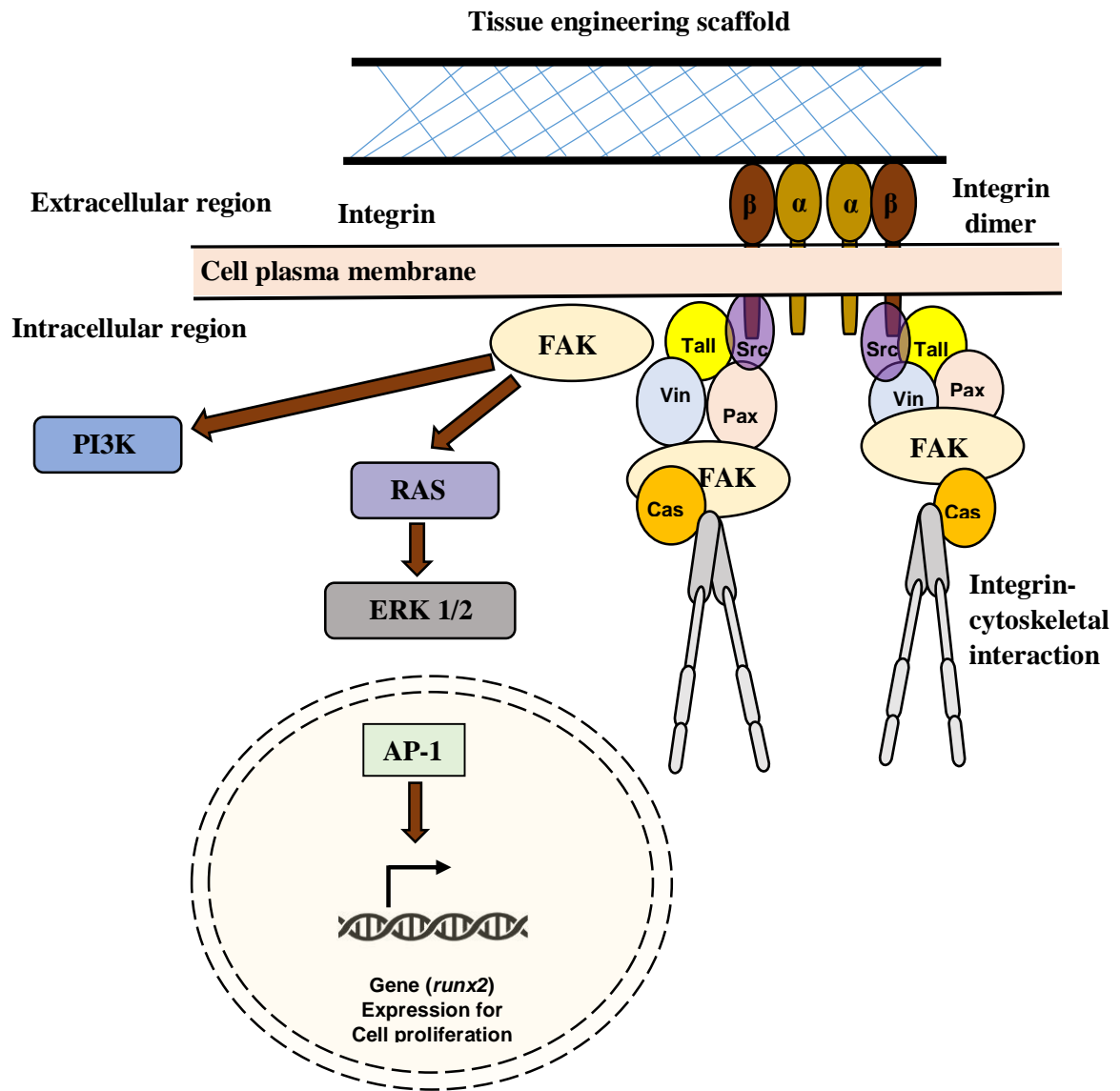


Figure 17. Integrin mediated signaling and Integrin-Scaffold interaction  
 (Self-representation based on Giancotti and Ruoslahti, 1999 and Marie et al., 2014  
 125, 128)



## **1.9 Cell and cell biology in BTR**

### **1.9.1. Bone cells**

Bone is a dynamic and powerful structure of human body. The maintenance of the animal bone structure includes periodical process of bone formation and bone resorption<sup>17</sup>. The bone majorly consists of 3 types of cells.

#### **A. Bone forming cells or Osteoblast**

The surface of animal bone harbors 4-6% cuboidal cells with numerous rough endoplasmic reticulum, notable Golgi apparatus and secretory vesicle. These cells are called *Osteoblast*<sup>129</sup>. The principal functions of the osteoblast cells are the synthesis and secrete the bone matrix; thus these cells facilitate bone formation. Hence, these cells are called bone forming cells<sup>7</sup>. The osteoblast cells are derived from mesenchymal stem cells and have following fates: a. osteoblast remains dormant and become bone lining cells or b. formation of *osteoclast*.

#### **B. Bone resorbing cells or Osteoclasts**

*Osteoclasts* are multinucleated cells sourced from mononuclear cells of hematopoietic stem cell lineage under significant cellular factors; especially, macrophage colony-stimulating factor (M-CSF) which is secreted by mesenchymal stem cells and osteoblasts<sup>7, 129</sup>. Osteoclast secretes tartrate-resistant acid phosphatase (TRAP) and Cathepsin K enzymes and hydrogen ions; which facilitates bone resorption process. Thus, these cells are also termed as bone resorbing cells.

#### **C. Mechano-sensing cells or Osteocytes**

*Osteocytes* are derived from osteoblast and present in the lacuna canalicular bone network system. Unlike osteoblast, they do not express bone marker like alkaline phosphatase but they express other bone matrix proteins. Osteocyte identifies the physiological deformation of bone matrix due to mechanical loading and shear stress

originating from canalicular fluid flow by the lacuna canalicular system. Thus osteocytes are considered as mechano-sensing cells <sup>7, 129</sup>.

Along with the above-mentioned cells, bone also harbors the following cells:

### **Osteoprogenitor cells or Mesenchymal stem cell (MSC)**

*Mesenchymal stem cells* (MSC) are considered as “Osteoprogenitor cell” as they produce osteoblast cells <sup>7</sup>. The MSC is stromal cell which are generally differentiate into osteoblast, chondroblast and adipocyte lineages. Additionally, they also express the biomarkers like CD73, CD90, CD105 <sup>130</sup>. The expressions of the specific genes like of bone morphogenetic proteins (BMPs) and members of the Wingless (*wnt*) signaling pathway are required for the commitment of MSC as osteoprogenitor lineage <sup>129</sup>.

### **1.9.2 Types of cells utilized in bone tissue engineering**

The biological evaluation of the interaction between bone implant/scaffold and different bone cell lines (like osteoblast and osteoclast) is utmost important factor in the context of healthy bone regeneration <sup>26, 131</sup>. The selection of cell source in bone tissue engineering study is a significant criterion for successful application. On the other hand, different *in vitro* studies with appropriate cell lines are also important <sup>26, 75</sup>. The criteria for the cell source selections involve, the availability of cells and its proper utilization, the osteogenic potential of the cells and the immunogenicity etc <sup>26</sup>. In general, appropriate selection of cell line or appropriate cell source will indicate the efficiency of the tissue engineering scaffold material in the context of its application. Different cell lines have been used as *in vitro* model for bone tissue engineering are discussed below in **Table 9**. <sup>26, 75, 131</sup>

**Table 9.** Cell lines have been used as *in vitro* model for BTE

Application	Cell lines		
<i>Bone Tissue Engineering</i>	<i>Differentiated cell lines</i>	Osteoblast	MC3T3-E1 cell line; Primary culture of human osteoblast
		Fibroblast	COS-7 cells; NIH3T3 cells
		Osteosarcoma	MG-63 cell line; Saos-2 cell line
	<i>Undifferentiated cell line (Stem cells)</i>	Adipose-Derived Stem cells (AD-SC)	
		Bone Marrow-Derived Stem Cell (BM-SC)	
		Embryonic Stem cell (ESC)	
		Induced pluripotent stem cells (iPSC)	
		Umbilical Cord Mesenchymal Stem Cells	
		Endothelial Progenitor Cells	
		Periosteum-Derived Progenitor Cells	
		Synovium-Derived Mesenchymal Stem Cells	
Muscle-Derived Stem Cells			

## 1.10 Scaffold and cell interaction

Cell and scaffold interaction is a crucial factor for the tissue regeneration event. The physiochemical characteristics of scaffold material significantly influence the cell proliferation and differentiation <sup>26</sup>. On the other hand, the efficient interaction between cell and scaffold results in notable cell motility and cell migration. The significant ligand-integrin interaction between cell and scaffold further leads to cytoskeletal contraction and remodeling events which can determine also the fate of the corresponding cell <sup>132, 133, 134, 135</sup>. In the context of cell proliferation and migration, the mechanical property of the scaffold is an important aspect. The mechanical characteristic of a scaffold material facilitates mechano-transduction related biochemical signaling which ultimately results in diverse cellular responses (Figure.

18). This mechano-transduction process involves cell-ECM or cell-scaffold adhesion, cell-cell adhesion, function of membrane-cytoskeletal-nuclear structural components <sup>56</sup>. It has been reported that, cell adhesion and proliferation of mesenchymal stem cells (MSC), fibroblast cells, and endothelial cells were significant on stiff substrates <sup>136</sup>. The cellular trans-membrane receptor, Integrin; whose primary function is cell-extracellular matrix adhesion, plays an important role in establishing the mechanical contact related adhesion between scaffold and actinomyosin system of cell cytoskeleton. Integrin promotes the focal adhesion between scaffold (i.e. extracellular matrix) and cell which subsequently results Integrin receptor conformational change and thus activates a cellular biochemical signaling cascade. The additional force to this Integrin in bound state also promotes cellular actin filament polymerization and stimulates further cytoskeletal contraction event. The significant interaction between actin and myosin-II filaments of cellular cytoskeletal stress fibers develops notable contractile forces. This contractile force helps the cell to identify the mechanical property and elasticity of the surrounding matrix <sup>137</sup>. However, cells also contain local mechano-sensing biomolecules to recognize and respond to the change in local mechanical force and property provided by the scaffold <sup>56</sup>. Porosity and interconnectivity of the pores of the scaffold material are also important factor for cell growth and nutrient flow. The pore size of the scaffold is also considered as a significant criterion for healthy tissue regeneration <sup>56</sup>. The cell migration was found restricted if the pore size is too small; on the other hand, cell adhesion was found limited if the pore size become too large. The pore size affects significantly the cell morphology.

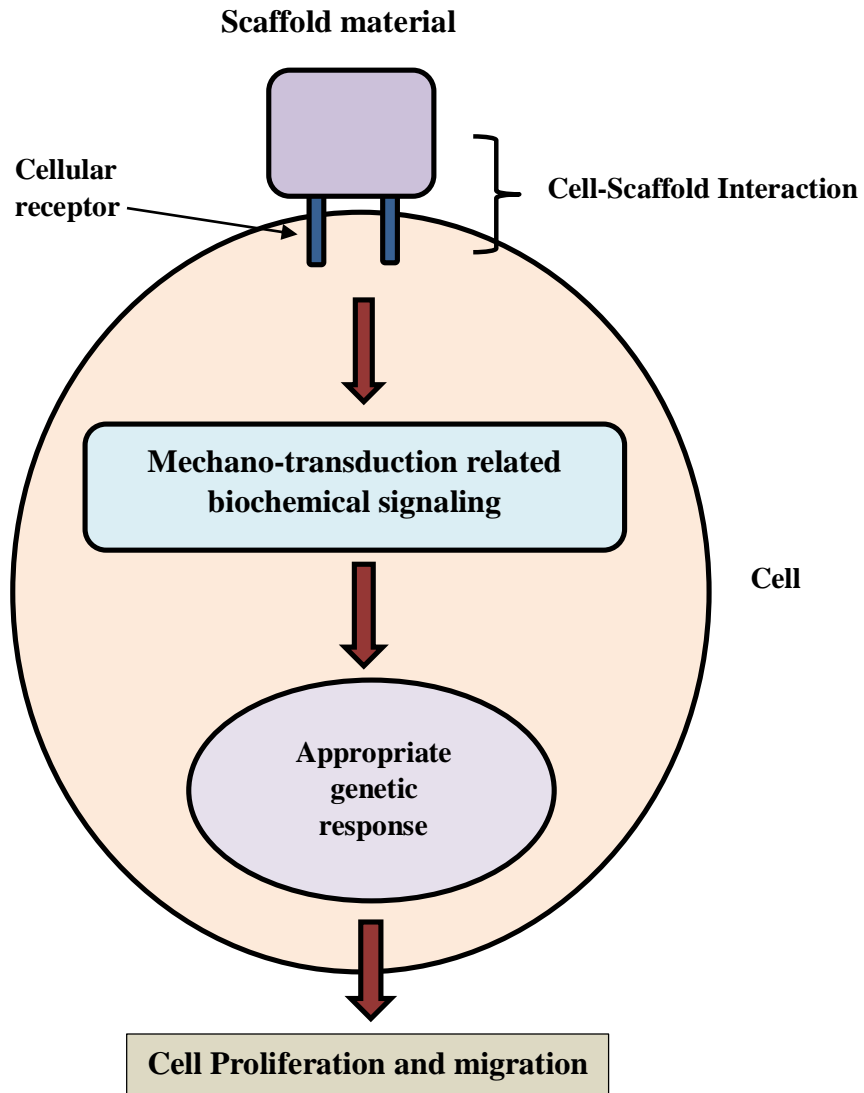


*Figure.18 Scaffold and cell Interaction (Self-representation)*

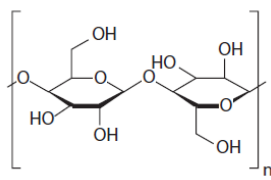
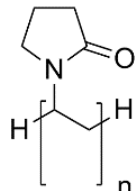
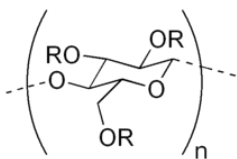
## Chapter 2. EXPERIMENTATION

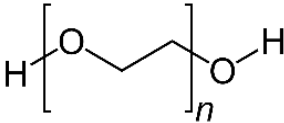
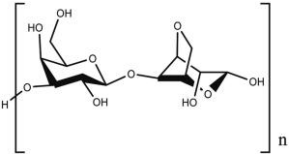
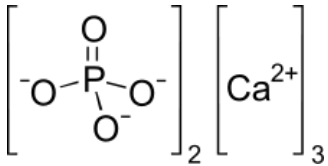
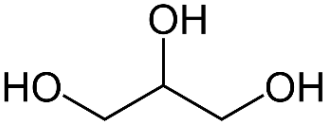
### 2.1 Materials for calcium reinforced BC based hydrogel preparation

#### 2.1.a The materials used in this study

The materials used in this doctoral study are explained below in **Table 10**.

**Table 10.** Materials used in the preparation of hydrogel scaffolds

Materials	Chemical formula	Description
<i>Bacterial cellulose</i> (BC)		BC is cellulose, which majorly synthesized by bacteria of the genera, <i>Gluconobacter</i> . BC is composed of a linear homopolysachharides developed by $\beta$ -D-glucopyranose units linked through $\beta$ -1, 4 glycosidic bonds. BC is devoid of lignin and hemicellulose and thus differs from the plant cellulose <sup>3, 55</sup> .
<i>Polyvinylpyrrolidone</i> (PVP)		PVP is a water-soluble polymer made from the monomer <i>N</i> -vinylpyrrolidone. It is a biocompatible polymer used in biomedical purposes like wound dressing <sup>138</sup> .
<i>Carboxy-methyl cellulose</i> (CMC)	 <p>R = H or CH<sub>2</sub>CO<sub>2</sub>H</p>	CMC is a water-soluble polymer. It is a biocompatible polymer. It is used in cosmetic application and other biomedical uses <sup>138</sup> .

<p><i>Polyethylene glycol</i> (PEG)</p>		<p>PEG is a hydrophilic polymer. It is also biocompatible polymer and reduces cell and tissue cytotoxicity<sup>3, 55, 138</sup>.</p>
<p><i>Agar</i></p>		<p>Agar is a jelly-like substance. It is a mixture of two components: the linear polysaccharide agarose, and a heterogeneous mixture of smaller molecules called agarpectin. Agar is considered as a gelling agent<sup>3, 55, 138</sup>.</p>
<p><i>β-tricalcium phosphate</i> (β-TCP)</p>		<p>β-TCP is a calcium salt of phosphoric acid. It is considered as a biocompatible bio-ceramics<sup>3, 55</sup>.</p>
<p><i>Hydroxyapatite</i> (HA)</p>	$\text{Ca}_{10}(\text{PO}_4)_6(\text{OH})_2$	<p>HA is a naturally occurring mineral form of calcium apatite. It is an integral component of animal bone<sup>3, 55</sup>.</p>
<p><i>Glycerin</i></p>		<p>Glycerin or Glycerol is a simple hydrophilic polyol compound. It is used as a humectant in the preparation of hydrogel<sup>3, 55, 138</sup>.</p>

### 2.1.b. Polymers and their purpose of use for the preparation of the hydrogel scaffold

The polymers and their advantages and specific purpose in this study are described below in **Table 11**.

**Table.11** Polymers and their advantages and specific purpose in this study

Polymers	Advantages	Specific purpose of use
<i>BC</i>	BC nano-fibers contain similar diameter like collagen. <sup>97</sup>	Biocompatibility and mechanical strength.
<i>PVP</i>	Biocompatible and water soluble	Biocompatibility
<i>CMC</i>	Swelling property and biocompatibility	Biocompatibility
<i>PEG</i>	Reduces cellular toxicity and biocompatibility	Biocompatibility and cellular toxicity lowering agent
<i>Agar</i>	Gelling agent and swelling ability	Gelling of hydrogel and swelling ability

### 2.1.c. Sources of the utilized materials in this study

The sources of the utilized materials in the study are described in **Table 12**.

**Table 12.** Sources of the materials in this study

Materials	Description	Source
<i>For CaP reinforced BC based hydrogel scaffolds</i>		
<i>BC (Raw material)</i>	Synthesized polymer	<i>G. xylinus</i> CCM 3611 <sup>T</sup> bacteria



<b>Polymers</b>	<i>PVP</i>	PVP K30, mol wt: 40, 000	Fluka, Switzerland
	<i>CMC</i>	Sodium carboxymethyl cellulose	Sinopharm Chemical Reagent Co Ltd. (SCRC), China
	<i>PEG</i>	PEG 3000, mol wt. 2700-3300	Fluka, Switzerland
	<i>Agar</i>	Agar powder for gelling agent	Fluka, Switzerland
<b>Other agents</b>	<i>Glycerin</i>	Humidity retention agent	Lach-Ner Ltd., Neratovice, Czech Republic
<b>Calcium Phosphates</b>	<i>Hydroxyapatite</i>	CaP powder, mol. Wt.: 502.31 g/mol	Sigma Aldrich, St. Louis, MO, USA
	<i><math>\beta</math>-tri calcium phosphate</i>	CaP powder, mol. Wt.: 310.18 g/mol	Fluka, Switzerland
For <i>in vitro</i> bio-mineralization of CaP reinforced BC based hydrogels to prepare <i>calcium phosphate and calcium carbonate reinforced BC based hydrogel scaffolds</i>			
<b>Sodium carbonate</b>	Na <sub>2</sub> CO <sub>3</sub> ; molecular weight 286.14 g/mol		Sigma Aldrich, St. Louis, MO, USA
<b>Calcium chloride</b>	CaCl <sub>2</sub> ; molecular weight 110.99 g/mol, 97.0%		Penta, Czech Republic

## 2.2 Methodology of calcium reinforced BC based hydrogel scaffold preparation

### 2.2.1 Synthesis of raw material i.e. Bacterial cellulose

The methodology of BC synthesis is described as follows:

BC (holding 99% H<sub>2</sub>O) was synthesized in presence of basal synthetic Hestrin-Schramm (HS) nutritive medium (pH 7.0) using *Gluconacetobacter xylinus* CCM 3611<sup>T</sup> (syn. *Acetobacter xylinum*) at 30°C for 15 days. 100 mL bacteriological culture bottles were inoculated with 5 mL of H.S. medium containing  $96 \times 10^8$  cells/mL bacteria [bacteria counted at 550 nm wavelength]. The freshly prepared BC pellicle was treated with 0.5N NaOH solution and then heated at 80°C for 1 hour to remove the possible contaminations from the BC pellicle (Figure. 19). The newly produced BC pellicle was then treated with deionized water and the water was refreshed after 2h of interval until the pH reached a neutral value. Thereafter, a homogenous suspension of BC (particle size: ranging from 159 nm-351.03 nm) from the obtained BC mat was prepared by grinding [10-12 mins] the BC mat in distilled water<sup>3, 55</sup>.

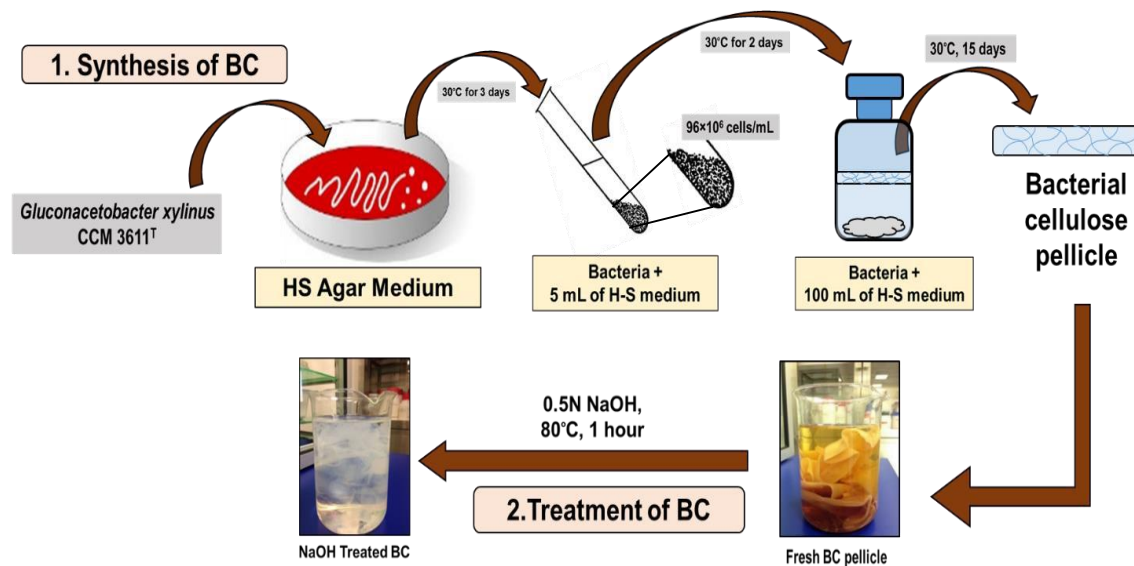


Figure 19. BC production in H.S. medium. (Self-representation)

### 2.2.2 Preparation of calcium reinforced BC based hydrogel scaffolds

The *calcium reinforced BC based hydrogel scaffolds* were developed in the form of *calcium phosphate reinforced BC based hydrogel scaffolds* and *calcium phosphate and calcium carbonate reinforced BC based hydrogel scaffolds*. The preparation of the hydrogel scaffolds is described below:

#### (a) Preparation of calcium phosphate reinforced BC based hydrogel scaffolds

*Calcium reinforced filled BC based hydrogel scaffolds* were prepared by applying the BC (holding 99% water) with CMC and PVP (**Table 13.**). Polyethylene glycol (PEG) was also used to reduce the risk of tissue damage and other significant cytotoxic effects. Agar was used as gelling agent and glycerin was used as humectant. Additionally, calcium phosphates like  $\beta$ -TCP and HA were given to develop the inorganic *calcium phosphate filled BC based hydrogel scaffolds* (Figure. 20) .

The hydrogel scaffolds were developed following the solvent casting method, applying moist heat and pressure. 100 mL polymer solutions were prepared in 250mL sealed glass bottles under 15 lbs (107 KPa) pressure and 120°C temperature for 20 minutes. Two sets of polymer solutions were prepared; where one set was without inorganic calcium phosphate, and another set was with inorganic calcium phosphates ( $\beta$ -TCP/HA). 25 mL polymer solution from each sealed glass bottles was then poured into 75 mm diameter petri-dishes and then allowed to cool at room temperature (22-25°C). Finally, smooth, round shaped, off white color BC based scaffolds with and without calcium phosphate were achieved. The hydrogel scaffolds without calcium phosphate were termed as “*BC-PVP*” and “*BC-CMC*” and the calcium phosphate reinforced scaffolds were termed as “*BC-PVP- $\beta$ -TCP/HA*” and “*BC-CMC- $\beta$ -TCP/HA*”.

Furthermore, on the basis of cell biological study, the “*BC-PVP- $\beta$ -TCP/HA*” scaffold was selected and then different *calcium phosphate reinforced BC based hydrogel scaffolds* (BC-PVP- $\beta$ -TCP/HA\_10:90; BC-PVP- $\beta$ -TCP/HA\_20:80; BC-PVP- $\beta$ -TCP/HA\_40:60; BC-PVP- $\beta$ -TCP/HA\_50:50; BC-PVP- $\beta$ -TCP/HA\_60:40) (Diameter: 75 mm; Thickness: 5.9-6.2 mm) were prepared with different calcium phosphate i.e.  $\beta$ -TCP and HA ratios (**Table 14**).

**Table 13.** *Composition of calcium reinforced BC based hydrogel scaffold.*

Sample index		PVP (g)	CMC (g)	BC (g)	PEG (g)	Agar (g)	Glycerin (mL)	$\beta$ -TCP/HA (g)	Water (mL)
Scaffolds without calcium	BC-PVP	0.5	0.0	0.5	1	2	1	0.0/0.0	95
	BC-CMC	0.0	0.5	0.5	1	2	1	0.0/0.0	95
Scaffolds with calcium phosphate	BC-PVP- $\beta$ -TCP/HA	0.5	0.0	0.5	1	2	1	0.2/0.8	94
	BC-CMC- $\beta$ -TCP/HA	0.0	0.5	0.5	1	2	1	0.2/0.8	94
Scaffolds with calcium phosphate and calcium carbonate	BC-PVP- $\beta$ -TCP/HA-CaCO <sub>3</sub>	0.5	0.0	0.5	1	2	1	0.2/0.8	94
	BC-CMC- $\beta$ -TCP/HA-CaCO <sub>3</sub>	0.0	0.5	0.5	1	2	1	0.2/0.8	94

**Table 14.** *Composition of calcium phosphate reinforced BC based hydrogel scaffold*

Calcium phosphate reinforced BC based hydrogel scaffolds	PVP (g)	BC (g)	PEG (g)	Agar (g)	Glycerin (mL)	$\beta$ -TCP/HA (g)	Water (mL)
BC-PVP	0.5	0.5	1	2	1	0.0/0.0	95
BC-PVP $\beta$ -TCP/HA _10:90	0.5	0.5	1	2	1	0.1/0.9	94
BC-PVP- $\beta$ -TCP/HA _20:80	0.5	0.5	1	2	1	0.2/0.8	94
BC-PVP- $\beta$ -TCP/HA _40:60	0.5	0.5	1	2	1	0.4/0.6	94
BC-PVP- $\beta$ -TCP/HA _50:50	0.5	0.5	1	2	1	0.5/0.5	94
BC-PVP- $\beta$ -TCP/HA _60:40	0.5	0.5	1	2	1	0.6/0.4	94

*(b) Preparation of calcium phosphate and calcium carbonate reinforced BC based hydrogel scaffolds*

The *calcium phosphate reinforced BC based hydrogel scaffolds* (only BC-PVP- $\beta$ -TCP/HA\_20:80 and “BC-CMC- $\beta$ -TCP/HA\_20:80) were further *in vitro* bio-mineralized for incorporation of additional  $\text{CaCO}_3$ . The *in vitro* bio-mineralization process was performed following the simple liquid diffusion technique. Two different ionic solutions (i.e.,  $\text{Na}_2\text{CO}_3$  and  $\text{CaCl}_2$ ) were used at fixed concentration ratios (5.25/100 mL and 7.35/100 mL) to prepare *calcium phosphate and  $\text{CaCO}_3$  filled BC based hydrogel scaffolds*. In this study, the bio-mineralization of hydrogel matrix was carried out for 60 min by keeping the test samples in each ionic solution. The *calcium phosphate reinforced BC based hydrogel scaffolds* were first immersed in 100 mL solution of  $\text{CaCl}_2 \cdot \text{H}_2\text{O}$  for 30 min and then transferred into 100 mL of  $\text{Na}_2\text{CO}_3$  solution and kept them for 30 min. In this procedure, *calcium phosphate and  $\text{CaCO}_3$  filled BC based in vitro bio-mineralized hydrogel scaffolds* were achieved, which were finally termed as “BC-PVP- $\beta$ -TCP/HA- $\text{CaCO}_3$ ” and “BC-CMC- $\beta$ -TCP/HA- $\text{CaCO}_3$ ” respectively (Figure. 20).

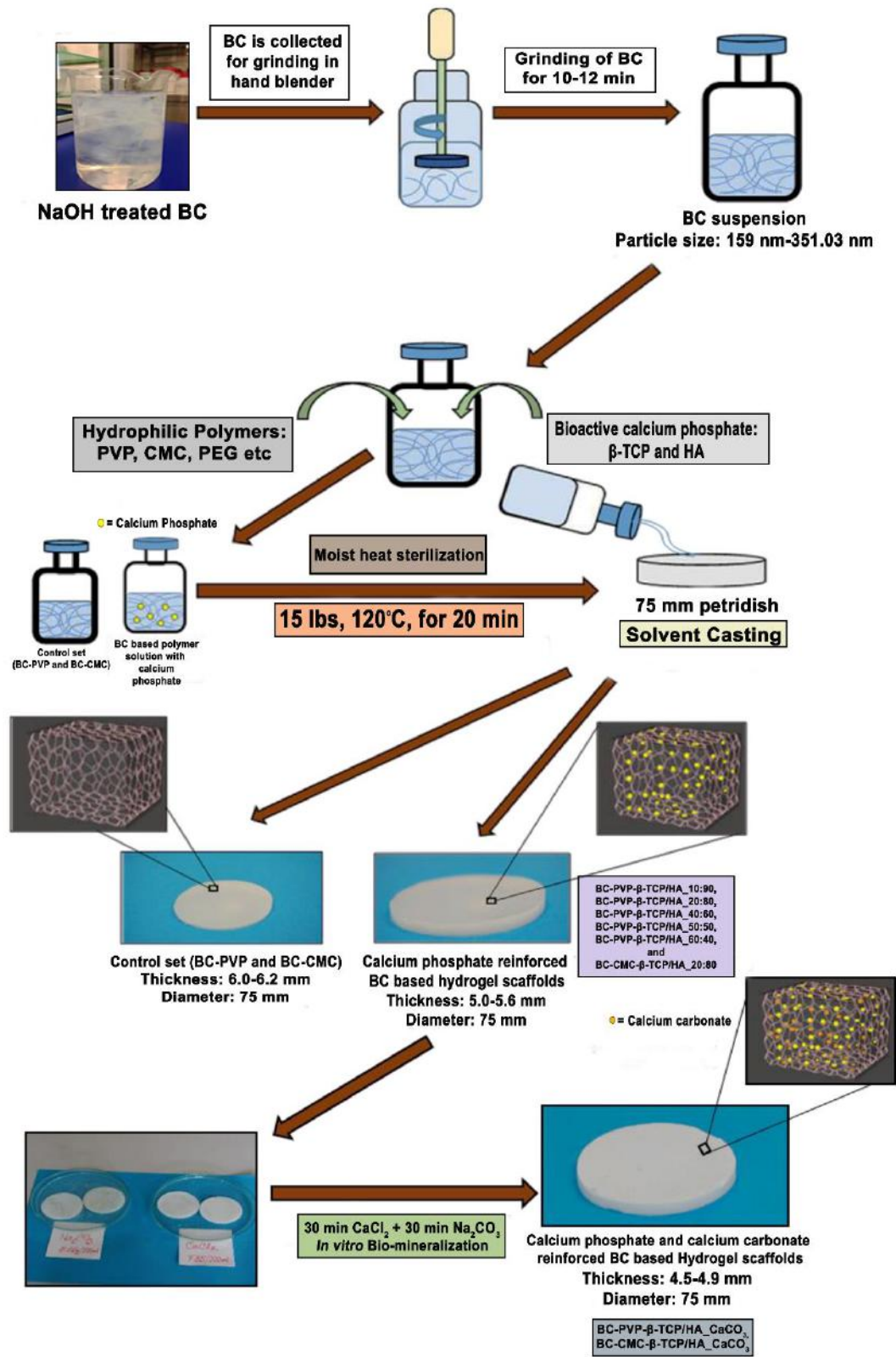


Figure. 20 Preparation of calcium reinforced BC based hydrogel scaffolds. (Self-representation)

## 2.3 Physical characterization

The physical characterization of *calcium reinforced BC based hydrogel scaffolds* were performed.

Most of the characterization study was performed with freeze dried or lyophilized samples. The calcium reinforced hydrogel scaffolds were freeze dried for 24 h, using Scanvac Cool Safe 110-4 PRO, Lyngø; at -80°C temperature and 0–5 kPa pressure.

Thereafter, specific dimensions of the sample sections were selected for the characterization analysis. The methodologies of the physical properties characterization are the following:

### 2.3.1 Swelling study

Polymeric hydrogel has been used as potential scaffold material for bone tissue engineering scaffold. It composed of hydrophilic cross-linked polymeric three dimensional networks structure, which can absorb and retain high quantity of water and thus has the similarity with a living tissue <sup>3, 55, 71</sup>.

High swelling ability of hydrogel is attributed by the notable hydrophilic groups like hydroxyl group, carboxyl group of the chains of its structural polymers <sup>75</sup>. The *swelling analysis* was performed through *gravimetric study* with physiological saline solution (Ringers solution; pH 7.40) at human physiological temperature (37°C± 1°C) and human fever temperature (39°C). Circular sections (20 mm diameter) of the hydrogel scaffolds were soaked for specific time intervals (5 min, 60 min, 120 min, 180 min, 240 min, 300 min, 360 min). The absorptivity of the hydrogel scaffolds is measured by the degree of swelling (Figure. 21) which is defined by the following equation:

$$\text{Degree of swelling (\%)} = [(W_s - W_d) / W_d] \times 100 \dots \dots \dots (1)$$

Where,  $W_s$  and  $W_d$  are weight of the swollen and dried hydrogel scaffold sections.

The data for swelling study was presented as the mean  $\pm$  standard error of the mean. Three repeats of experiments were conducted ( $n=3$ ). Statistical differences between control and treated groups, as well as between the studied samples were assessed using one-way analysis of variance (ANOVA) followed by a suitable post-hoc test (Dunnett/Bonferonni) by using GraphPad Prism version 5.00 for Windows (San Diego, CA, USA) and MS Office 2010 (Redmond, WA, USA). The P value is expressed as  $P < 0.0001_{n=3}$  for the level of significance.

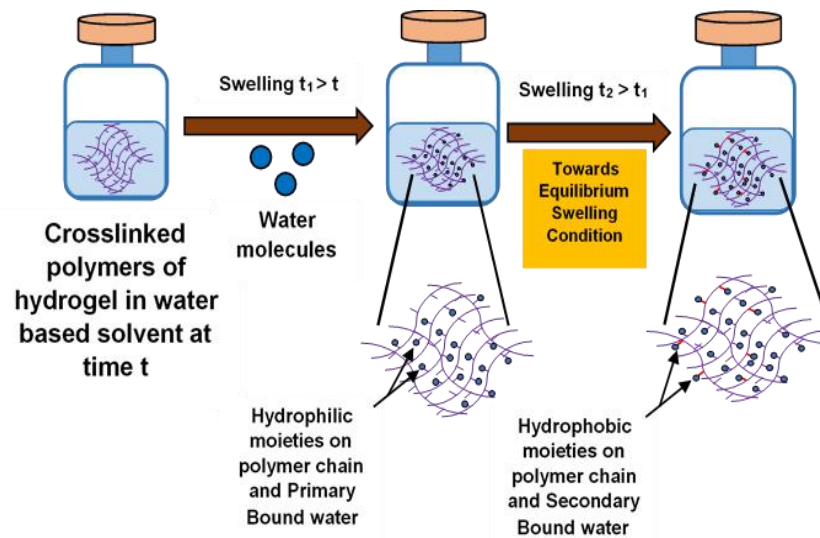


*Figure 21. Interaction of water and polymer chains of a hydrogel during swelling. (Self-representation)*

### 2.3.2 Porosity

*Porosity* is one of important factors of bone tissue engineering scaffold. The porosity can be defined as the percentage of void spaces inside a tissue engineering scaffold<sup>18, 139, 140</sup>. Porosity induces protein adsorption which ultimately stimulates bone cells<sup>141</sup>.



The *liquid displacement method* used for the determination of porosity. This method involves the immersion of freeze dried sample sections with specific dimensions (10 mm<sup>2</sup>) into absolute ethanol for 48 hours. The porosity of the sample is calculated by the following:

$$P = (W_2 - W_1) / \rho V_1 \dots \dots \dots (2)$$

Where, Where, W1 and W2 are the weight of the hydrogel scaffolds before and after the immersion into absolute ethanol and V1 is the volume of the scaffolds before immersion into ethanol, ρ is the constant of the density of ethanol at room temperature <sup>55,142</sup>.

The data for porosity study was presented as the mean ± standard error of the mean. Three repeats of experiments were conducted (n=3). Statistical differences between control and treated groups, as well as between the studied samples were assessed using one-way analysis of variance (ANOVA) followed by a suitable post-hoc test (Dunnett/Bonferonni) by using GraphPad Prism version 5.00 for Windows (San Diego, CA, USA) and MS Office 2010 (Redmond, WA, USA). The P value is expressed as P<0.0001<sub>n=3</sub> for the level of significance.

### **2.3.3 Biodegradation study**

One of the objectives of tissue engineering is to facilitate the growth of the host body cells and eventual replacement of the applied scaffold material by newly grown cell and tissue. Hence, a controlled *degradability* of the tissue engineering scaffold is an important consideration <sup>143, 144, 145, 146</sup>.

The degradation or bio-resorption profile of a material involves following steps <sup>147</sup>: Water adsorption and absorption, reduction of mechanical behavior and reduction of weight of the sample.

In hydrolysis, the long polymer chains in the amorphous region of the polymeric scaffold material become shortened. This is followed by reduction of molecular weight of the polymers and this leads to the loss of mechanical property of the scaffold. This ultimately leads to the weight loss of the polymeric device <sup>147</sup>.

The biodegradation study was performed through the analysis of the following methods:

**(a) Weight Loss profile**

The hydrolytic degradation experiment was performed through *gravimetrically* by incubation of the freeze dried sample sections (20 mm diameter) in solution (Physiological Saline [i.e. Ringer] solution; pH: 7.4) maintaining at 37°C for 28 days (i.e. 4 weeks). The saline solution was changed weekly. The sample sections were removed at specific time (i.e. 7 days, 14 days, 21 days, 28 days) from the solution. They were then freeze dried after being washed by distilled water. The percentage of weight loss was evaluated according to the following equation:

$$\text{Weight loss (\%)} = [(W_0 - W_t)/W_0] \times 100 \dots \dots \dots (3)$$

Where,  $W_0$  = weight at before degraded sample and  $W_t$  = weight of degraded samples at time t.

**(b) Gel content analysis**

Changes in gel content of the hydrolytically degraded calcium phosphate reinforced BC based hydrogel scaffolds samples (20 mm diameter) were analyzed to indicate the degradation phenomenon. The weights of the freeze dried hydrogel scaffolds were measured initially ( $W_0$ ) and after a specific time (7, 14, 21, or 28 days) ( $W_t$ ). The gel content of the scaffolds was measured through the following equation:

$$\text{Gel content} = W_t/W_0 \times 100 \dots \dots \dots (4)$$

**(c) Gel Density Study**

The density of the freeze dried *calcium phosphate reinforced BC based hydrogel scaffolds* samples (20 mm diameter) was studied at specific times (7, 14, 21, and 28 days) during the degradation study (in a physiological saline solution). The gel density ( $\rho$ ) was determined by the following equation:

$$\rho = W/\pi \times (d/2)^2 \times h \dots \dots \dots (5)$$

where; W = weight of the scaffold,  $\pi = 3.14$ , d = diameter of the samples, and h = thickness of the samples.

**(d) pH Change and Calcium Release in the medium**

The pH change of the medium (i.e., a physiological saline solution in which *calcium phosphate reinforced BC based hydrogel scaffolds* sections were immersed) was also analyzed with a pH meter (Lovobond pH meter, Amesbury, UK). Additionally, the percentage of calcium released by the *calcium phosphate reinforced BC based hydrogel scaffolds* at specific times (i.e., 7, 14, 21, and 28 days) during degradation was also studied because loss of calcium from the scaffolds might also indicate the loss of mechanical property. The percentage of calcium release from the scaffolds was studied by X-ray fluorescence (ARL Quant X, Spectrometer, Thermo Scientific, Waltham, MA, USA) in the presence of helium atmosphere.

Moreover, the bio-degradation phenomenon of the *calcium phosphate reinforced BC based hydrogel scaffolds* was further confirmed and reported through analysis of morphological changes (i.e. SEM) and chemical characterization (i.e. FTIR).

The data for biodegradation study was presented as the mean  $\pm$  standard error of the mean. Three repeats of experiments were conducted (n=3). Statistical differences between control and treated groups, as well as between the studied samples were

assessed using one-way analysis of variance (ANOVA) followed by a suitable post-hoc test (Dunnett/Bonferonni) by using GraphPad Prism version 5.00 for Windows (San Diego, CA, USA) and MS Office 2010 (Redmond, WA, USA). The P value is expressed as  $P < 0.0001_{n=3}$  for the level of significance.

## 2.4 Morphological characterization

*Morphology* is one of important factors of bone tissue engineering scaffold. Sample surface topography can provide the idea of surface roughness which is significant in respect of bone cell attachment, growth, proliferation and differentiation<sup>141, 148, 149</sup>.

Morphological characterization of *calcium reinforced BC based hydrogel scaffolds* was performed through *scanning electron microscope (SEM) analysis*. Small sections from different regions of the freeze dried scaffold were selected and analyzed through SEM by:

- (1) “*Phenome Pro*” (Phenome World, The Netherlands) table SEM, operating in the secondary electron imaging mode at an accelerating voltage of 5–20 kV. The image magnification was 100X – 10kX.
- (2) “*NOVA nanoSEM*” (FEI, USA), operating in the secondary electron imaging mode at an accelerating voltage of 5–20 kV. The image magnification was 100X–10kX.

On the other hand, the pore size is an important factor for bone tissue engineering scaffold. The pore size distributions were measured through SEM image analysis by ImageJ/Fiji software (NIH, USA).

The data for pore size distribution was analyzed and presented as the mean  $\pm$  standard error of the mean. Statistical differences between control and treated groups, as well as between the studied samples were assessed using one-way analysis of variance (ANOVA) followed by a suitable post-hoc test

(Dunnett/Bonferonni) by using GraphPad Prism version 5.00 for Windows (San Diego, CA, USA) and MS Office 2010 (Redmond, WA, USA). The P value is expressed as  $P < 0.0001$  and  $P < 0.01$  for the level of significance.

## **2.5 Chemical characterization**

Different chemical cues from the scaffold material could initiate specific signaling cascade and finally results in bone cell growth and proliferation<sup>150, 151, 152</sup>. Additionally, the chemical characterization of the scaffolds also indicates the compositional ingredients that have been used to develop the tissue engineering scaffold material.

The *chemical characterization of calcium reinforced BC based hydrogel scaffolds* was performed by:

### ***(1) Fourier Transform Infrared Spectroscopy (FTIR)***

The freeze dried samples of *calcium reinforced BC based hydrogel scaffolds* were used for *FTIR* analysis and performed at room temperature (20–22°C). A small amount of sample section with flat surface was selected from each freeze dried hydrogel scaffolds. Three repeats of experiments were conducted. FTIR was performed at wave number 600–4000  $\text{cm}^{-1}$  with a uniform resolution of 2  $\text{cm}^{-1}$ . The ATR-FTIR analysis was conducted by using NICOLET 320 FTIR spectrophotometer with the “Omic” software package.

### ***(2) Energy Dispersive X-ray Fluorescence (EDX) Study***

The presence of calcium (Ca), phosphate (P) in the *calcium phosphate reinforced BC based hydrogel scaffolds* were determined by *scanning electron microscope enabled energy dispersive X-ray fluorescence (SEM-EDX)* at an accelerated voltage of 15 kV. For this study, sections from freeze dried samples were selected.

The SEM-EDX study was also performed in triplicate.

## 2.6 Thermal characterization

Thermal characterization of tissue engineering scaffolds is also considered as an important criterion for knowing its thermal stability and behavior<sup>153, 154</sup>.

The thermal behavior of *calcium reinforced BC based hydrogel scaffolds* was analyzed by the following methods:

### (1) *Thermo-gravimetric analysis (TGA)*

*TGA of calcium reinforced BC based hydrogel scaffolds* was performed by the TA Q500 apparatus (TA Instruments, USA). The analysis was performed with 7-8 mg amount of freeze dried sample with platinum pan, at the constant heating rate of 10°C/min between the temperature ranges from 25–700°C under nitrogen atmosphere (50 mL/min).

The TGA was performed in triplicate (n = 3).

### (2) *Differential scanning calorimetry (DSC)*

*DSC of freeze dried samples of calcium phosphate reinforced BC based hydrogel scaffolds* was performed to determine the thermal characteristics of the hydrogel scaffolds. 5–8 mg of the sample was taken. The DSC was measured with a differential scanning calorimeter (Mettler Toledo, Columbus, Ohio, USA) at a temperature range of -50 to 500°C in the presence of the nitrogen gas flow rate at 50 mL/min.

The DSC study was performed in triplicate (n = 3).

## 2.7 Mechanical Property analysis

Mechanical property is one of the most important characteristics of bone tissue engineering scaffold. Appropriate mechanical property of bone scaffold ensures the bone cell growth and proliferation and thereby facilitates tissue regeneration<sup>155</sup>.

The mechanical characterization of *calcium reinforced BC based hydrogel scaffolds* was performed through the following methods:

### (1) *Viscoelastic behavior analysis*

The viscoelastic property of the *calcium reinforced BC based hydrogel scaffolds* samples was studied by using a modular compact rheometer testing device (Anton Paar, MCR 502, Austria) and “Rheoplus” software package for data analysis. Dynamic frequency sweep analysis was conducted in the linear viscoelastic region (LVR) at 1% strain amplitude at room temperature (28°C), and human physiological temperature (37°C). The viscoelastic behavior was analyzed with both “before dry sample” sections (i.e. samples before freeze dried) and “swelled samples” sections (i.e. sample sections after swelling in physiological saline solution) (20 mm diameter) in the oscillation mode with the angular frequency range from 0.1 to 100 rad s<sup>-1</sup> and in some fixed angular frequencies (0.39 rad s<sup>-1</sup>, 3.9 rad s<sup>-1</sup>, 39 rad s<sup>-1</sup>) at 37°C. In addition, viscoelastic behavior of swelled *calcium phosphate reinforced BC based hydrogel scaffolds* were studied at human fever temperature (39°C) from 0.1 to 100 rad s<sup>-1</sup>. The tan δ value was also determined. The influence of angular frequency on storage (G′) and loss (G′′) modulus and complex viscosity (η\*) was calculated by the following equation:

$$\eta^* = [(G'/\omega)^2 + (G''/\omega)^2]^{1/2} \dots \dots \dots (6)$$

The viscoelastic analysis was performed in triplicate (n = 3). The data were presented as mean± standard error of the mean.

## **(2) Compression test**

The compressive strength of *calcium reinforced BC based hydrogel scaffolds* was determined by using Testometric M350-5CT, England, UK at room temperature (20°C) with a load cell having a full scale 300 kgf. Sections (20 mm diameter) from freeze dried hydrogel samples were taken for the study. The study was done with a compression rate of 1 mm.min<sup>-1</sup>.

The compression study was performed in triplicate (n = 3). The data were presented as mean±standard deviation of the mean.

## **2.8 Biological Property analysis**

Biological characterization is most important parameter in assessing the efficiency of scaffold for bone tissue engineering application<sup>156</sup>. Biological characterizations of the bone tissue engineering scaffold were performed on the basis of antibacterial study and *in vitro* analysis.

### **2.8.1 Antimicrobial study**

Antibacterial property is an important aspect of hydrogel scaffold<sup>157</sup>. The antibacterial activity of all *calcium reinforced BC based hydrogel scaffolds* were studied by following the *agar disc diffusion* method. The bacteria selected for this study are *Staphylococcus aureus* (*S. aureus* CCM 4516; Gram + ve bacteria) and *Escherichia coli* (*E. coli* CCM 4517; Gram – ve bacteria). 8 mm circular specimens were selected from the all *calcium reinforced BC based hydrogel scaffolds*. Specimens were sterilized by treating with 1 mL of 96% ethanol for 40 min. Then the specimens were dried at 30–32°C and again UV sterilized for 30 minutes. 100 mL of bacterial suspension was used for this study. The analysis was performed using sterile nutrient agar (2%) medium. Finally, testing plates were then incubated



in a temperature controlled incubator at 37°C for 24 h. The antibacterial property was analyzed by observing the zone of inhibition (Figure. 22). The antibacterial property analysis was performed in triplicate (n = 3).

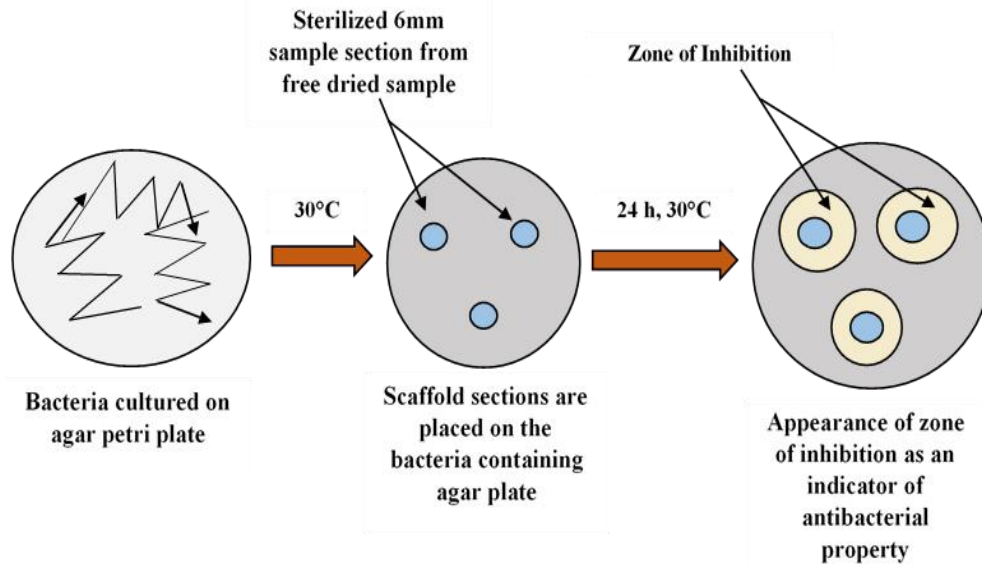


Figure 22. Agar Disc Diffusion method for antibacterial test. (Self-representation)

### 2.8.2 Cell biological study

The *in vitro* efficiency of the TE scaffolds was analyzed through *cell biological studies*. Different aspects for cellular studies are considered for establishment of cell biological efficiency of scaffolds. The cell biological analysis of *calcium reinforced BC based hydrogel scaffolds* was performed through the following studies:

#### 2.8.2. a Biocompatibility study

Assessment of bio-compatibility of a tissue engineering scaffold material is a complex procedure<sup>158</sup>. It involves different safety and pre-clinical evaluation. The biological assessment of medical devices is regulating by internationally recognized standards i.e. International Organization for Standardization (ISO) standard ISO-

10993-5. Cell cytotoxicity and viability is the most important consideration of biological assessment of the scaffold <sup>159</sup>.

*i. Cell culture*

Cells (Human fibroblast, Lep-3; Mouse bone explant cells, BEC; human osteosarcoma cells, Saos-2; Human mesenchymal stem cells, MSC) were used as model systems in our study. Cells were obtained from the Cell culture collection of the Institute of Experimental Morphology, Pathology and Anthropology with Museum—Bulgarian Academy of Sciences (IEMPAM-BAS). The cultures were grown in Dulbecco's Modified Eagle Medium (DMEM) supplemented with 10% fetal bovine serum, 100 U/mL penicillin and 100 µg/mL streptomycin. The cultures were kept in a humidified incubator (Thermo Scientific, HEPA Class 100, Waltham, MA, USA) at 37°C under 5% CO<sub>2</sub> in air. For routine passages, the cells were detached using a mixture of 0.05% trypsin and 0.02% EDTA. The cell cultures were passaged 2–3 times per week (1:2 to 1:3 split). The experiments were performed during the exponential phase of cell growth. During investigations performed the BEC cells were on their 44–50<sup>th</sup> passages.

*ii. Sample preparation*

Circular sections (6 mm in diameter) of the six freeze dried *calcium reinforced BC based hydrogel scaffolds* were taken for this study. Sections were placed in the 48-well cell culture plate, treated with 50 µL of 96% ethanol for 40 min after which the ethanol was removed and dried at 30–32°C to complete dryness. Then, the materials were sterilized under the exposure of UV radiation for 80–90 min.

*Indirect and direct experiments* were performed for evaluating the influence of the materials on cell viability and proliferation which finally indicated the biocompatibility of the scaffolds.

### *iii. Indirect experiments*

For cell viability/proliferation study, the cells (i.e., Lep-3, BEC, Saos-2, MSC) were seeded in 96-well flat-bottomed microplates at a specific concentration of ( $1 \times 10^4$  cells/well for Lep-3 and BEC;  $7.5 \times 10^3$  cells/well for Saos-2) in fresh DMEM medium with 10% FBS. At the 24<sup>th</sup> h, the culture medium from each well was removed and changed with 100  $\mu$ L DMEM containing hydrogel scaffolds extract (sample extracts, obtained after 1-, 3-, 5-and 7-day incubation periods).

The percent of viable cells was determined using MTT (*3-(4, 5-Dimethylthiazol-2-yl)-2,5-diphenyltetrazolium bromide*) test. The cells were incubated for 3 h with MTT solution (0.3 mg MTT in 10 mL DMEM) at 37°C under 5% CO<sub>2</sub> condition. The formed blue MTT formazan was extracted with a mixture of absolute ethanol and DMSO (1:1, v/v). The quantitative analysis was performed by absorbance measurements in an automated microplate reader (Tecan, Sunrise™, Grödig, Austria) at 540/620 nm.

### *iv. Direct experiment*

Each material was placed in bottom of a 48 well cell culture plate on the drop (20  $\mu$ L) of FBS for 30 min at 30–32°C in order to stick the sample to the surface of the well. Thereafter, 1 mL of DMEM (containing 10% FBS and antibiotics) was given to the wells (containing sterilized sample sections as well as empty wells that serve as controls).

The cells ( $5 \times 10^4$  cells/well, Lep-3, BEC, Saos-2) were seeded directly on the material sample placed on the bottom of a 48-well cell culture plate and incubated for 1, 3, 5, and 7 days in CO<sub>2</sub> incubator at 37°C. The number and viability of the cells were determined before seeding using an automated cell counter and the trypan blue dye exclusion technique (zero time). The cell viability was found to be >95% in all experiments performed. At the start of the experiment the cell numbers were

equal in all wells/ between all different samples, and they were cultured in equal conditions. Cells were grown in wells without materials, which served as controls. The effect of the materials on cell viability and proliferation was studied by MTT test. MTT concentration corresponded to the volume of the plate. Like those discussed in *indirect experiment*, the cells here were also incubated in MTT solution at 37°C under a 5% CO<sub>2</sub> condition. The quantitative analysis was performed following the extraction of blue colored formazan.

The data were presented as mean± standard error of the mean. Statistical differences between control and treated groups were assessed using one-way analysis of variance (ANOVA) followed by suitable post-hoc test by using GraphPad Prism version 5.00 (San Diego, CA, USA) for Windows and MS Office 2010 (Redmond, WA, USA).

#### 2.8.2.b DNA damage analysis

The presence of single and double stranded DNA damages within the cells induced by the effect of *calcium reinforced BC based hydrogel scaffolds* was assessed by single cell gel electrophoresis (Comet assay) at alkaline pH. Cells (Lep-3) were seeded in 6-well flat-bottomed microplates at a concentration of  $3 \times 10^5$  cells/well. At the 24<sup>th</sup> hour the culture medium was removed and changed with sample extract media (3-days modified media) and control media was also prepared. The cells were mixed with 1.4% of low-gelling agarose (Sigma Type II) and immediately spread onto microscopic slides pre-coated with 0.5% normal agarose. Then the cells were lysed for 1 h in a lysis solution (1 M NaCl, 50 mM EDTA pH 8, 30 mM NaOH, 0.1% N-lauroylsarcosine; pH 10). After 1-h incubation in the denaturing solution (30 mM NaOH, 10 mM EDTA; pH 12.6) for DNA unwinding, the slides were electrophoresed for 20 min at 0.46 V/cm in the same denaturing buffer. At the end of the electrophoresis, the slides were subsequently dehydrated for 5 min in 75% and

in 96% of ethanol. Comets were observed under Leitz epifluorescent microscope (Orthoplan, VARIO ORTHOMAT 2) using a 450–490 nm band-pass filter following staining of microgels with the fluorescent dye SYBR green I (Molecular Probes, Eugene, OR, USA). 1000 randomly chosen objects per each probe and treatment were taken for quantification. Two repetitions of the experiment were done and standard deviations were quantified. In all cases they were very small.

### *2.8.2.c Apoptosis/necrosis analysis*

The ability of the materials to induce cells death was evaluated by APOPTOSIS detection kit, (ANNEXINV—GFP-Certified Apoptosis/Necrosis detection kit, Enzo Life Sciences). Cells were spinned down at 400 g for 5 min at room temperature and carefully re-suspended in 1 mL cold 1×PBS (2.68mM KCl, 1.47mM KH<sub>2</sub>PO<sub>4</sub>, 1.37mM NaCl, 8mM Na<sub>2</sub>HPO<sub>4</sub>), pH 7. Spinning down follows at the same conditions and the pellet was re-suspended in 510 µL Dual Detection Reagent (500µL 1×binding buffer, 5µL Apoptosis Detection reagent/Annexin V-Enzo Gold; 5µL Necrosis Detection Reagent). Samples were incubated at room temperature for 10 min at dark and were analyzed via cytometry using 488 nm laser at FL 2 and FL 3 channels for apoptosis and necrosis detection respectively. Results were quantified with FlowJo software. Two repetitions of the experiment were done. Data quantitation included estimation of the percentage of cells undergoing apoptosis and necrosis and the ratio between these percentages in comparison to the control cells is given in PDU (procedure data units).

### *2.8.2. d Bone marker analysis*

The activity of alkaline phosphatase (ALP) was assessed in the 5 days modified cell culture medium with cells (Saos-2 and MSC cells). The cells were seeded in 6-well flat-bottomed microplates at a concentration of  $2 \times 10^4$  for Saos-2 cells/well to  $4 \times 10^4$  for MSC cells/well. Sample volume was adjusted with 80 µL/well with assay buffer.

Alkaline phosphatase (ALP) activity was evaluated by standard colorimetric kit as recommended by the manufacturer protocol. The data presented here as mean±error of the mean.

#### *2.8.2.e Cell-biomaterial interaction study*

The samples prepared as described in biocompatibility analysis. The cells ( $7 \times 10^5$  cells/well, Lep-3) were seeded directly on sample materials in a 48-well cell culture plate and left in an incubator (Thermo Scientific) at 37 °C, 5% CO<sub>2</sub>. After 7 days' incubation period, the culture medium was removed and the sample sections were washed with 4% glutaraldehyde for 1h followed by washing with double distilled water. The samples were then subjected to dry by filter system CORNING 431097 (0.22 μm) under low pressure for 2 h and were left for 2 days at 30–32 °C for complete drying. Finally, samples were prepared for SEM analysis by a standard procedure and observed under scanning electron microscope (JEOL JSM-5510, Tokyo, Japan) at an accelerating voltage of 10 kV.

### **Chapter 3. MOTIVATION OF THE DOCTORAL STUDY**

Different pathological and traumatic events lead to significant bone fracture situation<sup>1, 160</sup>. On the other hand, aging and bone related diseases also increase the probability of bone fracture<sup>161</sup>. Research indicated that about 75 million individuals have been troubled by osteoporosis in Europe, USA and Japan<sup>11</sup>. Study has shown that bone related diseases like osteoporosis causes two million bone fractures every year and this number will increase to three million by 2025<sup>162</sup>.

Treatment methods including bone-autografting and allografting have been used for so long. However, various limitations also exist for the successful utilization of these methods<sup>1</sup>. The autograph based approach involves the application of implant, which has obtained from the host body. In addition, the potential surgical risks like infection and inflammation, bleeding, hypersensitivity, and damage of donor tissue are also prominent<sup>1</sup>. Thus, a novel approach is important to solve this fracture related problem.

Tissue engineering is an emerging therapeutic field, where the regeneration of tissue can be achieved through application of bioactive scaffold. Application of polymeric hydrogel scaffolds can be a suitable approach<sup>2</sup>. The use of polymeric degradable biomaterials will not require a secondary surgical procedure for implant removal. Thus bone tissue engineering with polymeric biomaterial can become an exciting alternative therapeutic alternative<sup>163, 164</sup>.

Different biomaterial and scaffolds from metal to ceramic have been successfully used in tissue engineering application. However, they have also limitations. On the other hand, a number of studies have been conducted with polymeric hydrogels in bone tissue engineering from 2006 to 2020 (Figure. 23), however; there is a

prominent scarcity of a bone tissue engineering scaffold materials in the commercial market which has both, osteoconductive and osteoinductive property (**Table.2**).

Cellulose is considered as significant and naturally abundant biopolymer <sup>95</sup>. Bacterial cellulose has been extensively used in biomedical application. The advantage of BC over other polymers involves the fact that BC has significant controllable three dimensional fibrous network structures and notable biocompatibility <sup>3, 55</sup>. BC has a significant use as bone tissue engineering scaffold due to its remarkable similarity with bone extra cellular matrix and collagen <sup>110</sup>. BC based biomaterial and composite like BC/collagen, BC/chitosan has been already utilized also in wound dressing, development of vascular grafts and artificial blood vessel <sup>120</sup>. The BC based 3D hydrogel thus can be also utilized in BTR application.

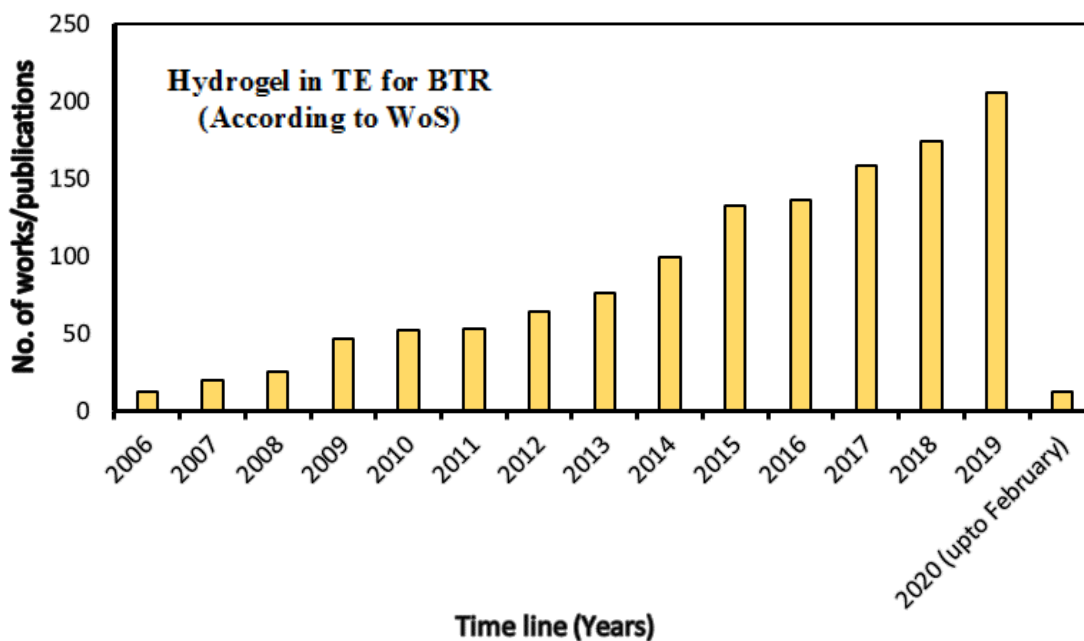


*Figure 23. Hydrogel application for BTR from 2006 to 2020 (According to Web of Science [WoS])*

The inorganic phase of bone predominantly consists of calcium <sup>2</sup>. Bone cells composed of different receptors and ion channels which can successfully receive



extracellular calcium that is also responsible for the growth of the cells <sup>1, 2</sup> (Figure.24). Studies demonstrated that incorporation of bioactive compounds within a bone tissue engineering scaffold has a significant role in increase of *osteoconductive* and *osteoinductive* property of the scaffold <sup>2</sup>. This doctoral study focuses the development of *calcium reinforced BC based hydrogel scaffolds*, which could provide “osteconduction” through its efficient scaffold structure and also “osteinduction” through providing osteogenic signal to the bone cells by calcium phosphate like hydroxyapatite (HA),  $\beta$  tri-calcium phosphate ( $\beta$ -TCP) and calcium carbonate ( $\text{CaCO}_3$ ) (Figure. 24). The novel polymeric calcium reinforced hydrogel scaffold contains the BC, PVP, PEG etc. as a polymeric component and calcium phosphate/calcium carbonate as bioactive filler agent. These scaffolds will mimic the animal extracellular matrix and will facilitate bone tissue regeneration <sup>165,166</sup>.

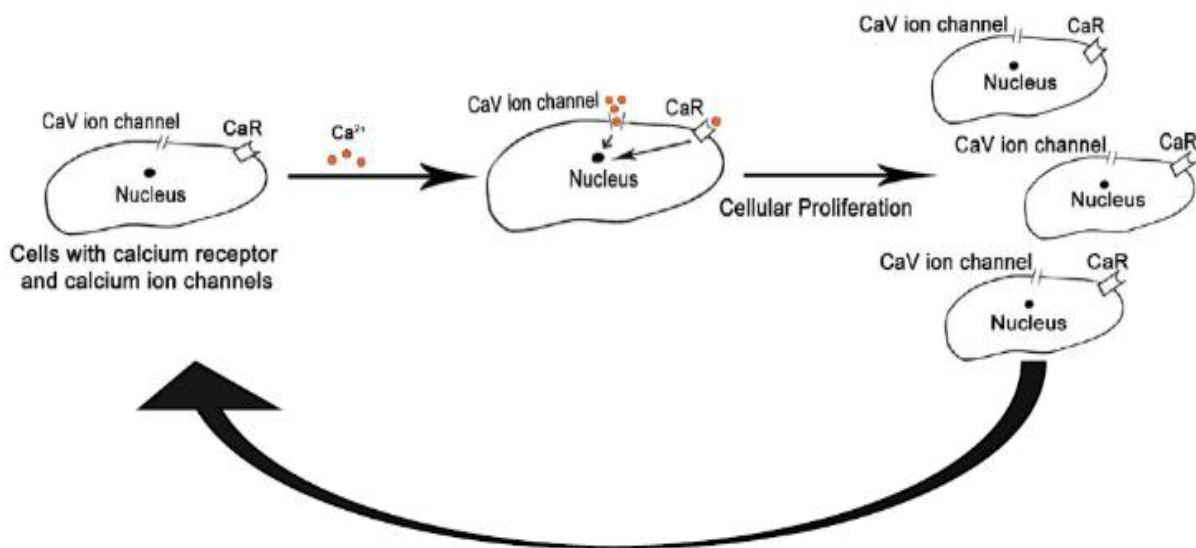


Figure 24. Outline of extracellular calcium stimulation for bone cell growth and development. Bone cells has extracellular calcium specific receptors (CaR) and voltage gated ion channels for calcium (Self-representation based on Aquino-Martínez et al., 2017 <sup>167</sup>).

## Chapter 4. AIM AND BRIEF SUMMARY OF THE THESIS

The major *aim* of this doctoral study is the *preparation and characterization of calcium reinforced BC based hydrogel scaffold for bone tissue regeneration application*. Hence, this doctoral thesis work is directed on the following aspects (as mentioned below).

- **Preparation of calcium reinforced BC based hydrogel scaffolds**
  - *Preparation of raw material, i.e. bacterial cellulose*  
BC, one of the key raw material is synthesized for the preparation of hydrogel scaffolds.
  - *Preparation of calcium reinforced polymeric hydrogel scaffolds*
    - *Calcium phosphate reinforced BC based hydrogel scaffolds*
    - *Calcium phosphate and calcium carbonate reinforced BC based hydrogel scaffolds.*
- **Evaluation of properties of the calcium reinforced BC based polymeric hydrogel scaffolds** on the basis of:
  - *Structural property*
    - Morphology (Surface/Cross section)
    - Physio-chemical property
    - Swelling
    - Porosity
    - Biodegradation
    - Thermal analysis
    - Mechanical property analysis
  - *Functional property*
    - Biological property analysis
      - *Antibacterial property analysis*
      - *Cell biological property analysis*
- **Selection of a suitable composition for polymeric hydrogel scaffold** on the basis of *its structural and functional* (biological activity) *properties* to recommend for its application for bone tissue regeneration.

The *brief summary* of this doctoral work which were also submitted/accepted, published and in preparation in the form of 7 articles are explained below:

*Article I* entitled “*Inorganic calcium filled bacterial cellulose based hydrogel scaffold: novel biomaterial for bone tissue regeneration*” emphasized the structure, physio-chemical characterization of *calcium reinforced BC based hydrogel scaffolds* (i.e. *calcium phosphate reinforced BC based hydrogel scaffolds* and *calcium phosphate and calcium carbonate reinforced BC based hydrogel scaffolds*). At first, the raw material, BC was synthesized in presence of basal synthetic Hestrin-Schramm (HS) nutritive medium (pH 7.0) using *Gluconacetobacter xylinus* CCM 3611<sup>T</sup> (syn. *Acetobacter xylinum*), incubated at 30°C for 15 days. Then the BC was treated in 0.5N NaOH solution and heated at 80°C for 2 hours for decontamination. Thereafter, a homogenous suspension of BC (particle size range: 159 nm -351.03 nm) from the obtained BC mat was prepared by grinding (10-12 mins) the BC mat in distilled water. The grinded BC suspension (50 mL BC suspension  $\cong$  0.5 g of BC) was then used to prepare BC based hydrogel. Additionally, synthetic polymers like PVP and/or CMC (used for biocompatibility), PEG (used for reducing the cytotoxic effect), Agar (used as a gelling agent), and Glycerin (used as a humectant) were also utilized to prepare BC-PVP and BC-CMC hydrogel matrix. Furthermore, *calcium reinforced BC based hydrogel scaffolds* were then prepared in the form of *calcium phosphate reinforced BC based hydrogel scaffolds* & *calcium phosphate and calcium carbonate reinforced BC based hydrogel scaffolds* (i.e. *in vitro* bio-mineralized scaffolds). Earlier research by other researchers reported that the ratio of  $\beta$ -TCP: HA= 20:80 was found significant for osteogenic growth of bone cells. Thus,  $\beta$ -TCP: HA= 20:80 was initially selected for this study. *Calcium phosphate reinforced BC based hydrogel scaffolds* (BC-PVP- $\beta$ -TCP/HA\_20:80 and BC-CMC- $\beta$ -TCP/HA\_20:80) were prepared by incorporating calcium phosphate [in the form of  $\beta$ -tri-calcium phosphate ( $\beta$ -TCP) and hydroxyapatite (HA) in the ratio of 20:80]

within the BC-PVP and BC-CMC hydrogel matrix. Thereafter, the *calcium phosphate reinforced BC based scaffolds* were *in vitro* bio-mineralized for the preparation of *calcium phosphate and calcium carbonate reinforced BC based hydrogel scaffolds* (BC-PVP- $\beta$ -TCP/HA-CaCO<sub>3</sub> and BC-CMC- $\beta$ -TCP/HA-CaCO<sub>3</sub>). BC-PVP and BC-CMC were kept as control set. Thereafter, the hydrogel scaffolds were characterized for BTR application. FTIR and TG analysis indicated the presence of BC and calcium phosphate and calcium carbonate within the hydrogel scaffolds. SEM study established the porous structures (50-200  $\mu$ m) within the scaffolds. Swelling study indicated significant swelling ability of *calcium phosphate reinforced BC based hydrogel scaffolds*. Compressive strength (0.24-0.60 MPa) of the *calcium reinforced BC based hydrogel scaffolds* were found similar like human trabecular bone. On the other hand, antibacterial study indicated that *calcium phosphate & calcium carbonate reinforced BC based hydrogel scaffold*, especially BC-CMC- $\beta$ -TCP/HA-CaCO<sub>3</sub> hydrogel scaffold has a faint antibacterial property only for *S. aureus*. Furthermore, notable human fibroblast (Lep-3) cell viability was also found. The results indicated that *calcium reinforced BC based hydrogel scaffolds* have the necessary characteristics to be utilized in bone regeneration application. These above mentioned observations and results were **reported and published** in “*International Journal of Polymeric Materials and Polymeric Biomaterials*” (2019), 68:1-3, 134-144. DOI: <https://doi.org/10.1080/00914037.2018.1525733> (Web of Science Indexed, Q2 [Polymer Science], J<sub>imp</sub>: 2.263)

**Article II** entitled “*Rheological Performance of Bacterial Cellulose based non-mineralized and mineralized hydrogel scaffolds*” focused the analysis of rheological/viscoelastic property of *calcium reinforced BC based hydrogel scaffolds*. Here non-mineralized hydrogel scaffolds referred to *calcium phosphate*

*reinforced BC based hydrogel scaffolds (BC-PVP- $\beta$ -TCP/HA\_20:80 and BC-CMC- $\beta$ -TCP/HA\_20:80) and mineralized hydrogel scaffolds referred to calcium phosphate and calcium carbonate reinforced in vitro bio-mineralized BC based hydrogel scaffolds (BC-PVP- $\beta$ -TCP/HA-CaCO<sub>3</sub> and BC-CMC- $\beta$ -TCP/HA-CaCO<sub>3</sub>). BC-PVP and BC-CMC were kept as control set. The viscoelastic property analysis indicated the mechanical strength of the hydrogel scaffolds in room temperature (28°C). It is observed that all the calcium reinforced BC based hydrogel scaffolds (BC-PVP- $\beta$ -TCP/HA\_20:80 and BC-CMC- $\beta$ -TCP/HA\_20:80, BC-PVP- $\beta$ -TCP/HA-CaCO<sub>3</sub> and BC-CMC- $\beta$ -TCP/HA-CaCO<sub>3</sub>) were significantly viscoelastic in nature. They maintained high elastic property (expressed in terms of storage modulus [G']) than viscous property (expressed in terms of loss modulus [G'']). These above-mentioned results were **reported and published** in “AIP Conference Proceedings related to Novel Trends in Rheology VII” (2017), 1843, 050008-1–050008-7. DOI: <https://doi.org/10.1063/1.4983000> (Web of Science Indexed; Book Chapter, ISBN: 978-0-7354-1513-3)*

**Article III** entitled “**Biocompatibility and Biological Efficiency of Inorganic Calcium Filled Bacterial Cellulose Based Hydrogel Scaffolds for Bone Bioengineering**” focused the study of biocompatibility and cell biological efficiency analysis of *calcium reinforced BC based hydrogel scaffolds* (ie. *calcium phosphate reinforce BC based hydrogel scaffold [BC-PVP- $\beta$ -TCP/HA\_20:80 and BC-CMC- $\beta$ -TCP/HA\_20:80] and calcium phosphate and calcium carbonate reinforced BC based hydrogel scaffolds [BC-PVP- $\beta$ -TCP/HA-CaCO<sub>3</sub> and BC-CMC- $\beta$ -TCP/HA-CaCO<sub>3</sub>]). BC-PVP and BC-CMC were also kept as control set. Earlier, the *Article I* and *Article II* indicated that *calcium reinforced BC based hydrogel scaffolds* has the necessary physiochemical and mechanical property to induce the cell growth for bone tissue regeneration. To analyse the effect of hydrogel scaffolds on the cellular*

level, the biocompatibility study was performed with human diploid fibroblast, Lep-3 (from 3 month's old human embryo) cell and mouse bone explant cells (BEC; from 2-3 months old ICR mice). The cell proliferation was found notable for 3-7 days of incubation with *calcium reinforced BC based hydrogel scaffolds*. In addition, the fibroblast (Lep-3) apoptosis was found insignificant for *BC-PVP- $\beta$ -TCP/HA\_20:80* hydrogel scaffold. Additionally, cell-biomaterial interaction study through SEM analysis demonstrated the notable growth of Lep-3 cell on to the surface of *BC-PVP- $\beta$ -TCP/HA\_20:80* hydrogel scaffold. Thus, according to the research observation, the "***BC-PVP- $\beta$ -TCP/HA***" hydrogel scaffold was found a better combination among the *scaffolds* that can be further analysed for bone tissue regeneration application. The above-mentioned observations were ***reported and published*** in "*International Journal of Molecular Sciences*" (2018), 19 (12):3980. DOI: 10.3390/ijms19123980 (Web of Science Indexed, Q2 [Multidisciplinary, Chemistry, Biochemistry & Molecular Biology], J<sub>imp</sub>: 4.183)

***Article IV*** entitled "***Swelling and rheological study of calcium phosphate filled bacterial cellulose based hydrogel scaffold***" involved the analysis of swelling and thereby study of viscoelastic property of the swelled *calcium reinforced BC based hydrogel scaffolds*. Earlier, *Article III* demonstrated that the "***BC-PVP- $\beta$ -TCP/HA***" hydrogel scaffold has the necessary physiochemical and cell biological characteristics to be utilized bone regeneration application. Thus, in this work, keeping the *BC-PVP- $\beta$ -TCP/HA\_20:80* as a reference sample, different "***BC-PVP- $\beta$ -TCP/HA***" scaffolds were developed and analysed on the basis of swelling and viscoelasticity. The  $\beta$ -TCP and HA were incorporated in the ratio of 10:90, 20:80, 40:60, 50:50, 60:40 into the scaffold matrix to achieve the *calcium phosphate reinforced BC based hydrogel scaffolds* and were termed as, "***BC-PVP- $\beta$ -TCP/HA\_10:90***" (for  $\beta$ -TCP: HA= 10:90), ***BC-PVP- $\beta$ -TCP/HA\_20:80***" (for  $\beta$ -TCP:

HA= 20:80), BC-PVP- $\beta$ -TCP/HA\_40:60” (for  $\beta$ -TCP: HA= 40:60), BC-PVP- $\beta$ -TCP/HA\_50:50” (for  $\beta$ -TCP: HA= 50:50), BC-PVP- $\beta$ -TCP/HA\_60:40” (for  $\beta$ -TCP: HA= 60:40). *BC-PVP- $\beta$ -TCP/HA\_20:80* was kept as reference sample. BC-PVP scaffold was also used as a control. Analyses of swelling and viscoelastic property is important in respect to the utilization of the *calcium phosphate reinforced BC based hydrogel scaffolds* in bone tissue regeneration application. Thus, *the developed calcium phosphate reinforced hydrogel scaffolds (i.e. BC-PVP- $\beta$ -TCP/HA\_10:90, BC-PVP- $\beta$ -TCP/HA\_20:80, BC-PVP- $\beta$ -TCP/HA\_40:60, BC-PVP- $\beta$ -TCP/HA\_50:50, BC-PVP- $\beta$ -TCP/HA\_60:40)* were first analyzed on the basis of swelling at physiological temperature (37°C) in physiological saline solution (Ringer solution; pH. 7.4), then the viscoelastic property of the scaffolds was analyzed both at room temperature (28°C) and physiological temperature (37°C) regime. Furthermore, the morphological characterization of the hydrogel scaffolds at “before swelling” and “after swelling” was also analyzed. All the BC based hydrogel scaffolds have shown notable viscoelastic property both at 28°C and 37°C. However, among the all *calcium phosphate reinforced BC based hydrogel scaffolds*, the *BC-PVP- $\beta$ -TCP/HA\_20:80* and *BC-PVP- $\beta$ -TCP/HA\_50:50* hydrogel scaffolds were found significant in the context of swelling and rheological property. The above-mentioned results were **reported and published** in “*Journal of Applied Polymer Sciences*” (2020), 137, 48522. DOI: 10.1002/app.48522. [Web of Science Indexed, Q2 [Polymer Science], J<sub>imp</sub>: 2.188).

**Article V** entitled “**Viscoelastic behavior of Calcium Phosphate Packed Bacterial Cellulose -Polyvinylpyrrolidone based Hydrogel Scaffolds at Human Fever Temperature**” emphasized the analysis of swelling and viscoelastic property of *calcium phosphate reinforced BC based hydrogel scaffolds* at altered human physiological temperature i.e. human fever temperature (39°C). Earlier, **Article IV**

demonstrated and reported that all *calcium phosphate reinforced BC based hydrogel scaffolds* showed significant swelling and rheological behavior at both room temperature (28°C) and human physiological temperature (37°C). Especially, *BC-PVP- $\beta$ -TCP/HA\_20:80*, *BC-PVP- $\beta$ -TCP/HA\_50:50* and also *BC-PVP- $\beta$ -TCP/HA\_40:60* hydrogel scaffolds were showing notable swelling and rheological property among all *calcium phosphate reinforced BC based hydrogel scaffolds*. Thus, this work focused the analysis of swelling and viscoelastic property at human fever temperature (39°C) with *BC-PVP- $\beta$ -TCP/HA\_20:80*, *BC-PVP- $\beta$ -TCP/HA\_40:60* and *BC-PVP- $\beta$ -TCP/HA\_50:50* hydrogel scaffolds. It has been observed that all the three *calcium phosphate reinforced BC based hydrogel scaffolds* were showing significant swelling ability and viscoelastic behavior at human fever temperature (39°C). The above-mentioned result was **reported and accepted for publication** in “*AIP conference proceedings related to PPS Europe-Africa 2019 Regional Conference*” (2020) (Will be indexed in Web of Science, Book Chapter).

**Article VI** entitled “*Calcium Phosphate Incorporated Bacterial Cellulose-Polyvinylpyrrolidone Based Hydrogel Scaffold: Structural Property and Cell Viability Study for Bone Regeneration Application*” emphasized the physical property analysis like void fraction, porosity, study of biodegradability and primary cell viability property. Earlier, *Article IV* and *Article V* were reported the analysis of the important implant properties like swelling and viscoelastic behavior of *calcium phosphate reinforced BC based hydrogel scaffolds*. It has been observed at human physiological temperature regime (37°C), *BC-PVP- $\beta$ -TCP/HA\_20:80*, and *BC-PVP- $\beta$ -TCP/HA\_50:50* hydrogel scaffolds have indicated notable swelling and viscoelastic behavior. Furthermore, at human fever temperature (39°C), *BC-PVP- $\beta$ -TCP/HA\_20:80*, *BC-PVP- $\beta$ -TCP/HA\_40:60* and *BC-PVP- $\beta$ -TCP/HA\_50:50*



hydrogel scaffolds also have demonstrated notable swelling and rheological property. Hence, in this work, the physical property and primary cell viability behavior study were performed with *BC-PVP- $\beta$ -TCP/HA\_20:80*, *BC-PVP- $\beta$ -TCP/HA\_40:60* and *BC-PVP- $\beta$ -TCP/HA\_50:50* hydrogel scaffolds. BC-PVP was kept as control set. The porosity and void fraction of *BC-PVP- $\beta$ -TCP/HA\_50:50* hydrogel scaffold was found higher than other two calcium reinforced BC based hydrogel scaffolds. Additionally, *BC-PVP- $\beta$ -TCP/HA\_50:50* hydrogel scaffold has the highest degree degradation than *BC-PVP- $\beta$ -TCP/HA\_20:80* and *BC-PVP- $\beta$ -TCP/HA\_40:60* hydrogel scaffolds. On the other hand, compressive strengths of all the *calcium reinforced hydrogel scaffolds* were found comparable with the human cancellous bone. Furthermore, Saos-2 cell viability was found significant for all the *calcium phosphate reinforced BC based hydrogels*. Thus, in this work, this was suggested that the *BC-PVP- $\beta$ -TCP/HA\_20:80*, *BC-PVP- $\beta$ -TCP/HA\_40:60* and *BC-PVP- $\beta$ -TCP/HA\_50:50* hydrogel scaffolds can be further evaluated on the basis of detailed *in vitro* efficiency in the context of bone tissue regeneration application. The above-mentioned observations were **reported and published** in “*Polymers*” (2019), 11, 1821. DOI:10.3390/polym11111821 (Web of Science Indexed, Q1 [Polymer Science],  $J_{imp}$ : 3.164).

**Article VII** entitled “*In vitro efficiency of calcium phosphate incorporated bacterial cellulose based hydrogel scaffold for bone regeneration*” emphasizes the *in vitro* efficiency of *calcium reinforced BC based hydrogel scaffolds*. Earlier in **Article VI**, according to the physical, biodegradable, mechanical and primary cell viability property of three *calcium phosphate reinforced BC based hydrogel scaffolds*: *BC-PVP- $\beta$ -TCP/HA\_20:80*, *BC-PVP- $\beta$ -TCP/HA\_40:60* and *BC-PVP- $\beta$ -TCP/HA\_50:50* were suggested for the further analysis in the context of biological applicability for bone regeneration application. Thus, this work focuses in-depth

analysis of *in vitro* cell biological efficiency of the *BC-PVP- $\beta$ -TCP/HA\_20:80*, *BC-PVP- $\beta$ -TCP/HA\_40:60* and *BC-PVP- $\beta$ -TCP/HA\_50:50 hydrogel scaffolds*. BC-PVP scaffold was kept as control set. The *in vitro* efficiency was studied on the basis of comparative analysis of the biocompatibility (through MTS analysis) with human osteosarcoma cell line, Saos-2 and human adipose derived mesenchymal stem cells (MSC). Additionally, ki-67 protein expression (marker for cell proliferation) analysis was performed. Furthermore, bone marker study (Alkaline phosphatase expression) was also analyzed. Finally, cell-biomaterial interaction was analyzed by SEM study. Albeit, notable biocompatibility was observed with all the hydrogel scaffolds however, a significant MSC biocompatibility was found for *BC-PVP-  $\beta$ -TCP/HA\_20:80* and *BC-PVP-  $\beta$ -TCP/HA\_50:50*. Both Saos-2 and MSC cells also expressed ki-67 protein for cell proliferation. Additionally, it was observed that both the cell line expressed notable alkaline phosphatase (bone marker) in presence of the *BC-PVP-  $\beta$ -TCP/HA\_20:80* and *BC-PVP-  $\beta$ -TCP/HA\_50:50* scaffolds extracts. Finally, the SEM study indicated a significant growth of Saos-2 cells on to the surface of the *calcium phosphate reinforced BC based hydrogel scaffolds: BC-PVP-  $\beta$ -TCP/HA\_20:80* and *BC-PVP-  $\beta$ -TCP/HA\_50:50*. Thus, these results indicated the future possibility of *BC-PVP-  $\beta$ -TCP/HA\_20:80* and *BC-PVP-  $\beta$ -TCP/HA\_50:50* hydrogel scaffolds to be utilized in bone tissue engineering application. These scaffolds were recommended for further analysis on the basis of *in vivo* evaluation for soft bone tissue engineering. The ***above-mentioned results are being prepared and will be submitted*** in a Web of Science indexed impact factor journal.

## Chapter 5. CONCLUDING REMARKS

### 5.1 Conclusion

This doctoral work focuses the *development and characterization of a novel calcium reinforced BC based hydrogel scaffold suitable for BTR application*. The hydrogel scaffolds were developed with natural polymer, BC. Additionally, other synthetic polymers: PVP, CMC, PEG etc. were also utilized. *Calcium reinforced BC based hydrogel scaffolds* were prepared in the form of *calcium phosphate reinforced BC based hydrogel scaffolds (BC-PVP- $\beta$ -TCP/HA and BC-CMC-  $\beta$ -TCP/HA)* and *calcium phosphate and calcium carbonate reinforced BC based hydrogel scaffolds (BC-PVP- $\beta$ -TCP/HA\_ CaCO<sub>3</sub> and BC-CMC-  $\beta$ -TCP/HA\_ CaCO<sub>3</sub>)*. The calcium phosphate was initially given in the form of  $\beta$ -TCP and HA in the ratio of 20:80. Then the *calcium phosphate reinforced BC based hydrogel scaffolds* were *in vitro* bio-mineralized to develop *calcium phosphate and calcium carbonate reinforced BC based hydrogel scaffolds*. They were then characterized on the basis of structural (i.e. *physiochemical property, thermal, optical and morphological, degradation, mechanical property*) and functional properties (*antibacterial property and in vitro efficiency of bone specific cell lines*).

The **structural property** of calcium reinforced BC based hydrogel scaffolds was analyzed on the basis of *physiochemical property, thermal, optical and morphological, degradation, mechanical behavior*. Study indicated that the swelling ability and porosity of *calcium phosphate reinforced BC based hydrogel scaffolds (BC-PVP- $\beta$ -TCP/HA\_20:80 and BC-CMC- $\beta$ -TCP/HA\_20:80)* were significant and higher than *calcium phosphate and calcium carbonate reinforced BC based hydrogel scaffolds (BC-PVP- $\beta$ -TCP/HA\_ CaCO<sub>3</sub> and BC-PVP- $\beta$ -TCP/HA\_ CaCO<sub>3</sub>)*. Moreover, among *calcium phosphate reinforced hydrogel scaffolds*, the swelling

property was found notable for *BC-PVP- $\beta$ -TCP/HA\_20:80*, and *BC-PVP- $\beta$ -TCP/HA\_50:50* scaffolds. On the other hand, the FTIR and TGA studies indicated the presence of all of the necessary ingredients within the hydrogel scaffolds. The biodegradation of the *calcium phosphate reinforced hydrogel scaffolds* was also analyzed. Albeit, all the hydrogels were found hydrolytically degradable; however, *BC-PVP- $\beta$ -TCP/HA\_50:50* scaffold has shown notable hydrolytic degradation. On the other hand, all the hydrogel scaffolds were found to be viscoelastic in nature at room temperature (28°C); however, the viscoelastic property of *BC-PVP- $\beta$ -TCP/HA\_20:80* and *BC-PVP- $\beta$ -TCP/HA\_50:50* scaffolds was notable at human physiological temperature (37°C) and human fever temperature (39°C). Additionally, the mechanical strength (i.e. compressive strength) of all *calcium reinforced BC based hydrogel scaffolds* were found similar with the human cancellous bone.

On the other hand, the **functional properties** of the *calcium reinforced BC based hydrogel scaffolds* were analyzed majorly on the basis of cell biological efficiency analysis. Antibacterial property of the hydrogel scaffolds was also analyzed with *Staphylococcus aureus* (*S. aureus* CCM<sup>4516</sup>) [gram +ve bacteria] and *Escherichia coli* (*E. coli* CCM<sup>4517</sup>) (Gram – ve bacteria). No significant antibacterial property was found. However, a faint antibacterial efficiency was only for *BC-CMC- $\beta$ -TCP/HA\_CaCO<sub>3</sub>* with *S. aureus*. The *cell biological efficiency* was analyzed with *bone specific cells* with different cell lines like human fibroblast (Lep-3) cells, mouse bone explant cell line (BEC), human osteosarcoma cell line (Saos-2) and human mesenchymal stem cells (MSC); that established the biocompatibility of the hydrogel scaffolds. Albeit, all the *calcium phosphate reinforced BC based hydrogel scaffolds* and *calcium phosphate and calcium carbonate BC based hydrogel scaffolds* shown notable biocompatibility with human fibroblast (Lep-3) and bone

explant cells (BEC); however, it was also observed that biocompatibility was significant for “*BC-PVP- $\beta$ -TCP/HA\_20:80*” hydrogel scaffold. Furthermore, the cellular apoptosis was also notably less for the above-mentioned scaffold. Thus, the “*BC-PVP- $\beta$ -TCP/HA*” hydrogel scaffold was selected for further analysis and different “*BC-PVP- $\beta$ -TCP/HA*” hydrogel scaffolds were prepared by applying different  $\beta$ -TCP and HA concentration ratios (w/w): *BC-PVP- $\beta$ -TCP/HA\_10:90*, *BC-PVP- $\beta$ -TCP/HA\_20:80*, *BC-PVP- $\beta$ -TCP/HA\_40:60*, *BC-PVP- $\beta$ -TCP/HA\_50:50*, *BC-PVP- $\beta$ -TCP/HA\_60:40*. On the basis of structural, physiochemical, mechanical/viscoelastic properties of the above-mentioned scaffolds, the *in vitro* efficiency was analyzed with *BC-PVP- $\beta$ -TCP/HA\_20:80*, *BC-PVP- $\beta$ -TCP/HA\_40:60*, *BC-PVP- $\beta$ -TCP/HA\_50:50* hydrogel scaffolds. Finally, the cell viability and biocompatibility of human osteoblast like cell line Saos-2 and human MSC confirmed the efficiency of the *BC-PVP- $\beta$ -TCP/HA\_20:80*, *BC-PVP- $\beta$ -TCP/HA\_50:50* hydrogel scaffolds. Additionally, cell biomaterial interaction and bone marker expression were also found significant for the *BC-PVP- $\beta$ -TCP/HA\_20:80*, *BC-PVP- $\beta$ -TCP/HA\_50:50* hydrogel scaffolds.

Hence, on the basis of above observations, the *calcium phosphate reinforced BC based hydrogel scaffolds: **BC-PVP- $\beta$ -TCP/HA\_20:80** and **BC-PVP- $\beta$ -TCP/HA\_50:50*** were further recommended for the *in vivo* analysis and application in BTR.

## 5.2 Contribution of the doctoral work to society

In the present scenario, bone fracture caused by bone related disorders is a serious problem of the society. This doctoral work focuses the preparation and characterization of novel *calcium reinforced polymeric hydrogel scaffold* that can be utilized for bone tissue regeneration application.

Different combinations of polymeric components have been utilized to develop hydrogel scaffolds which can be utilized as bone implant. However, a very less number of bone implant is currently functional in the commercial market, which have both osteoconductive and osteoinductive property. This work focuses the preparation of hydrogel scaffold with osteoconductive and osteoinductive property. The hydrogel scaffolds were prepared with biopolymer, *BC*. Additionally, the bioactivity of the *BC* based hydrogel scaffold has been enhanced by reinforcing the scaffold with the incorporation of calcium mineral (calcium phosphate and/or calcium carbonate). Thus a bioactive biocompatible *calcium reinforced BC based hydrogel scaffold* is developed, which is especially prepared for bone tissue engineering and regeneration application.

This study will elaborate the use of natural polymer based *calcium reinforced polymeric hydrogel scaffold* in bone tissue engineering application and can provide opportunity to the next generation scientific researchers to develop further modified and extremely specific polymeric hydrogel scaffolds intended for bone tissue regeneration application.

### 5.3 Future plan

The goal of this doctoral work is the *development and characterization of a novel calcium reinforced BC based hydrogel scaffold suitable for BTR application*. However, the following studies should be performed before the final application of the scaffolds.

- Analysis of mechanical property linked to degradation of the scaffolds to understand the change in mechanical strength with degradation phenomenon.
- Gene and mRNA expression analysis to understand the genetic response especially for bone regeneration, induced/stimulated by these hydrogel scaffolds.
- Finally, *in vivo* analysis with different animal models is required.

### REFERENCES

1. IAQUINTA, Maria Rosa, Elisa MAZZONI, Marco MANFRINI, Antonio D'AGOSTINO, Lorenzo TREVISIOL, Riccardo NOCINI, R., Leonardo TROMBELLI, Giovanni BARBANTI-BRODANO, Fernanda MARTINI, Mauro TOGNON. Innovative Biomaterials for Bone Regrowth, *International Journal of Molecular Sciences*. 2019, vol. 20, no. 3, pp. 618. ISSN 1422-0067.
2. CHOCHOLATA, Petra, Vlastimil KULDA, Vaclav BABUSKA. Fabrication of Scaffolds for Bone-Tissue Regeneration, *Materials*. 2019, vol. 12, no. 4, pp. 568. ISSN 1996-1944.
3. BASU, Probal, Nabanita SAHA, Radostina ALEXANDROVA, Boika ANDONOV-LILOVA, Milena GEORGIEVA, George MILOSHEV, Petr SAHA. Biocompatibility and Biological Efficiency of Inorganic Calcium Filled Bacterial Cellulose Based Hydrogel Scaffolds for Bone Bioengineering, *International Journal of Molecular Sciences*. 2018, vol. 19, no.12, pp. 3980. ISSN 1422-0067.

4. BUENZLI Pascal and Natalie SIMS. Quantifying the osteocyte network in the human skeleton, *Bone*. 2015, vol. 75, pp. 144-150. ISSN: 8756-3282.
5. WOLDE-SEMAIT, Henock and KOMLOS, Daniel. *Vertebral Compression Fractures in Osteoporotic and Pathologic Bone*. Springer Nature, Switzerland, 2020, pp. 1-8. Chapter 1. Normal Bone Physiology. ISBN 978-3-030-33860-2.
6. REY C, C COMBES, C DROUET, MJ GLIMCHER. Bone mineral: update on chemical composition and structure, *Osteoporosis International*. 2009, vol. 20, no. 6, pp. 1013-1021. ISSN: 0937-941X.
7. EI SAYED Suzan, Trevor A. NEZWEK, Matthew VARACALLO. Physiology, Bone. *StarPearls Publishing, NCBI* [online] © 2019 [cit. 21.07.2019] Available from: <https://www.ncbi.nlm.nih.gov/books/NBK441968/>
8. CLARKE Bart. Normal Bone Anatomy and Physiology, *Clinical Journal of American Society of Nephrology*. 2008, vol. 3, pp. S131-S139. ISSN: 1555-9041.
9. AI-AQI Z S, Adel AIaGI, Dana GRAVES, Louis GERSTENFELD, Thomas EINHORN. Molecular Mechanisms Controlling Bone Formation during Fracture Healing and Distraction Osteogenesis, *Journal of Dental Research*. 2008, vol. 87, 107-118. ISSN: 0022-0345.
10. LANGER Robert and Joseph VACANTI. Tissue Engineering, *Science*. 1993, vol. 260, no. 5110, pp. 920-926. ISSN: 0036-8075.
11. IOF: *International Osteoporosis Foundation* [online]. © 2017 [viewed 30.08.2017]. Available from: <https://www.iofbonehealth.org/facts-statistics>
12. NEJADDEHBASHI Fereshteh, Mahmoud HASHEMITABAR, Vahid BAYATI, Eskandar MOGHIMIPOUR, Jabrael MOVAFFAGH, Mahmoud ORAZIZADEH, Mohammadreza ABBASPOUR. Incorporation of silver sulfadiazine into an electrospun composite of polycaprolactone as an antibacterial scaffold for wound healing in rats, *Cell Journal*, vol. 21, no. 4, pp. 379-390. ISSN: 2228-5806.
13. FAROKHI Maryam, Farinaz Jonidi SHARIATZADEH, Atefeh SOLOUK & Hamid MIRZADEH (2019): Alginate Based Scaffolds for Cartilage Tissue Engineering: A Review, *International Journal of Polymeric Materials and Polymeric Biomaterials*, vol. 69, no. 4, pp. 230-247. DOI: 10.1080/00914037.2018.1562924 ISSN: 0091-4037.
14. ROBERTS, Timothy and Andrew ROSENBAUM. Bone grafts, bone substitutes and orthobiologics: The bridge between basic science and clinical advancements in fracture healing, *Organogenesis*. 2012, vol. 8, pp. 114-124. ISSN: 1547-6278



15. KHAN Safdar, Frank CAMMISA, Harvinder SANDHU, Ashish DIWAN, Federico GIRARDI, Joseph LANE. The biology of bone grafting, *Journal of American Academic Orthopaedic Surgeons*. 2005, vol.13, pp. 77-86. ISSN: 1067-151X.
16. WANG Wenhao and Kelvin W.K. YEUNG. Bone grafts and biomaterials substitutes for bone defect repair: A review, *Bioactive Materials*. 2017, vol. 2, pp. 224-247. ISSN: 2452-199X.
17. SALGADO António, Olga P. COUTINHO, Rui L. REIS. Bone Tissue Engineering: State of the Art and Future Trends, *Macromolecular Bioscience*. 2004, vol. 4, pp. 743-765. ISSN: 1616-5195.
18. JAN, MARIA A. Woodruff, Devakara R. EPARI, Roland STECK, Vaida GLATT, Ian C. DICKINSON, Peter CHOONG, Michael SCHUETZ, Dietmar W. HUTMACHER. Bone Regeneration Based on Tissue Engineering Conceptions – A 21st Century Perspective, *Bone Research*. 2013, vol. 3, pp. 216-248. ISSN: 2095-6231.
19. NANDI Samit Kumar, S ROY, Prasenjit MUKHERJEE, Biswanath KUNDU. Orthopaedic application of bone grafts & graft substitutes: A review. *Indian Journal of Medical Research*. 2010, vol. 132, pp. 15-30. ISSN: 0971-5916.
20. Biomatlante solutions [online] © 2019 [cit. 2019-07-26], Available from: <https://biomatlante.com/en/products/orthopaedics/mbcp-synthetic-bone-graft-substitute>
21. KYERON ® [online] © 2019 [cit. 2019-07-25], Available from: [http://www.kyeron.com/HATCPGRANULES\\_en.html](http://www.kyeron.com/HATCPGRANULES_en.html)
22. Graftys [online] © 2016 [cit. 2019-07-28], Available from: <https://www.graftys.com/injectable-ceramic-products/>
23. Bio Sport Project [online] © 2015 [cit. 2019-07-2018], Available from: Products on the market/ in development : Autologous Chondrocyte Implantation (ACI) and Cartilage Allografts, 2015, Also available from <http://www.biosportproject.org.uk/technologies/aci/aci-products>
24. Summary of typical bone-graft substitutes that are commercially available – 2010, Available in: <https://www.aatb.org/sites/default/files/BoneGraftSubstituteTable2010.pdf>
25. MATHEW Ansuja, AUGUSTINE Robin, KALARIKAL Nandakumar, THOMAS Sabu. *Tissue engineering: principles, recent trends and the future*. Apple Academic Press, USA, 2016, pp. 31-82. Chapter 2. Nanomedicine and

- Tissue Engineering: State of the Art and Recent Trends. ISBN 978-1-771-88118-0.
26. KARGOZAR Saeid, Masoud MOZAFARI, Sepideh HAMZEHLOU, Peiman Brouki MILAN, Hae Won KIM, Francesco BAINO. Bone Tissue Engineering Using Human Cells: A Comprehensive Review on Recent Trends, Current Prospects, and Recommendations, *Applied Sciences*. 2019, vol. 9, no. 1, pp. 174. ISSN: 2076-3417.
  27. VASITA Rajesh and Dharendra S. KATTI. Nanofibers and their applications in tissue engineering, *International Journal of Nanomedicine*, 2006, vol. 1, no. 1, pp. 15-30. ISSN: 1176-9114.
  28. VARGHESE Shyni and Jennifer H. ELISSEEFF. *Hydrogels for Musculoskeletal Tissue Engineering*. Springer, Berlin, Heidelberg, 2006, pp. 95-144. Polymers for Regenerative Medicine. ISBN 978-3-540-33353-1.
  29. ROSETI Livia, Valentina PARISI, Mauro PETRETTA, Carola CAVALLO, Giovanna DESANDO, Isabella BARTOLOTTI, Brunella GRIGOLO. Scaffolds for Bone Tissue Engineering: State of the art and new perspectives, *Materials Science and Engineering C*. 2017, vol. 78, pp. 1246-1262. ISSN: 0928-4931.
  30. HERMAN AR. The history of skin grafts. *Journal of Drugs in Dermatology*. 2002, vol. 1, pp. 298–301. ISSN: 1545-9616.
  31. CHARDACK William, Dewane BRUESKE, Anthony P. SANTOMAURO, George FAZEKAS. Experimental Studies on Synthetic Substitutes for Skin and Their Use in the Treatment of Burns, *Annals of Surgery*. 1962, vol. 155, no. 1, pp. 127-139. ISSN: 1528-1140
  32. VIOLA Jessica, Bhavya LAL, Oren GRAD. The emergence of tissue engineering as a research field. [online] © 2003, Available at: [http://www.nsf.gov/pubs/2004/nsf0450/exec\\_summ.pdf](http://www.nsf.gov/pubs/2004/nsf0450/exec_summ.pdf)
  33. LANZA Robert, Robert LANGER, Joseph VACANTI. Principles of Tissue Engineering 3rd Edition, Academic press, 2007, pp. 1-1307. ISBN 978-0123983589
  34. SHIN Heungsoo, Seongbong JO, Antonios G. MIKOS. Biomimetic materials for tissue engineering, *Biomaterials*. 2003, vol. 24, no. 24, pp. 4353-4364. ISSN: 0142-9612.
  35. BERTHIAUME Francois, Timothy J. MAGUIRE, Martin L. YARMUSH. Tissue engineering and regenerative medicine: history, progress, and challenges,

- Annual Review of *Chemical and Biomolecular Engineering*, 2011, vol. 2, pp. 403-30. ISSN: 1947-5438.
36. PETERSEN Thomas H, Elizabeth CALLE, Liping ZHAO, Eun Jung LEE, Liqiong GUI, MichaSam B. RAREDON, Kseniya GAVRILOV, Tai YI, Zhen W. ZHUANG, Christopher BREUER, Erica HERZOG, Laura E. NIKLASON. Tissue-engineered lungs for in vivo implantation, *Science*. 2010, vol. 329, no. 5991, pp. 538-541. ISSN: 0036-8075.
  37. SUKEGAWA Atsusi, Iwasaki NORIMASA, Kasahara YASUHIKO, Onodera TOMOHIRO, Igarashi TATSUYA, Minami AKIO. Repair of rabbit osteochondral defects by an acellular technique with an ultra-purified alginate gel containing stromal cell-derived factor-1, *Tissue Engineering Part A*. 2012, vol. 18, no. 9-10, pp. 934-945. ISSN: 1937-3341
  38. TODHUNTER Michael E, Noel Y JEE, Alex J HUGHES, Maxwell C COYLE, Alec CERCHIARI, Justin FARLOW, James C GARBE, Mark A LABARGE, Tejal A DESAI, Zev J GARTNER. Programmed synthesis of three-dimensional tissues, *Nature Methods*, 2015, vol. 12, pp. 975-981. ISSN: 1548-7105.
  39. SCHLOSS, Ashley C, Danielle M. WILLIAMS, Lynne J. REGAN. *Protein-Based Hydrogels for Tissue Engineering*, Springer, Cham, 2016, vol., 940, pp. 167-177. Protein-based Engineered Nanostructures. ISBN 978-3-319-39194-6.
  40. KHADEMHOSEINI Ali and Robert LANGER. A decade of progress in tissue engineering, *Nature Protocols*, 2016, vol. 11, no. 10, pp. 1775-1781. ISSN: 1750-2799.
  41. LIU Mei, Xin ZENG, Chao MA, Huan YI, Zeeshan ALI, Xianbo MOU, Song LI, Yan DENG, Nongyue HE. Injectable hydrogels for cartilage and bone tissue engineering, *Bone research*, 2017, vol.5, pp.17014. ISSN: 2095-6231
  42. CADDEO Silvia, Monica BOFFITO, Susanna SARTORI. Tissue Engineering Approaches in the Design of Healthy and Pathological In Vitro Tissue Models, *Frontiers in Bioengineering and Biotechnology*, vol. 5, no. 40, pp. 1-22. ISSN: 2296-4185.
  43. STRATAKIS Emmanuel. Novel Biomaterials for Tissue Engineering 2018, *International Journal of Molecular Sciences*. 2018, vol. 19, no. 3960, pp. 1-4. ISSN: 1422-0067
  44. BACAKOVA Lucie, Julia PAJOROVA, Marketa BACAKOVA, Anne SKOGBERG, Pasi KALLIO, Katerina KOLAROVA, Vaclav SVORCIK.

- Versatile Application of Nanocellulose: From Industry to Skin Tissue Engineering and Wound Healing, *Nanomaterials*. 2019, vol. 9, no. 164, pp. 2-39. ISSN: 2079-4991.
45. LIU Yannan, Juan GU, Daidi FAN. Fabrication of High-Strength and Porous Hybrid Scaffolds Based on Nano-Hydroxyapatite and Human-Like Collagen for Bone Tissue Regeneration, *Polymers*. 2020, vol 12, no.1, pp.61. ISSN 2073-4360.
46. MARTA Peña Fernández, Cameron BLACK, Jon DAWSON, David GIBBS, Janos KANCZLER, Richard OREFFO, Gianluca TOZZI. Full-Field Strain Analysis of Regenerated Bone Tissue from Osteoinductive Biomaterials, *Materials*, 2020, vol. 13, no. 168, pp. 1-16. ISSN 1996-1944.
47. DARIŜ Barbara and KNEZ Źeljko, Poly(3-hydroxybutyrate): Promising biomaterial for bone tissue engineering, *Acta Pharmaceutica*. 2020, vol. 70, pp. 1-15. ISSN: 1846-9558.
48. QIU Yan-Ling, Xiao CHEN, Ya-Li HOU, Song-Bo TIAN, Yu-He CHEN, Li YU, Min-Hai NIE, Xu-Qian LIU. Characterization of different biodegradable scaffolds in tissue engineering, *Molecular Medicine Reports*. 2019, vol. 19, pp. 4043-4056. ISSN: 791-2997.
49. WILLIAMS, David. There is no such thing as a biocompatible material, *Biomaterials*. 2014, vol. 35, no. 38, pp. 10009-10014. ISBN: 0142-9612.
50. WILL Julia, Rainer DETSCH, Aldo. R. BOCCACCINI. Structural and Biological Characterization of Scaffolds, Susmita Bose, Academic Press, USA, 2013, pp. 299-310, Chapter 7.1. Characterization of Biomaterials. ISBN 9780124158009.
51. GULREZ Syed, Saphwan AL-ASSAF, Glyn O. PHILLIPS. *Hydrogels: Methods of Preparation, Characterisation and Applications*, In Tech, 2011, Chapter 5, Progress in Molecular and Environmental Bioengineering - From Analysis and Modeling to Technology Applications. ISBN 978-953-307-268-5.
52. DAVID Anu, James DAY, Ariella SHIKANOV. Immuno-isolation to prevent tissue graft rejection: Current knowledge and future use, *Experimental Biology and Medicine*. 2016, vol. 241, no. 9, pp. 955-961. ISSN: 15353699.
53. CROISIER Florence and Chistine JÉRÔME. Chitosan-based biomaterials for tissue engineering, *European Polymer Journal*. 2013, vol. 49, pp. 780-792. ISSN: 0014-3057.

54. GERVASO Francesca, Alessandro SANNINO, Giuseppe M. PERETTI. The biomaterialist's task: scaffold biomaterials and fabrication technologies, *Joints*. 2013, vol. 1, no. 3, pp. 130-137. ISSN: 2282-4324.
55. BASU Probal, Nabanita SAHA & Petr SAHA. Inorganic calcium filled bacterial cellulose based hydrogel scaffold: novel biomaterial for bone tissue regeneration, *International Journal of Polymeric Materials and Polymeric Biomaterials*. 2019, vol. 68, no. 1-3, pp. 134-144. ISSN: 0091-4037
56. MURPHY Ciara, Fergal J. O'BRIEN, David G. LITTLE, Aaron SCHINDELER. Cell-Scaffold Interactions in the Bone Tissue Engineering Triad, *European Cells and Materials*. 2013, vol. 26, pp. 120-132. ISSN: 1473-2262.
57. NING Chengyun, Lei ZHOU, Guoxin TAN. Fourth-generation biomedical materials, *Materials Today*. 2016, vol. 19, no. 1, pp. 2-3. ISSN: 1369-702.
58. HENCH Larry and Ian THOMPSON. Twenty-first century challenges for biomaterials, *Journal of the Royal Society Interface*. 2010, vol. 7, pp. S379-S391. ISSN: 1742-5689.
59. JACOB Jaicy, Namdev MORE, Kiran KALIA, Govinda KAPUSETTI. Piezoelectric smart biomaterials for bone and cartilage tissue engineering, *Inflammation and Regeneration*, 2018, vol. 38, no. 2, pp. 2-11. ISSN: 1880-8190.
60. GUO Baolin and Peter MA. Conducting Polymers for Tissue engineering, *Biomacromolecules*, 2018, vol. 19, no. 6, pp. 1764-1782. ISSN: 1525-7797.
61. LECH Christopher Jacques and Anh Tuan PHAN. Ball with hair: Modular functionalization of highly stable G-quadruplex DNA nano-scaffolds through N2-guanine modification, *Nucleic Acid Research*. 2017, vol. 45, pp. 6265-6274. ISSN: 0305-1048.
62. BOUET Guenaelle, David MARCHAT, Magali CRUEL, Luc MALAVAL, Laurence VICO. In vitro three-dimensional bone tissue models: from cells to controlled and dynamic environment, *Tissue Engineering Part B: Reviews*. 2014, vol. 21, no. 1, pp. 133-156. ISSN: 1937-3368.
63. TURNBULL, Gareth, Jon CLARKE, Frédéric PICARD, Philip RICHES, Luanluan JIA, Fengxuan HAN, Bin LI, Wenmiao SHU. 3D bioactive composite scaffolds for bone tissue engineering, *Bioactive Materials*. 2018, vol. 3, no. 3, pp. 278-314. ISSN: 2452-199X.
64. JANOUŠKOVÁ Olga. Synthetic Polymer Scaffolds for Soft Tissue Engineering, *Physiological Research*, 2018. vol. 67, pp. S3335-S348. ISSN: 1802-9973.

65. GERHARDT Lutz-Christian and Aldo. R. BOCCACCINI. Bioactive Glass and Glass-Ceramic Scaffolds for Bone Tissue Engineering, *Materials*. 2010, vol. 3, pp. 3867-3910. ISSN: 1996-1944.
66. MISCH Carl, Zhimin QU, Martha BIDEZ. Mechanical properties of trabecular bone in the human mandible: Implications for dental implant treatment planning and surgical placement. *Journal of Oral Maxillofacial Surgery*. 1999, vol. 57, no. 6, pp. 700-706. ISSN: 0278-2391.
67. GATTI Antonietta and Jonathan C. KNOWLES. *Biocompatibility and biological tests*. Springer, Boston, 2011, pp. 793-794, Chapter 27, Integrated Biomaterials Science. ISBN 978-0-306-46678-6.
68. AMINI Ami, Cato LAURENCIN, Syam NUKAVARAPU. Bone Tissue Engineering: recent advances and challenges, *Critical Reviews in Biomedical Engineering*. 2012, vol. 40, pp. 363-408. ISSN: 0278-940X
69. HOFFMAN Sandra, Marcos GARCIA-FUENTES. *Bioactive scaffolds for the controlled formation of complex skeletal tissues*. In Tech, 2011, pp. 393-432, Chapter 18, Regenerative Medicine and Tissue Engineering - Cells and Biomaterials. ISBN 978-953-307-663-8.
70. CHEN Qiaoping, Judith A ROETHER, Aldo Roberto BOCCACCINI. *Tissue engineering scaffolds from bioactive glass and composite materials*. Topics in Tissue Engineering (Ebook), 2008, pp. 1-27. Available at: [https://www.oulu.fi/spareparts/ebook\\_topics\\_in\\_t\\_e\\_vol4/abstracts/q\\_chen.pdf](https://www.oulu.fi/spareparts/ebook_topics_in_t_e_vol4/abstracts/q_chen.pdf)
71. JUN Fu and Marc PANHUIS. Hydrogel properties and applications, *Journal of Material Chemistry B*. 2019, vol. 7, pp. 1523-1525. ISSN: 2050-750X
72. MORI, Arianna De, Marta Peña FERNANDEZ, Gordon BLUNN, Gianluca TOZZI, Marta ROLDO. 3D printing and electrospinning of composite hydrogels for cartilage and bone tissue engineering, *Polymers*. 2018, vol. 10, no. 3, pp. 285. ISSN 2073-4360.
73. CHAI Yoke Chin, Scott J ROBERTS, Jan SCHROOTEN, Frank P LUYTEN. Probing the Osteoinductive Effect of Calcium Phosphate by Using an In Vitro Biomimetic Model, *TISSUE ENGINEERING: Part A*. 2011, vol. 17, pp. 1083-1097. ISSN: 1937-3341.
74. CHIRANI Naziha, L'Hocine YAHIA, Lukas GRISTSCH, Federico Leonardo MOTTA, Soumia CHIRANI, Silvia FARÈ. History and Applications of Hydrogels, *Journal of Biomedical Science*. 2016, vol. 4, pp. 1-23. ISSN: 1021-7770.

75. EI-SHERBINY Ibrahim and Magdi YACOUB. Hydrogel scaffolds for tissue engineering: Progress and challenges, *Global Cardiology Science and Practice*. 2013, vol. 38, pp. 2-27. ISSN: 2305-7823.
76. GUARINO Vincenzo, Antonio GLORIA, Maria Grazia RAUCCI, Luigi AMBROSIO. Hydrogel-Based Platforms for the Regeneration of Osteochondral Tissue and Intervertebral Disc, *Polymers*. 2012, vol. 4, pp. 1590-1612. ISSN: 2073-4360.
77. RIZZI Roberto, Claudia BEARZI, Arianna MAURETTI, Sergio BERNARDINI, Stefano CANNATA, Cesare GARGIOLI. Tissue engineering for skeletal muscle Regeneration, *Muscles, Ligaments and Tendons Journal*. 2012, vol. 2, pp. 230-234. ISSN: 2240-4554.
78. SCHOTT Hans. Swelling kinetics of polymers, *Journal of Macromolecular Science Part B*. 1992, vol. 1, pp. 1-9. ISSN: 0022-2348.
79. DE Sudipta, N R ALURU, B JHONSON, Wendy CRONE, David BEEBE, Jeffrey MOORE. Equilibrium swelling and kinetics of pH-responsive hydrogels: Models, experiments, and simulations, *Journal of Microelectromechanical System*. 2002, vol. 11, pp. 544-555. ISSN: 1057-7157.
80. NEGRINI Nicola Contessi, CELIKKIN Nehar, TARSINI Paolo, Silvia FARÈ, Wojciech ŚWIĘSZKOWSKI, 3D printing of chemically crosslinked gelatin hydrogels for adipose tissue engineering, *Biofabrication*, 2020, vol. 12, pp. 1-16. ISSN: 1758-5082
81. LUETCHFORD, Kim, Julian CHAUDHURI, Paul De BANK. Silk fibroin/gelatin microcarriers as scaffolds for bone tissue engineering, *Material Science & Engineering C*. 2020, vol. 106, no. 110116, pp. 1-9. ISSN: 0928-4931.
82. JUNG Hyungjin and Ozan AKKUS. Activation of intracellular calcium signaling in osteoblasts colocalizes with the formation of post-yield diffuse microdamage in bone matrix, *BoneKEy Reports*. 2016, vol. 5, pp. 1-7. ISSN: 2047-6396.
83. SHAH Rushita, Zdenka KUČEKOVÁ, Petr HUMPOLICEK, Petr SAHA. Properties of biomineralized (CaCO<sub>3</sub>) PVP-CMC hydrogel with reference to its cytotoxicity, *International Journal of Polymeric Materials and Polymeric Biomaterials*. 2016, vol. 65, no. 12, pp. 619-628. ISSN: 0091-4037.
84. CHAI Yoke Chin, Scott J ROBERTS, Jan SCHROOTEN, Frank P LUYTEN. Probing the Osteoinductive Effect of Calcium Phosphate by Using an In Vitro Biomimetic Model, *TISSUE ENGINEERING: Part A*. 2011, vol. 17, pp. 1083-1097. ISSN: 1937-3341.

85. MANFERDINI Cristina, Francesco GRASSI, Anna PIACENTINI, Luca CATTINI, Giuseppe FILARDO, Elisabetta LAMBERTINI, Roberta PIVA, Nicoletta ZINI, Andrea FACCHINI, Gina LISIGNOLI. Extracellular Calcium Chronically Induced Human Osteoblasts Effects: Specific Modulation of Osteocalcin and Collagen Type XV, *Journal of Cellular Physiology*. 2011, vol. 227, pp. 3151-3161. ISSN: 1097-4652.
86. DVORAK-EWELL Melita and Daniela RICCARDI. Ca<sup>2+</sup> as an extracellular signal in bone, *Cell Calcium*. 2004, vol. 35, pp. 249-255. ISSN: 0143-4160.
87. BUWALDA Sytze, Kristel BOERE, Pieter DIJKSTRA, Jan FEIJEN, Tina VERMONDEN, Wim HENNINK. Hydrogels in a historical perspective: From simple networks to smart materials, *Journal of Controlled Release*. 2014, vol. 190, pp. 254-273. ISSN: 0168-3659.
88. WICHTERLE O and D LIM. Hydrophilic Gels for Biological Use, *Nature*. 1960, vol. 185, pp. 117-118. ISSN: 1476-4687.
89. KIM Jungju, In Sook KIM, Soon Jung HWANG, Ho Chul KIM, Yongdo PARK, Kyung SUN. Bone regeneration using MMP sensitive-hyaluronic acid based hydro gels, 2009 IEEE 35th Annual Northeast Bioengineering Conference, Available at: <https://ieeexplore.ieee.org/stamp/stamp.jsp?tp=&arnumber=4967789>
90. TREERATTRAKOON Kiatnida. *In vitro analysis of injectable hyaluronic acid hydrogel scaffold containing strontium as a carrier for rhBMP-2 for bone regeneration* [online]. Sweden, 2013 [viewed 2019-30-08]. Doctoral Thesis. Uppsala University, Biology Education Centre and Department of Surgical Sciences, Orthopaedics, Akademiska Sjukhuset. Supervisor: Professor Sune Larsson. Available from: [https://www.ibg.uu.se/digitalAssets/147/c\\_147660-1\\_1-k\\_report-kiatnida-treerattrakoon.pdf](https://www.ibg.uu.se/digitalAssets/147/c_147660-1_1-k_report-kiatnida-treerattrakoon.pdf)
91. TOZZI Gianluca, Arianna De MORI, Antero OLIVEIRA, Marta ROLDO. Composite Hydrogels for Bone Regeneration, *Materials*. 2016, vol. 9, pp. 1-24. ISSN: 1996-1944.
92. BAI Xin, Mingzhu GAO, Sahla SYED, Jerry ZHUANG, Xiaoyang XU, Xue-Qing ZHANG. Bioactive hydrogels for bone regeneration, *Bioactive materials*. 2018, vol. 3, pp. 401-417. ISSN: 2452-199X
93. CARLSTRÖM Ingeborg Elisabeth, Ahmad RASHAD, Elisabetta CAMPODONI, Monica SANDRI, Kristin SYVERUD, Anne Isine BOLSTAD,



- Kamal MUSTAFA, Cross-linked gelatin-nanocellulose scaffolds for bone tissue engineering, *Material Letters*, vol. 264, pp.1-5. ISSN: 0167-577X.
94. AZEREDO Henriette MC, Hernane BARUD, Cristiane S FARINAS, Vanessa M VASCONCELLOS, Amanda M CLARO. Cellulose as a Raw Material for Food and Food Packaging Applications. *Frontiers in Sustainable Food Systems*. 2019, vol. 3, no. 7, pp. 1-14. ISSN: 2571-581X.
95. PORTELA Raquel, Catarina R LEAL, Pedro L ALMEIDA, Rita G SOBRAL. Bacterial cellulose: a versatile biopolymer for wound dressing applications, *Microbial Biotechnology*. vol. 12, pp. 586-610. ISSN: 1751-7915.
96. MONIRI Mona, Amin Boroumand MOGHADDAM, Susan AZIZI, Raha Abdul RAHIM, Arbakariya Bin ARIFF, Wan Zuhainis SAAD, Mohammad NAVADERI, Rosfarizan MOHAMAD. Production and Status of Bacterial Cellulose in Biomedical Engineering, *Nanomaterials*. 2017, vol. 7, pp. 2-26. ISSN: 2079-4991.
97. TORRES Fernando, Solene COMMEAUX, Omar TRONCOSO. Biocompatibility of Bacterial Cellulose Based Biomaterials, *Journal of Functional Biomaterials*, 2012, vol. 3, pp. 864-878. ISSN: 2079-4983.
98. EI-SAIED Houssni, Altaf H BASTA, Raid H GOBRAN. Research progress in friendly environmental technology for the production of cellulose products (bacterial cellulose and its application), *Polymer-Plastics Technology and Engineering*, 2004, vol. 43, pp. 797-820. ISSN: 2574-0881.
99. COSTA Andréa, Fabiola Carolina Gomes DE ALMEIDA, Glória M. VINHAS, Leonie SARUBBO. Production of Bacterial Cellulose by *Gluconacetobacter hansenii* Using Corn Steep Liquor As Nutrient Sources, *Frontiers in Microbiology*. 2017, vol. 8, pp. 1-12. ISSN: 1664-302X.
100. HESTRIN Shlomo and Matthias SCHRAMM. Synthesis of cellulose by *Acetobacter xylinum*. II. Preparation of freeze-dried cells capable of polymerizing glucose to cellulose, *Biochemical Journal*. 1954, vol. 58, pp. 345-352. ISSN: 0264-6021.
101. BROWN Adrian. An acetic ferment which forms cellulose, *Journal of the Chemical Society, Transactions*. 1886, vol. 49, pp. 432-439. ISSN: 0368-1645.
102. HICKEY Ryan and Andrew PELLING. Cellulose Biomaterials for Tissue Engineering. *Frontiers in Bioengineering and Biotechnology*. 2019, vol. 7, pp. 1-15. ISSN: 2296-4185.

103. DUTTA Sayan Deb, Dinesh K PATEL, Ki-Taek LIM, Functional cellulose-based hydrogels as extracellular matrices for tissue engineering, *Journal of Biological Engineering*. 2019, vol. 13, pp. 2-19. ISSN: 1754-1611.
104. UL-ISLAM Mazhar, Muhammad Wajid ULLAH, Shaukat KHAN, Nasrullah SHAH, Joong Kon PARK. Strategies for cost-effective and enhanced production of bacterial cellulose, *International Journal of Biological Macromolecules*. 2017, vol. 102, pp. 1166-1173. ISSN: 0141-8130.
105. TYAGI Neha and Suresh SUMATHI. Production of cellulose from sugarcane molasses using *Gluconacetobacter intermedius* SNT-1, optimization and characterization, *Journal of Cleaner Production*. 2016, vol. 112, pp. 71-80. ISSN: 0959-6526.
106. HUNGUND Basavaraj Shrishailappa, Shruti PRABHU, Chetan SHETTY, Srilekha ACHARYA, Veena PRABHU, Shantikumar GUPTA. Production of bacterial cellulose from *Gluconacetobacter persimmonis* GH-2 using dual and cheaper carbon sources, *Journal of Microbial and Biochemical Technology*. 2013, vol. 5, pp. 31-33. ISSN: 1948-5948.
107. SURESH Sumathi. *Biosynthesis and Assemblage of Extracellular Cellulose by Bacteria*. Springer, Cham, 2018, pp. 1-43. Handbook of Environmental Materials Management. ISBN 978-3-319-58538-3. Available at: [https://link.springer.com/referenceworkentry/10.1007%2F978-3-319-58538-3\\_71-1](https://link.springer.com/referenceworkentry/10.1007%2F978-3-319-58538-3_71-1)
108. ESA Faezah, Siti Masrinda TASIRIN, Norliza Abd RAHMAN. Overview of Bacterial Cellulose Production and Application, *Agriculture and Agricultural Science Procedia*. 2014, vol. 2, pp. 113-119. ISSN: 2210-7843.
109. GATENHOLM Paul and Dieter KLEMM. Bacterial nanocellulose as a renewable material for biomedical applications. *Materials from Renewable Resources Bulletin*. 2010, vol. 35, pp. 208-213. ISSN: 0883-7694.
110. PETERSEN Nathan and Paul GATENHOLM. Bacterial cellulose-based materials and medical devices: Current state and perspectives, *Applied Microbiology and Biotechnology*. 2011, vol. 91, pp. 1277-1286. ISSN: 0175-7598.
111. GUESMI Youssef, Hassen AGOUGUI, Mahjoub JABLI & Amir ALSHARABASY. Bioactive composites of hydroxyapatite/polyvinylpyrrolidone for bone regeneration applications,

- Chemical Engineering Communications*. 2019, vol. 3, pp. 279-288. ISSN: 0098-6445.
112. SUBRAMANIAN Uma Maheshwari, Samuel VASANTH KUMAR, Naveen NAGIAH & Uma Tiruchirapally SIVAGNANAM. Fabrication of Polyvinyl Alcohol-Polyvinylpyrrolidone Blend Scaffolds via Electrospinning for Tissue Engineering Applications, *International Journal of Polymeric Materials and Polymeric Biomaterials*. 2014, vol. 63, no. 9, pp. 476-485. ISSN: 0091-4037.
113. ROY Niladri and Nabanita SAHA. PVP-based Hydrogels: Synthesis, Properties and Applications. Nova Science Publishers, 2012. pp.02-33. ISBN: 978-1-61942-842-3.
114. KUMAR Anuj & Sung Soo HAN. PVA-based hydrogels for tissue engineering: A review, *International Journal of Polymeric Materials and Polymeric Biomaterials*. 2017, vol. 66, no. 4, pp. 159-182. ISSN: 0091-4037.
115. REVURU Sainitya, Sriram MUTHUKUMAR, Kalyanarman VAIDYANATHAN, Dhivya SHANKAR, Saravanan SEKARAN, M VAIRAMANI, Thotapalli SASTRY, Nagarajan SELVAMURUGAN. Scaffolds containing chitosan/carboxymethyl cellulose/mesoporous wollastonite for bone tissue engineering, *International Journal of Biological Macromolecules*. 2015, vol. 80, pp. 481-488. ISSN: 0141-8130.
116. VERMA Vipin, Poonam VERMA, Santosh KAR, Pratima RAY, Alok RAY. Fabrication of Agar-Gelatin Hybrid Scaffolds Using a Novel Entrapment Method for In Vitro Tissue Engineering Applications, *Biotechnology & Bioengineering*. 2007, vol. 96, pp. 392-400. ISSN: 1097-0290.
117. LOGITHKUMAR R, A. KESHAVNARAYAN, Selvaraj DHIVYA, Anjali CHAWLA, Saravanan SEKARAN, Nagarajan SELVAMURUGAN. A review of chitosan and its derivatives in bone tissue engineering, *Carbohydrate Polymers*. 2016, vol. 151, pp. 172-188. ISSN: 0144-8617.
118. HENCH Larry and Ian THOMPSON. Twenty-first century challenges for biomaterials, *Journal of the Royal Society Interface*. 2010, vol. 7, pp. S379-S391. ISSN: 1742-5689.
119. LOWE Baboucarr, Mark OTTENSMEYER, Chun XU, Yan HE, Qingsong YE, Maria J TROULIS. The Regenerative Applicability of Bioactive Glass and Beta-Tricalcium Phosphate in Bone Tissue Engineering: A Transformation

- Perspective, *Journal of Functional Materials*. 2019, vol. 10, pp. 2-18. ISSN: 2079-4983.
120. TORGBO Selorm and Prakrit SUKYAI. Bacterial cellulose-based scaffold materials for bone tissue engineering, *Applied Materials Today*. 2018, vol. 11, pp. 34-49. ISSN: 2352-9407
121. LEE Mi Nam, Hee-Su HWANG, Sin-Hye OH, Amir ROSHANZADEH, Jung-Woo KIM, Ju Han SONG, Eung-Sam KIM, Jeong-Tae KOH. Elevated extracellular calcium ions promote proliferation and migration of mesenchymal stem cells via increasing osteopontin expression, *Experimental & Molecular Medicine*. 2018, vol. 50, no. 142, pp. 2-16. ISSN: 2092-6413.
122. LAI Chung-Fang, Lala CHAUDHARY, Aurora FAUSTO, Linda R HALSTEAD, Daniel S ORY, Louis V AVIOLI, Su-Li CHENG. Erk is essential for growth, differentiation, integrin expression, and cell function in human osteoblastic cells, *Journal of Biological Chemistry*. 2001, vol. 276, pp. 14443-14450. ISSN: 0021-9258.
123. NEW David and Yung H WONG. Molecular mechanisms mediating the G protein-coupled receptor regulation of cell cycle progression, *Journal of Molecular Signaling*. 2007, vol. 2, pp. 1-15. ISSN: 0022-2836.
124. SHEENOY Aroon, *Rheology of Filled Polymer Systems*, Illustrated ed., Springer, © 1999. ISBN 978-0-412-83100-3.
125. GIANCOTTI Filippo and Erkki RUOSLAHTI. Integrin Signaling, *Science*. 1999, vol. 285, pp. 1028-1033. ISSN: 1095-9203.
126. RUBIN Janet, Clinton RUBIN, Christopher R JACOBS. Molecular pathways mediating mechanical signaling in bone, *Gene*. 2006, vol. 367, pp. 1-16. ISSN: 0378-1119.
127. CHUA Ing Loon Sean, Hae-Won KIM, Jae Ho LEE. Signaling of extracellular matrices for tissue regeneration and therapeutics, *Tissue Engineering and Regenerative Medicine*. 2016, vol. 13, pp. 1-12. ISSN: 1738-2696.
128. MARIE Pierre, Eric HAÏ, Zuzana SAIDAK. Integrin and cadherin signaling in bone: role and potential therapeutic targets, *Trends in Endocrinology and Metabolism*. 2014, vol. 25, pp. 567-574. ISSN: 1043-2760.
129. FLORENCIO-SILVA Rinaldo, Gisela Rodrigues da Silva SASSO, Estela SASSO-CERRI, Manuel Jesus SIMÕES, Paulo Sérgio CERRI. *Biology of Bone*

- Tissue: Structure, Function, and Factors That Influence Bone Cells, *BioMed Research International*. 2015, vol. 2015, pp. 1-17. ISSN: 2314-6141.
130. JIN Yuan-Zhe and LEE Jae Hyup. Mesenchymal Stem Cell Therapy for Bone Regeneration, *Clinics in Orthopedic Surgery*. 2018, vol. 10, pp. 271-278. ISSN: 2005-291X.
  131. BAO Chao Le Meng, Erin Y TEO, Mark S K CHONG, Yuchun LIU, Mahesh CHOOLANI, Jerry K Y CHAN. *Advances in Bone Tissue Engineering*, InTech, 2013, pp.599-614. Chapter 24. Regenerative Medicine and Tissue Engineering. ISBN 978-953-51-1108-5.
  132. RIDLEY Anne, Martin A SCHWARTZ, Keith BURRIDGE, Richard A FIRTEL, Mark H GINSBERG, Gary BORISY, J Thomas PARSONS, Alan Rick HORWITZ. Cell migration: integrating signals from front to back, *Science*. 2003, vol. 302, pp. 1704-1709. ISSN: 1095-9203.
  133. FRIEDI Peter, Kurt S. ZÄNKER, Eva-B. BRÖCKER. Cell migration strategies in 3-D extracellular matrix: differences in morphology, cell matrix interactions, and integrin function, *Microscopy Research & Technique*. 1998, vol. 43, pp. 369-378. ISSN: 1097-0029.
  134. HUTTENLOCHER Anna, Rebecca R SANDBORG, Alan F HORWITZ. Adhesion in cell migration, *Current Opinion in Cell Biology*. 1995, vol. 7, pp. 697-706. ISSN: 0955-0674.
  135. LAUFFENBURGER Doughlas and Alan HORWITZ. Cell migration: A physically integrated molecular process, *Cell*. 1996, vol. 84, pp. 359-369. ISSN: 0092-8674.
  136. DISCHER Dennis, Paul JANMEY, Yu-li WANG. Tissue cells feel and respond to the stiffness of their substrate, *Science*. 2005, vol. 310, pp. 1139-1143. ISSN: 1095-9203.
  137. ZAJAC Alison and Dennis E DISCHER. Cell differentiation through tissue elasticity-coupled, myosin-driven remodeling, *Current Opinion in Cell Biology*. 2008, vol. 20, pp. 609-615. ISSN: 0955-0674.
  138. ROY, Niladri, Nabanita SAHA, Takishi KITANO, Petr SAHA. Biodegradation of PVP-CMC hydrogel film: a useful food packaging material, *Carbohydrate Polymers*. 2012, vol. 89, no. 2, pp. 346–353. ISSN: 0144-8617.
  139. LAWRENCE Mike and Yunhong JIANG. *Porosity, Pore Size Distribution, Micro-structure*. Springer, 2017, pp. 39-71. Chapter 2. Bio-aggregates Based Building Materials. ISBN 9789402410303.

140. NAKANISHI Kazuki. Porosity Measurement. Springer, Cham, © 2016. ISBN978-3-319-19454-7. Available from: [https://link.springer.com/referenceworkentry/10.1007%2F978-3-319-19454-7\\_38-1](https://link.springer.com/referenceworkentry/10.1007%2F978-3-319-19454-7_38-1)
141. KARAGEORGIOU Vassilis and David KAPLAN. Porosity of 3D biomaterial scaffolds and osteogenesis, *Biomaterials*. 2005, vol. 26, pp. 5474-5491. ISSN: 0142-9612.
142. SOWMYA Srinivasan, Pandian Thodi SUDHEESH KUMAR, Krishna Prasad CHENNAZHI, Shantikumar Vasudevan NAIR, K P CHENNAZHI, Jayakumar RANGASAMY. Biocompatible  $\beta$ -chitin Hydrogel/Nanobioactive Glass Ceramic Nanocomposite Scaffolds for Periodontal Bone Regeneration, *Trends in Biomaterials and Artificial Organs*. 2011, vol. 25, pp. 1-11. ISSN: 0971-1198.
143. FERFERA-HARRAR Hafida, Nacera AOUAZ, Nassima DAIRI. Environmental-sensitive chitosan-g-polyacrylamide/carboxymethylcellulose superabsorbent composites for wastewater purification I: synthesis and properties, *Polymer Bulletin*. 2016, vol. 73, pp. 815-840. ISSN: 0170-0839.
144. SAHA Nabanita, Amarjargal SAARAI, Niladri ROY, Takeshi KITANO, Petr SAHA. Polymeric Biomaterial Based Hydrogels for Biomedical Applications, *Journal of Biomaterials and Nanobiotechnology*. 2011, vol. 2, pp. 85-90. ISSN: 2158-7027.
145. O'BRIEN Fergal. Biomaterials & scaffolds for tissue engineering, *Materials Today*. 2011, vol. 3, pp. 88-95. ISSN: 1369-7021.
146. KUMAR P T Sudheesh, Sowmya SRINIVASAN, Vinoth Kumar LAKSHMANAN, Hiroshi TAMURA, S V NAIR, R JAYAKUMAR. Chitin hydrogel/nano hydroxyapatite composite scaffolds for tissue engineering applications, *Carbohydrate Polymers*. 2011, vol. 85, pp. 584-591. ISSN: 0144-8617.
147. GAJJAR Chirag and Martin KING. Resorbable Fiber-Forming Polymers for Biotextile Applications Springer, Cham, © 2014. ISBN 978-3-319-08305-6.
148. DENG Yi, Xiaochen LIU, Anxiu XU, Lixin WANG, Zuyuan LUO, Yunfei ZHENG, Feng DENG, Jie WEI, Zhihui TANG, Shicheng WEI. Effect of surface roughness on osteogenesis in vitro and osseointegration in vivo of carbon fiber-reinforced polyetheretherketone– nanohydroxyapatite composite, *International Journal of Nanomedicine*. 2015, vol. 10, pp. 1425-1447. ISSN: 1176-9114.

149. RAHMAN Md. Shirajur, Md Minhajul ISLAM, Md Sazedul ISLAM, Asaduz ZAMAN, Tanvir AHMED, Shanta BISWAS, Sadia SHARMEEN, Taslim Ur RASHID, Mohammed Mizanur RAHMAN. Morphological Characterization of Hydrogels. Springer Nature, 2019, pp. 8919-862. ISBN 978-3-319-77829-7. Available from: [https://link.springer.com/referenceworkentry/10.1007%2F978-3-319-77830-3\\_28](https://link.springer.com/referenceworkentry/10.1007%2F978-3-319-77830-3_28)
150. HIRSCH Edit, Márió NACSA, Ferenc ENDER, Miklós MOHAI, Zsombor Kristof NAGY, György J. MAROSI. Preparation and Characterization of Biocompatible Electrospun Nanofiber Scaffolds, *Periodica Polytechnica Chemical Engineering*. 2018, vol. 62, pp. 510-518. ISSN: 0324-5853.
151. MANCILLA León Benjamin, M A ARAIZA-TÉLLEZ, J O FLORES-FLORES, Maria Cristina PINA-BARBA. Physico-chemical characterization of collagen scaffolds for tissue engineering, *Journal of Applied Research and Technology*. 2016, vol. 1, pp. 77-85. ISSN: 1665-6423.
152. BERTHOMIEU Catherine and Rainer Hienerwadel. Fourier transform infrared (FTIR) spectroscopy, *Photosynthesis Research*, 2009, vol. 101, pp. 157-70. ISSN: 0166-8595.
153. THÜRMER Mônica Beatriz, Carlos Eduardo DIEHL, Fábio José Bento BRUM, Luis Alberto Loureiro Dos SANTOS. Preparation and characterization of hydrogels with potential for use as biomaterials, *Materials Research*. 2014, vol. 17, pp. 109-113. ISSN: 1516-1439.
154. GILL Pooria, Tahereh Tohidi MOGHADAM, Bijan RANJBAR. Differential Scanning Calorimetry Techniques: Applications in Biology and Nanoscience, *Journal of Biomolecular Techniques*. 2010, vol. 21, pp. 167-193. ISSN: 1524-0215.
155. OYEN Michelle. Mechanical characterisation of hydrogel materials, *International Materials Reviews*. 2014, vol. 59, pp. 44-59. ISSN: 0950-6608.
156. SAHA, Nabanita, Rushita SHAH, Prerak GUPTA, Biman MANDAL, Radostina ALEXANDROVA, Maja Dutour SIKIRIC, Petr SAHA. PVP - CMC hydrogel: An excellent bioinspired and biocompatible scaffold for osseointegration, *Material Science and Engineering: C*. 2019, vol. 95, pp. 440-449. ISSN: 0928-4931.
157. BALOUIRI Mounyr, Sadiki MOULAY, Saad SADIKI, Ibnsouda KORAICHI (2016) Methods for *in vitro* evaluating antimicrobial activity: A

- review, *Journal of Pharmaceutical Analysis*. 2016, vol. 6, pp.71-79. ISSN: 2095-1779.
158. KUMAR Nita, Rayhaneh AFJEI, Tarik MASSOUD, Ramasamy PAULMURUGAN. Comparison of cell-based assays to quantify treatment effects of anticancer drugs identifies a new application for Bodipy-L-cystine to measure apoptosis, *Scientific Reports*. 2018, vol. 8, no. 16363, pp. 1-11. ISSN: 2045-2322.
159. BERNARD Mélisande, Emile JUBELI, Michael PUNGENETE, Najet YAGOUBI. Biocompatibility of polymer-based biomaterials and medical devices – regulations, *in vitro* screening and risk-management, *Biomaterials Science*. 2018, vol. 6, pp. 2025-2053. ISSN: 2047-4849.
160. CHAUVIN-KIMOFF Laurel, Claire ALLARD-DANSEREAU, Margaret COLBOURNE. The medical assessment of fractures in suspected child maltreatment: Infants and young children with skeletal injury, *Paediatrics & Child Health*. 2018, vol. 23, no.2, pp. 156–160. ISSN: 1205-7088.
161. ORYAN, Ahmad, Soodeh, ALIDADI, Ali MOSHIRI. Current concerns regarding healing of bone defects, *Hard tissue*. 2013, vol. 2, no.2, pp. 1-12. ISSN: 2050-2303.
162. NOF: *National Osteoporosis Foundation* [online]. © 2018 [viewed 10.02.2018]. Available from: <https://www.nof.org/patients/what-is-osteoporosis/>
163. SEKULA Małgorzata and Ewa K. ZUBA-SURMA. Biomaterial and Stem cells: Promising Tools in Tissue Engineering and Biomedical Applications. IntechOpen, 2018, pp. 361-378. Chapter 16. Biomaterial in Regenerative Medicine. ISBN 978-953-51-3776-4.
164. KROEZE Robert, HELDER, Marco, GOVAERT Leon, & SMIT Theo. Biodegradable Polymers in Bone Tissue Engineering, *Materials*. 2009, vol 2, pp. 833-856. ISSN: 1996-1944.
165. SHAH Rushita, Nabanita SAHA, Takishi KITANO, Petr SAHA. Preparation of CaCO<sub>3</sub>-Based Biomineralized Polyvinylpyrrolidone-Carboxymethylcellulose Hydrogels and Their Viscoelastic Behavior, *Journal of Applied Polymer Science*. 2014, vol. 40237, pp. 1-9. ISSN: 1097-4628.
166. BASU Probal, Nabanita SAHA, Radostina ALEXANDROVA, Petr SAHA. Calcium Phosphate Incorporated Bacterial Cellulose-Polyvinylpyrrolidone Based Hydrogel Scaffold: Structural Property and Cell Viability Study for Bone



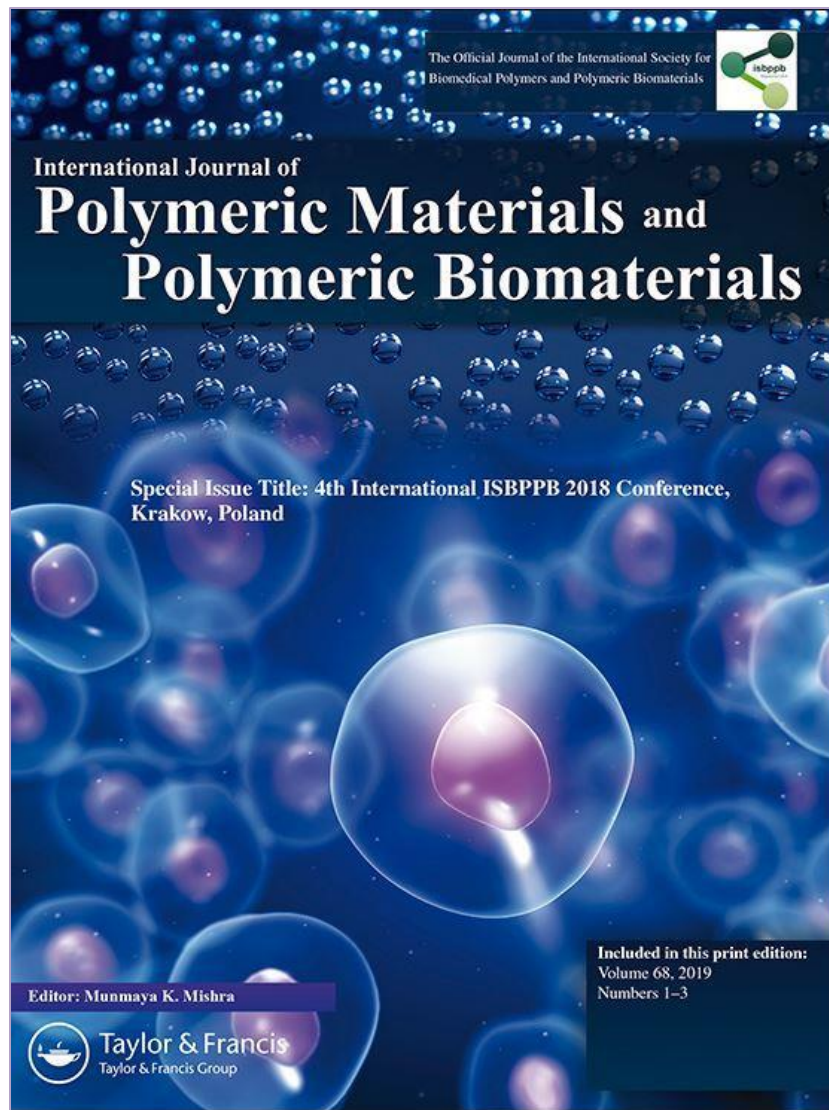
Regeneration Application. *Polymers*, 2019, vol. 11, no. 1821, pp. 1-24. ISSN: 2073-4360.

167. AQUINO-MARTÍNEZ Rubén, Natalia ARTIGAS, Beatriz GÁMEZ, José Luis ROSA, Francesc VENTURA. Extracellular calcium promotes bone formation from bone marrow mesenchymal stem cells by amplifying the effects of BMP-2 on SMAD signaling, *PLoS ONE*. 2017, vol. 12, no. 5, pp. e0178158. ISSN: 1932-6203.

# **PUBLICATIONS**

## PUBLICATION I

**Basu P. (50%), Saha N & Saha P. (2019)** “Inorganic calcium filled bacterial cellulose based hydrogel scaffold: novel biomaterial for bone tissue regeneration”, *International Journal of Polymeric Material and Polymeric Biomaterial* (Web of Science indexed, Q2 [Polymer Science], **J<sub>imp</sub>: 2.263**), 68:1-3, 134-144. DOI: <https://doi.org/10.1080/00914037.2018.1525733>



The Official Journal of the International Society for  
Biomedical Polymers and Polymeric Biomaterials



International Journal of  
**Polymeric Materials and  
Polymeric Biomaterials**

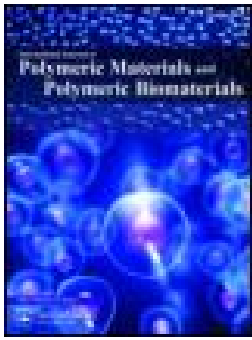
Special Issue Title: 4th International ISBPPB 2018 Conference,  
Krakow, Poland

Editor: Munmaya K. Mishra



**Taylor & Francis**  
Taylor & Francis Group

Included in this print edition:  
Volume 68, 2019  
Numbers 1-3



## Inorganic calcium filled bacterial cellulose based hydrogel scaffold: novel biomaterial for bone tissue regeneration

Probal Basu, Nabanita Saha & Petr Saha

To cite this article: Probal Basu, Nabanita Saha & Petr Saha (2018): Inorganic calcium filled bacterial cellulose based hydrogel scaffold: novel biomaterial for bone tissue regeneration, International Journal of Polymeric Materials and Polymeric Biomaterials, DOI: [10.1080/00914037.2018.1525733](https://doi.org/10.1080/00914037.2018.1525733)

To link to this article: <https://doi.org/10.1080/00914037.2018.1525733>



Published online: 31 Dec 2018.



Submit your article to this journal [↗](#)



Article views: 5



View Crossmark data [↗](#)



## Inorganic calcium filled bacterial cellulose based hydrogel scaffold: novel biomaterial for bone tissue regeneration

Probal Basu, Nabanita Saha, and Petr Saha

Centre of Polymer Systems, University Institute, Tomas Bata University in Zlín, Zlín, Czech Republic

### ABSTRACT

This work emphasizes the structural, physio-chemical characterization and cell biological efficiency analysis of novel inorganic calcium (only calcium phosphate and in combination of calcium phosphate &  $\text{CaCO}_3$ ) filled bacterial cellulose (BC) based hydrogel scaffolds. FTIR and TG analysis indicates the presence of BC and inorganic calcium within the hydrogel scaffolds. SEM establishes the porous structures (50–200  $\mu\text{m}$ ). Swelling study indicates significant swelling ability in both calcium phosphate filled and calcium phosphate &  $\text{CaCO}_3$  filled hydrogel scaffolds. Compressive strength (0.24–0.60 MPa) of the calcium filled hydrogel scaffolds are similar like trabecular bone. Significant cell viability (Lep-3) was further noticed until 72,120 and 168 h.

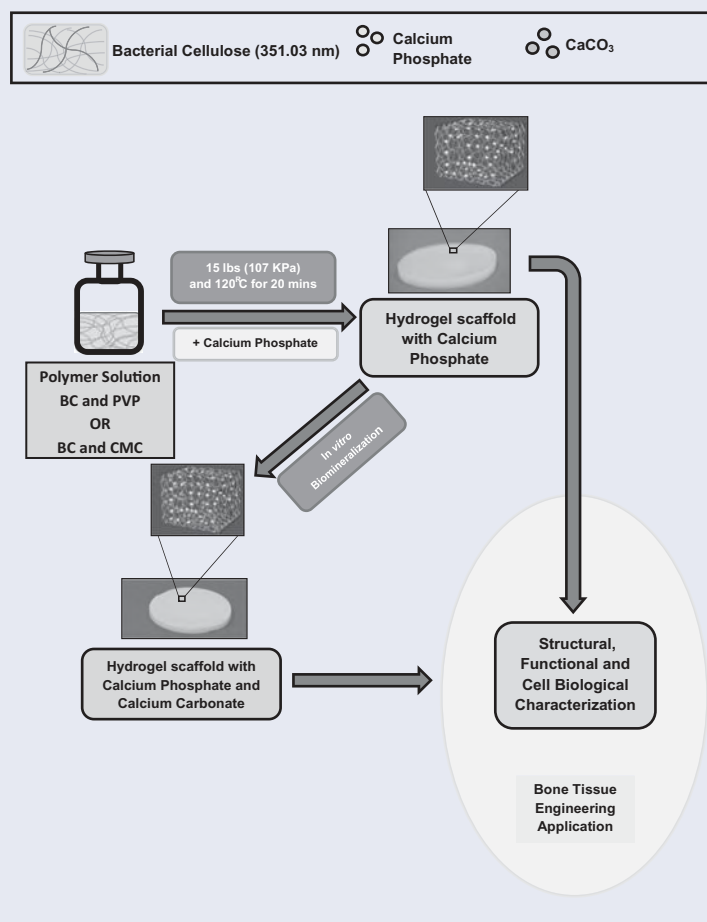
### ARTICLE HISTORY

Received 21 July 2018  
Accepted 25 August 2018

### KEYWORDS

Bacterial cellulose; bone regeneration; calcium phosphate; calcium carbonate; *in vitro* biomineralization

### GRAPHICAL ABSTRACT



## 1. Introduction

Bone is an extremely specified structure of animal body<sup>[1]</sup>. Research indicated that about 75 million individuals have been troubled by osteoporosis in Europe, USA and Japan. Moreover, studies showed that osteoporosis causes more than 8.9 million fractures worldwide annually, with a condition where an osteoporotic fracture occurs in every 3 seconds<sup>[2]</sup>. The treatment methods related to the fracture resulted from osteoporosis include utilization of either auto/allografts or ceramic coated/inert metallic implant which are expensive for application<sup>[3]</sup>. In this regard, the application of bioactive hydrogel scaffold can become a significant approach in bone tissue engineering due to its osteoconduction and osteoinduction property, notable mechanical property and cost-effective production attributes<sup>[4]</sup>.

The objective of the tissue engineering approach can be fulfilled by development of a tissue engineering scaffold which will act as an extra cellular matrix (ECM) to give the necessary platform for bone regeneration<sup>[5]</sup>. Hydrogel is a three dimensional polymeric network structure which can retain significant amount of water<sup>[6–8]</sup>. The primary function of tissue engineering scaffolds (e.g., hydrogel scaffolds) include cell adhesion, stimulation of cell proliferation at the desired site and facilitation of cell-biomaterial interaction<sup>[9]</sup>. The significant properties of scaffold materials involve efficient architecture, cyto-compatibility and notable mechanical property<sup>[10]</sup>.

Different polymers, co-polymers, polymer blends, polymer-composite scaffolds were utilized to design an efficient tissue engineering scaffold material. Several synthetic polymers PLA, PLLA, PLGA, and PCL etc. were applied to develop novel tissue engineering scaffolds<sup>[11]</sup>. In addition, several natural polymers like collagen, hyaluronic acid, fibrin, fibronectin, alginate, chitosan, silk were also used in the fabrication of scaffold<sup>[12–15]</sup>. Different polyesters like Poly-epsilon-caprolactone (PCL) based materials is also considered as exciting material for tissue engineering applications<sup>[16]</sup>. Additionally, different nano-filler filled polymer material like hydroxyapatite, silica, carbon nanotube can also act as a potential biomaterial<sup>[17,18]</sup>.

On the other hand, studies indicated that bioactive inorganic fillers like calcium phosphate e.g., tri-calcium phosphate ( $\beta$ -TCP), octa-calcium phosphate (OCP) and hydroxyapatite (HA) could enhance the osteoconduction and osteoinduction property of the biomaterial<sup>[19]</sup>. In addition, calcium carbonate ( $\text{CaCO}_3$ ) is found also effective in respect to providing stiffness which is a very important factor for the development of a bioactive hydrogel scaffold. Diverse methods of the organic-inorganic hybridization (i.e. solvent casting/particle leaching, scaffold coating etc.) were found useful for the inclusion of  $\text{CaCO}_3$  within the polymer matrix<sup>[20]</sup>.

Interestingly, cellulose based hydrogel scaffolds are considered as a promising material for tissue engineering applications<sup>[21]</sup>. Research demonstrated that cellulose and its derivatives can be utilized to improve the structural properties of different types of polymer systems<sup>[22]</sup>. Bacterial cellulose (BC) based hydrogel scaffolds has also the attributes to become a potential biomaterial<sup>[23]</sup>. BC is biocompatible biopolymer<sup>[24]</sup>. It has high crystallinity, ultra-fine network structure and high water absorption capability<sup>[25,26]</sup>.

The PVP-CMC hydrogel scaffold were previously developed at our laboratory in combination of synthetic polymers like polyvinylpyrrolidone (PVP), carboxymethyl cellulose (CMC)<sup>[6, 27]</sup>. Further, following the biomimetic biomineralization technique,  $\text{CaCO}_3$  filled PVP -CMC hydrogel scaffold was prepared for bone tissue engineering application<sup>[20]</sup>. Moreover, in our previous work, hydrogel scaffold developed using bacterial cellulose (BC) and polyvinylpyrrolidone (PVP), were also reported<sup>[25]</sup>. However, all the above mentioned hydrogel scaffolds have a significant elastic and mechanical property, which is the prerequisite for tissue engineering application; but for bone tissue engineering application more specific bioactive and suitable biomaterial (in the form of scaffold) is needed. Studies showed that calcium phosphates,  $\beta$ -tri calcium phosphate ( $\beta$ -TCP) and hydroxyapatite (HA) have the potentiality to induce osteogenesis<sup>[12]</sup> and thereby facilitate bone tissue engineering. Hence, in this work, inorganic calcium filled BC based hydrogel scaffold is developed by addition of  $\beta$ -TCP and HA and then followed by simple biomimetic biomineralization technique to incorporate ( $\text{CaCO}_3$ ) within the calcium phosphate filled hydrogel scaffold.

Earlier studies indicated the preparation of the hydrogel scaffolds through a variety of means; involving chemical cross linking and irradiation techniques<sup>[28,29]</sup>. Albeit, these methods have been considered as significant approach to achieve a hydrogel structure but, it has also some adverse effects (like introduction of possible DNA damage by the effects of chemicals and/or ionizing radiation), which can bring the negative consequences on the cellular level; especially, on the genome level. On the other hand, instead of chemical crosslinking method, physical crosslinking method can also be beneficial and efficient to develop hydrogel scaffolds<sup>[30]</sup> which can be effectively used in the biomedical field. This work focuses on the development of novel inorganic calcium filled BC based hydrogel scaffolds which are prepared with the unique combination of blending that involves biocompatible and bioadhesive biopolymers like BC, polyvinylpyrrolidone (PVP) and carboxymethylcellulose (CMC) through physical crosslinking method (i.e., moist heat treatment). Additionally, inorganic calcium filler i.e. calcium phosphate was administered to increase their osteoinductive property. Then through *in vitro* biomineralization method,  $\text{CaCO}_3$  mineral was also incorporated in the calcium phosphate filled BC based hydrogel scaffold in order to increase its stiffness and mechanical property for making it suitable for its potential application in bone tissue regeneration. The analysis of structure (FTIR, TGA, and SEM), function (compressive strength, swelling, porosity) and biological efficiency (cell viability) study with the novel inorganic calcium filled BC based hydrogel scaffolds were the principal goal of investigation in regard to its potential utilization in bone tissue engineering application.

## 2. Experimentation

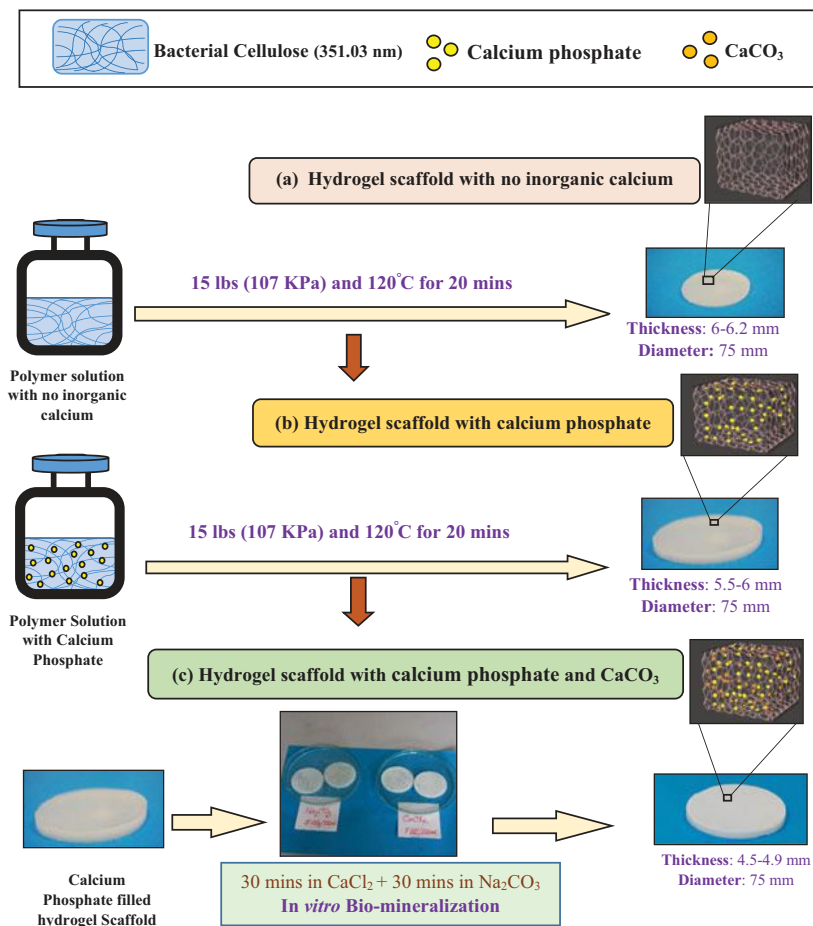
### 2.1. Materials

#### 2.1.1. Materials for preparation of inorganic calcium phosphate filled BC based hydrogel scaffold

Polyvinylpyrrolidone K30 (PVP K30; molecular weight: 40,000), polyethylene glycol 3000 (PEG; average molecular

**Table 1.** Composition of BC-PVP, BC-CMC and  $\beta$ -TCP/HA filled BC based hydrogel scaffold.

Sample index	PVP (g)	CMC (g)	BC (g)	PEG (g)	Agar (g)	Glycerin (mL)	$\beta$ -TCP/HA (g)	Water (mL)
BC-PVP	0.5	0.0	0.5	1	2	1	0.0/0.0	95
BC-CMC	0.0	0.5	0.5	1	2	1	0.0/0.0	95
BC-PVP $\beta$ -TCP/HA	0.5	0.0	0.5	1	2	1	0.2/0.8	94
BC-CMC- $\beta$ -TCP/HA	0.0	0.5	0.5	1	2	1	0.2/0.8	94

**Figure 1.** Preparation of BC based hydrogel scaffolds: (a) scaffold with no inorganic calcium: BC-PVP and BC-CMC; (b) Scaffold with calcium phosphate: BC-PVP- $\beta$ -TCP/HA, BC-CMC- $\beta$ -TCP/HA (c) Scaffold with calcium phosphate and  $\text{CaCO}_3$ : BC-PVP- $\beta$ -TCP/HA- $\text{CaCO}_3$ , and BC-CMC- $\beta$ -TCP/HA- $\text{CaCO}_3$ .

weight: 2700–3300), agar,  $\beta$ -tri calcium phosphate ( $\beta$ -TCP; molecular weight: 310.18 g/mol) were supplied by Fluka, Switzerland; sodium carboxy-methyl cellulose (CMC) was purchased from Sinopharm Chemical Reagent Co Ltd (SCRC), China; anhydrous calcium chloride ( $\text{CaCl}_2$ ; molecular weight 110.99 g/mol, 97.0%) was obtained from Penta, Czech Republic; and sodium carbonate-decahydrate ( $\text{Na}_2\text{CO}_3$ ; molecular weight 286.14 g/mol), hydroxyapatite (HA; molecular weight: 502.31 g/mol) were obtained from Sigma Aldrich.

BC was synthesized and derived from the microbiological laboratory of Centre of Polymer System, Tomas Bata University in Zlin. BC (holding 99%  $\text{H}_2\text{O}$ ) was synthesized in presence of basal synthetic Hestrin-Schramm (HS) nutritive medium (pH 7.0) using *Gluconacetobacter xylinus* CCM 3611<sup>T</sup> (syn. *Acetobacter xylinum*), incubated at 30 °C for 15 days. The freshly prepared BC pellicle is treated with 0.5 N NaOH solution and then heated at 80 °C for 1 h to remove

the possible contaminations from the BC pellicle. Thereafter, a homogenous suspension of BC (particle size: 351.03 nm) from the obtained BC mat was prepared by grinding the BC mat in distilled water.

### 2.1.2. Materials for antibacterial study and cell viability study

For antibacterial study, the bacteria selected for antibacterial study are *Staphylococcus aureus* (*S. aureus* CCM 4516) (Gram + ve bacteria) and *Escherichia coli* (*E. coli* CCM 4517) (Gram – ve bacteria).

For cell viability study, the Dulbecco's modified Eagle's medium (DMEM) and fetal bovine serum (FBS) were obtained from Gibco-Invitrogen (UK). Dimethyl sulfoxide (DMSO) and trypsin were obtained from AppliChem (Germany). The antibiotics (Penicillin and Streptomycin) for cell cultures were from Lonza (Belgium).



Ethylenediaminetetraacetic acid (EDTA) was purchased from local agents and distributors.

## 2.2. Methods

### 2.2.1. Preparation of calcium phosphate filled BC based hydrogel scaffolds

Calcium phosphate filled BC based hydrogel scaffolds were prepared with polymer solution of BC (holding 99% water) with CMC and PVP and other ingredients and bioactive materials (as shown in Table 1)<sup>[31]</sup>. PEG was added in all the hydrogel solutions to reduce the risk of tissue damage and other significant cytotoxic effects<sup>[32]</sup>. Glycerin used as humectant<sup>[6, 8, 31]</sup>. Agar is a hydrophilic polymer<sup>[33]</sup> performed as a gelling agent, might help in the increase of the degree of swelling. The bioactive materials ( $\beta$ -TCP and HA) were incorporated in the ratio of 20:80<sup>[34]</sup> to achieve calcium phosphate filled biomaterial considering its application in bone tissue engineering; finally termed as “BC-PVP- $\beta$ -TCP/HA” and “BC-CMC-  $\beta$ -TCP/HA” (as shown in Figure 1). Both “BC-PVP” and “BC-CMC” scaffolds were used as base scaffolds/control sets. All the hydrogel scaffolds were prepared following the solvent casting method, applying the physical cross-linking agent (moist heat and pressure). The polymer solutions (100 mL) were prepared in 250 mL sealed glass bottles under 15 lbs (107 KPa) pressure and 120 °C temperature for 20 min<sup>[6, 30]</sup>. Two sets of polymer solutions were prepared. One set was free form bioactive materials (i.e. inorganic calcium) and another set was with bioactive materials (i.e. calcium phosphate, in the form of  $\beta$ -TCP and HA). 25 mL polymer solutions from each bottles were poured into 75 mm diameter petri-dishes and allowed to cool at room temperature (22–25 °C). Finally, smooth, round shaped, off white color BC based scaffold (BC-PVP, BC-CMC) without inorganic calcium/bioactive materials (Diameter: 75 mm; Thickness: 6.0–6.2 mm) and calcium phosphate filled/with bioactive materials (i.e. BC-PVP- $\beta$ -TCP/HA and “BC-CMC-  $\beta$ -TCP/HA) hydrogel scaffolds (Diameter: 75 mm; Thickness: 5.5–6 mm) were achieved.

### 2.2.2. Preparation of calcium phosphate and CaCO<sub>3</sub> filled BC based hydrogel scaffolds

The calcium phosphate and CaCO<sub>3</sub> filled BC based hydrogel scaffolds was prepared following in *vitro* bio-mineralization technique. The calcium phosphate filled hydrogel scaffolds were placed for in *vitro* biomineralization process to incorporate CaCO<sub>3</sub> for the development of stronger bioactive polymeric scaffold material. The in *vitro* bio-mineralization process was performed following the simple liquid diffusion technique<sup>[35]</sup>. Two different ionic solutions (i.e., Na<sub>2</sub>CO<sub>3</sub> and CaCl<sub>2</sub>) were operated at fixed concentration ratios (5.25/100 mL and 7.35/100 mL) to prepare inorganic calcium phosphate and CaCO<sub>3</sub> filled BC based hydrogel scaffolds. Research demonstrated that the deposition and accumulation of CaCO<sub>3</sub> within the hydrogel scaffold are notable between 60–90 min of in *vitro* bio-mineralization<sup>[20]</sup>. Thus, in this study, the bio-mineralization of hydrogel matrix was

performed for 60 mins by keeping the test samples in each ionic solution. The calcium phosphate filled BC based hydrogel scaffolds were first immersed in 100 mL solutions of CaCl<sub>2</sub>. H<sub>2</sub>O for 30 mins and then transferred into 100 mL of Na<sub>2</sub>CO<sub>3</sub> solution and kept them for 30 mins. In this procedure, calcium phosphate and CaCO<sub>3</sub> filled BC based in *vitro* bio-mineralized hydrogel scaffold were achieved (Diameter: 75 mm; Thickness: 4.5–4.9 mm), which are finally termed as “BC-PVP- $\beta$ -TCP/HA-CaCO<sub>3</sub>” and “BC-CMC- $\beta$ -TCP/HA-CaCO<sub>3</sub>” respectively.

## 2.3. Characterization of BC Based hydrogel scaffolds

### 2.3.1. Scanning Electron Microscopy (SEM)

The morphology of the BC based hydrogel scaffolds were established by SEM analysis. The surface and cross sectional structures were discussed. The hydrogel scaffolds were first lyophilized for 24 h, using Scanvac Cool Safe 110-4 PRO, Lyng; lyophilization at –80 °C temperature and 0–5 kPa pressure. Thereafter, the SEM study was performed by “Phenome Pro” (Phenome World, Netherlands) table SEM, operating in the secondary electron imaging mode at an accelerating voltage of 5–20 kV. The image magnification was 100X – 10kX. Additionally, the average pore diameters of the hydrogel scaffold samples were investigated by using Image J software (NIH, USA).

### 2.3.2. Fourier Transform Infrared Spectroscopy (FT-IR)

Fourier Transform Infrared Spectroscopy (FT-IR) analysis of all the BC based hydrogel scaffolds were performed at room temperature at wave number 600–4000 cm<sup>-1</sup> with uniform resolution of 2 cm<sup>-1</sup>. The ATR-FTIR analysis was conducted by using NICOLET 320 FT-IR Spectrophotometer with Omnic software package.

### 2.3.3. Thermal analysis

The thermogravimetric analysis (TGA) of all six different hydrogel scaffolds was done by the TA Q500 apparatus (TA Instruments, USA). The analysis was performed with 8 mg amount of sample with platinum pan, at the constant heating rate of 10 °C/min between the temperature ranges from 25–700 °C under nitrogen atmosphere (50 mL/min).

### 2.3.4. Swelling study

The swelling analysis was performed with physiological saline solution (pH 7.40) at 37 °C ( $\pm 1$  °C). Sections (10 mm<sup>2</sup>) of the hydrogel scaffolds were soaked for specific time intervals (5 min, 60 min, 120 min, 180 min, 240 min, 300 min, 360 min and 1020 min). The absorptivity of the hydrogel scaffolds is measured by the degree of swelling which is defined by the following equation:

$$\text{Degree of swelling (\%)} = \left( \frac{W_s - W_d}{W_d} \right) \times 100$$

Where,  $W_s$  and  $W_d$  are weight of the swollen and dried hydrogel.

Additionally, the equilibrium liquid content (ELC), where the liquid is physiological saline solution; was calculated<sup>[36]</sup> by using following equation:

$$\text{ELC (\%)} = (M_s - M_0 / M_s) \times 100$$

Where,  $M_s$  is the weight of swollen hydrogel at equilibrium.

### 2.3.5. Porosity study

The porosity of the hydrogel samples was examined by liquid displacement method<sup>[37]</sup>. Sections (10 mm<sup>2</sup>) of six studied samples were carefully immersed into absolute ethanol for 48 h until the saturation was reached. The porosity of the samples was calculated by the following equation:

$$P = (W_2 - W_1) / \rho V_1$$

Where,  $W_1$  and  $W_2$  are the weight of the hydrogel scaffolds before and after the immersion into absolute ethanol and  $V_1$  is the volume of the scaffolds before immersion into ethanol,  $\rho$  is the constant of the density of ethanol.

### 2.3.6. Compression study

Compression study was done by using Testometric M350-5CT, England at room temperature (20 °C) with a load cell having a full scale 300 kg. 20 mm diameter sections from freeze dried hydrogel samples were taken for the study. The study was done with a compression rate of 1 mm. min<sup>-1</sup>. The result was expressed as the mean  $\pm$  S.D.

### 2.3.7. Antibacterial study

The antibacterial activity of all BC based hydrogel scaffolds were studied by following agar disc diffusion method<sup>[38]</sup>. The bacteria selected for this study are *Staphylococcus aureus* (*S. aureus* CCM 4516) (Gram + ve bacteria) and *Escherichia coli* (*E. coli* CCM 4517) (Gram - ve bacteria). 100  $\mu$ L of bacterial suspension was used and 8 mm circular specimens were selected from the all the hydrogel samples. The antibacterial study was performed using sterile nutrient agar (2%) medium. Finally, testing plates were then incubated in a temperature controlled incubator at 37 °C for 24 h.

### 2.3.8. Cell biological study

**2.3.8.1. Cell and cell culture.** The human diploid fibroblast cell from the lung of 3 months' normal embryo, Lep-3<sup>[39]</sup> was used as model systems in our study. The cell line was obtained from cell culture collection of the Institute of Experimental Morphology, Pathology and Anthropology with Museum - Bulgarian Academy of Sciences (IEMPAM-BAS), Sofia, Bulgaria.

The cell culture was cultivated in DMEM supplemented with 5–10% fetal bovine serum, 100 U/mL penicillin and 100  $\mu$ g/mL streptomycin. The cultures were kept in a humidified incubator (Thermo Scientific, HEPA Class 100) at 37 °C under 5% CO<sub>2</sub> in air. For routine passages, the adherent cells were detached using a mixture of 0.05% trypsin and 0.02% EDTA. The cell lines were passaged 2–3 times

per week. The experiments were performed during the exponential phase of cell growth.

**2.3.8.2. Cell viability study.** Cell viability was examined with the extract of the sterilized samples of the hydrogel scaffolds. 6 mm circular sections from all BC based hydrogel scaffolds were taken for this study. Sections were placed in the culture plate and treated with 50  $\mu$ L of 96% ethanol and dried in the room temperature (30–32 °C) for 60 min. Then, they were sterilized under the exposure of UV radiation for 80–90 min. Thereafter, 4 mL of DMEM (containing 10% FBS) was given to the wells containing sterilized sample sections and then placed in the humidified incubator at 37 °C under 5% CO<sub>2</sub> in air.

The cells were seeded in 96-well flat-bottomed microplates at a concentration of  $1 \times 10^4$  cells/well. At the 24<sup>th</sup> hour, the culture medium withdrawn and changed with 100  $\mu$ L DMEM containing the extract of the BC based hydrogel scaffolds sections. Cells were further grown in non-modified medium (culture medium control). The effects of the scaffold extract on the cell viability was evaluated using thiazolyl blue tetrazolium bromide (MTT) test, after 72 h, 120 h and 168 h of incubation. The cells were incubated for 180 min of MTT solution (5 mg MTT in 10 mL DMEM) at 37 °C under 5% CO<sub>2</sub> condition. The formed blue MTT formazan was extracted with a mixture of absolute ethanol and DMSO (1:1, v/v).

The quantitative analysis was performed by absorbance measurements in an automated microplate reader (Tecan, Sunrise<sup>TM</sup>, Austria) at 540/620 nm.

## 3. Statistical analysis

The data are presented as mean  $\pm$  standard error of the mean. Statistical differences between control and treated groups, as well as between the studied samples were assessed using one-way analysis of variance (ANOVA) followed by suitable post-hoc test (Dunnnett/Bonferroni) by using GraphPad Prism version 5.00 for Windows, GraphPad Software, San Diego California USA, [www.graphpad.com](http://www.graphpad.com).

## 4. Result and discussion

Inorganic calcium filled BC based hydrogel scaffolds are either filled with calcium phosphate or with both calcium phosphate and CaCO<sub>3</sub>. These novel biomaterials/scaffolds were designated as “BC-PVP- $\beta$ -TCP/HA”, “BC-CMC- $\beta$ -TCP/HA”, “BC-PVP- $\beta$ -TCP/HA-CaCO<sub>3</sub>”, and “BC-CMC- $\beta$ -TCP/HA-CaCO<sub>3</sub>” respectively. The “BC-PVP” and “BC-CMC” scaffolds were considered as control set of scaffolds. To analyze the structure, function and biological efficiency of these scaffolds, the following investigations were performed and discussed below.

### 4.1. Scanning electron microscopy

The morphological structures (surface, cross section and porosity) of BC based hydrogel scaffolds were analyzed and

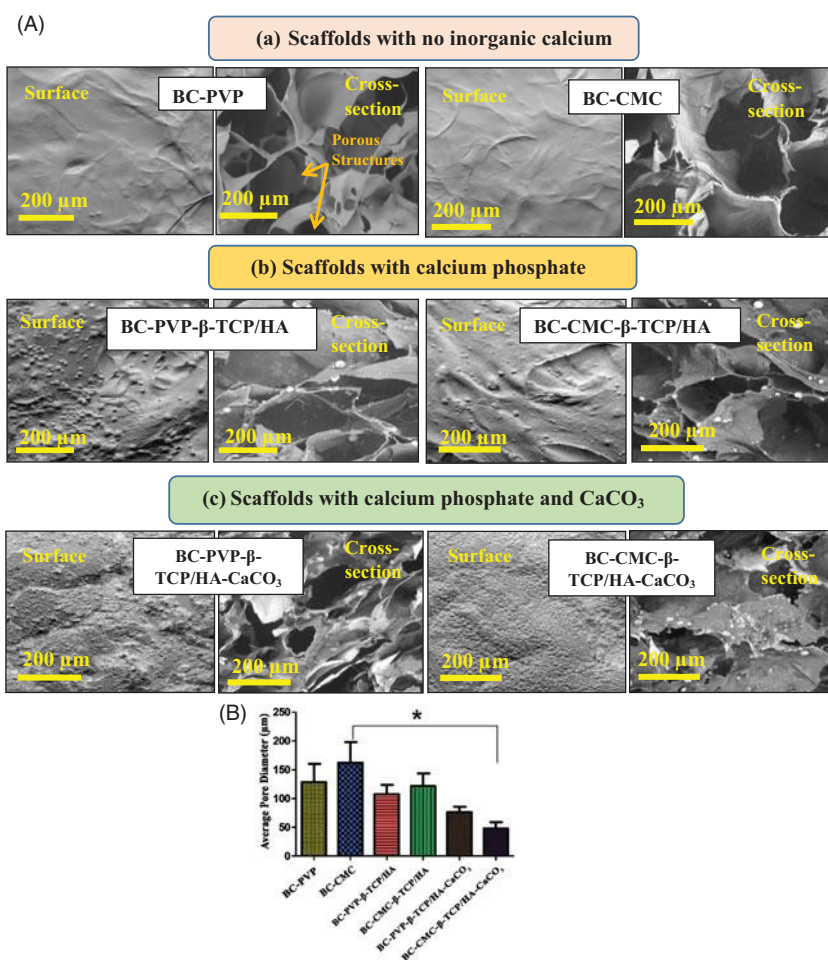


**Figure 2.** (A) SEM image of BC based hydrogel scaffolds: (a) scaffold with no inorganic calcium: BC-PVP and BC-CMC; (b) Scaffold with calcium phosphate: BC-PVP-β-TCP/HA, BC-CMC-β-TCP/HA, (c) Scaffold with calcium phosphate and CaCO<sub>3</sub>: BC-PVP-β-TCP/HA-CaCO<sub>3</sub>, and BC-CMC-β-TCP/HA-CaCO<sub>3</sub>. (B) The average pore diameters of all six the BC based hydrogel scaffolds. Pore diameter of scaffold without inorganic calcium (BC-CMC) is significantly (\**P* < .05) higher than the biomineralized scaffold (BC-CMC-β-TCP/HA-CaCO<sub>3</sub>).

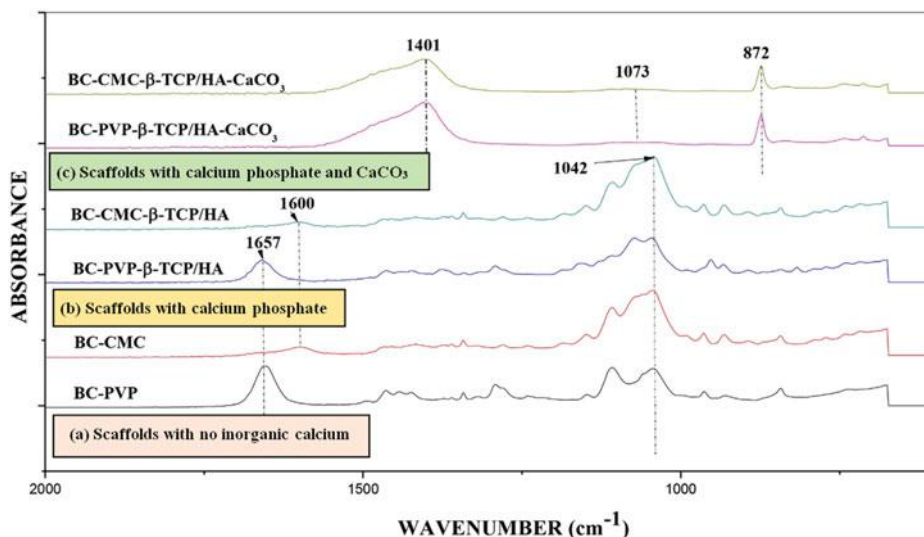


**Figure 3.** FTIR spectra of BC based hydrogel scaffolds: (a) scaffold with no inorganic calcium: BC-PVP and BC-CMC; (b) Scaffold with calcium phosphate: BC-PVP-β-TCP/HA, BC-CMC-β-TCP/HA (c) Scaffold with calcium phosphate and CaCO<sub>3</sub>: BC-PVP-β-TCP/HA-CaCO<sub>3</sub>, and BC-CMC-β-TCP/HA-CaCO<sub>3</sub>.

illustrated in Figure 2. It can be observed from Figure 2A, that the surface structure of BC-PVP and BC-CMC hydrogels is much smoother than the surfaces of inorganic calcium filled BC based hydrogel scaffolds. Moreover, surfaces

of BC-PVP-β-TCP/HA and BC-CMC-β-TCP/HA scaffolds are comparatively smoother than the surface of biomineralized hydrogel scaffolds. Significant rough surface of these scaffold is attributed due to the deposition of further CaCO<sub>3</sub>

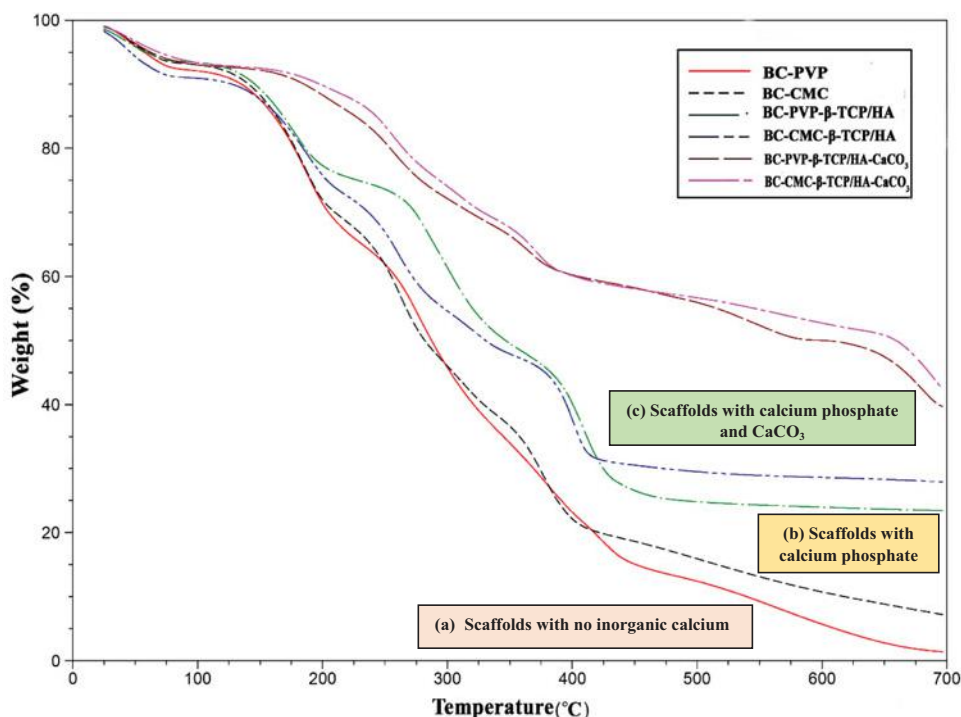


**Figure 4.** The TG analysis of different BC based hydrogel scaffolds: (a) Scaffold with no inorganic calcium: BC-PVP, BC-CMC, (b) Scaffold with calcium phosphate: BC-PVP- $\beta$ -TCP/HA, BC-CMC- $\beta$ -TCP/HA (c) Scaffold with calcium phosphate and  $\text{CaCO}_3$ : BC-PVP- $\beta$ -TCP/HA- $\text{CaCO}_3$ , and BC-CMC- $\beta$ -TCP/HA- $\text{CaCO}_3$ .

into the calcium phosphate filled hydrogel scaffolds during *in vitro* bio-mineralization process. On the other hand, cross sectional images of BC based scaffolds were confirmed that all these biomaterials are comprised of substantially porous structures. The average pore diameter of calcium phosphate filled hydrogel scaffolds is comparatively less than the BC-PVP and BC-CMC hydrogel scaffolds. This is due to the accumulation of calcium phosphate within BC-PVP or BC-CMC blend polymeric biomaterials, as showed in the Figure 2A. The average pore diameter of all the six BC based hydrogel scaffolds are ranging from 50–200  $\mu\text{m}$ . However, the average pore diameter of non-mineralized hydrogel scaffolds is 100–200  $\mu\text{m}$ . The additional deposition of  $\text{CaCO}_3$  is the cause of a decrease in pore size further. The pore diameter of BC-CMC hydrogel was significantly higher ( $P < .05$ ) than the biomineralized BC-CMC- $\beta$ -TCP/HA- $\text{CaCO}_3$  (Figure 2B). On the basis of difference in pore diameter, the hydrogel scaffolds were classified as follows: BC-PVP, BC-CMC > BC-PVP- $\beta$ -TCP/HA, BC-CMC- $\beta$ -TCP/HA > BC-PVP- $\beta$ -TCP/HA- $\text{CaCO}_3$ , BC-CMC- $\beta$ -TCP/HA- $\text{CaCO}_3$ . Research indicated that the tissue engineering scaffold with a pore diameter of 100  $\mu\text{m}$  and above is important for its efficiency<sup>[40,41]</sup>. Thus, the morphological study confirmed the significant applicability of BC based hydrogel scaffolds in regard to their effect.

#### 4.2. Fourier Transform Infrared Spectroscopy (FT-IR)

FT-IR analysis of all BC based hydrogel scaffolds is shown in Figure 3. Here, the data represented in the range between 600–2000  $\text{cm}^{-1}$ , as all the notable bands and peaks were revealed in this region. The FT-IR spectra exhibit characteristic bands of bond stretching patterns for C–O, C=O groups.

Research indicated that cellulose and its carboxymethyl derivative, CMC contain very similar functional groups with the same absorption band for the C–O bond stretching in FTIR analysis<sup>[42]</sup>. The peak at 1042  $\text{cm}^{-1}$  and band at 1073  $\text{cm}^{-1}$  correspond to the C–O bond stretching is caused by the presence of cellulose<sup>[42]</sup>. Additionally, the absorption band at 1600  $\text{cm}^{-1}$  in CMC containing hydrogel scaffolds (BC-CMC, BC-CMC- $\beta$ -TCP/HA) is typical for CMC<sup>[43]</sup>. On the other hand, the peak at 1657  $\text{cm}^{-1}$  indicates the C=O stretching of pyrrolidone, confirming the existence of PVP. This similar type of result was also reported by Kesavan et al.<sup>[44]</sup> and Shah et al.<sup>[45]</sup>. The potential interaction of calcium phosphate with the extra ingredients mask the functional groups of calcium phosphate. However, significant peaks at 1401  $\text{cm}^{-1}$  and at 872  $\text{cm}^{-1}$  in BC-PVP- $\beta$ -TCP/HA- $\text{CaCO}_3$ , and BC-PVP- $\beta$ -TCP/HA- $\text{CaCO}_3$  indicate the notable presence and interaction of  $\text{CO}_3^{2-}$  group with other components<sup>[46,47]</sup>. In some cases, some peaks in FTIR can be masked by the strong band peaks<sup>[48]</sup>. During the *in vitro* biomineralization for 60–90 min, the  $\text{CaCO}_3$  mineral is deposited on the surface of the hydrogel scaffold and the mineral also gradually nucleated on the polymer chains. Thus, there is a high possibility to mask the presence of phosphate due to higher concentration of  $\text{CaCO}_3$ . This is evident with the FTIR results where the significant peaks at 1401  $\text{cm}^{-1}$  and at 872  $\text{cm}^{-1}$  for  $\text{CaCO}_3$  is clearly visible. Moreover, the band at 3352  $\text{cm}^{-1}$  (not shown in the range of depicted in Figure 3) is the characteristics of a hydroxyl group (-OH) stretching<sup>[45, 49]</sup>.

#### 4.3. Thermogravimetric Analysis (TGA)

The rate of mass change as a function of temperature of six separate BC based hydrogel scaffolds is shown in the

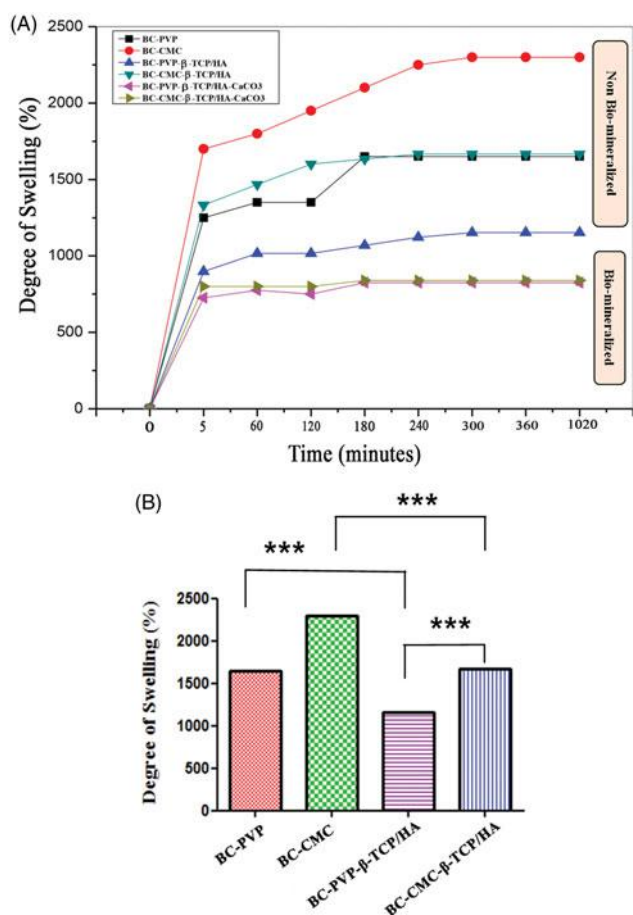


**Figure 5.** (A) Swelling effect of BC based hydrogel scaffolds (BC-PVP, BC-CMC, BC-PVP-β-TCP/HA, BC-CMC-β-TCP/HA, BC-PVP-β-TCP/HA-CaCO<sub>3</sub>, and BC-CMC-β-TCP/HA-CaCO<sub>3</sub>). (B) The degree of swelling of BC-CMC hydrogel scaffolds is significantly higher than BC-CMC-β-TCP/HA. Additionally, the degree of swelling of BC-PVP is also higher than BC-PVP-β-TCP/HA. On the other hand, swelling degree is found higher with BC-CMC-β-TCP/HA than BC-PVP-β-TCP/HA. Asterisk (\*\*\*) indicates level of significance at  $P < .0001$ ; where  $n = 3$ .

**Figure 4.** It can be seen from the figure that the initial stage of decomposition up to 150 °C shows the moisture loss from all the six hydrogels. The second stage exhibits the decomposition (nearly 57.07% weight losses) of bacterial cellulose (BC) at 300–350 °C<sup>[50]</sup>. In addition to it, the decomposition of CMC (nearly 80.59% weight loss) also occurred at 300–400 °C. Furthermore, significant weight loss of PVP generally starts from 200 °C, up to 400 °C<sup>[45, 51]</sup>. On the other hand, the pyrolytic decomposition of inorganic calcium present at high temperature. For calcium phosphate filled BC based hydrogel scaffolds, the significant weight loss profile was seen between 200 °C to 400 °C. This indicates the decomposition of calcium phosphate (especially hydroxyapatite) in between that temperature range, which was comparable with earlier research report<sup>[52]</sup>. Again, for the calcium phosphate & CaCO<sub>3</sub> filled bio-mineralized hydrogel scaffolds, the TG profile is not similar to the calcium phosphate filled hydrogels. This might arise from the significant distribution of CaCO<sub>3</sub> along with the calcium phosphate throughout the polymeric matrix. The thermal breakdown of CaCO<sub>3</sub> requires a higher temperature (i.e., over 700 °C)<sup>[53]</sup>. It can be also seen from the figure that there very less thermal breakdown was occurred until

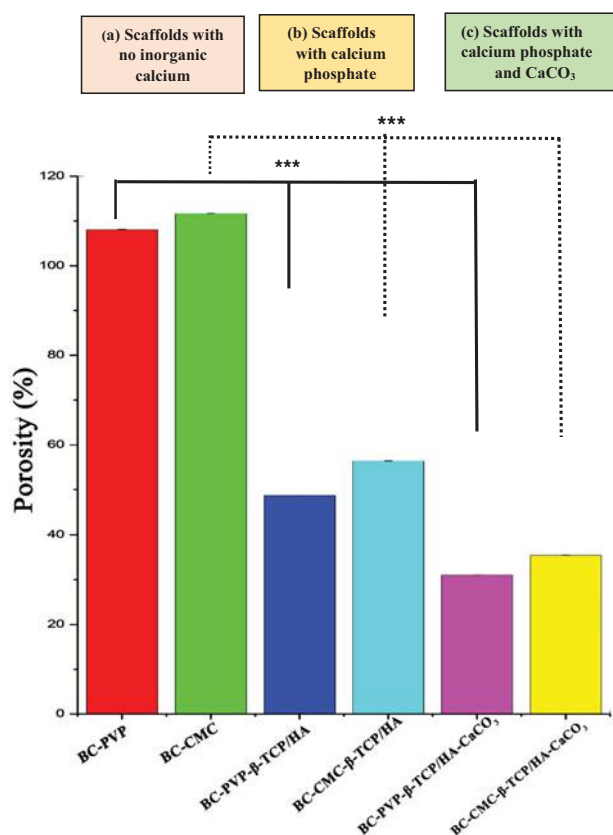


**Figure 6.** Percentage of porosity of different BC based hydrogel scaffolds: (a) Scaffold with no inorganic calcium: BC-PVP, BC-CMC, (b) Scaffold with calcium phosphate: BC-PVP-β-TCP/HA, BC-CMC-β-TCP/HA (c) Scaffold with calcium phosphate and CaCO<sub>3</sub>: BC-PVP-β-TCP/HA-CaCO<sub>3</sub>, and BC-CMC-β-TCP/HA-CaCO<sub>3</sub>. Asterisk (\*\*\*) indicates the significant difference ( $P < .0001$ ;  $n = 3$ ) of porosity among the BC based hydrogel samples. Regular line indicates relation between BC-PVP based scaffolds and dotted line indicates BC-CMC based scaffolds.

700 °C. Thus, the high concentration of inorganic calcium of biomineralized hydrogel matrices went thermal decomposition at high temperature (>700 °C).

#### 4.4. Swelling study

The swelling characteristics with physiological saline solution (pH 4.2, 37 °C ± 1 °C) of six different BC based hydrogel samples is indicated in Figure 5. The study was performed for 17 h to confirm the equilibrium rate of absorptivity of the hydrogel samples. As can be seen from the Figure 5A that the degree of swelling of BC-CMC scaffold was significant ( $P < .001$ ). This hydrogel scaffold is reached at equilibrium nearly after 5 h, whereas BC-PVP scaffold reached at equilibrium nearly after 3 h. Additionally, it can also be seen that, the degree of swelling is higher ( $P < .001$ ) for calcium phosphate filled hydrogels than both calcium phosphate and CaCO<sub>3</sub> filled bio-mineralized hydrogel. However, the degree of swelling of the bio-mineralized hydrogels is lower than the BC-PVP and BC-CMC hydrogel. Moreover, the biomineralized samples took nearly 3 h to arrive at the equilibrium swelling. Additionally, these biomineralized scaffolds reach to nearly equilibrium level after 5 min, whereas calcium phosphate filled hydrogel scaffolds were showing a significant increase ( $P < .0001$ ) at the same time duration. In

**Table 2.** The compressive strength (MPa) of inorganic calcium filled BC based hydrogel scaffolds.

BC based hydrogel scaffolds		Compressive Strength (MPa)
Scaffold with no inorganic calcium	BC-PVP	0.21 ± 0.02
	BC-CMC	0.20 ± 0.03
Scaffold with calcium phosphate	BC-PVP-β-TCP/HA	0.31 ± 0.01
	BC-CMC-β-TCP/HA	0.24 ± 0.007
Scaffold with calcium phosphate and CaCO <sub>3</sub>	BC-PVP-β-TCP/HA-CaCO <sub>3</sub>	0.50 ± 0.03
	BC-CMC-β-TCP/HA-CaCO <sub>3</sub>	0.60 ± 0.01

context of degree of swelling, it is relevant to mention that the compositions of all hydrogels contain agar. Agar is a hydrophilic polymer<sup>[33]</sup>. Thus, the hydrophilic nature of agar could further increase the degree of swelling of BC-PVP β-TCP/HA) and BC-CMC- β-TCP/HA hydrogel scaffolds. However, this effect can not be seen in *In vitro* bio-mineralized hydrogel scaffolds due to the deposition of CaCO<sub>3</sub> which reduces the degree of swelling. The deposition of high concentration of inorganic calcium to the crosslinking polymeric network affects notably the swelling capacity of the bio mineralized hydrogels. Thus, for bio-mineralized samples, although the equilibrium swelling reached early, but the degree of swelling is not significant. Research showed that increased polymeric interaction contributes the water or solution absorbance/retention ability of hydrogel scaffold<sup>[20, 54]</sup>. Interestingly, PVP has low water absorption capacity<sup>[55, 56]</sup>. CMC blended with BC increases the absorption capacity of the CMC containing hydrogel scaffolds (BC-CMC, BC-CMC-β-TCP/HA), compared to the PVP containing hydrogels (BC-PVP, BC-PVP-β-TCP/HA) (Figure 5B). The significant absorptivity is majorly attributed by BC in PVP containing hydrogels<sup>[26]</sup>.

Furthermore, all the six hydrogels retain a high amount of physiological saline solution. The ELC of BC-CMC hydrogel is sizeable (95.83 ± 0.0131) at its equilibrium swelling condition. Additionally, the ELC of BC-PVP-β-TCP/HA (92.01 ± 0.01) and BC-CMC-β-TCP/HA (94.34 ± 0.02) are also notable. The scaffolds, BC-PVP-β-TCP/HA-CaCO<sub>3</sub> (89.18 ± 0.05), BC-CMC-β-TCP/HA-CaCO<sub>3</sub> (89.36 ± 0.01) also showed high liquid (physiological saline solution) retention ability.

#### 4.5. Porosity study

Porosity of the six BC based scaffolds are shown in Figure 6. As it can be seen from the figure that BC-PVP to BC-PVP-β-TCP/HA-CaCO<sub>3</sub> and BC-CMC to BC-CMC-β-TCP/HA-CaCO<sub>3</sub> hydrogel scaffolds, the percentage of porosity were gradually decreasing. Additionally, the porosity of calcium phosphate filled BC based hydrogel scaffold is significantly ( $P < .0001$ ) different than the calcium phosphate and CaCO<sub>3</sub> filled BC based biomaterialized hydrogel scaffolds: for BC-PVP based scaffolds: BC-PVP > BC-PVP-β-TCP/HA > BC-PVP-β-TCP/HA-CaCO<sub>3</sub> and for BC-CMC based scaffolds: BC-CMC > BC-CMC-β-TCP/HA > BC-CMC-β-TCP/HA-CaCO<sub>3</sub>. Calcium phosphate particles were distributed throughout the polymer matrix and filling up the space of the porous structures. Moreover, *in vitro* bio mineralization causes the further deposition of CaCO<sub>3</sub> near the porous structures which in turn influence the porosity and pore size of the bio mineralized samples.

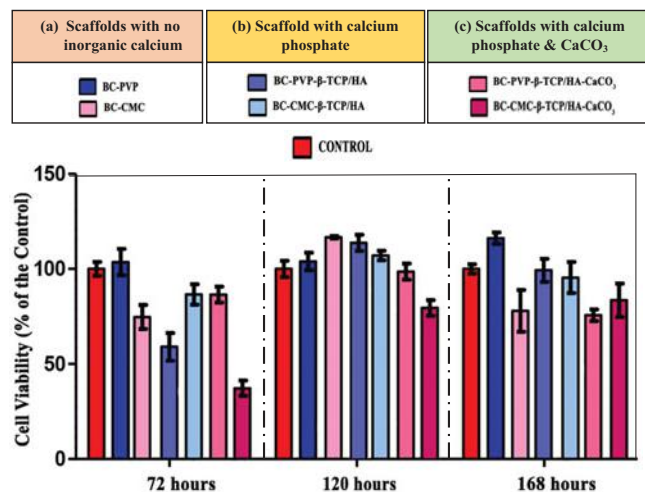


**Figure 7.** The cell viability profile of Lep-3 cells (after 72 h, 120 h and 168 h of incubation) in presence of extract of BC based hydrogel scaffolds: (a) scaffold with no inorganic calcium: BC-PVP and BC-CMC; (b) Scaffold with calcium phosphate: BC-PVP-β-TCP/HA, BC-CMC-β-TCP/HA (c) Scaffold with calcium phosphate and CaCO<sub>3</sub>: BC-PVP-β-TCP/HA-CaCO<sub>3</sub>, and BC-CMC-β-TCP/HA-CaCO<sub>3</sub>.

#### 4.6. Compression study

Mechanical property of all six different BC based hydrogel scaffolds are depicted in Table 2. Research reported that, the compressive strength of the trabecular bone ranged from 0.22 to 10.44 MPa<sup>[57]</sup>. As it can be observed in the table, the calcium phosphate filled hydrogel scaffolds and calcium phosphate & CaCO<sub>3</sub> filled BC based *in vitro* bio-mineralized hydrogel scaffolds are showing similar compressive strength values like the trabecular or cancellous bones. This might be explained the presence of inorganic fillers like calcium phosphate and CaCO<sub>3</sub> within the scaffolds. The compressive strength of all BC based scaffolds (Table. 2) can be categorized as follows: BC-PVP, BC-CMC < BC-PVP-β-TCP/HA, BC-CMC-β-TCP/HA < BC-PVP-β-TCP/HA-CaCO<sub>3</sub>, and BC-CMC-β-TCP/HA-CaCO<sub>3</sub>. The CaCO<sub>3</sub> deposition of *in vitro* bio-mineralization process within the calcium phosphate filled BC based scaffold slightly changes the compressive strength of them compared to only calcium phosphate filled BC based hydrogel scaffold.

#### 4.7. Antibacterial study

Antibacterial study showed that there no clear zone of inhibition in the presence of BC based hydrogel scaffolds with *E. coli*. However, BC-PVP and BC-CMC were shown a faint zone of inhibition with *S. aureus*. Interestingly, BC-CMC-β-TCP/HA-CaCO<sub>3</sub> hydrogel showed notable zone of inhibition with *S. aureus*. However, BC-CMC-β-TCP/HA

scaffold did not show any significant antibacterial property. Previous study indicated that  $\text{CaCO}_3$  has notable antibacterial activity<sup>[58]</sup>. Moreover, studies also showed that  $\text{Ca}^{2+}$ -ion has the significant ability to disrupt the membrane of *S. aureus* but does not show any similar effect on the *E. coli*<sup>[59]</sup>. The BC-CMC- $\beta$ -TCP/HA- $\text{CaCO}_3$  scaffolds contains a high concentration of  $\text{Ca}^{2+}$ -ion, which provides a notable antibacterial activity to it, specifically against the *S. aureus*. On the other hand, the antibacterial activity was not found for BC-PVP- $\beta$ -TCP/HA- $\text{CaCO}_3$  with *S. aureus*. This might have resulted from a possible introduction of potential chemical modifications within the compositional ingredients which result in the loss of the antibacterial ability<sup>[60]</sup>.

#### 4.8. Cell viability study

The cell viability of six different BC based hydrogel scaffolds showed in Figure 7. The study was performed in three separate time intervals i.e., 72 h, 120 h and 168 h. As can be seen from the Figure 7, the cell viability with BC-PVP remained notable than the other hydrogel scaffolds from 72 h to 168 h of incubation. However, the cell viability with BC-PVP in 168 h incubation is seen higher than 72 h and 120 h duration. Polymer like BC, PVP, and CMC have significant biocompatibility. BC together with PVP or CMC may provide the combinatorial stimulated biological effect on the cells, which ultimately reflected in high cellular viability. On the other hand, the cell viability is found more than 90% for BC-PVP- $\beta$ -TCP/HA and BC-CMC- $\beta$ -TCP/HA hydrogel scaffold in both 120 h and 168 h of incubation than 72 h. This might be due to the presence and activity of calcium phosphate. According to earlier studies, calcium phosphate like  $\beta$ -TCP and HA can facilitate osteoconduction, which ultimately results in high cell viability<sup>[61]</sup>. Interestingly, the cell viability is gradually increased from 72 h to 168 h for BC-CMC- $\beta$ -TCP/HA- $\text{CaCO}_3$  and 72 h to 120 h for BC-PVP- $\beta$ -TCP/HA- $\text{CaCO}_3$ . This phenomenon is similar to the assumption of earlier research which indicates  $\text{CaCO}_3$  facilitates cell viability for fibroblasts<sup>[62]</sup>. However, all the BC based hydrogel scaffold showed notable cell viability throughout the study period (72 h, 120 h, and 168 h). In this context, it is relevant to mention that, the Lep-3 cells are embryonic fibroblast cells<sup>[39]</sup> and not specified to elicit a prompt response in the presence of notable calcium content in the surrounding environment like that of the specified bone fibroblast. Thus, through acclimatization with the significant inorganic calcium environment within the DMEM containing scaffold extract, the cells exhibit high viability with the gradually increasing incubation period from 72 h to 168 h.

#### 5. Conclusions

The present work focuses the preparation of novel inorganic calcium filled BC based hydrogel scaffolds which contains calcium phosphate (in the form of  $\beta$ -TCP and HA) and  $\text{CaCO}_3$ . The structure, function and cell biological attributes were thereafter investigated. FTIR and thermal characterization studies prove the presence of the ingredients like BC, PVP,

CMC, inorganic calcium. The SEM study revealed significantly different pore diameters (50–200  $\mu\text{m}$ ) within six different BC based hydrogel samples. Additionally, the degree of swelling of calcium phosphate filled BC based hydrogel samples was found higher than the bio-mineralized samples. Furthermore, inorganic calcium filled BC based hydrogel scaffolds has the similar compressive strength (0.24–0.60 MPa) like the trabecular bones. Moreover, study demonstrated that BC-CMC- $\beta$ -TCP/HA- $\text{CaCO}_3$  has antibacterial property (only for *S. aureus*). Finally, cell viability study demonstrates the cell biological efficiency of inorganic calcium filled BC based hydrogel scaffolds. Thus, inorganic calcium filled BC based hydrogel scaffolds might provide a significant stimulating environment as a bone implant that facilitate the soft bone tissue regeneration process. Generally, the trabecular or cancellous bone are primarily found at the metaphysis region of the femur bone<sup>[63]</sup>. Hence, *inorganic calcium filled bacterial cellulose based hydrogel scaffolds* can be used for the metaphyseal bone regenerations.

#### Disclosure statement

The author declares that there is no conflict of interest.

#### Funding

This work is mainly supported by the Internal Grant Agency (Project No. IGA/CPS/2017/003 and IGA/CPS/2018/008), Tomas Bata University in Zlin, Czech Republic and Ministry of Education, Youth and Sports of The Czech Republic – NPU Program I (LO1504). Moreover, this work was performed within the framework of COST Action MP1301 “New Generation Biomimetic and Customized Implants for Bone Engineering” ([www.cost.eu](http://www.cost.eu)). Authors are thankful to COST Action MP1301 partner institution “Institute of Experimental Morphology, Pathology and Anthropology with Museum-Bulgarian Academy of Sciences (IEMPAM-BAS)”, Sofia, Bulgaria; especially, Assoc. Prof. Radostina Alexandrova as the cell viability and cell proliferation study of inorganic calcium filled hydrogel scaffold was performed under her supervision during STSM visit supported by COST Action MP1301.

#### References

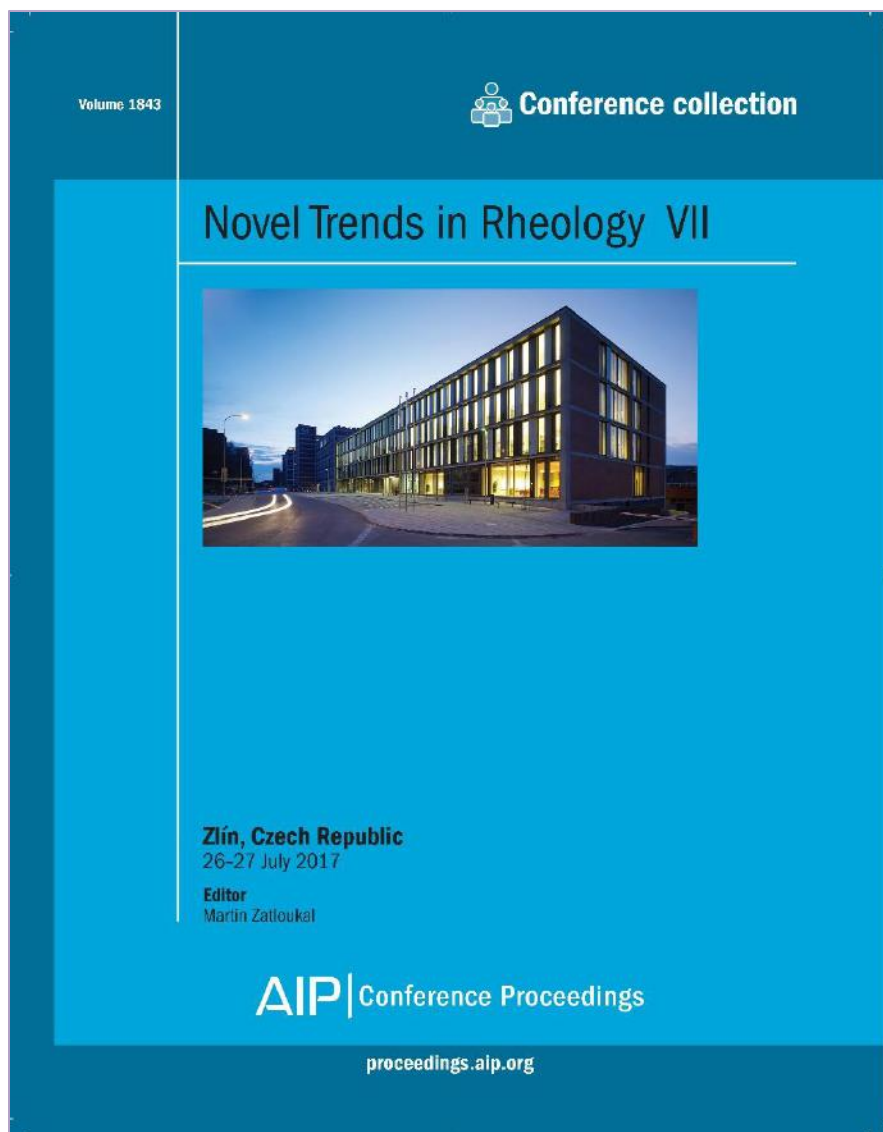
- [1] Kini, U.; Nandeesh, B. N. Physiology of Bone Formation, Remodelling and Metabolism. In *Radionuclide and Hybrid Bone Imaging*, Fogelman et al. Eds.; Springer-Verlag Berlin: Heidelberg, 2012, pp 29–57. doi:10.1007/978-3-642-02400-9\_2
- [2] International Osteoporosis Foundation (IOF), <https://www.iof-bonehealth.org/facts-statistics>, (accessed on 30.08.2017).
- [3] Castilho, M.; Dias, M.; Vorndran, E.; Gbureck, E.; Gbureck, U.; Fernandes, P.; Pires, I.; Gouveia, B. Armes, H.; Pires, E.; et al. *Biofabrication*. 2014, 6(025005), 1–13. doi:10.1088/1758-5082/6/2/025005
- [4] Deligkaris, K.; Tadele, T. S.; Olthuis, W. *Sens Actuators B*. 2010, 147, 765–774. doi:10.1016/j.snb.2010.03.083
- [5] Polo-Corrales, L.; Latorre-Esteves, M.; Ramirez-Vick, J. E. *J. Nanosci. Nanotechnol.* 2014, 14(1), 15–56. doi:10.1166/jnn.2014.9127

- [6] Roy, N.; Saha, N.; Kitano, T.; Saha, P. *Carbohydr Polym.* **2012**, *89*, 346–353. doi:10.1016/j.carbpol.2012.03.008
- [7] Roy, S. G.; De, P. *Polymer.* **2014**, *55*, 5425–5434. doi:10.1016/j.polymer.2014.08.072
- [8] Saha, N.; Shah, R.; Vyroubal, R.; Kitano, T.; Saha, P. *AIP Conf. Proc.* **2013**, *1526*, 292–300. doi: 10.1063/1.4802623.
- [9] Burg, K. J. L.; Porter, S.; Kellam, J. F. *Biomaterials.* **2000**, *21*, 2347–2359. doi:10.1016/S0142-9612 doi:(00)00102-2
- [10] Chan, B. P.; Leong, K. W. *Eur Spine J.* **2008**, *17*(Suppl 4), 467–479. doi:10.1007/s00586-008-0745-3
- [11] Thavornutikarn, B.; Chantarapanich, N.; Sitthiseripratip, K.; Thouas, G. A.; Chen, Q. *Prog. Biomater.* **2014**, *3*, 61–102. doi: 10.1007/s40204-014-0026-7
- [12] Stratton, S.; Shelke, N.B.; Hoshino, K.; Rudraiah, S.; Kumbar, S.G. *Bioact Mater.* **2016**, *1*(2): 93–108. doi:10.1016/j.bioactmat.2016.11.001
- [13] Venkatesan, J.; Jayakumar, R.; Anil, S.; Chalisserry, E. P.; Pallela, R.; Kim, S. J. *Biomater. Tiss. Eng.* **2015**, *5*, 458–464. doi: 10.1166/jbt.2015.1338
- [14] Walimbe, T.; Panitch, A.; Sivasankar, P. M. J. *Voice.* **2017**, *31*(4), 416–423. doi:10.1016/j.voice.2016.11.014.
- [15] Zustiak, S. P.; Wei, Y.; Leach, J. B. *Tissue Eng. Part B Rev.* **2012**, *19*(2), 160–171. doi:10.1089/ten.teb.2012.0458
- [16] Abedalwafa, M.; Wang, F., Wang, L.; Li, C. *Rev. Adv. Mater. Sci.* **2013**, *34*, 123–140.
- [17] Stodolak-Zycha, E.; Frączek-Szczypta, A.; Wiecheć, A.; Błażewicz, M. *Acta Physica Polonica A.* **2012**, *121*(2), 518–521 doi:10.12693/APhysPolA.121.518
- [18] Paluszkiwicz, P.; Weselucha-Birczyn, A.; Stodolak-Zyc, E.; Hasik, M. *Vib. Spectrosc.* **2012**, *60*, 185–188. doi:10.1016/j.vibspec.2011.12.004
- [19] Muthukumar, T.; Aravinthan, A.; Sharmila, J.; Kim, N. M. *Carbohydr. Polym.* **2016**, *152*, 566–574. doi:10.1016/j.carbpol.2016.07.003
- [20] Shah, R.; Saha, N.; Kitano, T.; Saha, P. *J. Appl. Polym. Sci.* **2014**, *40237*, 1–9. doi:10.1002/APP.40237
- [21] del Valle, L. J.; Díaz, A.; Puiggali, J. *Gels.* **2017**, *3*(27), 2–28. doi:10.3390/gels3030027
- [22] Wu, S.; Liu, X.; Yeung, K. W. K.; Liu, C.; Yang, X. *Mater. Sci. Eng. R Rep.* **2014**, *80*, 1–36. doi:10.1016/j.mser.2014.04.001
- [23] Pandey, M.; Mohamad, N.; Iqbal Mohd Amin, M. C. *Mol. Pharm.* **2014**, *11*, 3596–3608. doi:10.1021/mp500337r
- [24] Keshk, S. M. A. S. *J. Bioprocess. Biotech.* **2014**, *4*(2), 1000150. doi:10.4172/2155-9821.1000150
- [25] Shah, R.; Vyroubal, R.; Fei, H.; Saha, N.; Kitano, T.; Saha, P. *AIP Conf. Proc.* **2015**, *1662*, 040007-1–040007-7. doi:10.1063/1.4918895
- [26] Ul-Islam, M.; Khan, T.; Kon Park, J. *Carbohydr. Polym.* **2012**, *88*(2), 596–603. doi:10.1016/j.carbpol.2012.01.006.
- [27] Saha, N.; Shah, R.; Gupta, P.; Mandal, B. B.; Alexandrova, R.; Sikiric, M. D.; Saha, P. *Mater. Sci. Eng. C.* **2018**, Accepted Manuscript. doi:10.1016/j.msec.2018.04.050
- [28] Mohamad, N.; Iqbal Mohd Amin, M.C.; Pandey, M.; Ahmad, N.; Rajab, N. F. *Carbohydr. Polym.* **2014**, *114*, 312–320. doi: 10.1016/j.carbpol.2014.08.025
- [29] Numata, Y.; Kono, H.; Tsuji, M.; Tajima, K. *Carbohydr. Polym.* **2017**, *173*, 67–76. doi:10.1016/j.carbpol.2017.05.077
- [30] Roy, N.; Saha, N.; Kitano, T.; Saha, P. *J. Appl. Polym. Sci.* **2010**, *117*, 1703–1710. doi:10.1002/app.32056
- [31] Basu, P.; Saha, N.; Bandyopadhyay, S.; Saha, P. *AIP Conf. Proc.* **2017**, *1843*, 050008. doi:10.1063/1.4983000
- [32] Alcantar, N. A.; Aydil, E. S.; Israelachvili, J. N. *J. Biomed. Mater. Res.* **2000**, *51*(3), 343–351. doi:10.1002/1097-4636(20000905)51:3 < 343: AID-JBM7 > 3.0.CO;2-D
- [33] Nayak, K. K.; Gupta, P. *Int. J. Biol. Macromol.* **2015**, *81*, 1–10. DOI: doi:10.1016/j.ijbiomac.2015.07.025
- [34] Struillou, X.; Rakic, M.; Badran, Z.; Macquigneau, L.; Colombeix, C.; Pilet, P.; Verner, C.; Gauthier, O.; Weiss, P.; Soueidan, A. *J. Mater. Sci. Mater. Med.* **2013**, *24*, 2749–2760. doi:10.1007/s10856-013-5019-x
- [35] Rauch, M. W.; Dressler, M.; Scheel, H.; Opendbosch, D. V.; Zollfrank, C. *Eur. J. Inorg. Chem.* **2012**, *32*, 5192–5198. doi: 10.1002/ejic.201200575
- [36] Wong, R. S. H.; Ashton, M.; Dodou, K. *Pharmaceutics.* **2015**, *7*, 305–3019. doi:10.3390/pharmaceutics7030305
- [37] Liyun, J.; Yubao, L.; Chengdong, X. *J. Biomed. Sci.* **2009**, *16*(65), 1–10. doi:10.1186/1423-0127-16-65
- [38] Balouiri, M.; Sadiki, M.; Ibsouda, S. K. *J. Pharm. Anal.* **2016**, *6*(2), 71–79. doi:10.1016/j.jpha.2015.11.005
- [39] Dyakova, L.; Culita, D.-C.; Marinescu, G.; Alexandrov, M.; Kalfin, R.; Patron, L.; Alexandrova, R. *Biotechnol. Biotechnol. Equip.* **2014**, *28*(3), 543–551. doi:10.1080/13102818.2014.927973
- [40] Martín, L.; Alonso, M.; Girotti, A.; Arias, F. J.; Rodríguez-Cabello, J. *Biomacromolecules.* **2009**, *10*, 3015–3022. doi: 10.1021/bm900560a
- [41] Roach, P.; Eglin, D.; Rohde, K.; Perry, C. C. *J. Mater. Sci. Mater. Med.* **2007**, *18*, 1263–1277. doi:10.1007/s10856-006-0064-3
- [42] Liu, Y. *Materials.* **2013**, *6*, 299–313. doi:10.3390/ma610299
- [43] Khafizov, M. M. *Int. Polym. Sci. Tech.* **2005**, *32*(12), T5–T7.
- [44] Kesavan, K.; Rajendran, S.; Mathew, C. M. *Polym. Sci. Ser. B.* **2014**, *56*(4), 520–529. doi:10.1134/S1560090414040034
- [45] Shah, R.; Saha, N.; Kuceková, Z.; Humpolicek, P.; Saha, P. *Int. J. Polym. Mater.* **2016**, *65*(12), 619–628. doi:10.1080/00914037.2016.1157793
- [46] Costa, S. N.; Freire, V. N.; Caetano, E. W. S.; Maia, F. F. Jr.; Barboza, C. A.; Fulco, U. L.; Albuquerque, E. L. *J. Phys. Chem. A.* **2016**, *120*, 5752–5765. doi:10.1021/acs.jpca.6b05436
- [47] Habibovic, P.; Barrère, F.; van Blitterswijk, C. A.; de Groot, K.; Layrolle, P. *J. Am. Chem. Soc.* **2002**, *85*(3), 517–522. doi: 10.1111/j.1151-2916.2002.tb00126.x
- [48] Horn, M.; Nienhaus, K.; Nienhaus, G. U. *F1000Research.* **2014**, *3*, 290.
- [49] Thürmer, M. B.; Diehl, C. E.; Brum, F. J. B.; dos Santos, L. A. *Mater. Res.* **2014**, *17*(Suppl. 1), 109–113. doi:10.1590/1516-1439.223613
- [50] Saska, S.; Barud, H. S.; Gaspar, A. M. M.; Marchetto, R.; Ribeiro, S. J. L.; Messaddeq, Y. *Int. J. Biomater.* **2011**, 175362, 1–8. doi:10.1155/2011/175362
- [51] Otsuka, T.; Chujo, Y. *Polym. J.* **2008**, *40*(12), 1157–1163. doi: 10.1295/polymj. PJ2008167
- [52] Liao, C. J.; Lin, F. H.; Chen, S.; Sun, J. S. *Biomaterials.* **1999**, *20*, 1807–1813. doi:10.1016/S0142-9612 (99) 00076-9
- [53] Abdolmohammadi, S.; Siyamak, S.; Ibrahim, N. A.; Md Zin Wan Yunus, W.; Ab Rahman, M. Z.; Azizi, S.; Fatehi, A. *Int. J. Mol. Sci.* **2012**, *13*, 4508–4522. doi:10.3390/ijms13044508
- [54] Sienkiewicz, A.; Krasucka, P.; Charmas, B.; Stefaniak, W.; Goworek, J. *J. Therm. Anal. Calorim.* **2017**, *130*, 85–93. doi: 10.1007/s10973-017-6131-9.
- [55] Roy, N.; Saha, N.; Kitano, T.; Saha, P. *Soft Mater.* **2010**, *8*(2), 130–148. doi:10.1080/15394451003756282
- [56] Singh, R.; Singh, D. *J. Mater. Sci. Mater. Med.* **2012**, *23*(11), 2649–2658. doi:10.1007/s10856-012-4730-3
- [57] Misch, C. E.; Zhimin, Q.; Bidez, M. W. *J. Oral. Maxillofac. Surg.* **1999**, *57*(6), 700–706. doi:10.1016/S0278-2391 (99)90437-8
- [58] Ataee R. A.; Derakhshanpour, J.; Mehrabi Tavana A.; Eydi A. *J. Mil. Med.* **2011**, *13*(2), 65–70. <http://militarymedj.ir/article-1-794-en.html>
- [59] Xie, Y.; Yang, L. *Sci. Rep.* **2016**, *6*, 20628. doi:10.1038/srep20628
- [60] Madkour, A. E.; Dabkowski, J. M.; Nüsslein, K.; Tew, G. N. *Langmuir.* **2009**, *25*(2), 1060–1067. doi:10.1021/la802953v
- [61] Lee, J. H.; Ryu, M. Y.; Baek, H.-R.; Lee, K. M.; Seo, J.-H.; Lee, H.-Y. *Sci. World J.* **2013**, *481789*, 1–9. doi:10.1155/2013/481789
- [62] Kamba, A. S.; Ismail, M.; Ibrahim, T. A. T.; Zakaria, Z. A. B. *Afr. J. Tradit. Complement Altern. Med.* **2014**, *11*(4), 31–38. doi: 10.4314/ajtcam.v11i4.5
- [63] Burr, D. B.; Akkus, O. Bone Morphology and Organization, Chapter 1. In *Basic and Applied Bone Biology*, Burr D, Allen, M., Eds.; Academic Press (Elsevier): USA, **2014**; pp 3–25.



## PUBLICATION II

**Basu P. (50%),** Saha N, Bandyopadhyay S, Saha P. (2017) “Rheological Performance of Bacterial Cellulose based non-mineralized and mineralized hydrogel scaffolds”, *AIP Conference Proceedings of Novel Trends in Rheology VII* (Web of Science Indexed; Book Chapter) 1843, 050008-1–050008-7. DOI: <https://doi.org/10.1063/1.4983000>. ISBN: 978-0-7354-1513-3



Volume 1843

 **Conference collection**

# Novel Trends in Rheology VII

---



**Zlín, Czech Republic**  
26-27 July 2017

**Editor**  
Martin Zatloukal

**AIP** | Conference Proceedings

[proceedings.aip.org](http://proceedings.aip.org)

# Rheological Performance of Bacterial Cellulose based Nonmineralized and Mineralized Hydrogel Scaffolds

Probal Basu<sup>a)</sup>, Nabanita Saha<sup>b)</sup>, Smarak Bandyopadhyay<sup>c)</sup> and Petr Saha<sup>d)</sup>

Centre of Polymer Systems, University Institute, Tomas Bata University in Zlin, Trida Tomase Bati 5678, 760 01 Zlin, The Czech Republic

<sup>a)</sup>probal@cps.utb.cz

<sup>b)</sup>Corresponding author: nabanita@cps.utb.cz

<sup>c)</sup>bandyopadhyay@cps.utb.cz

<sup>d)</sup>saha@utb.cz

**Abstract.** Bacterial cellulose (BC) based hydrogels (BC-PVP and BC-CMC) are modified with  $\beta$ -tri-calcium phosphate ( $\beta$ -TCP) and hydroxyapatite (HA) to improve the structural and functional properties of the existing hydrogel scaffolds. The modified hydrogels are then biomineralized with  $\text{CaCO}_3$  following liquid diffusion technique, where salt solutions of  $\text{Na}_2\text{CO}_3$  (5.25 g/100 mL) and  $\text{CaCl}_2$  (7.35 g/100 mL) were involved. The BC-PVP and BC-CMC are being compared with the non-mineralized (BC-PVP- $\beta$ -TCP/HA and BC-CMC- $\beta$ -TCP/HA) and biomineralized (BC-PVP- $\beta$ -TCP/HA- $\text{CaCO}_3$  and BC-CMC- $\beta$ -TCP/HA- $\text{CaCO}_3$ ) hydrogels on the basis of their structural and rheological properties. The Fourier Transform Infrared (FTIR) spectral analysis demonstrated the presence of BC, CMC, PVP,  $\beta$ -TCP, HA in the non-mineralized and BC, CMC, PVP,  $\beta$ -TCP, HA and  $\text{CaCO}_3$  in the biomineralized samples. Interestingly, the morphological property of non-mineralized and biomineralized, hydrogels are different than that of BC-PVP and BC-CMC based novel biomaterials. The Scanning Electron Microscopic (SEM) images of the before mentioned samples reveal the denser structures than BC-PVP and BC-CMC, which exhibits the changes in their pore sizes. Concerning rheological analysis point of view, all the non-mineralized and biomineralized hydrogel scaffolds have shown significant elastic property. Additionally, the complex viscosity ( $\eta^*$ ) values have also found in decreasing order with the increase of angular frequency ( $\omega$ ) 0.1  $\text{rad}\cdot\text{sec}^{-1}$  to 100  $\text{rad}\cdot\text{sec}^{-1}$ . All these BC based hydrogel scaffolds are elastic in nature, can be recommended for their application as an implant for bone tissue engineering.

## INTRODUCTION

Viscoelasticity represents a combinatorial properties of viscosity and elasticity of a material with the parallel contribution of each being dependent on time, temperature, stress and strain rate [1]. The viscoelastic property of a biomaterial is significantly contingent upon composition and the concentration of the administered material as well as the preparation condition of the hydrogels. [1,2]. Viscoelastic properties of hydrogel scaffold correspond significantly with its microstructures and might give useful information for modulating their performance characteristics [3]. Bacterial cellulose (BC) is a cellulose, which has a wide ranging applications. BC has been produced by *Gluconacetobacter xylinus* (*syn. Acetobacter xylinum*), a gram negative, aerobic bacterium which uses a wide range of carbon and nitrogen source from the growth medium and produce a pellicle of cellulose on the surface of the medium [4]. Due to its significant mechanical strength and biocompatibility, it has a notable demand in the field of biomedical research [5]. Tissue of human bone is a viscoelastic material. This property is responsible for its significant toughness and strength [6]. The hydrogel scaffold with significant elastic property will ensure its efficiency as a bone implant material. Thus, the hydrogel scaffolds become a poignant interest for researchers working in bone tissue engineering [7]. Hydrogels are the three dimensional polymeric network structure containing pores and facilitate the growth of inorganic minerals by providing an efficient structural framework [8]. Researchers of Center of Polymer systems, University Institute, Tomas Bata University in Zlin have already reported the rheological characteristics of “BC-PVP” and “BC-CMC” hydrogels in their previous studies. In the present study,

these bacterial cellulose (BC) based hydrogels are modified with  $\beta$ -tri-calcium phosphate ( $\beta$ -TCP) and hydroxyapatite (HA) to improve the structural and functional properties of the existing hydrogel scaffolds. The modified hydrogels are then biomineralized for the formation of calcium carbonate ( $\text{CaCO}_3$ ), a natural biomineral. The modified/non-mineralized BC based hydrogels are designated as “BC-PVP- $\beta$ -TCP/HA” and “BC-CMC- $\beta$ -TCP/HA” and the biomineralized scaffolds are termed as “BC-PVP- $\beta$ -TCP/HA- $\text{CaCO}_3$ ” and “BC-CMC- $\beta$ -TCP/HA- $\text{CaCO}_3$ ” respectively. The BC-PVP and BC-CMC scaffolds are being compared with the BC-PVP- $\beta$ -TCP/HA, BC-CMC- $\beta$ -TCP/HA, BC-PVP- $\beta$ -TCP/HA- $\text{CaCO}_3$  and BC-CMC- $\beta$ -TCP/HA- $\text{CaCO}_3$  on the basis of their structural and rheological properties. The present work is an endeavor to study the viscoelastic and the structural properties of all the six different BC based hydrogels.

## EXPERIMENTAL

The BC based hydrogels were prepared by using the polymers: BC suspension (particle size: 250 nm), dry polyvinylpyrrolidone (PVP) and carboxymethylcellulose (CMC).  $\beta$ -Tri-Calcium Phosphate ( $\beta$ -TCP) and Hydroxyapatite (HA) were added to achieve calcium phosphate filled composite biomaterials. These calcium phosphate filled wet hydrogels were then biomineralized for 60 minutes following liquid diffusion technique [7], where salt solutions of  $\text{Na}_2\text{CO}_3$  (5.25 g/100 mL) and  $\text{CaCl}_2$  (7.35 g/100 mL) were involved and finally get  $\text{CaCO}_3$  filled novel biomaterials. PVP, a synthetic polymer, has a variety of applications in the pharmaceutical and biomedical field because of high absorption capacity and high mechanical property [9,10]. Whereas, CMC is an ether derivative of cellulose used in the field of foods, cosmetics and paint as a viscosity modifier, thickener and water retention agent [11].  $\beta$ -Tri-Calcium Phosphate ( $\beta$ -TCP) has considered as an attractive additive/compound for bone tissue engineering because of its efficient biocompatibility, biosafety and long shelf life.  $\beta$ -TCP exhibit an excellent balance in absorption, degradation [12]. Moreover, HA is generally used as a bone filling material [13]. The  $\beta$ -TCP and HA added in the ratio of 20:80 [14].

All the chemicals used in this study are AR grade and purchased from Sigma-Aldrich. The BC mat (holding 99%  $\text{H}_2\text{O}$ ), obtained from the microbiological laboratory of the Centre of Polymer System, Tomas Bata University in Zlin, was synthesized in presence of basal synthetic HS nutritive medium using *Gluconacetobacter xylinus* CCM 3611<sup>T</sup>. The composition of the polymeric solutions for each hydrogel scaffolds are described in Table 1.

**TABLE 1.** Composition of BC-PVP, BC-CMC and  $\beta$ -TCP/HA filled BC based hydrogel scaffold.

Sample index	PVP (g)	CMC (g)	BC (g)	PEG (g)	AGAR (g)	GLYCERINE (mL)	$\beta$ -TCP/HA (g)	Water (mL)
BC-PVP	0.5	0.0	0.5	1	2	1	0.0/0.0	95
BC-CMC	0.0	0.5	0.5	1	2	1	0.0/0.0	95
BC-PVP $\beta$ -TCP/HA	0.5	0.0	0.5	1	2	1	0.2/0.8	94
BC-CMC- $\beta$ -TCP/HA	0.0	0.5	0.5	1	2	1	0.2/0.8	94

The BC based hydrogels mentioned in Table 1 were prepared following the solvent casting technique [15]. The polymer solutions were treated under moist heat and pressure (15 lbs pressure and 120°C temperature) for 20 minutes in a sealed glass bottle. The 30 mL polymer solution was poured into 75 mm diameter petri-dishes and allowed to cool at room temperature (22-25°C) for 5-10 minutes. Finally, smooth, round shaped and off white (diameter: 75 mm; thickness: 5.5-6.0 mm) hydrogel scaffolds were obtained. The  $\beta$ -TCP/HA filled BC based hydrogel scaffold were selected for biomineralization for further incorporation of additional  $\text{CaCO}_3$  for the development of more stiff and strong bioactive polymeric material as an implant for bone tissue regeneration. Finally, soft, smooth, round shaped milky white (diameter:75mm; thickness: 1.8-2.4 mm) hydrogel scaffolds were achieved.

The structural analysis of hydrogel scaffolds had done by ATR-FTIR spectroscopy by using NICOLET 320 FTIR Spectrophotometer with “Omic” software package with the Germanium ATR crystal within the wave number of 600–4000  $\text{cm}^{-1}$  at room temperature. The morphological characteristics of all of the hydrogel samples were ascertained by scanning electron microscopy (SEM). The analysis has done with “Phenome Pro” (PhenomeWorld, Netherlands) SEM, operating in the electron imaging mode at an accelerating voltage of 5-20 kV. The images were taken at a magnification of 100X – 10kX.

The nonmineralized i.e. BC-PVP, BC-CMC and  $\beta$ -TCP/HA filled BC based hydrogel scaffold and biomineralized ( $\text{CaCO}_3$ ) incorporated  $\beta$ -TCP/HA filled BC based hydrogel scaffolds (at before dry state) were measured to evaluate their viscoelastic properties. The viscoelastic properties of the hydrogel samples were studied

by using a modular compact rheometer testing device (Anton Paar, Austria) and “Rheoplus” software package for data analysis. A 20 mm diameter parallel plate measuring geometry with a gap between the plates adjusted according to the sample thickness (5.5-6.0 mm for nonmineralized hydrogel and 1.8-2.4 mm for mineralized hydrogel). Dynamic frequency sweep analyses were conducted at room temperature to obtain the storage ( $G'$ ) and loss ( $G''$ ) modulus and complex viscosity ( $\eta^*$ ). The measurement had done in the oscillation mode with the angular frequency range from 0.1 to 100  $\text{rad}\cdot\text{s}^{-1}$  at 1% strain amplitude. The influence of angular frequency and mineralization on storage ( $G'$ ) and loss ( $G''$ ) modulus and complex viscosity ( $\eta^*$ ) will be calculated by the following equation:

$$\eta^* = [(G'/\omega)^2 + (G''/\omega)^2]^{1/2} \quad (1)$$

## RESULTS AND DISCUSSION

### Structural Analysis of BC based Nonmineralized and Bio-mineralized Hydrogel Scaffold

The morphological (surface and cross section) images of BC-PVP and BC-CMC hydrogels (before modification and biomineralization); BC-PVP- $\beta$ -TCP/HA and BC-CMC- $\beta$ -TCP/HA hydrogels (after modification and before mineralization); PVP-BC- $\beta$ -TCP/HA/ $\text{CaCO}_3$  and CMC-BC- $\beta$ -TCP/HA- $\text{CaCO}_3$  hydrogels (after biomineralization) are shown in Fig. 1. It can be seen from SEM images that the surfaces of the PVP-BC and BC-CMC hydrogels are smoother than the surfaces of the other hydrogels. This can be a result of the aggregation of the BC particles in the CMC-BC and PVP-BC hydrogels. However, the visible coarse surfaces of PVP-BC- $\beta$ -TCP/HA, CMC-BC- $\beta$ -TCP/HA hydrogels and biomineralized ( $\text{CaCO}_3$ ) hydrogels confirm the presence of  $\beta$ -TCP, HA, and  $\text{CaCO}_3$  respectively within the hydrogel scaffolds. On the other hand, the observed porous structures in the SEM images (cross section) confirmed that the resultant scaffolds are nothing but polymeric hydrogel.

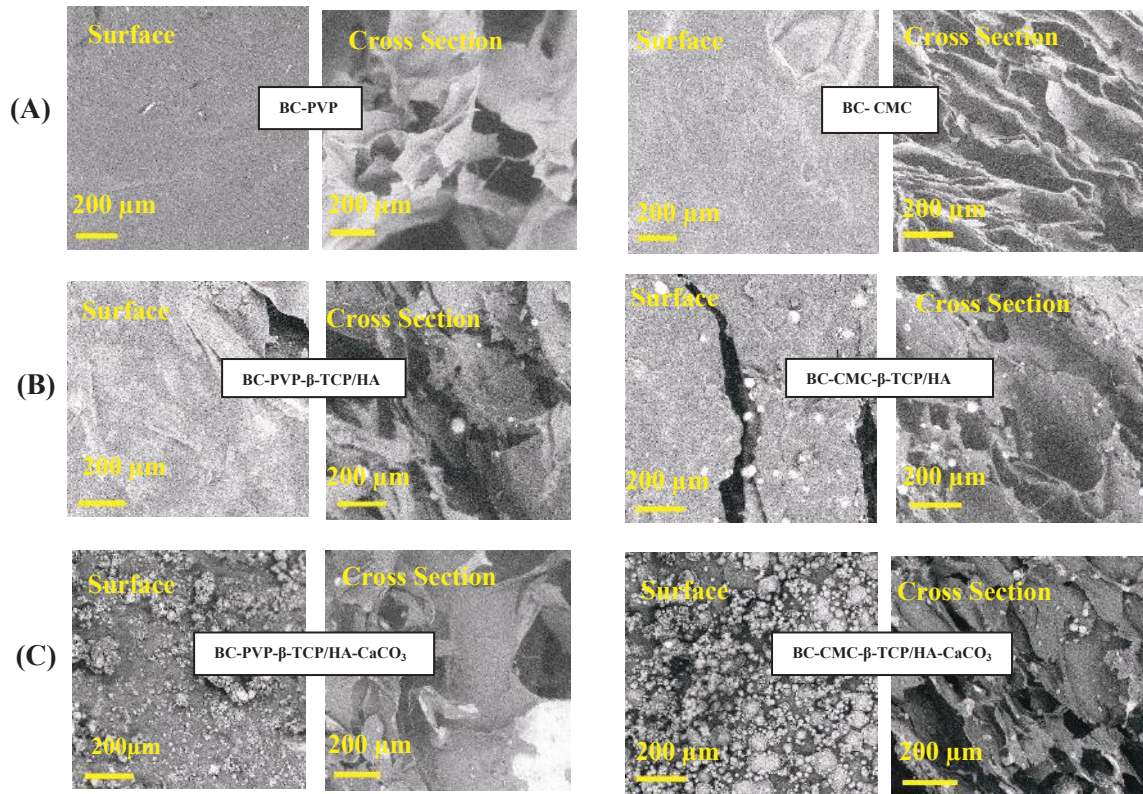


**FIGURE 1.** SEM Micrographs of Hydrogel Scaffolds: BC-PVP and BC-CMC (before modification and biomineralization) (A), BC-PVP- $\beta$ -TCP/HA and BC-CMC- $\beta$ -TCP/HA (after modification and before mineralization) (B), and PVP-BC- $\beta$ -TCP/HA/ $\text{CaCO}_3$  and CMC-BC- $\beta$ -TCP/HA- $\text{CaCO}_3$  (after biomineralization) (C).

The presence of  $\beta$ -TCP/HA particles can be seen like white dots on the surface as well as within the porous structure of PVP-BC- $\beta$ -TCP/HA, CMC-BC- $\beta$ -TCP/HA hydrogels. Additionally, it can be noticed that pore sizes were gradually changed from the PVP-BC, CMC-BC to PVP-BC- $\beta$ -TCP/HA- $\text{CaCO}_3$  and CMC-BC- $\beta$ -TCP/HA- $\text{CaCO}_3$  hydrogels. This change in pore size results in the development of much denser structures which is caused by an increase in inter-polymeric network. These hydrogels with porous structures can facilitate the diffusion of water, drug and other bioactive agents like growth factors, vitamin D, etc.

The FTIR spectra of PVP-BC, CMC-BC, PVP-BC- $\beta$ -TCP/HA, CMC-BC- $\beta$ -TCP/HA, PVP-BC- $\beta$ -TCP/HA/ $\text{CaCO}_3$ , CMC-BC- $\beta$ -TCP/HA- $\text{CaCO}_3$  hydrogels are shown in Fig. 2. A significant band seen between  $3338\text{ cm}^{-1}$  to  $3388\text{ cm}^{-1}$  that corresponds to the hydroxyl group (-OH) stretching. The band between  $1044\text{ cm}^{-1}$  to  $1073\text{ cm}^{-1}$  corresponds to the C-O bond stretching of cellulose, which can be found all the BC based hydrogels. Moreover, the peak present at  $1657\text{ cm}^{-1}$  exhibits the presence of C=O stretching of pyrrolidone, which can be found in all PVP containing hydrogels. Additionally, the peak between  $963\text{ cm}^{-1}$  to  $1110\text{ cm}^{-1}$  which corresponds to phosphate ( $\text{PO}_4^{3-}$ ) group confirms the presence of  $\beta$ -TCP and HA within the BC based hydrogels. Furthermore, the peak between  $1401\text{ cm}^{-1}$  to  $1405\text{ cm}^{-1}$  corresponds to C-O stretching of HA. The peak at  $872\text{ cm}^{-1}$  to  $874\text{ cm}^{-1}$  confirms the presence of  $\text{CO}_3^{2-}$  in the biomineralized samples.

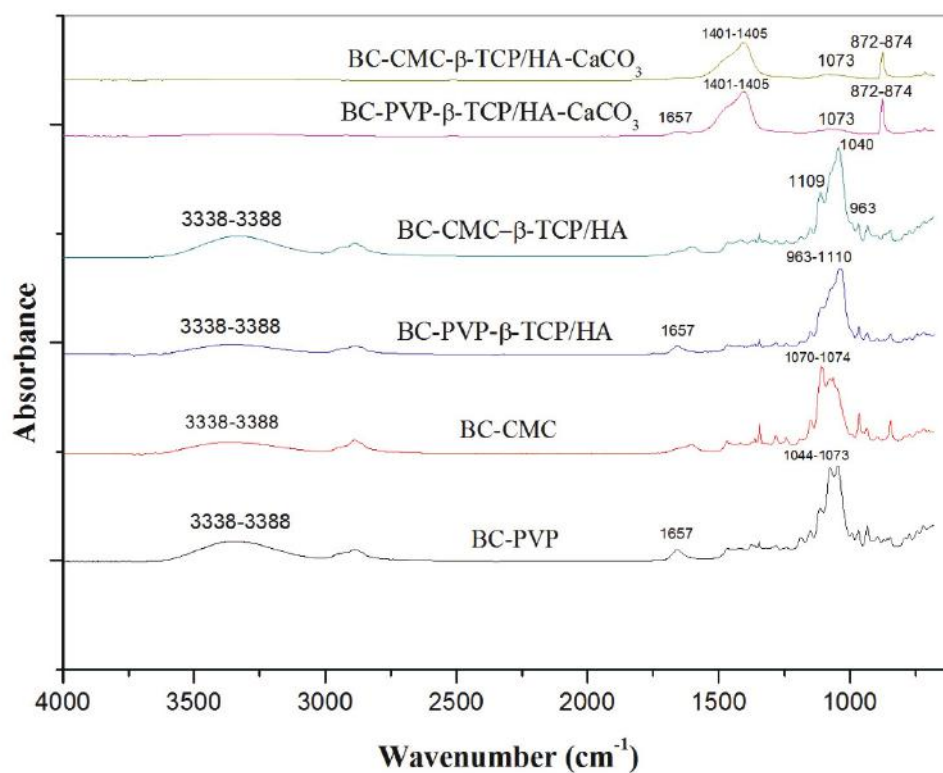


**FIGURE 2.** FTIR Spectra of Hydrogel Scaffolds: PVP-BC, CMC-BC (before modification and biomineralization), PVP-BC- $\beta$ -TCP/HA, CMC-BC- $\beta$ -TCP/HA (after modification and before mineralization) PVP-BC- $\beta$ -TCP/HA/ $\text{CaCO}_3$ , CMC-BC- $\beta$ -TCP/HA- $\text{CaCO}_3$  (after biomineralization).

The viscoelastic property of the BC based hydrogel [non-mineralized and mineralized (60 mins) with  $\text{CaCO}_3$ ] samples were measured at room temperature. Fig. 3 exhibits the storage ( $G'$ ) and loss modulus ( $G''$ ) of the non-mineralized and biomineralized BC based hydrogels against the angular frequency ( $\omega$ ). It was observed that for all samples, the storage modulus is greater than the loss modulus and exhibit a rubbery consistency throughout the entire measurement. The overall trend of the storage moduli sustained a plateau behavior which indicates that the material is rigid cross-linked gel. Moreover, it is also seen that storage modulus ( $G'$ ) is not dependent on the angular frequency ( $\omega$ ). However, the values of the loss modulus ( $G''$ ) for all samples are found to be somewhat dependent on angular frequency ( $\omega$ ). From the Fig. 3, it can be noticed that the values of the loss modulus of PVP-BC hydrogel and CMC-BC hydrogel is higher than that of other non-mineralized and the biomineralized hydrogels, which

demonstrates their lower viscous behavior. This trend might be contributed by the presence of the additive like  $\beta$ -TCP and HA in the BC based hydrogels. Furthermore, the  $\text{CaCO}_3$  influences significantly the viscous behavior in the biomaterialized hydrogel.

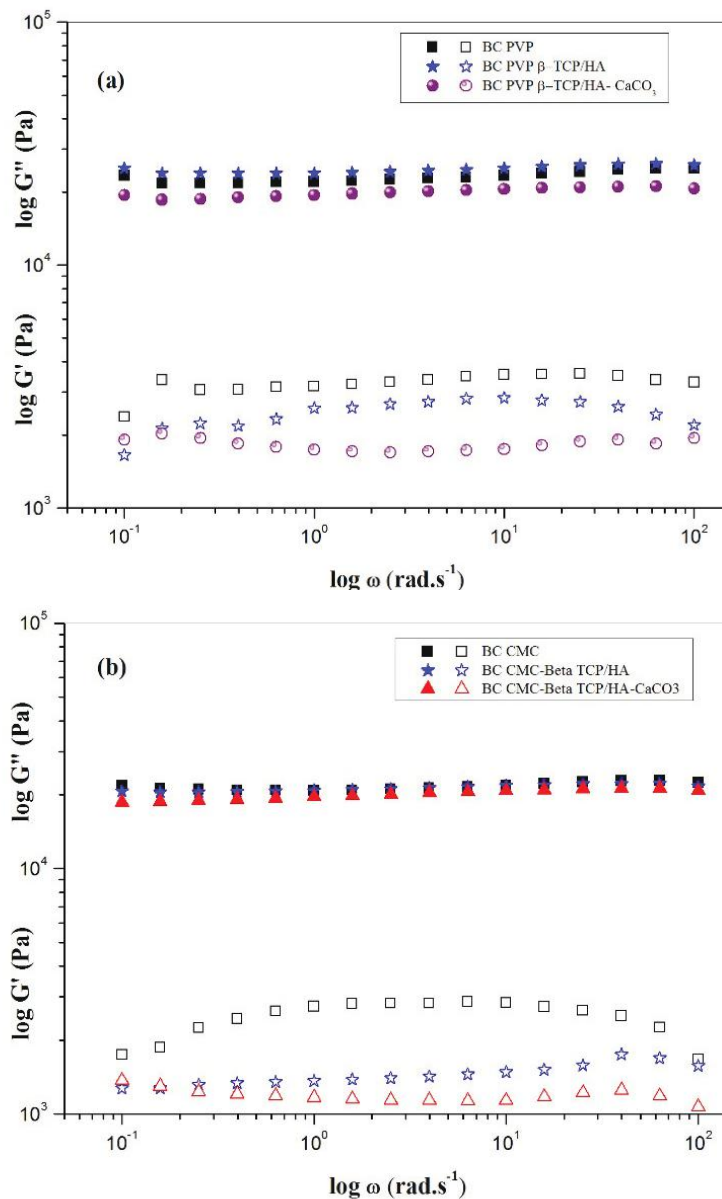


**FIGURE 3** Viscoelastic Nature of Hydrogel Scaffolds: PVP-BC, PVP-BC-  $\beta$ -TCP/HA, PVP-BC-  $\beta$ -TCP/HA/ $\text{CaCO}_3$  (a), and CMC-BC, CMC-BC-  $\beta$ -TCP/HA, CMC-BC-  $\beta$ -TCP/HA- $\text{CaCO}_3$  (b) where storage modulus ( $G'$ , filled symbols) and loss modulus ( $G''$ , open symbol) as a function of angular frequency ( $\omega$ ) at 1% strain for non-mineralized and bio-mineralized BC based hydrogels.

Fig. 4 exhibits effect of angular frequency on complex viscosity of PVP-BC and CMC-BC and biomaterialized hydrogels. It is noticeable from the figure that at 1% strain, all the nonmineralized and biomaterialized hydrogels demonstrates a similar relationship trend among angular frequency and complex viscosity i.e., from low to high angular viscosity at 1% strain the values of complex viscosity is decreasing. All of the BC based hydrogels have significantly maintained elastic nature throughout the study.

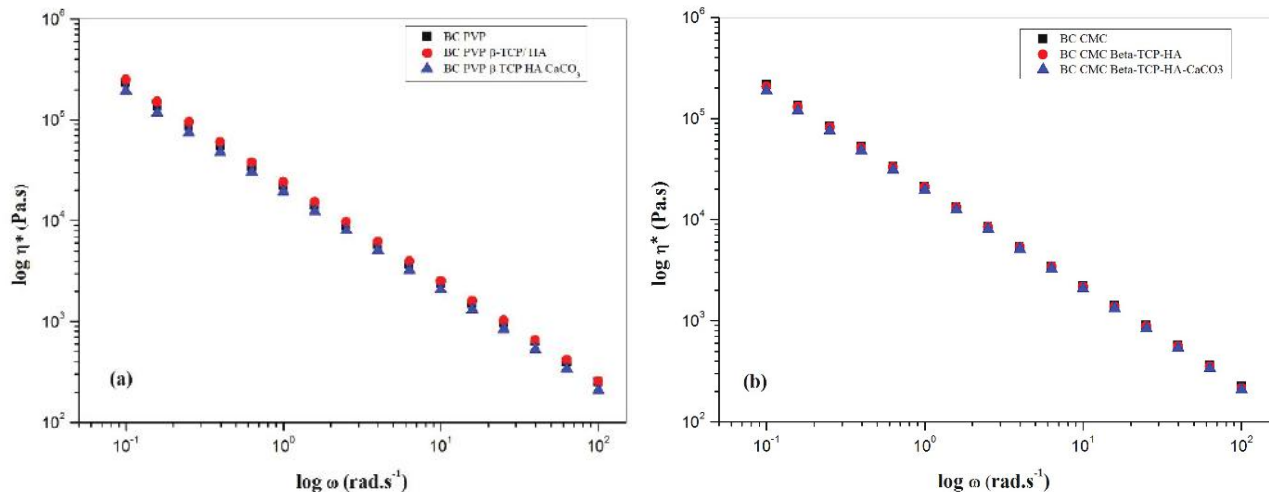


**FIGURE 4.** Effect of angular frequency ( $\omega$ ) at 1% strain on complex viscosity ( $\eta^*$ ) of non-mineralized and biomineralized BC based hydrogels (a and b).

## CONCLUSION

This work includes the study of the viscoelastic properties of the novel bacterial cellulose (BC) based hydrogel scaffolds which involve the  $\beta$ -Tri-Calcium Phosphate ( $\beta$ -TCP) and Hydroxyapatite (HA) as additional bio-active materials. The modified hydrogel composites are then subjected to bio-mineralization for the incorporation of  $\text{CaCO}_3$  within the BC based hydrogel matrix, to achieve an efficient functional property oriented polymeric scaffold/implant for bone tissue regeneration or drug delivery. The electron microscopic study entails the structural characteristics of all BC based nonmineralized and biomineralized ( $\text{CaCO}_3$ ) hydrogels. Further, the non-mineralized and biomineralized hydrogel scaffolds are confirmed by FTIR examination. The rheological study suggests that all BC based nonmineralized and biomineralized ( $\text{CaCO}_3$ ) hydrogels have a significant elastic property. The result indicates about the potential application of BC based hydrogels in the field of biomedical application, especially as an implant for transdermal drug delivery and bone tissue engineering. All the hydrogels are exhibiting significant porous structures which may facilitate the diffusion of electrolytes, drugs and other bioactive agents like growth factors, vitamin D etc.

## ACKNOWLEDGEMENTS

The authors extend their sincere gratitude to the Internal Grant Agency (Project No. IGA/CPS/2017/003), Tomas Bata University in Zlin, the Czech Republic for their financial support. Authors also thank for the partial funding given by Ministry of Education, Youth and Sports of the Czech Republic - NPU Program I (LO1504). Authors are thankful to Dr. Zandraa Oyunchimeg, Microbiology Laboratory, Center of Polymer Systems, Tomas Bata University in Zlin for providing the Bacterial Cellulose mat.

## REFERENCES

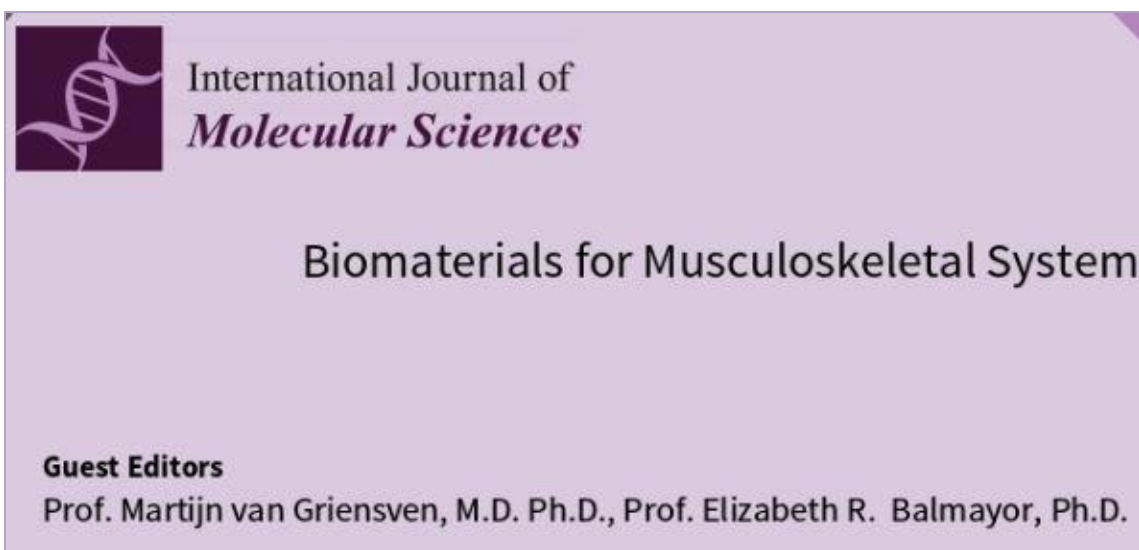
1. N. Roy, N. Saha, T. Kitano and P. Saha, *AIP Conference Proceedings* **1152**, 210-216 (2009).
2. N. Saha, R. Vyroubal, R. Shah, T. Kitano and P. Saha, *AIP Conference Proceedings* **1526**, 301-309 (2013).
3. L. Weng, X. Chen and W. Chen, *Biomacromolecules* **8**, 1109-1115 (2007).
4. T. Oikawa, T. Morino and M. Ameyama, *Biosci. Biotechnol. Biochem.* **59**, 1564-1565 (1995).
5. R. Shah, R. Vyroubal, H. Fei, N. Saha, T. Kitano and P. Saha, *AIP Conference Proceedings* **1662**, 040007 (2015).
6. M. Pawlikowski, *Archive of Mechanical Engineering*, **LIX**(1), 31-51 (2012).



7. R. Shah, N. Saha, Z. Kucekova, P. Humpolicek and P. Saha, [Int. J. Polym. Mat. Polym. Biomat.](#) **65**, 619-628 (2016).
8. V Keskar, NW Marion, JJ Mao, RA. Gemeinhart, [Tissue Engineering Part A.](#) **15**(7), 1695-1707 (2009).
9. R. Meena, R. Lehnen and B. Saake, [Cellulose](#) **21**, 553-568 (2014).
10. H. V. Chavda, R. D. Patel, I. P. Modhia and C. N. Patel, [Int. J. Pharmaceut. Inv.](#) **2**, 134-138 (2012).
11. G. Leone, M. Consumi, G. Greco, C. Bonechi, S. Lamponi, C. Rossi and A. Magnani, [J. Biomedic. Mat. Research B: App. Biomat.](#) **97b**, 278-288 (2011).
12. P. Gao, H. Zhang, Y. Liu, B. Fan, X. Li, X. Xiao et. al., [Scientific Reports](#) **6**(23367), 1-14 (2016).
13. T. Nonoyama, H. Ogasawara, M. Tanaka, M. Higuchi and T. Kinoshita, [Soft Matter](#) **8**, 11531 (2012).
14. X. Struillou, M. Rakic, Z. Badran, L. Macquigneau, C. Colombeix, P. Pilet, C. Verner, O. Gauthier, P. Weiss and A. Soueidan, [J. Mater. Sci.: Mater. Med.](#) **24**, 2749-2760 (2013).
15. N. Roy, N. Saha, T. Kitano and N. Saha, [J. App. Polym. Sci.](#) **117**, 1703-1710 (2010).
16. M. W. Rauch, M. Dressler, H. Scheel, D. V. Opdenbosch and C. Zollfrank, [Eur. J. Inor. Chem.](#) **32**, 5192-5198 (2012).

## PUBLICATION III

**Basu P (50%)**, Saha N, Alexandrova R, Andonova-Lilova B, Georgieva M, Miloshev G, Saha P. (2018) “Biocompatibility and Biological Efficiency of Inorganic Calcium Filled Bacterial Cellulose Based Hydrogel Scaffolds for Bone Bioengineering”, *International Journal of Molecular Sciences* (Web of Science Indexed, Q2 [Multidisciplinary, Chemistry, Biochemistry & Molecular Biology], **Jimp: 4.183**) **19** (12): 3980. DOI: 10.3390/ijms19123980





## Biomaterials for Musculoskeletal System

Guest Editors:

**Prof. Martijn van Griensven,  
M.D. Ph.D.**

Experimental Trauma Surgery,  
Klinikum rechts der Isar,  
Technical University of Munich,  
Munich, Germany

Martijn.vanGriensven@tum.de

**Prof. Elizabeth R. Balmayor,  
Ph.D.**

Experimental Trauma Surgery,  
Klinikum rechts der Isar,  
Technical University of Munich,  
Munich, German

Elizabeth.Rosado-Balmayor@  
tum.de

Deadline for manuscript  
submissions:

**closed (26 December 2018)**

### Message from the Guest Editors

Dear Colleagues,

In this special issue, we would like to present new developments in biomaterials for musculoskeletal tissue engineering. Particularly, this special issue seeks for studies describing radically new and smart materials, innovative material processing techniques that may allow for new scaffold design, multi-phase scaffolds for interface tissue engineering e.g. osteochondral and tendon/ligament-to-bone enthesis. Contributions (reviews and/or original papers) on new biomaterials for bone, cartilage, muscle, tendon and ligaments are welcome.

- Biomaterials
- Smart materials
- Nanomaterials
- Multi-phase scaffolds
- Interface tissue engineering
- Musculoskeletal tissue engineering
- Cartilage tissue regeneration
- Muscle tissue regeneration
- Tendon and/or Ligament tissue regeneration





Article

# Biocompatibility and Biological Efficiency of Inorganic Calcium Filled Bacterial Cellulose Based Hydrogel Scaffolds for Bone Bioengineering

Probal Basu <sup>1</sup>, Nabanita Saha <sup>1,\*</sup>, Radostina Alexandrova <sup>2</sup>, Boyka Andonova-Lilova <sup>2</sup>, Milena Georgieva <sup>3</sup>, George Miloshev <sup>3</sup> and Petr Saha <sup>1</sup>

<sup>1</sup> Centre of Polymer Systems, University Institute, Tomas Bata University in Zlín, Trida Tomase Bati 5678, 760 01 Zlín, Czech Republic; probal@utb.cz (P.B.); saha@utb.cz (P.S.)

<sup>2</sup> Institute of Experimental Morphology, Pathology and Anthropology with Museum, Bulgarian Academy of Sciences, 1113 Sofia, Bulgaria; rialexandrova@hotmail.com (R.A.); boika\_andonova@hotmail.com (B.A.-L.)

<sup>3</sup> Laboratory of Molecular Genetics, Institute of Molecular Biology “Acad. R. Tsanev”, Bulgarian Academy of Sciences, 1113 Sofia, Bulgaria; milenageorgy@gmail.com (M.G.); miloshev@bio21.bas.bg (G.M.)

\* Correspondence: nabanita@utb.cz; Tel.: +420-57603-8156

Received: 19 October 2018; Accepted: 27 November 2018; Published: 11 December 2018



**Abstract:** The principal focus of this work is the in-depth analysis of the biological efficiency of inorganic calcium-filled bacterial cellulose (BC) based hydrogel scaffolds for their future use in bone tissue engineering/bioengineering. Inorganic calcium was filled in the form of calcium phosphate ( $\beta$ -tri calcium phosphate ( $\beta$ -TCP) and hydroxyapatite (HA)) and calcium carbonate ( $\text{CaCO}_3$ ). The additional calcium,  $\text{CaCO}_3$  was incorporated following *in vitro* bio-mineralization. Cell viability study was performed with the extracts of BC based hydrogel scaffolds: BC-PVP, BC-CMC; BC-PVP- $\beta$ -TCP/HA, BC-CMC- $\beta$ -TCP/HA and BC-PVP- $\beta$ -TCP/HA- $\text{CaCO}_3$ , BC-CMC- $\beta$ -TCP/HA- $\text{CaCO}_3$ ; respectively. The biocompatibility study was performed with two different cell lines, i.e., human fibroblasts, Lep-3 and mouse bone explant cells. Each hydrogel scaffold has facilitated notable growth and proliferation in presence of these two cell types. Nevertheless, the percentage of DNA strand breaks was higher when cells were treated with BC-CMC based scaffolds i.e., BC-CMC- $\beta$ -TCP/HA and BC-CMC- $\beta$ -TCP/HA- $\text{CaCO}_3$ . On the other hand, the apoptosis of human fibroblasts, Lep-3 was insignificant in BC-PVP- $\beta$ -TCP/HA. The scanning electron microscopy confirmed the efficient adhesion and growth of Lep-3 cells throughout the surface of BC-PVP and BC-PVP- $\beta$ -TCP/HA. Hence, among all inorganic calcium filled hydrogel scaffolds, ‘BC-PVP- $\beta$ -TCP/HA’ was recommended as an efficient tissue engineering scaffold which could facilitate the musculoskeletal (i.e., bone tissue) engineering/bioengineering.

**Keywords:** bacterial cellulose; *in vitro* bio-mineralization; bone tissue engineering; biocompatibility; apoptosis; DNA damage

## 1. Introduction

Bone is an important part of the animal musculoskeletal system. The structural framework of an animal is preserved by the bones through modelling and remodeling events [1,2]. Extensive research indicated that bone related disorders like osteoporosis affect 75 million individuals throughout Europe, USA and Japan. In addition, many studies also showed that osteoporosis causes more than 8.9 million fractures worldwide annually; with a condition where an osteoporotic fracture occurs in every 3s [3]. The possible treatment methods for this comprise the use of either auto/allografts or

ceramic coated/inert metallic implants, which in many cases are far too expensive for application [4]. In this context, the hydrogel based bioactive scaffold can become a notable approach in bone tissue engineering/bone bioengineering; due to its osteo-conduction and osteo-induction properties, notable mechanical property and further its cost-effective production attributes [5].

The hydrogel is a three dimensional polymeric network structure which can retain significant amount of water [6–8]. The hydrogel based bioactive scaffolds have the necessary attributes to become an efficient extra cellular matrix (ECM) that has the potential to execute the primary functions of the tissue engineering scaffolds like cell adhesion, stimulation for cell proliferation and others [9,10]. Different polymers, polymer-composite scaffolds are often utilized in the design of an efficient scaffold material. Additionally, a variety of synthetic polymers like poly(lactic-co-glycolic) acid (PLGA), poly(glycolic acid) (PGA) poly(caprolactone) (PCL) and natural polymers like collagen, hyaluronic acid have also been used in the fabrication of tissue engineering scaffold [11–16].

Research showed that bacterial cellulose (BC) based hydrogel scaffolds could also become a potential biomaterial for tissue regeneration application [17]. BC is a biocompatible biopolymer [18] and has high crystallinity, ultra-fine network structure and high water absorption capability [19,20]. These significant structural and functional properties of BC increase its importance in musculoskeletal/tissue engineering/bone bioengineering applications.

The inorganic phase of the bone tissue is composed majorly of calcium mineral [21]. However, recent research data reported that the extracellular calcium had a significant role in cellular growth and development [22]. Bone cells are comprised of different calcium ion channels and extracellular calcium receptors that receive the signals from the extracellular  $\text{Ca}^{2+}$  [23,24], which in turn generates specific genetic responses related to cell growth and proliferation [25]. Studies indicated that the biocompatibility and the mechanical properties of the tissue engineering scaffolds can be modified and improved by addition of calcium phosphate [26,27]. Bioactive calcium phosphate fillers like  $\beta$ -tri-calcium phosphate ( $\beta$ -TCP), octa-calcium phosphate (OCP) and hydroxyapatite (HA) improve the osteo-conduction and osteo-induction properties of the biomaterial [17,28]. On the other hand, inorganic calcium can also be incorporated in the tissue engineering scaffold through organic-inorganic hybridization. A variety of methods of the organic-inorganic hybridization (i.e., solvent casting/particle leaching, scaffold coating, etc.) have been developed for the inclusion of bioactive  $\text{CaCO}_3$  within the polymer matrix in order to obtain improvement in the structural and functional properties of the scaffold [29].

Polyvinylpyrrolidone (PVP) is a synthetic polymer which has significant biocompatibility. Several studies indicated that the application of PVP is not so widespread due to its poor mechanical properties and low swelling capacity [30]. However, the properties of PVP can be improved when it is blended with polysaccharides. On the other hand, carboxymethyl cellulose (CMC) is the cellulose derivative which has also significant utilization in cosmetology and as a water retention agent. Additionally, CMC has notable biocompatibility [30,31]. The blending of the above mentioned polymers, PVP-CMC hydrogel scaffold; has been previously successfully prepared in our laboratory. The biological efficiency of PVP-CMC scaffold has also been found suggestive [30–32]. BC is a natural polymer which also has significant biocompatibility and notable mechanical properties. Recent data indicated that a variety of composite materials prepared with BC such as BC/Chitosan, BC/collagen were used in biomedical applications; especially in tissue engineering/bone bioengineering [33,34]. The hydrogel scaffolds prepared from the natural polymers like BC and synthetic polymers PVP and CMC have also been reported in our previous work [19]. Albeit all the above-mentioned hydrogel scaffolds have the necessary material characteristics (like mechanical, rheological properties) for tissue engineering application; however, in order to develop a more specific bone tissue engineering scaffold, inorganic calcium (in the form of calcium phosphate or/and  $\text{CaCO}_3$ ) filled BC based hydrogel scaffolds were developed. In the present work, the focus is given on the *in vitro* characterization of the novel inorganic calcium filled BC based hydrogel scaffolds through evaluation of their biocompatibility and biological efficiency in a series of cell-based assays.

## 2. Results

The novel inorganic calcium filled scaffolds “BC-PVP- $\beta$ -TCP/HA”, “BC-CMC- $\beta$ -TCP/HA”, “BC-PVP- $\beta$ -TCP/HA-CaCO<sub>3</sub>”, and “BC-CMC- $\beta$ -TCP/HA-CaCO<sub>3</sub>” were prepared and their biocompatibility and biological efficiency (in a series of cell based assays) were evaluated in order to recommend for its application for bone tissue engineering/bioengineering, where, the “BC-PVP” and “BC-CMC” scaffolds were considered as a control set of scaffolds. To analyze the biological efficiency of these scaffolds, the following investigations were performed and discussed below.

### 2.1. Cell Viability and Biocompatibility Study

Cell viability studies have been performed through MTT(3-(4,5-Dimethylthiazol-2-yl)-2,5-diphenyltetrazolium bromide) test in indirect (IDE) and direct experiments (DE) using human embryonic fibroblasts (Lep-3) and mouse bone explant cells (BEC), and are summarized in Figure 1.

It can be seen from Figure 1 that the detected cytotoxicity of the calcium filled scaffolds was low in the studied cell cultures, when determined in IDEs and incubated in 3, 5 and 7 days' extract culture medium. In contrast, it is clearly visible that the existence of the viable Lep-3 and BEC cells has been specially affected by the presence of BC-CMC- $\beta$ -TCP/HA-CaCO<sub>3</sub> and decreased in number after 5 days. However, both the cells were affected more or less in the presence of all the scaffolds after 7 days except “BC-PVP- $\beta$ -TCP/HA” in DE and in presence of BEC. In general, “BC-CMC- $\beta$ -TCP/HA-CaCO<sub>3</sub>” exhibited the highest cytotoxic activity in DEs for both human and mouse cells (i.e., Lep-3 and BEC).

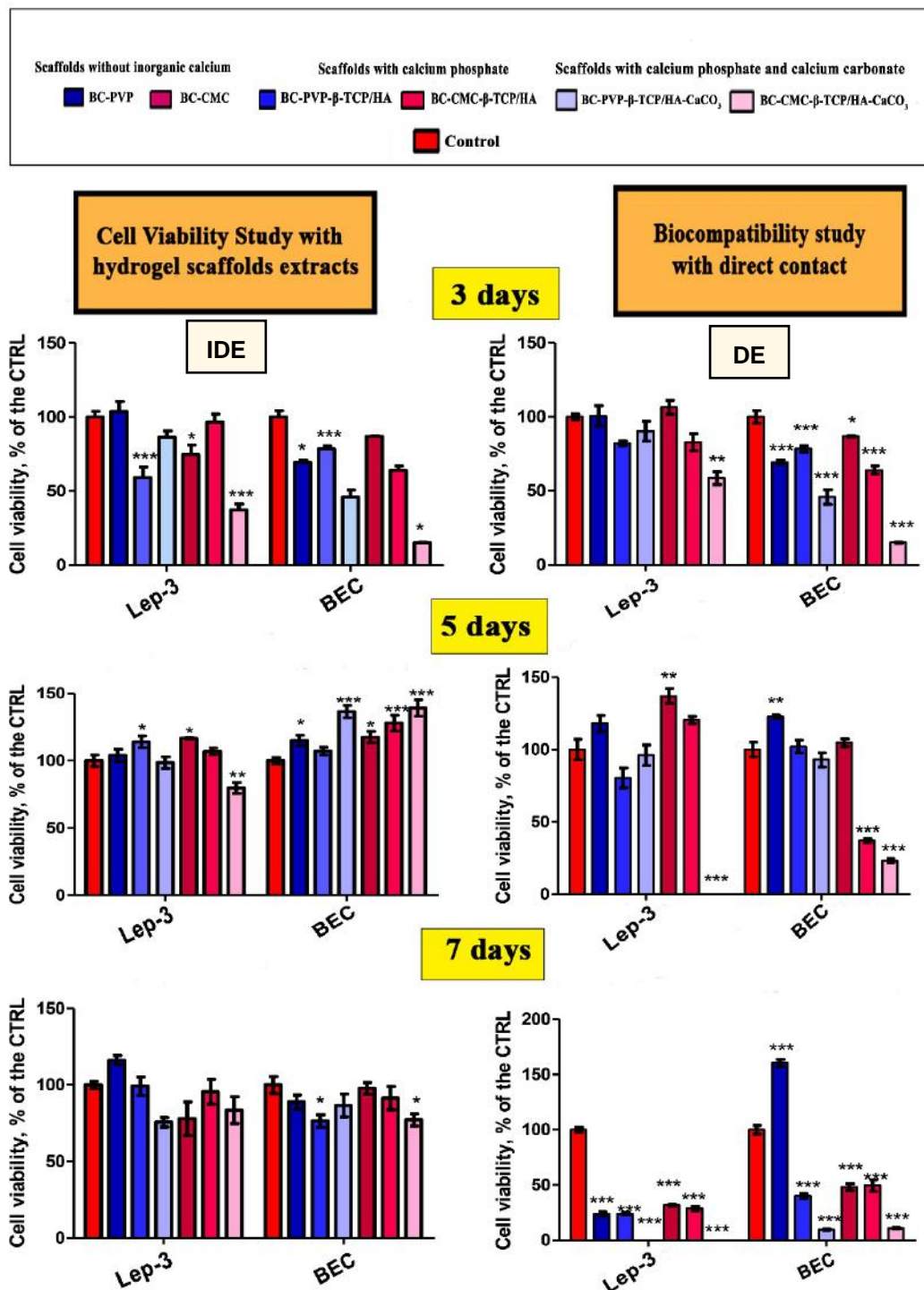


**Figure 1.** Human fibroblast, Lep-3 and mouse bone explant cells (BEC) cellular viability (proliferation profiles) after incubation with six different BC based hydrogel scaffolds (scaffolds without inorganic calcium, scaffolds with calcium phosphate, scaffolds with calcium phosphate and CaCO<sub>3</sub>); established by indirect (IDE) and direct experiments (DE). \*  $p < 0.05$ ; \*\*  $p < 0.005$ ; \*\*\*  $p < 0.0001$  as compared to the control.

## 2.2. Genotoxic Potential of the Studied BC Based Inorganic Calcium Filled Hydrogel Scaffolds

The genotoxic potential of the studied BC based inorganic calcium filled hydrogel scaffolds was determined by the method of Comet Assay in alkaline conditions in order to detect all kinds of DNA breaks; in which the tested scaffolds can potentially induce genotoxic effect (i.e., DNA breaks) in

the cells. Lep-3 cells were used as the model cellular system in this study. The Comet Assay data quantitation included calculation of the percentage of comets, i.e., cells with damaged DNA in all tested probes and results are displayed on Figure 2. It can be seen that, the higher percentage of comets (cells with damaged DNA) was observed in Lep-3 cells grown in 3 days' extract culture medium from BC-CMC- $\beta$ -TCP/HA and BC-CMC- $\beta$ -TCP/HA-CaCO<sub>3</sub>; where more than 60% of all observed cells per probe were with damaged DNA. On the other hand, more than 60% of cells incubated with BC-PVP- $\beta$ -TCP/HA and BC-PVP- $\beta$ -TCP/HA-CaCO<sub>3</sub> were found with native, i.e., untouched/unaffected DNA, in comparison to the control and cells with BC-CMC- $\beta$ -TCP/HA and BC-CMC- $\beta$ -TCP/HA-CaCO<sub>3</sub> scaffolds.

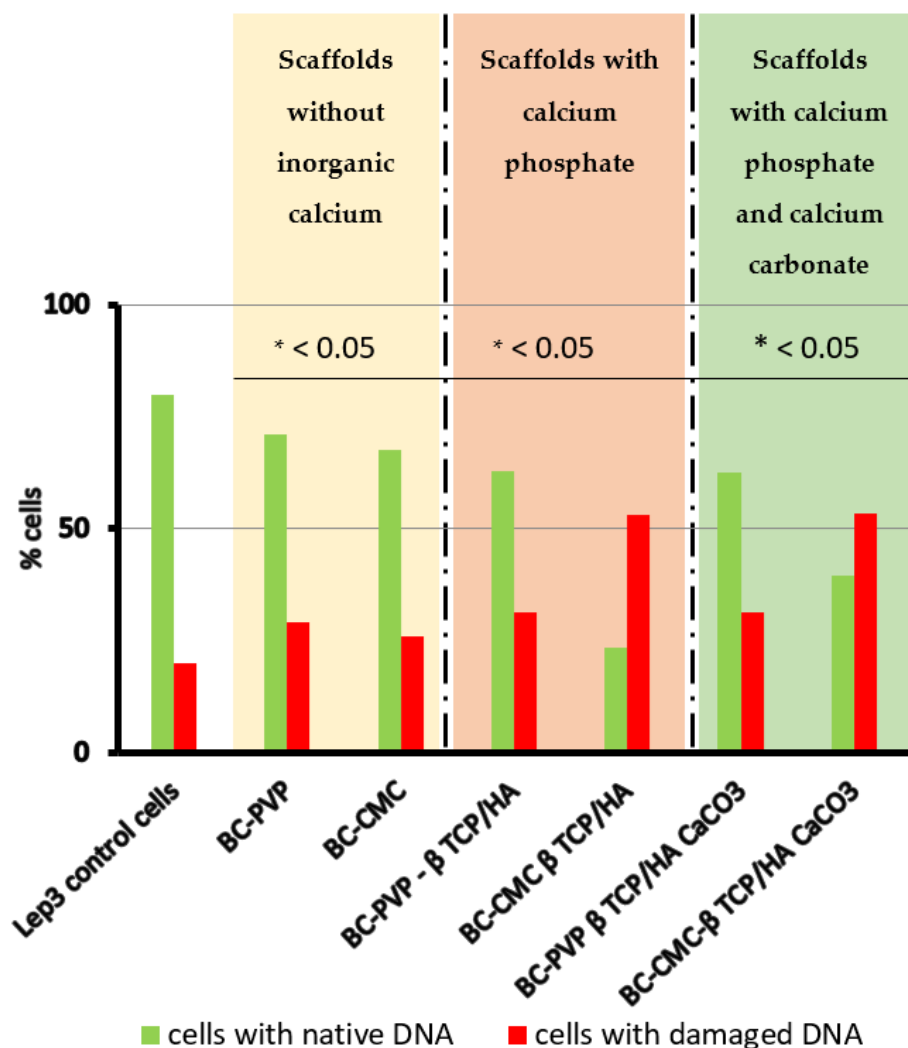


**Figure 2.** Genotoxicity testing of the studied biocompatible scaffolds was done by the method of Comet Assay in Lep-3 cells in the presence of extracts of all six BC based hydrogel scaffolds. Data quantitation proceeded with estimation of the percentage of comets by assuming the total number of objects per probe ( $n = 1000$ ) as 100% and the percentage of comets, i.e., cells with damaged DNA was estimated and represented as a graph. Student  $t$  test was performed and the estimated  $p$  values for all probes in comparison to the control were statistically significant  $p < 0.05$ .

### 2.3. Study on Apoptosis/Necrosis

In order to elucidate the mechanisms of the biological action of the tested scaffolds on the studied cellular model systems and to understand the reasons for the detected genotoxic potential of those with calcium phosphate and carbonate functionalization, i.e., BC-CMC- $\beta$ -TCP/HA and



BC-CMC- $\beta$ -TCP/HA-CaCO<sub>3</sub> (already detected with the Comet Assay Figure 2), FACS analysis (fluorescence activated cell sorting) with Annexin V-FITC kit performed for evaluation of the percentage of cells undergoing apoptosis and necrosis when layered onto all studied scaffolds. The percentage of apoptotic and necrotic cells together with the percentage of live cells was estimated by software data quantitation. Further on the ratio among cells in apoptosis and necrosis and alive cells was done and is displayed in procedure data values (PDU) on Figure 3. The last represents the ratio between apoptotic and necrotic cells in the probes versus these percentages in the controls (Lep-3 control cells). The blue bars on Figure 3 represent the ratio between the percentages of apoptotic cells in the probes versus the control, while the red bars represent the ratio between the percentages of necrotic cells in the tested probes versus the necrotic cells in the control. As it is easily seen on Figure 3 an increased number (around 40%) of apoptotic cells was detected in the probes of human Lep-3 cells grown in 3 days' extract culture medium in presence of BC-CMC- $\beta$ -TCP/HA, BC-PVP- $\beta$ -TCP/HA-CaCO<sub>3</sub> and BC-CMC- $\beta$ -TCP/HA-CaCO<sub>3</sub>. Interestingly, the trend with the observed increase of apoptosis between BC-PVP and BC-PVP- $\beta$ -TCP/HA was similar but when compared to BC-CMC- $\beta$ -TCP/HA, BC-PVP- $\beta$ -TCP/HA-CaCO<sub>3</sub> and BC-CMC- $\beta$ -TCP/HA-CaCO<sub>3</sub> it was not so well pronounced as previously expected.

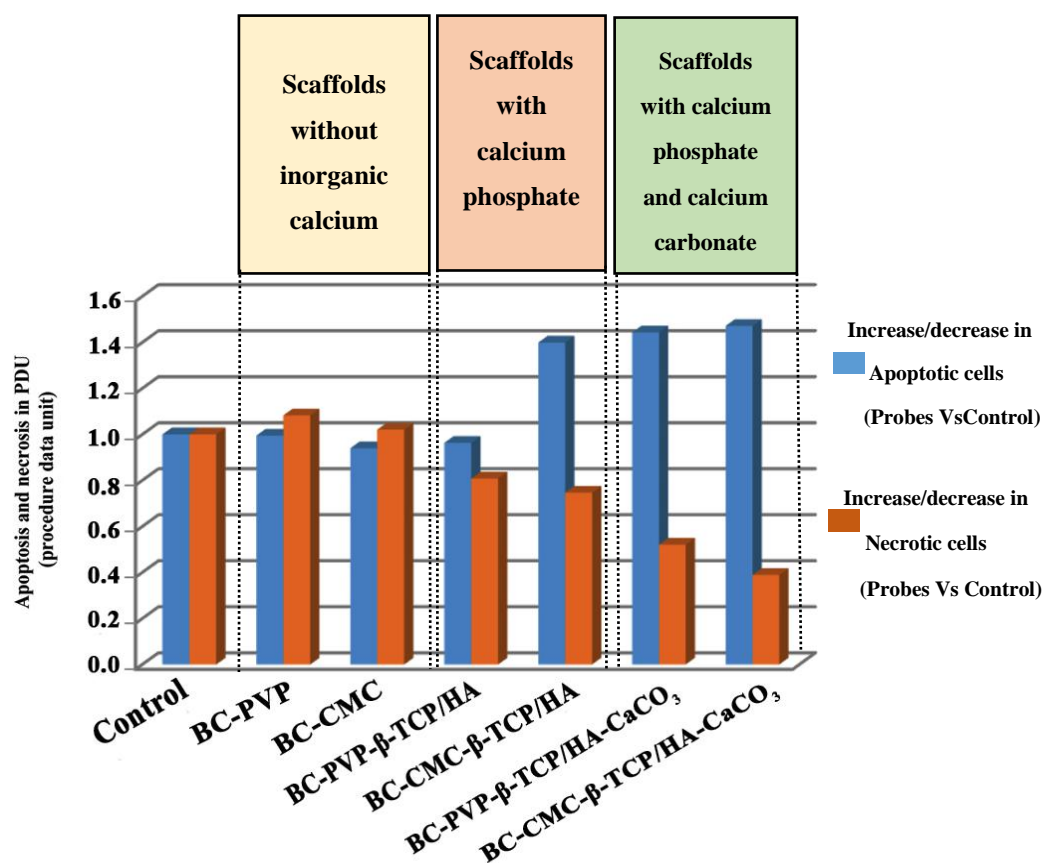


**Figure 3.** Discrimination between apoptotic and necrotic types of cell death induced by the tested scaffolds in Lep-3 cells. FACS analysis with Annexin V-FITC kit for apoptosis/necrosis detection was applied on Lep-3 cells cultivated in presence of six studied scaffolds. Data quantitation included estimation of the percentage of cells undergoing apoptosis and necrosis and the ratio between these percentages in comparison to the control cells is given in PDU (procedure data units).

Noteworthy, the results from the FACS analysis for discrimination between apoptosis and necrosis are in correspondence with the results from the alkaline Comet Assay. The detected genotoxic potential of BC-CMC- $\beta$ -TCP/HA and BC-CMC- $\beta$ -TCP/HA-CaCO<sub>3</sub> is also reflected in the experiments for studying of the mechanisms for the induction of different types of cell death. In the cases when

cells were cultivated in the presence of these types of scaffolds (i.e., BC-CMC- $\beta$ -TCP/HA and BC-CMC- $\beta$ -TCP/HA-CaCO<sub>3</sub>), the higher levels of apoptosis were seen. It could be a result from the possible genotoxic effect of these substances/scaffolds.

#### 2.4. SEM Analysis

The SEM analysis of hydrogel scaffolds-Lep-3 cell interaction is depicted in Figure 4. The analysis was performed with BC-PVP and BC-PVP- $\beta$ -TCP/HA, as these materials showed better cyto-compatibility in direct (DE) and indirect experiments (IDE). The presence of Lep-3 cells including groups of 2–3 cells was observed on the surface of both materials (Figure 4). The adhered Lep-3 cells on the surface of BC-PVP- $\beta$ -TCP/HA can be seen notably.

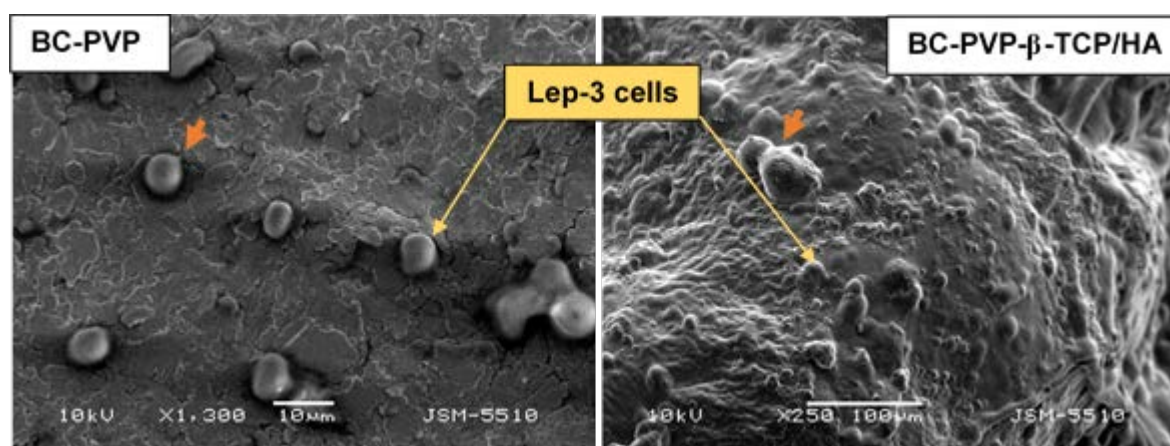


**Figure 4.** SEM images of Lep-3 cells grown on BC based hydrogel (BC-PVP and BC-PVP- $\beta$ -TCP/HA). The orange colored arrow indicates developing projections.

### 3. Discussion

Generally, the significant properties of scaffold materials involve efficient architecture, cyto-compatibility and notable mechanical property. Recently many different scaffold materials have been developed with a variety of synthetic and natural polymers [11]. However, the application of natural polymers like bacterial cellulose (BC) for tissue regeneration is also very promising [35]. In this study, BC was used with different biocompatible polymers like PVP, CMC, etc. Calcium phosphate (in the form of  $\beta$ -TCP/HA) was added within the polymer matrix. Moreover, the calcium phosphate filled scaffolds were further *in vitro* biomineralized to develop calcium phosphate and calcium carbonate filled biomineralized hydrogel scaffold. The applied cell based assays for studying of their biological properties demonstrated the promising cyto-compatibility.

Calcium phosphate like  $\beta$ -TCP and HA can facilitate osteo-conduction, which ultimately results in high cell viability [36]. In the cell viability study with sample extract in IDE, the BEC viability was significant for BC-PVP- $\beta$ -TCP/HA-CaCO<sub>3</sub> after 5 days of incubation. Additionally, there was a trend of increase also seen in BEC viability with BC-CMC and calcium phosphate and calcium carbonate filled hydrogel scaffolds after 5 day of incubation. Moreover, until the 7 day of incubation, cell viability for Lep-3 and BEC was still significant for all the BC based hydrogels. Other authors studies indicated that CaCO<sub>3</sub> facilitates cell viability for fibroblasts [37]. In this context, it is relevant to mention that; the Lep-3 cells are embryonic fibroblast cells [38] and not at all are specified to elicit prompt response in the presence of notable calcium content in the surrounding environment. Thus, through acclimatization with the significant inorganic calcium environment, the cells exhibit high viability with the gradually increasing incubation period from 72 to 168 h. In regard to the biocompatibility study in the direct contact (DE) with the scaffolds, the BEC and Lep-3 cells initially acclimatized with the chemical and physical environment that has been provided by the scaffold sections and thus showed cell growth and viability after 3 days of incubation. Then gradually the higher cell viability started to be visible

after 5 days of incubation. Interestingly, after 7 days of incubation, the Lep-3 and BEC cell viability decreased in comparison to cell viability after 3 days and 5 days of incubation. In any case, the BEC viability was found higher for BC-PVP after 7 days of incubation.

Porosity is an important factor for bone cell growth and proliferation [39]. Thus, the significant porous structures of BC-PVP scaffold section might provide the necessary environment for BEC growth efficiently after 7 days of incubation. On the other hand, research indicated that high levels of  $\text{Ca}^{2+}$  can negatively influence DNA repair ability to the cells [40] and thereby can cause less cell viability. Interestingly, after 7 days of incubation, the BEC and Lep-3 cell viability was significantly fewer when incubation performed with *in vitro* biomineralized samples. Lep-3 cells were unable to get any proliferation stimulation in contact (DE) with the *in vitro* biomineralized samples (BC-PVP- $\beta$ -TCP/HA- $\text{CaCO}_3$ , BC-CMC- $\beta$ -TCP/HA- $\text{CaCO}_3$ ) after 7 days of incubation. This indicates that *in vitro* biomineralized hydrogels can only provide an initial stimulatory signals to Lep-3 cells. As Lep-3 cells are sensitive human embryonic cells (but not stem cells), the initial high concentration of calcium in the cell culture environment causes them to significantly proliferate up to 3 days of incubation in the presence of all six hydrogel scaffolds, while no proliferation was observed after 5 days of incubation during direct experiments (DE). However, the Lep-3 cell viability after 5 days of incubation with BC-PVP- $\beta$ -TCP/HA- $\text{CaCO}_3$  very possibly resulted from the combined positive effect provided by the polymers (BC and PVP) and the inorganic calcium content. Finally, the high calcium content most probably inhibits the subsequent proliferation of both human and mouse cells after 7 days of incubation.

The results from the method of comet assay signified the occurrence of DNA damage in the cells when Lep-3 cells were used in the study to evaluate the genotoxic effect of hydrogel scaffolds. Albeit, BC and CMC have been proved to be biocompatible polymers, together with calcium phosphate in BC-CMC- $\beta$ -TCP/HA hydrogel scaffold, they might develop a cellular burden by possible induction of considerable number of DNA breaks. Earlier reports showed that several polymers and ceramics can indeed cause oxidative stress [41,42] in the cells, which ultimately resulted in DNA strand breaks [43]. The possible interaction of BC, CMC and calcium phosphate (for BC-CMC- $\beta$ -TCP/HA hydrogel scaffold) might develop oxidative stress to the cells which could finally result in high percentage of comets (cells with damaged DNA). Moreover, research indicated that the elevation of the calcium ion ( $\text{Ca}^{2+}$ ) concentration can also influence DNA repair ability of the cells [40]. This phenomenon is evident of Figure 1, where the percentage of live cells was found less for the BC-CMC- $\beta$ -TCP/HA- $\text{CaCO}_3$  hydrogel scaffold. The degree of DNA damage might be greater than the DNA repair ability for BC-CMC- $\beta$ -TCP/HA- $\text{CaCO}_3$ . On the other hand, the notable percentage of live cells for BC-PVP- $\beta$ -TCP/HA and BC-PVP- $\beta$ -TCP/HA- $\text{CaCO}_3$  indicated the introduction of less DNA damage into the fibroblast cells (Lep-3).

Regarding apoptosis/necrosis study, the necrosis level was found gradually decreasing compared to apoptosis (Necrosis: BC-PVP > BC-CMC > BC-PVP- $\beta$ -TCP/HA > BC-CMC- $\beta$ -TCP/HA > BC-PVP- $\beta$ -TCP/HA- $\text{CaCO}_3$  > BC-CMC- $\beta$ -TCP/HA- $\text{CaCO}_3$ ). Other researchers demonstrated that, an elevated extracellular  $\text{Ca}^{2+}$  can cause the production of reactive oxygen species (ROS) in cellular mitochondria, which thereby induces the destruction of the mitochondrial membrane that finally initiates the apoptosis through the release of cytochrome C into the cytoplasm [44]. Possibly, the *in vitro* biomineralized  $\text{CaCO}_3$  filled samples (BC-PVP- $\beta$ -TCP/HA- $\text{CaCO}_3$ , BC-CMC- $\beta$ -TCP/HA- $\text{CaCO}_3$ ), creates high  $\text{Ca}^{2+}$  environment around the Lep-3 cell population which might also increase the intracellular  $\text{Ca}^{2+}$  levels which could have resulted in apoptosis. Earlier research indicated that caspase-8; a cysteine aspartate protease involved in apoptosis, has a specific role in suppression of necrosis and facilitation of apoptosis [45]. Our studies show that, the apoptosis level is also seen increasing following incubation time with the calcium phosphate filled scaffolds and with the *in vitro* biomineralized  $\text{CaCO}_3$  filled hydrogel scaffolds. The possible formation of caspase-8 in some population of the cells might be responsible for the significant shift from necrosis to apoptosis in all biomineralized  $\text{CaCO}_3$  filled hydrogel scaffolds. Interestingly, the elevated level of apoptosis

compared to necrosis can also be seen in BC-CMC- $\beta$ -TCP/HA compared to BC-PVP- $\beta$ -TCP/HA hydrogel scaffold. This might be associated with the combinatorial effect of polymers (BC, CMC) and calcium phosphate ( $\beta$ -TCP/HA). In addition, the cell viability, rather than apoptotic/necrotic cell death is also found higher in BC-PVP- $\beta$ -TCP/HA, compared to BC-CMC- $\beta$ -TCP/HA and BC-CMC- $\beta$ -TCP/HA-CaCO<sub>3</sub>. Furthermore, the apoptotic/necrotic cell death is also found 10 folds less for BC-CMC than BC-PVP.

Scientific data revealed that different materials contains various surface characteristics like the surface topography, wettability, roughness, softness which notably influence a variety of cell behavior like cellular adhesion, growth, differentiation [46,47]. BC-PVP and BC-PVP- $\beta$ -TCP/HA hydrogel scaffolds contain the necessary attributes (mechanical and microstructural properties) [48] which facilitate efficient Lep-3 fibroblast cell adhesion on the surface of the hydrogel scaffolds. Additionally, the homogenous cell adhesion also signifies the efficient adsorption of cell adhesion proteins to the surface of the hydrogel scaffolds. This focal adhesion of cells on the surface of these hydrogel scaffolds will further facilitate the cell proliferation and growth events which ultimately elaborate the event of tissue regeneration [45].

## 4. Materials and Methods

### 4.1. Materials

Polyvinylpyrrolidone K30 (PVP K30; molecular weight: 40,000), Polyethylene glycol 3000 (PEG; average molecular weight: 2700–3300), Agar,  $\beta$ -tri calcium phosphate ( $\beta$ -TCP; molecular weight: 310.18 g/mol) were supplied by Fluka, Switzerland; Sodium carboxymethyl cellulose (CMC) was purchased from Sinopharm Chemical Reagent Co Ltd. (SCRC), China; anhydrous Calcium chloride (CaCl<sub>2</sub>; molecular weight 110.99 g/mol, 97.0%) was obtained from Penta, Czech Republic; and Sodium carbonate-decahydrate (Na<sub>2</sub>CO<sub>3</sub>; molecular weight 286.14 g/mol), Hydroxyapatite (HA; molecular weight: 502.31 g/mol) were obtained from Sigma Aldrich.

Dulbecco's modified Eagle's medium (DMEM) and Fetal bovine serum (FBS) were obtained from Gibco-Invitrogen (Loughborough, UK). Thiazolyl blue tetrazolium bromide (MTT). Dimethyl sulfoxide (DMSO) and Trypsin were obtained from AppliChem (Darmstadt, Germany). Agar is supplied by Fluka, Switzerland. The antibiotics (Penicillin and Streptomycin) for cell cultures were from Lonza (Verviers, Belgium). Ethylenediaminetetraacetic acid (EDTA), Glutaraldehyde, Ammonium hydroxide, Formaldehyde and all other chemicals of the highest purity commercially available were purchased from local agents and distributors. All sterile plastic ware and syringe filters were from Orange Scientific (Braine-l' Alleud, Belgium). Agarose (low-gelling) was purchased from Sigma-Aldrich. ANNEXINV—GFP-Certified Apoptosis/Necrosis detection kit was used from Enzo Life Sciences (Long Island, NY, USA).

### 4.2. Synthesis and Preparation of Homogenous Suspension of BC

BC (holding 99% H<sub>2</sub>O) was synthesized in presence of basal synthetic Hestrin-Schramm (HS) nutritive medium (pH 7.0) using *Gluconacetobacter xylinus* CCM 3611<sup>T</sup> (syn. *Acetobacter xylinum*) at 30 °C for 15 days. 100 mL bacteriological culture bottles were inoculated with 5 mL of H.S. medium containing  $96 \times 10^8$  cells/mL bacteria (bacteria counted at 550 nm wavelength with Grant-Bio McFarland Densitometer DEN-1B, Grant Instruments Ltd., UK). The freshly prepared BC pellicle is treated with 0.5 N NaOH solution and then heated at 80 °C for 1 h to remove the possible contaminations from the BC pellicle. Thereafter, a homogenous suspension of BC (particle size: 351.03 nm) from the obtained BC mat was prepared by grinding the BC mat in distilled water.

### 4.3. Preparation of Inorganic Calcium Phosphate Filled BC Based Hydrogel Scaffold

BC based hydrogel scaffolds were first developed by applying the BC (holding 99% water) with CMC and PVP (Table 1) [49]. Polyethylene glycol (PEG) was also used in all the solutions to reduce

the risk of tissue damage and other significant cytotoxic effects [50]. Agar used as gelling agent and glycerin used as humectant [49].

Additionally,  $\beta$ -TCP and HA were applied in the ratio of 20:80 [49,51] in the hydrogel scaffolds to produce the inorganic calcium phosphate filled BC based hydrogel scaffolds. The prepared scaffolds were termed as, “BC-PVP- $\beta$ -TCP/HA” and “BC-CMC- $\beta$ -TCP/HA” (Figure 5), where, BC-PVP and BC-CMC hydrogel scaffolds were used as base scaffolds/control set [19].

**Table 1.** Composition of inorganic calcium phosphate filled BC based hydrogel scaffold [48,49].

Sample Index	PVP (g)	CMC (g)	BC (g)	PEG (g)	Agar (g)	Glycerin (mL)	$\beta$ -TCP/HA (g)	Water (mL)
BC-PVP	0.5	0.0	0.5	1	2	1	0.0/0.0	95
BC-CMC	0.0	0.5	0.5	1	2	1	0.0/0.0	95
BC-PVP- $\beta$ -TCP/HA	0.5	0.0	0.5	1	2	1	0.2/0.8	94
BC-CMC- $\beta$ -TCP/HA	0.0	0.5	0.5	1	2	1	0.2/0.8	94

The BC based hydrogel scaffolds were prepared following the solvent casting method, applying moist heat and pressure. 100 mL polymer solutions were prepared in 250 mL sealed glass bottles under 15 lbs (107 KPa) pressure and 120 °C temperature for 20 min [6]. Two sets of polymer solutions were prepared; where one set was without inorganic calcium phosphate, and another set was with inorganic calcium phosphate ( $\beta$ -TCP/HA). 25 mL polymer solution from each sealed glass bottles was poured into 75 mm diameter petri-dishes and allowed to cool at room temperature (22–25 °C). Finally, smooth, round shaped, off white color BC based scaffold without inorganic calcium phosphate (“BC-PVP” and “BC-CMC”) were achieved; diameter: 75 mm; thickness: 6.0–6.2 mm in wet state. The inorganic calcium phosphate filled scaffolds are termed as “BC-PVP- $\beta$ -TCP/HA” and “BC-CMC- $\beta$ -TCP/HA”; diameter: 75 mm; thickness: 5.5–6 mm of hydrogel scaffolds were attained.

#### 4.4. Preparation of Biomineralized Inorganic Calcium Phosphate and Calcium Carbonate ( $\text{CaCO}_3$ ) Filled BC Based Hydrogel Scaffold

The calcium phosphate filled BC based hydrogel scaffolds were further bio-mineralized for incorporation of additional  $\text{CaCO}_3$  for the development of strong bioactive polymeric scaffold material. For achieving that, the *in vitro* bio-mineralization process was performed following the simple liquid diffusion technique [52]. Two different ionic solutions (i.e.,  $\text{Na}_2\text{CO}_3$  and  $\text{CaCl}_2$ ) were used at fixed concentration ratios (5.25/100 mL and 7.35/100 mL) to prepare inorganic calcium phosphate and  $\text{CaCO}_3$  filled BC based hydrogel scaffolds. Research demonstrated that the deposition and accumulation of  $\text{CaCO}_3$  within the hydrogel scaffold is notable between 60–90 min [29]. Thus, in this study, the bio-mineralization of hydrogel matrix was carried out for 60 min by keeping the test samples in each ionic solution. The calcium phosphate filled BC based hydrogel scaffolds were first immersed in 100 mL solution of  $\text{CaCl}_2 \cdot \text{H}_2\text{O}$  for 30 min and then transferred into 100 mL of  $\text{Na}_2\text{CO}_3$  solution and kept them for 30 min. In this procedure, calcium phosphate and  $\text{CaCO}_3$  filled BC based *in vitro* bio-mineralized hydrogel scaffold were achieved having diameter: 75 mm; thickness: 4.5–4.9 mm (in wet state), and as a result, they are finally termed as “BC-PVP- $\beta$ -TCP/HA- $\text{CaCO}_3$ ” and “BC-CMC- $\beta$ -TCP/HA- $\text{CaCO}_3$ ” respectively (Figure 5).

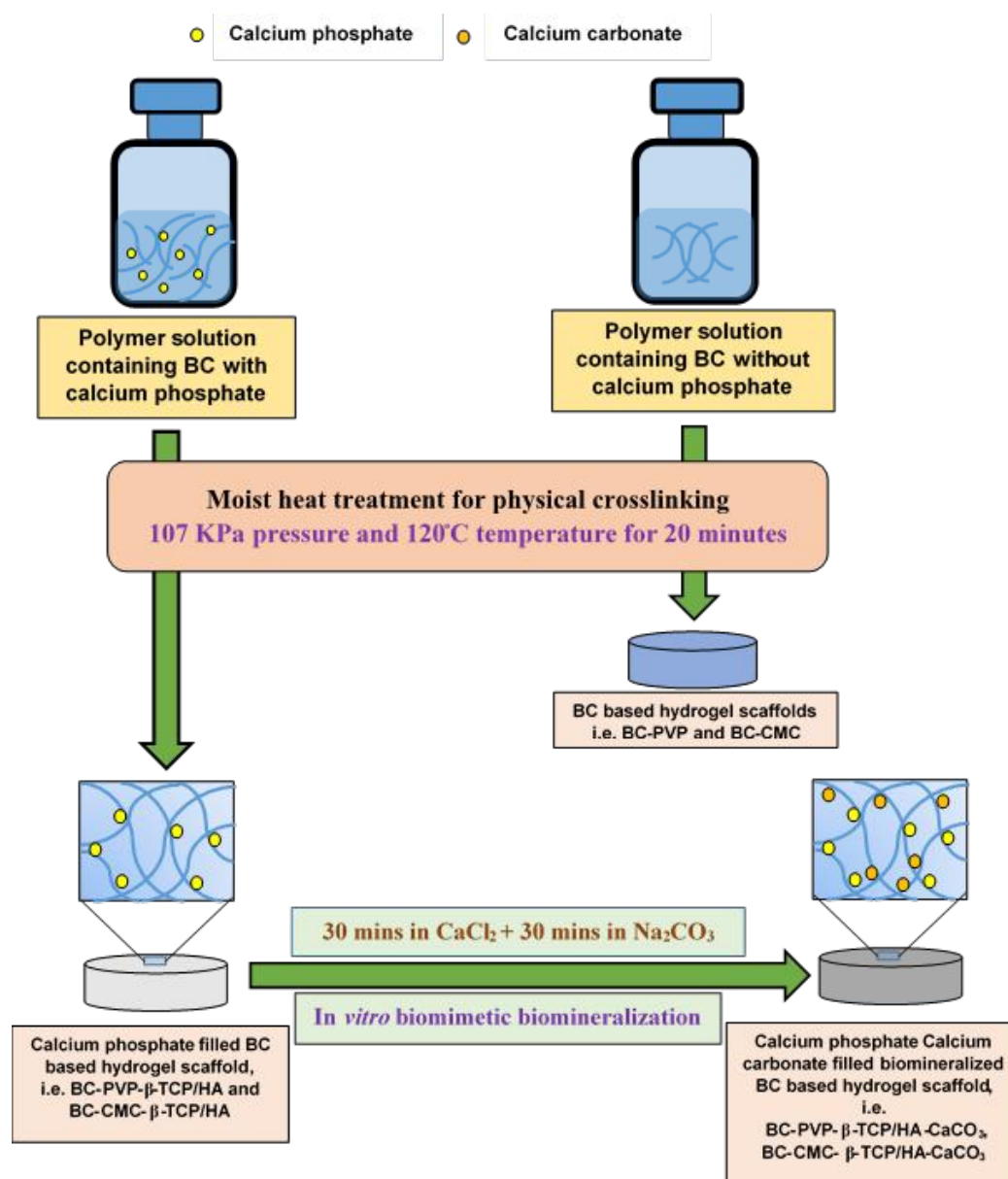


**Figure 5.** Schematic diagram: preparation of inorganic calcium filled BC based hydrogel scaffolds.

#### 4.5. Cell cultures

Human diploid fibroblast; Lep-3 cells from lung of 3-month old human embryo and cell culture established from bone explants of 2–3 months old ICR mice (Bone explant cells, BEC) as it was earlier described [39] were used as model systems in our study. Lep-3 and BEC cells were obtained from the Cell culture collection of the Institute of Experimental Morphology, Pathology and Anthropology with Museum—Bulgarian Academy of Sciences (IEMPAM-BAS).

Both the cultures were grown in DMEM medium supplemented with 10% fetal bovine serum, 100 U/mL penicillin and 100 µg/mL streptomycin. The cultures were kept in a humidified incubator (Thermo Scientific, HEPA Class 100, Waltham, MA, USA) at 37 °C under 5% CO<sub>2</sub> in air. For routine passages, the cells were detached using a mixture of 0.05% trypsin and 0.02% EDTA. The cell cultures were passaged 2–3 times per week (1:2 to 1:3 split). The experiments were performed during the exponential phase of cell growth. During investigations performed the BEC cells were on their 44–50th passages.

#### 4.6. Evaluation of Cell Viability and Proliferation

##### 4.6.1. Sample Preparation

Circular sections (size: 6 mm in diameter, 2–3 mm thickness) of the six freeze dried samples (BC-PVP, BC-CMC, BC-PVP- $\beta$ -TCP/HA, BC-CMC- $\beta$ -TCP/HA, BC-PVP- $\beta$ -TCP/HA-CaCO<sub>3</sub>, BC-CMC- $\beta$ -TCP/HA-CaCO<sub>3</sub>) were taken for this study. Sections were placed in the 48-well cell culture plate, treated with 50  $\mu$ L of 96% ethanol for 40 min after which the ethanol was removed and dried at 30–32 °C to complete dryness. Then, the materials were sterilized under the exposure of UV radiation for 80–90 min.

Indirect and direct experiments were performed for evaluating the influence of the materials on cell viability and proliferation

##### 4.6.2. Indirect Experiments (IDE)

Each material was placed in bottom of a 48 well cell culture plate on the drop (20  $\mu$ L) of FBS for 30 min at 30–32 °C in order to stick the sample to the surface of the well. Thereafter, 1 mL of DMEM (containing 10% FBS and antibiotics) was given to the wells (containing sterilized sample sections as well as empty wells that serve as controls) and then placed in the humidified incubator at 37 °C under 5% CO<sub>2</sub> in air for 3, 5 and 7 days. The cell culture medium (sample extracts and extract control medium) was collected and used in indirect experiments.

For cell viability/proliferation study, the cells (i.e., Lep-3 and BEC) were seeded in 96-well flat-bottomed microplates at a concentration of  $1 \times 10^4$  cells/well in fresh DMEM medium with 10% FBS. At the 24th h, the culture medium from each well was removed and changed with 100  $\mu$ L DMEM containing hydrogel scaffolds extract (sample extracts, obtained after 3-, 5- and 7-day incubation periods). The percent of viable cells was determined using MTT (3-(4,5-Dimethylthiazol-2-yl)-2,5-diphenyltetrazolium bromide) test.

MTT test was performed as it was earlier described [33]. Briefly, the cells were incubated for 3 h with MTT solution (0.3 mg MTT in 10 mL DMEM) at 37 °C under 5% CO<sub>2</sub> condition. The formed blue MTT formazan was extracted with a mixture of absolute ethanol and DMSO (1:1, *v/v*). The quantitative analysis was performed by absorbance measurements in an automated microplate reader (Tecan, Sunrise™, Grödig, Austria) at 540/620 nm.

##### 4.6.3. Direct Experiments (DE)

The cells ( $5 \times 10^4$  cells/well) were seeded directly on the material sample placed on the bottom of a 48-well cell culture plate and incubated for 3, 5 and 7 days in CO<sub>2</sub> incubator at 37 °C. The number and viability of the cells were determined before seeding using automated cell counter by trypan blue dye exclusion technique (zero time). The cell viability was found to be >95% in all experiments performed. At the start of the experiment the cell numbers are equal in all wells / between all different samples, and they are cultured in equal conditions. Cells were grown in wells without materials, served as controls. The effect of the materials on cell viability and proliferation was studied by MTT test as described in Section 4.6.2 with MTT concentration is corresponding to the volume of the plate.

#### 4.7. Study of DNA Damages

The presence of single and double stranded DNA damages was assessed by single cell gel electrophoresis (Comet assay) at alkaline pH. Lep-3 cells were seeded in 6-well flat-bottomed microplates at a concentration of  $3 \times 10^5$  cells/well. At the 24th hour the culture medium was removed and changed with sample extract media (3-days modified media) and control media prepared as described in Section 4.6.2.

The Lep-3 cells were mixed with 1.4% of low-gelling agarose (Sigma Type II) and immediately spread onto microscopic slides precoated with 0.5% normal agarose. Cells were lysed for 1 h in a lysis solution (1 M NaCl, 50 mM EDTA pH 8, 30 mM NaOH, 0.1% *N*-lauroylsarcosine; pH 10). After 1-h

incubation in the denaturing solution (30 mM NaOH, 10 mM EDTA; pH 12.6) for DNA unwinding, the slides were electrophoresed for 20 min at 0.46 V/cm in the same denaturing buffer. At the end of the electrophoresis the slides were subsequently dehydrated for 5 min in 75% and in 96% of ethanol. Comets were observed under Leitz epifluorescent microscope (Orthoplan, VARIO ORTHOMAT 2) using a 450–490 nm band-pass filter following staining of microgels with the fluorescent dye SYBR green I (Molecular Probes, Eugene, OR, USA). 1000 randomly chosen objects per each probe and treatment were taken for quantification. Two repetitions of the experiment were done and standard deviations were quantified. In all cases they were very small.

#### 4.8. Apoptosis/Necrosis Study via Annexin V-FITC

The ability of the materials to induce cells death was evaluated by APOPTOSIS detection kit, (ANNEXIN V—GFP-Certified Apoptosis/Necrosis detection kit, Enzo Life Sciences). Cells were spun down at 400 g for 5 min at room temperature and carefully re-suspended in 1 mL cold 1 × PBS (2.68 mM KCl, 1.47 mM KH<sub>2</sub>PO<sub>4</sub>, 1.37 mM NaCl, 8 mM Na<sub>2</sub>HPO<sub>4</sub>), pH 7. Spinning down follows at the same conditions and the pellet was re-suspended in 510 µL Dual Detection Reagent (500 µL 1 × binding buffer, 5 µL Apoptosis Detection reagent/Annexin V-Enzo Gold; 5 µL Necrosis Detection Reagent). Samples were incubated at room temperature for 10 min at dark and were analysed via cytometry using 488 nm laser at FL 2 and FL 3 channels for apoptosis and necrosis detection respectively. Results were quantified with FlowJo software. Two repetitions of the experiment were done. Data quantitation included estimation of the percentage of cells undergoing apoptosis and necrosis and the ratio between these percentages in comparison to the control cells is given in PDU (procedure data units).

#### 4.9. SEM Analysis

The samples prepared as described in Section 4.6.1. Lep-3 cells ( $7 \times 10^5$  cells/well) were seeded directly on sample materials in a 48-well cell culture plate and left in an incubator (Thermo Scientific) at 37 °C, 5% CO<sub>2</sub>. After 7 days' incubation period, the culture medium was removed and the sample sections were washed with 4% glutaraldehyde for 1 h followed by washing with double distilled water. The samples were then subjected to dry by filter system CORNING 431097 (0.22 µm) under low pressure for 2 h and were left for 2 days at 30–32 °C for complete drying. Finally, samples were prepared for SEM analysis by a standard procedure and observed under scanning electron microscope (JEOL JSM-5510, Tokyo, Japan) at an accelerating voltage of 10 kV.

#### 4.10. Statistical Analysis

The data are presented as mean ± standard error of the mean. Statistical differences between control and treated groups were assessed using one-way analysis of variance (ANOVA) and student's *t*-test followed by suitable post-hoc test by using GraphPad Prism version 5.00 (San Diego, CA, USA) for Windows and MS Office 2010 (Redmond, WA, USA).

## 5. Conclusions

The present work focuses the biocompatibility and biological efficiency of inorganic calcium filled hydrogel scaffold in bone regeneration/bone bioengineering. The comprehensive comparative study with two cell lines indicates the cell biological efficiency of the scaffolds. Lep-3 cell line represents non-specified human fibroblast and mouse bone explant cell (BEC) line represents specified bone cells. The comparative cell viability study (with the extracts of all the six BC based hydrogel scaffolds) and biocompatibility study with two different cell lines indicates that the PVP based hydrogel scaffold can facilitate the growth and proliferation of both types of cell lines. Additionally, the percentage of DNA strand break were found less in PVP based samples than CMC based samples. Furthermore, apoptosis events were not so significantly found in Lep-3 cells with BC-PVP-β-TCP/HA. Finally, SEM study indicates the efficient adhesion and growth of fibroblast (Lep-3) cells throughout the BC-PVP-β-TCP/HA hydrogel scaffold surface. Thus, this scaffold exhibits promising osteo-conduction.



Additionally, the notable cyto-compatibility of this scaffold suggests its putative ability to facilitate the process of bone regeneration. However, further studies are required with different osteogenic cell lines (i.e., osteoblast) and mesenchymal stem cell line to ascertain the efficiency of abovementioned hydrogel scaffold in bone tissue engineering.

**Author Contributions:** Conceptualization, N.S. and P.S.; Data curation, B.A.-L.; Formal analysis, P.B., R.A., M.G. and G.M.; Funding acquisition, N.S., R.A. and P.S.; Investigation, P.B.; Supervision, N.S.; Writing—original draft, P.B.; Writing—review and editing, N.S., R.A. and M.G.

**Funding:** This work is mainly supported by the Internal Grant Agency (Project No. IGA/CPS/2017/003 and IGA/CPS/2018/008), Tomas Bata University in Zlin, Czech Republic and Ministry of Education, Youth and Sports of the Czech Republic—NPU Program I (LO1504), National Scientific Fund, Bulgarian Ministry of Education and Science under Grant No. DFNI Б 02 30, Bulgarian Science Fund (Grant No. DN 11/15) and NATO science for Peace and Security program (Grant No. NATO SPS MYP G5266). Moreover, this work was performed within the framework of COST Action MP1301 “New Generation Biomimetic and Customized Implants for Bone Engineering” ([www.cost.eu](http://www.cost.eu)) and COST Action CA15214 “An integrative action for multidisciplinary studies on cellular structural networks”.

**Conflicts of Interest:** The authors declare no conflict of interest.

## References

1. Buenzli, P.R.; Sims, N.A. Quantifying the osteocyte network in the human skeleton. *Bone* **2015**, *75*, 144–150. [[CrossRef](#)] [[PubMed](#)]
2. Kini, U.; Nandeesh, B.N. *Physiology of Bone Formation, Remodeling and Metabolism*, In *Radionuclide and Hybrid Bone Imaging*; Springer: Heidelberg, Germany, 2012; pp. 29–57. ISBN 978-3-642-02400-9.
3. International Osteoporosis Foundation (IOF). 2017. Available online: <https://www.iofbonehealth.org/facts-statistics> (accessed on 30 August 2017).
4. Castilho, M.; Dias, M.; Vorndran, E.; Gbureck, E.; Fernandes, P.; Pires, I.; Gouveia, B.; Armes, H.; Pires, E.; Rodrigues, J. Application of a 3D printed customized Implant for canine cruciate ligament treatment by tibial tuberosity advancement. *Biofabrication* **2014**, *6*, 1–13. [[CrossRef](#)] [[PubMed](#)]
5. Deligkaris, K.; Tadele, T.S.; Olthuis, W. Hydrogel-based devices for biomedical applications. *Sens. Actuators B* **2010**, *147*, 765–774. [[CrossRef](#)]
6. Roy, N.; Saha, N.; Kitano, T.; Saha, P. Biodegradation of PVP–CMC hydrogel film: A useful food packaging material. *Carbohydr. Polym.* **2012**, *89*, 346–353. [[CrossRef](#)] [[PubMed](#)]
7. Roy, S.G.; De, P. Swelling properties of amino acid containing cross-linked polymeric organogels and their respective poly-electrolytic hydrogels with pH and salt responsive property. *Polymer* **2014**, *55*, 5425–5434. [[CrossRef](#)]
8. Saha, N. Morphology, Absorptivity and Viscoelastic Properties of Mineralized PVP-CMC Hydrogel. *AIP Conf. Proc.* **2013**, *1526*, 292–300. [[CrossRef](#)]
9. Burg, K.J.L.; Porter, S.J.F.; Kellam, J.F. Biomaterial developments for bone tissue engineering. *Biomaterials* **2000**, *21*, 2347–2359. [[CrossRef](#)]
10. Polo-Corrales, L.; Latorre-Esteves, M.; Ramirez-Vick, J.E. Scaffold design for bone Regeneration. *J. Nanosci. Nanotechnol.* **2014**, *14*, 15–56. [[CrossRef](#)]
11. Stratton, S.; Shelke, N.B.; Hoshino, K. Bioactive polymeric scaffolds for tissue engineering. *Bioact. Mater.* **2016**, *1*, 93–108. [[CrossRef](#)]
12. Thavorniyutikarn, B.; Chantarapanich, N.; Sitthiseripratip, K. Bone tissue engineering scaffolding: Computer-aided scaffolding techniques. *Prog. Biomater.* **2014**, *3*, 61–102. [[CrossRef](#)]
13. Walimbe, T.; Panitch, A.; Sivasankar, P.M. A Review of Hyaluronic Acid and Hyaluronic Acid-based Hydrogels for Vocal Fold Tissue Engineering. *J. Voice* **2017**, *31*, 416–423. [[CrossRef](#)] [[PubMed](#)]
14. Ritz, U.; Gerke, R.; Götz, H.; Stein, S.; Rommens, P.M. A New Bone Substitute Developed from 3D-Prints of Polylactide (PLA) Loaded with Collagen I: An In Vitro Study. *Int. J. Mol. Sci.* **2017**, *18*, 2569. [[CrossRef](#)] [[PubMed](#)]
15. Jo, Y.-Y.; Kim, S.-G.; Kwon, K.-J.; Kweon, H.; Chae, W.-S.; Yang, W.-G.; Lee, E.-Y.; Seok, H. Silk Fibroin-Alginate-Hydroxyapatite Composite Particles in Bone Tissue Engineering Applications In Vivo. *Int. J. Mol. Sci.* **2017**, *18*, 858. [[CrossRef](#)] [[PubMed](#)]

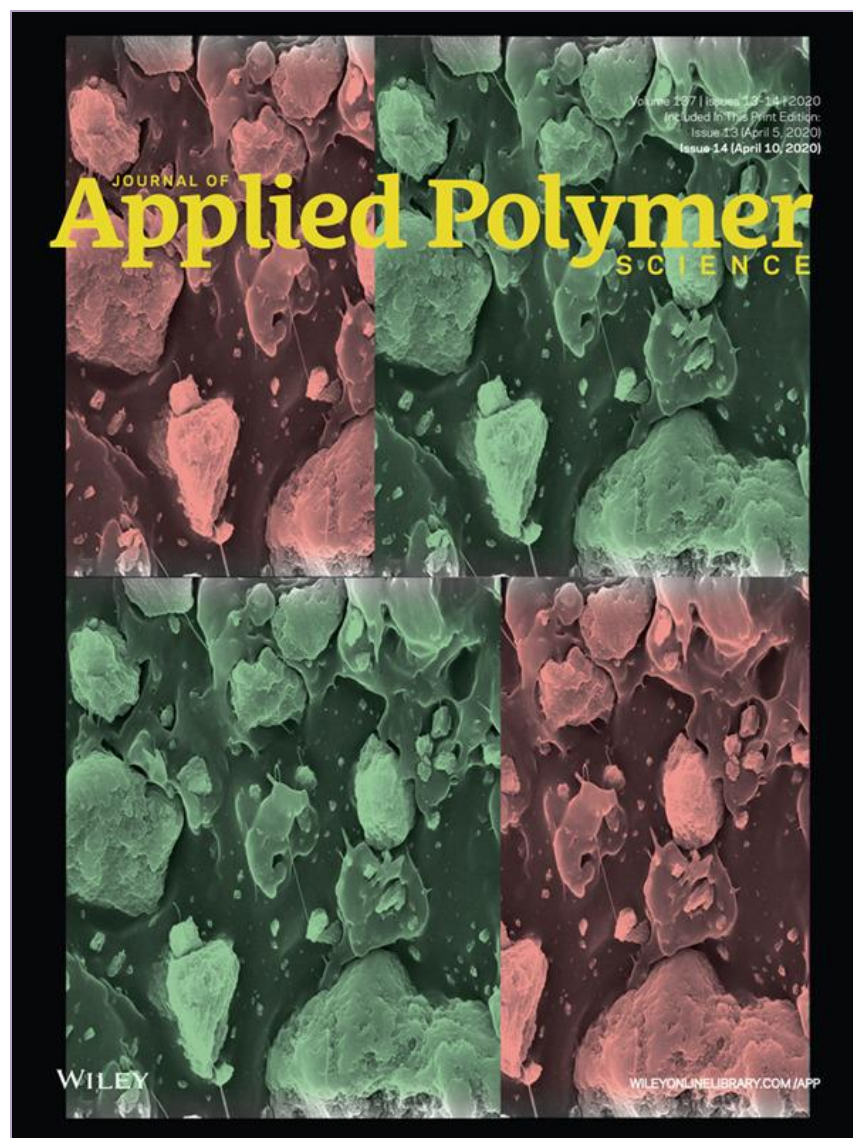
16. Gentile, P.; Chiono, V.; Carmagnola, I.; Hatton, P.V. An Overview of Poly(lactic-co-glycolic) Acid (PLGA)-Based Biomaterials for Bone Tissue Engineering. *Int. J. Mol. Sci.* **2014**, *15*, 3640–3659. [[CrossRef](#)] [[PubMed](#)]
17. Jiang, P.; Ran, J.; Yan, P.; Zheng, L.; Shen, X.; Tong, H. Rational design of a high-strength bone scaffold platform based on in situ hybridization of bacterial cellulose/nano-hydroxyapatite framework and silk fibroin reinforcing phase. *J. Biomater. Sci. Polym. Ed.* **2018**, *29*, 107–124. [[CrossRef](#)] [[PubMed](#)]
18. Keshk, S. Bacterial Cellulose Production and its Industrial Applications, Bacterial Cellulose Production and its Industrial Applications. *J. Bioprocess. Biotech.* **2014**, *4*, 1000150. [[CrossRef](#)]
19. Shah, R.; Vyroubal, R.; Fei, H.; Saha, N.; Kitano, T.; Saha, P. Preparation of bacterial cellulose based hydrogels and their viscoelastic behavior. *AIP Conf. Proc.* **2015**, 1662. [[CrossRef](#)]
20. Ul-Islam, M.; Khan, T.; Kon Park, J. Water holding and release properties of bacterial cellulose obtained by in situ and ex situ modification. *Carbohydr. Polym.* **2012**, *88*, 596–603. [[CrossRef](#)]
21. Rey, C.; Combes, C.; Drouet, C.; Glimcher, M.J. Bone mineral: Update on chemical composition and structure. *Osteoporos. Int.* **2009**, *20*, 1013–1021. [[CrossRef](#)] [[PubMed](#)]
22. Aquino-Martínez, R.; Artigas, N.; Gámez, B.; Rosa, J.L.; Ventura, F. Extracellular calcium promotes bone formation from bone marrow mesenchymal stem cells by amplifying the effects of BMP-2 on SMAD signaling. *PLoS ONE* **2017**, *12*, e0178158. [[CrossRef](#)]
23. McCleskey, E.W.; Fox, A.P.; Feldman, D.; Tsien, R.W. Different types of calcium channels. *J. Exp. Biol.* **1986**, *124*, 177–190. [[PubMed](#)]
24. Dvorak-Ewell, M.M.; Chen, T.H.; Liang, N.; Garvey, C.; Liu, B.; Tu, C.; Chang, W.; Bikle, D.D.; Shoback, D.M. Osteoblast Extracellular Ca<sup>2+</sup>-Sensing Receptor Regulates Bone Development, Mineralization and Turnover. *J. Bone Miner. Res.* **2011**, *26*, 2935–2947. [[CrossRef](#)] [[PubMed](#)]
25. Dvorak, M.M.; Siddiqua, A.; Ward, D.T. Physiological changes in extracellular calcium concentration directly control osteoblast function in the absence of calciotropic hormones. *Proc. Natl. Acad. Sci. USA* **2004**, *101*, 5140–5145. [[CrossRef](#)] [[PubMed](#)]
26. Ghassemi, T.; Shahroodi, A.; Ebrahimzadeh, M.H.; Mousavian, A.; Movaffagh, J.; Moradi, A. Current concepts in scaffolding for bone tissue engineering. *Arch. Bone Jt. Surg.* **2018**, *6*, 2–90.
27. Drzewiecka, K.; Kleczewska, J.; Krasowski, M.; Łapińska, B. Mechanical properties of composite material modified with amorphous calcium phosphate. *J. Achiev. Mater. Manuf. Eng.* **2016**, *74*, 22–28. [[CrossRef](#)]
28. Muthukumar, T.; Aravinthan, A.; Sharmila, J. Collagen/chitosan porous bone tissue engineering composite scaffold incorporated with Ginseng Compound, K. *Carbohydr. Polym.* **2016**, *152*, 566–574. [[CrossRef](#)] [[PubMed](#)]
29. Shah, R.; Saha, N.; Kitano, T.; Saha, P. Preparation of CaCO<sub>3</sub>-Based Biomineralized Polyvinylpyrrolidone-Carboxymethylcellulose Hydrogels and Their Viscoelastic Behaviour. *J. Appl. Polym. Sci.* **2014**, *40237*, 1–9. [[CrossRef](#)]
30. Roy, N.; Saha, N.; Kitano, T.; Saha, P. Novel hydrogels of PVP–CMC and their swelling effect on viscoelastic properties. *J. Appl. Polym. Sci.* **2010**, *117*, 1703–1710. [[CrossRef](#)]
31. Allou, N.B.; Yadav, A.; Pal, M.; Goswamee, R.L. Biocompatible nanocomposite of carboxymethyl cellulose and functionalized carbon–norfloxacin intercalated layered double hydroxides. *Carbohydr. Polym.* **2018**, *186*, 282–289. [[CrossRef](#)]
32. Saha, N.; Shah, R.; Gupta, P.; Mandal, B.B.; Alexandrova, R.; Sikiric, M.D.; Saha, P. PVP-CMC hydrogel: An excellent bioinspired and biocompatible scaffold for osseointegration. *Mater. Sci. Eng. C* **2018**. [[CrossRef](#)]
33. Kim, J.; Cai, Z.; Lee, H.S.; Choi, G.S.; Lee, D.H.; Jo, C. Preparation and characterization of bacterial cellulose/chitosan composite for potential biomedical application. *J. Polym. Res.* **2011**, *18*, 739–744. [[CrossRef](#)]
34. Saska, S.; Teixeira, L.N.; de Oliveira, P.T.; Gaspar, A.M.M.; Ribeiro, S.J.L.; Messaddeq, Y.; Marchetto, R. Bacterial cellulose-collagen nanocomposite for bone tissue engineering. *J. Mater. Chem.* **2012**, *22*, 22102–22112. [[CrossRef](#)]
35. Pértile, R.A.N.; Moreira, S.; Gil da Costa, R.M.; Correia, A.; Guãrdao, L.; Gartner, F.; Vilanova, M.; Gama, M. Bacterial Cellulose: Long-Term Biocompatibility Studies. *J. Biomater. Sci. Polym. Ed.* **2018**, *201223*, 1339–1354. [[CrossRef](#)] [[PubMed](#)]
36. Lee, J.H.; Ryu, M.Y.; Baek, H.-R.; Lee, K.M.; Seo, J.-H.; Lee, H.-K. Fabrication and Evaluation of Porous Beta-Tricalcium Phosphate/Hydroxyapatite (60/40) Composite as a Bone Graft Extender Using Rat Calvarial Bone Defect Model. *Sci. World J.* **2013**, *481789*, 1–9. [[CrossRef](#)] [[PubMed](#)]

37. Kamba, A.S.; Ismail, M.; Ibrahim, T.A.T.; Zakaria, Z.A.B. Biocompatibility of Bio Based Calcium Carbonate Nanocrystals Aragonite Polymorph on NIH 3T3 Fibroblast Cell Line. *Afr. J. Tradit. Complement. Altern. Med.* **2014**, *11*, 31–38. [[CrossRef](#)] [[PubMed](#)]
38. Andonova-Lilova, B.; Alexandrova, R.; Rabadjieva, D.; Tepavitcharova, S. Application of cultured murine cells for initial evaluation of the biocompatibility of Mg and Zn-modified tri-calcium phosphates. *C. R. Acad. Bulg. Sci.* **2012**, *65*, 1099–1104.
39. Martín, L.; Alonso, M.; Girotti, A.; Arias, F.J.; Rodriguez-Cabello, J.C. Synthesis and Characterization of Macroporous Thermosensitive Hydrogels from Recombinant Elastin-Like Polymers. *Biomacromolecules* **2009**, *10*, 3015–3022. [[CrossRef](#)] [[PubMed](#)]
40. Gafter, U.; Malachi, T.; Ori, Y.; Breitbart, H. The role of calcium in human lymphocyte DNA repair ability. *J. Lab. Clin. Med.* **1997**, *130*, 33–41. [[CrossRef](#)]
41. Buljan, Z.I.; Ribaric, S.P.; Abram, M.; Ivankovic, A.; Spalj, S. In vitro oxidative stress induced by conventional and self-ligating brackets. *Angle Orthod.* **2012**, *82*, 340–345. [[CrossRef](#)] [[PubMed](#)]
42. Guadagno, N.A.; Moriconi, C.; Licursi, V.; D'Acunto, E.; Nisi, P.S.; Carucci, N.; De Jaco, A.; Cacci, E.; Negri, R.; Lupo, G.; Miranda, E. Neuroserpin polymers cause oxidative stress in a neuronal model of the dementia FENIB. *Neurobiol. Dis.* **2017**, *103*, 32–44. [[CrossRef](#)] [[PubMed](#)]
43. Eliaz, N.; Metoki, N. Calcium Phosphate Bioceramics: A Review of Their History, Structure, Properties, Coating Technologies and Biomedical Applications: A Review. *Materials* **2017**, *10*, 334. [[CrossRef](#)] [[PubMed](#)]
44. Voccoli, V.; Tonazzini, I.; Signore, G.; Caleo, M.; Cecchini, M. Role of extracellular calcium and mitochondrial oxygen species in psychosine-induced oligodendrocyte cell death. *Cell Death Dis.* **2014**, *5*, 1–10. [[CrossRef](#)] [[PubMed](#)]
45. McIlwain, D.R.; Berger, T.; Mak, T.W. Review on Caspase Functions in Cell Death and Disease. *Cold Spring Harb. Perspect. Biol.* **2013**, *5*, 1–28. [[CrossRef](#)] [[PubMed](#)]
46. Chang, H.-I.; Wang, Y.I. Cell Responses to Surface and Architecture of Tissue Engineering Scaffolds. In *Regenerative Medicine and Tissue Engineering—Cells and Biomaterials*; Daniel, E., Ed.; InTech: London, UK, 2011; pp. 569–588. ISBN 978-953-307-6638.
47. Engler, A.J.; Sen, S.; Sweeney, H.L.; Discher, D.E. Matrix elasticity directs stem cell lineage specification. *Cell* **2006**, *126*, 677–689. [[CrossRef](#)] [[PubMed](#)]
48. Basu, P.; Saha, N.; Saha, P. Inorganic calcium filled bacterial cellulose based hydrogel scaffold: A novel biomaterial for bone tissue regeneration. *Int. J. Polym. Mater.* **2018**, in press.
49. Basu, P.; Saha, N.; Bandyopadhyay, S.; Saha, P. Rheological performance of bacterial cellulose based nonmineralized and mineralized hydrogel scaffolds. *AIP Conf. Proc.* **2017**, *1843*, 050008. [[CrossRef](#)]
50. Alcantar, N.A.; Aydil, E.S.; Israelachvili, J.N. Polyethylene glycol-coated biocompatible surfaces. *J. Biomed. Mater. Res.* **2000**, *51*, 343–351. [[CrossRef](#)]
51. Struillou, X.; Rakic, M.; Badran, Z.; Macquigneau, L.; Colombeix, C.; Pilet, P.; Verner, C.; Gauthier, O.; Weiss, P.; Soueidan, A. The association of hydrogel and biphasic calcium phosphate in the treatment of dehiscence-type peri-implant defects: An experimental study in dogs. *J. Mater. Sci. Mater. Med.* **2013**, *24*, 2749–2760. [[CrossRef](#)] [[PubMed](#)]
52. Rauch, M.W.; Dressler, M.; Scheel, H.; Opdenbosch, D.V.; Zollfrank, C. Mineralization of Calcium Carbonates in Cellulose Gel Membranes. *Eur. J. Inorg. Chem.* **2012**, *32*, 5192–5198. [[CrossRef](#)]



## PUBLICATION IV

**Basu P (50%), Saha N & Saha P. (2020)** “Swelling and rheological study of calcium phosphate filled bacterial cellulose based hydrogel scaffold”, *Journal of Applied Polymer Science* [Web of Science Indexed, Q2 [Polymer Science], **J<sub>imp</sub>: 2.188**), 137, 48522. DOI: 10.1002/app.48522



Volume 137 | Issues 13–14 | 2020

Included In This Print Edition:

Issue 13 (April 5, 2020)

Issue 14 (April 10, 2020)

JOURNAL OF  
**Applied Polymer**  
SCIENCE

The cover features four panels of microscopic images showing porous, interconnected polymer structures. The top-left and bottom-right panels are colored in shades of red and orange, while the top-right and bottom-left panels are colored in shades of green. The structures appear to be highly porous and interconnected, typical of membranes or porous polymers.

WILEY

WILEYONLINELIBRARY.COM/JAPP

## Swelling and rheological study of calcium phosphate filled bacterial cellulose-based hydrogel scaffold

Probal Basu , Nabanita Saha , Petr Saha 

Centre of Polymer Systems, University Institute, Tomas Bata University in Zlin, Trida Tomase Bati 5678, 760 01 Zlín, Czech Republic

Correspondence to: N. Saha (E-mail: nabanita@utb.cz)

**ABSTRACT:** This work focuses mainly about swelling and rheological properties of calcium phosphate filled bacterial cellulose (BC)-based hydrogel scaffolds. Calcium phosphate is incorporated in the form of hydroxyapatite (HA) and  $\beta$ -tricalcium phosphate ( $\beta$ -TCP) in different ratios, that is, 00:00, 10:90, 20:80, 40:60, 50:50, and 60:40. These scaffolds are also comprised with polyvinylpyrrolidone (PVP), poly(ethylene glycol), agar, and glycerin; designated as “BC-PVP” and “BC-PVP- $\beta$ -TCP/HA.” All the hydrogel scaffolds are showing the notable viscoelastic property at 28 and 37 °C temperatures. The degree of swelling is found significant in BC-PVP- $\beta$ -TCP/HA\_50:50 scaffold and it is notably elastic at 37 °C after 5 min of swelling. However, after 60 min of swelling and at equilibrium swelling state, the elastic property of BC-PVP- $\beta$ -TCP/HA\_20:80 is revealed the highest. Considering the degree of swelling and rheological properties, the BC-PVP- $\beta$ -TCP/HA\_50:50 and BC-PVP- $\beta$ -TCP/HA\_20:80 hydrogel scaffolds found suitable for their application in bone tissue engineering or bone tissue regeneration. © 2019 Wiley Periodicals, Inc. *J. Appl. Polym. Sci.* **2020**, *137*, 48522.

**KEYWORDS:** biomaterials; rheology; swelling

Received 27 April 2019; accepted 2 September 2019

DOI: [10.1002/app.48522](https://doi.org/10.1002/app.48522)

### INTRODUCTION

The human musculoskeletal system is comprised of bones,<sup>1</sup> which provide necessary mechanical support to the body.<sup>2,3</sup> However, the fracture of bone seldom happens in significant stressful mechanical and/or physiological conditions. Aging and bone-related diseases also enhance the propensity for bone fracture.<sup>3</sup> Study indicated that bone-related diseases like osteoporosis is the cause of 2 million bone fractures every year and this number will increase to 3 million by 2025.<sup>4</sup> Bone auto-grafting is a well-practiced method, which facilitates the fracture healing process through significant osteoconductivity and osteoinductivity.<sup>5</sup> However, the limitations of this method are also notable.<sup>5–7</sup> The autograph-based approach involves the application of implant which is obtained from the host body. The bone volume which can be collected is also limited. In addition, the potential surgical risks like infection and inflammation, bleeding, hypersensitivity, and damage of donor tissue are also prominent.<sup>8</sup> Hence, a new approach toward the potential solution of this problem is a current and immediate need.<sup>1,9</sup> The polymeric biomaterial can mimic the physical and biochemical attributes of the natural bone matrix.<sup>8</sup> In addition, the use of polymeric degradable biomaterials will not require a secondary surgical procedure for implant removal. Thus, bone tissue engineering with polymeric biomaterial

can become an efficient alternative approach to solve this problem.<sup>5,10</sup>

Biomaterials are the materials which can be used as scaffolds for tissue engineering.<sup>11,12</sup> It elaborates the cell–cell attachment and communication through the porous networks.<sup>13</sup> Different metal-based material like titanium along with calcium phosphate ceramics like hydroxyapatite (HA) and  $\beta$ -tricalcium phosphate ( $\beta$ -TCP) have been significantly and successfully utilized for bone tissue engineering applications.

Different composite materials for bone tissue engineering were developed by using synthetic polymers like poly(glycolic acid), poly( $\epsilon$ -caprolactone), poly(lactic-co-glycolic acid), poly(L-lactic acid), poly(vinyl alcohol), poly(acrylic acid), and poly(aldehyde gluconate).<sup>14–17</sup> In addition, natural polymers like collagen, gelatin, fibrin,<sup>18</sup> agar,<sup>19</sup> and cellulose<sup>20</sup> have also been used in tissue engineering application. Bacterial cellulose (BC) is considered as a significant biopolymer because of its high mechanical property, high crystallinity, and notable biocompatibility. Earlier studies reported that the BC-based biomaterial has applied in wound dressing, development of vascular grafts and artificial blood vessel, tissue engineering application, and so forth.<sup>21–24</sup> BC-based polymeric hydrogel scaffold can be efficiently utilized as three-dimensional scaffold material for bone tissue engineering.<sup>25–28</sup>

Appropriate mechanical property and biocompatibility are the two important concerns for the biomaterials for bone tissue engineering application. The major challenge of the recent materials is the proper tuning of these properties which are essential for their application.<sup>8,29</sup> Thus, in addition to the appropriate biocompatibility, the study of the mechanical property of biomaterial is necessary for its successful applicability.

The rheological analysis indicates the mechanical property of a composite biomaterial by explaining its nature of the internal structure and physical properties of the polymer–filler composite.<sup>30,31</sup> Various researches were conducted to understand the rheological behavior of the hydrogel scaffolds<sup>32–39</sup> utilized in bone tissue engineering applications. The frequency dependence of storage ( $G'$ ) and loss ( $G''$ ) modulus in the linear viscoelasticity region (LVR) provides significant information regarding gel structure and its mechanical behavior,<sup>39</sup> which confirms the applicability of the biomaterial.

Polymeric hydrogel scaffold [polyvinylpyrrolidone (PVP)-carboxymethyl cellulose (CMC)] was earlier developed in our laboratory in combination of synthetic polymers, PVP, and CMC.<sup>40,41</sup> Moreover, hydrogel scaffold was developed using BC and PVP in our previous work.<sup>34</sup> However, all the afore-mentioned hydrogel scaffolds had the notable elastic property; more specific bioactive suitable biomaterial is needed, especially for bone tissue engineering application. Very few researches have been performed which have indicated the swelling and rheological behavior of the scaffold material.<sup>42–44</sup> Previously, Tommasi *et al.*<sup>45</sup> have indicated the rheological behavior of injectable hydrogel (prepared with synthetic polymers and chemical crosslinking agents) after 14 days of swelling. However, there is no significant study that has indicated the viscoelastic changes of hydrogel scaffolds corresponding to their swelling effect. The present study only focuses on the swelling and viscoelastic changes at physiological temperature (37 °C). However, the change in chemical and surface properties of the calcium phosphate filled hydrogel scaffold with the gradual swelling can also be observed for a better degree of understanding regarding the physiochemical attributes of the scaffolds in the physiological conditions, which might be analyzed and reported in our future work.

Moreover, previous studies showed that the human body temperature and pH have also their effects on the viscoelastic behavior of the scaffolds.<sup>46,47</sup> Thus, the current study of viscoelasticity of the scaffolds at human physiological temperature ( $\pm 37$  °C) will finally lead to the selection of better calcium phosphate filled BC

based hydrogel scaffold material in regard to its rheological behavior/mechanical property for bone tissue engineering application.

## EXPERIMENTAL

### Materials

Polyvinylpyrrolidone K30 (PVP K30; molecular weight: 40 000 g/mol), poly(ethylene glycol) 3000 (PEG; average molecular weight: 2700–3300 g/mol), agar, and  $\beta$ -TCP (molecular weight: 310.18 g/mol) were supplied by Fluka, Switzerland. Hydroxyapatite (HA; molecular weight: 502.31 g/mol) were obtained from Sigma–Aldrich, St. Louis, USA. Glycerin was obtained from Lach-Ner s.r.o., Czech Republic.

### Synthesis and Preparation of Homogenous Suspension of BC

BC (holding 99% H<sub>2</sub>O) was synthesized in presence of basal synthetic Hestrin–Schramm nutritive medium (pH 7.0) using *Glucanacetobacter xylinus* CCM 3611<sup>T</sup> (syn. *Acetobacter xylinum*) at 30 °C for 15 days. Hundred milliliters of bacteriological culture bottles were inoculated with 5 mL of HS medium containing  $96 \times 10^8$  cells/mL bacteria [bacteria counted at 550 nm wavelength with Grant-Bio McFarland Densitometer DEN-1B, Grant Instruments Ltd., U.K.]. The freshly prepared BC pellicle was then treated with 0.5 N NaOH solution and then heated at 80 °C for 1 h to remove the possible contaminations from the pellicle. The newly produced BC pellicle was then treated with deionized water and the water was refreshed after 2 h of interval until the pH reached a neutral value. Thereafter, a homogenous suspension of BC [particle size: 159 nm (SD:  $\pm 11.33$ )] from the obtained BC mat was prepared by grinding (12 min) the BC mat in distilled water.

### Preparation of Calcium Phosphate Filled BC-Based Hydrogel Scaffolds

BC-based hydrogel scaffolds were developed by applying the BC (holding 99% water) with PVP<sup>48</sup> (Table I). PEG was also used in all the hydrogel solutions to reduce the risk of tissue damage and other significant cytotoxic effects.<sup>49</sup> Moreover, agar has used as a gelling agent and glycerin used as humectant.<sup>48</sup> Agar is a hydrophilic polymer<sup>50</sup> that performs as a gelling agent and help in the increase of the degree of swelling.

Additionally,  $\beta$ -TCP and HA were incorporated in the ratio of 00:00, 10:90, 20:80, 40:60, 50:50, and 60:40 into the hydrogel scaffold matrix to achieve the calcium phosphate filled BC-based

**Table I.** Composition of Calcium Phosphate Filled Bacterial Cellulose-Based Hydrogel Scaffolds with Varied  $\beta$ -TCP and HA

Sample index	PVP (g)	BC (g)	PEG (g)	Agar (g)	Glycerin (mL)	$\beta$ -TCP/HA (g)	Water (mL)
BC-PVP	0.5	0.5	1	2	1	0.0/0.0	95
BC-PVP- $\beta$ -TCP/HA_10:90	0.5	0.5	1	2	1	0.1/0.9	94
BC-PVP- $\beta$ -TCP/HA_20:80	0.5	0.5	1	2	1	0.2/0.8	94
BC-PVP- $\beta$ -TCP/HA_40:60	0.5	0.5	1	2	1	0.4/0.6	94
BC-PVP- $\beta$ -TCP/HA_50:50	0.5	0.5	1	2	1	0.5/0.5	94
BC-PVP- $\beta$ -TCP/HA_60:40	0.5	0.5	1	2	1	0.6/0.4	94

Abbreviations: BC, bacterial cellulose; HA, hydroxyapatite; PEG, poly(ethylene glycol); PVP, polyvinylpyrrolidone; TCP, tricalcium phosphate.

hydrogel scaffolds (Table I) and henceforth will be termed as, “BC-PVP- $\beta$ -TCP/HA\_10:90” (for  $\beta$ -TCP: HA = 10:90), “BC-PVP- $\beta$ -TCP/HA\_20:80” (for  $\beta$ -TCP: HA = 20:80), “BC-PVP- $\beta$ -TCP/HA\_40:60” (for  $\beta$ -TCP: HA = 40:60), “BC-PVP- $\beta$ -TCP/HA\_50:50” (for  $\beta$ -TCP: HA = 50:50), and “BC-PVP- $\beta$ -TCP/HA\_60:40” (for  $\beta$ -TCP: HA = 60:40). BC-PVP scaffold was used as a control.

All the BC-based hydrogel scaffolds were prepared by following the solvent casting method, applying only the physical crosslinking agent (moist heat and pressure). The polymer solutions (100 mL) were prepared in 250 mL sealed glass bottles under 15 lbs (107 kPa) pressure and 120 °C temperature for 20 min.<sup>26,40</sup> Twenty-five milliliters of polymer solutions from each sealed glass bottles were poured into 75 mm diameter petri-dishes and allowed to cool at room temperature (22–25 °C). Finally, smooth, round shaped, off white color BC-based scaffold without calcium phosphate (i.e., BC-PVP; diameter: 75 mm; thickness: 6.0–6.3 mm) and with calcium phosphate filled hydrogel scaffolds (BC-PVP- $\beta$ -TCP/HA\_10:90; BC-PVP- $\beta$ -TCP/HA\_20:80; BC-PVP- $\beta$ -TCP/HA\_40:60; BC-PVP- $\beta$ -TCP/HA\_50:50; BC-PVP- $\beta$ -TCP/HA\_60:40; diameter: 75 mm; thickness: 5.9–6.2 mm) were attained.

### Swelling Property Analysis

The swelling analysis was performed with physiological saline solution (pH 7.40) at 37 °C ( $\pm 1$  °C). Sections (diameter: 20 mm) of the hydrogel scaffolds were soaked for specific time (5, 30, 60, 120, 180, 240, 300, and 360 min). The water absorptivity of the hydrogel scaffolds was measured by the degree of swelling which is defined by the following equation:

$$\text{Degree of swelling (\%)} = [(W_s - W_d) / W_d] \times 100 \quad (1)$$

where  $W_s$  and  $W_d$  are the weight of the swollen and dried hydrogel scaffold section.

The swelling study was performed in triplicate ( $n = 3$ ) for all six samples BC-PVP, BC-PVP- $\beta$ -TCP/HA\_10:90, BC-PVP- $\beta$ -TCP/HA\_20:80, BC-PVP- $\beta$ -TCP/HA\_40:60, BC-PVP- $\beta$ -TCP/HA\_50:50, and BC-PVP- $\beta$ -TCP/HA\_60:40.

### Morphological Analysis

Morphological character is one of the important factors that also influence the viscoelastic property of the material. Thus, to identify the plausible influence of the morphological characters on the rheological aspects, the structure of the calcium phosphate filled BC-based hydrogel scaffolds were observed by the scanning electron microscopy (SEM) analysis. The surface and cross-sectional structures of all the six hydrogel samples were analyzed. The freshly prepared samples and equilibrium swelled samples (i.e., after 330 min) were lyophilized using Scanvac Cool Safe 110-4 PRO, Lyng; lyophilizer at  $-80$  °C temperature and 0–5 kPa pressure. Thereafter, the SEM study was performed by “NOVA nanoSEM” (FEI), operating in the secondary electron imaging mode at an accelerating voltage of 5–20 kV. The image magnification was  $\times 100$ – $\times 10k$ . Additionally, wet BC mat was lyophilized and then SEM images were taken at  $\times 250$  000 magnification with an accelerating voltage of 5 kV. The pore size and pore distribution of the different calcium phosphate

concentration containing hydrogel scaffolds were investigated by using ImageJ/Fiji software (NIH). In addition, the BC fiber orientation between 0° and 180° was also analyzed with SEM image by using directionality plug-in for Fiji software (Ashburn, VA) with default bin size.

### Rheological Property

The viscoelastic property of the hydrogel samples was studied by using a modular compact rheometer testing device (Anton Paar, Austria) and “Rheoplus” software package for data analysis. Dynamic frequency sweep analysis was conducted in the LVR at 1% strain amplitude at room temperature (28 °C) and physiological temperature (37 °C). The rheological measurements of “before dry” and “after swelled” (after 5 min of swelling) samples (20 mm diameter; thickness: 5.9–6.3 mm) were done in the oscillation mode with the angular frequency range from 0.1 to 100 rad  $s^{-1}$  and in some fixed angular frequencies (0.39 rad  $s^{-1}$ , 3.9 rad  $s^{-1}$ , 39 rad  $s^{-1}$ ) in the linear viscoelastic region, at 1% strain amplitude at 37 °C. The  $\tan \delta$  value was also determined. In addition, the viscoelastic properties of swelled samples after 60 min of swelling and after equilibrium swelling were also studied in 3.9 rad  $s^{-1}$  at 1% strain amplitude. The influence of angular frequency on storage ( $G'$ ) and loss ( $G''$ ) modulus and complex viscosity ( $\eta^*$ ) was calculated by the following equation:

$$\eta^* = [(G'/\omega)^2 + (G''/\omega)^2]^{1/2} \quad (2)$$

The rheological analysis was performed in triplicate ( $n = 3$ ) for all six samples BC-PVP, BC-PVP- $\beta$ -TCP/HA\_10:90, BC-PVP- $\beta$ -TCP/HA\_20:80, BC-PVP- $\beta$ -TCP/HA\_40:60, BC-PVP- $\beta$ -TCP/HA\_50:50, and BC-PVP- $\beta$ -TCP/HA\_60:40.

### Statistical Analysis

The data are presented as mean  $\pm$  standard error of the mean. Statistical differences between the studied samples were assessed using one-way analysis of variance (ANOVA) followed by the Bonferonni's post hoc test by using GraphPad Prism version 5.00 for Windows, GraphPad Software, San Diego, CA, www.graphpad.com.

## RESULTS AND DISCUSSION

BC-based hydrogel scaffolds filled with different concentrations of calcium phosphate (in the form of  $\beta$ -TCP and HA): BC-PVP- $\beta$ -TCP/HA\_10:90, BC-PVP- $\beta$ -TCP/HA\_20:80, BC-PVP- $\beta$ -TCP/HA\_40:60, BC-PVP- $\beta$ -TCP/HA\_50:50, and BC-PVP- $\beta$ -TCP/HA\_60:40 are characterized on the basis of swelling, morphology, and rheological property. The rheological characterization of the afore-mentioned hydrogel scaffold is performed and compared at room temperature (28 °C) and human physiological temperature (37 °C). In the context of the applicability of the scaffolds in the physiological environment, the swelling study is performed at physiological temperature (37 °C). Additionally, the rheological characterization has also been performed in the physiological temperature (37 °C) to analyze the change in viscoelastic behavior. BC-PVP hydrogel scaffold is kept for control in both the temperatures and the BC-PVP- $\beta$ -TCP/HA\_20:80 hydrogel scaffold kept as a reference sample for the rheological study, swelling study, SEM study, and pore size distribution.



### Swelling Analysis

One of the significant characteristics of a hydrogel is high water retention capacity. Figure 1(a) represents the swelling characteristics of calcium phosphate filled BC-based hydrogel scaffolds (BC-PVP- $\beta$ -TCP/HA\_10:90, BC-PVP- $\beta$ -TCP/HA\_20:80, BC-PVP- $\beta$ -TCP/HA\_40:60, BC-PVP- $\beta$ -TCP/HA\_50:50, BC-PVP- $\beta$ -TCP/HA\_60:40). Here, BC-PVP and BC-PVP- $\beta$ -TCP/HA\_20:80 hydrogel scaffolds are used as a control set.

The high degree of swelling of the polymeric gels is attributed by intermolecular noncovalent interactions like hydrogen bonding, coulombic repulsion.<sup>26,35</sup> The significant ( $P < 0.0001$ ) swelling degree of BC-PVP hydrogel scaffold has resulted from the notable interaction between the polymeric chains. Albeit, the swelling capacity of the only PVP is notably poor,<sup>26</sup> but in combination with BC the BC-PVP hydrogel scaffold can able to show a prominent ( $P < 0.0001$ ) degree of swelling. It can be observed that all the hydrogel scaffolds reach the equilibrium swelling nearly after 300 min, that is, 330 min. Interestingly, BC-PVP- $\beta$ -TCP/HA\_50:50 hydrogel scaffold is showing a significant degree of swelling ( $P < 0.0001$ ) from 180 min [Figure 1(b)]. At

equilibrium swelling (330 min), the degree of swelling of the BC-PVP- $\beta$ -TCP/HA\_50:50 hydrogel scaffold is also notably higher ( $P < 0.0001$ ) than the other calcium phosphate filled hydrogel scaffolds [Figure 1(c)]. BC-based hydrogel scaffolds contain calcium phosphate as filler. The swelling ability of the calcium phosphate filled hydrogels can be influenced by the degree of filling,<sup>51</sup> which might be the reason for a lower degree of swelling of calcium phosphate containing BC-based hydrogel samples compared to BC-PVP. The distribution of the calcium phosphate (in the form of  $\beta$ -TCP/HA) within the BC-based hydrogel matrix might affect their swelling degree<sup>51</sup> in the following way (from 180 to 300 min): BC-PVP- $\beta$ -TCP/HA\_50:50 > BC-PVP- $\beta$ -TCP/HA\_40:60 > BC-PVP- $\beta$ -TCP/HA\_20:80 > BC-PVP- $\beta$ -TCP/HA\_60:40 > BC-PVP- $\beta$ -TCP/HA\_10:90. Specifically, swelling capacity can be influenced by the presence of calcium phosphate fillers like  $\beta$ -TCP and HA.<sup>52,53</sup> The presence of  $\beta$ -TCP and HA as calcium phosphate fillers might influence the degree of swelling of the calcium phosphate filled hydrogel scaffolds. On the other hand, the significant swelling rate of BC-PVP- $\beta$ -TCP/HA\_50:50 hydrogel scaffold might be because of the presence of high

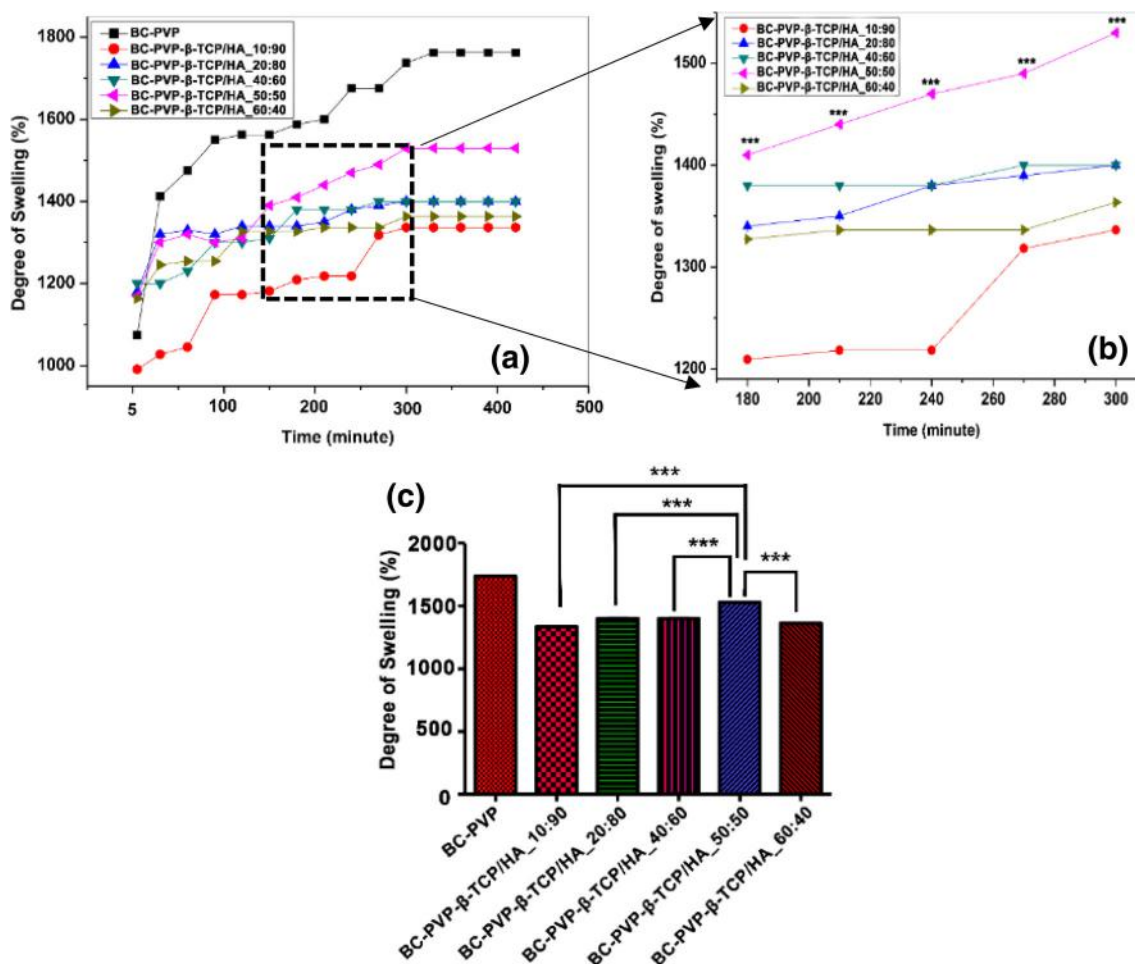


**Figure 1.** (a) Degree of swelling of bacterial cellulose (BC)-based calcium phosphate filled hydrogel scaffolds: BC-PVP- $\beta$ -TCP/HA\_10:90, BC-PVP- $\beta$ -TCP/HA\_20:80, BC-PVP- $\beta$ -TCP/HA\_40:60, BC-PVP- $\beta$ -TCP/HA\_50:50, BC-PVP- $\beta$ -TCP/HA\_60:40; (b) BC-PVP- $\beta$ -TCP/HA\_50:50 is showing high degree of swelling from 180 to 300 min of swelling. (c) Degree of swelling of the BC-based calcium phosphate filled hydrogel scaffolds at equilibrium swelling (i.e., 330 min). Asterisk (\*\*\*)  $P < 0.0001$  indicates the significant degree of swelling. [Color figure can be viewed at wileyonlinelibrary.com]

macroporous structure and high porosity.<sup>54</sup> The presence of high macroporous structures might facilitate the high degree of swelling of the afore-mentioned hydrogel scaffold than the other.

### SEM Study

The morphological characterization of BC is depicted in Figure 2 (a). BC is composed of different fibers, which are forming networks and interacting with each other to generate the meshlike structure. The rheological behavior of BC-based material depends on the orientation of the BC fibers. The difference in the orientation of fibers can affect rheological behavior.<sup>55</sup> It also influences the mechanical strength of the composite scaffold.<sup>56</sup> Different BC fibers have different structural orientation, which significantly confirms the structural anisotropy of the BC fibers. It can be seen in Figure 2(b) that a notable amount of BC fibers is found structurally oriented between the direction 120–160°. Additionally, the fiber diameter is one of the important factors that influences the rheological behavior of the material.<sup>57</sup> The average fiber diameter

of the BC mat is depicted in Figure 2(c). It can be seen that the BC mat is composed of BC fibers with different fiber diameter. These differences in the fiber diameter along with different calcium phosphate concentration influence the viscoelastic behavior of the scaffolds.

Figure 3 depicts the morphological characteristics (surface and cross sections) of fresh and equilibrium swelled (after 330 min of swelling) calcium phosphate filled BC-based hydrogel scaffolds (BC-PVP- $\beta$ -TCP/HA\_10:90, BC-PVP- $\beta$ -TCP/HA\_20:80, BC-PVP- $\beta$ -TCP/HA\_40:60, BC-PVP- $\beta$ -TCP/HA\_50:50, BC-PVP- $\beta$ -TCP/HA\_60:40). BC-PVP scaffold is used as the control. The surface structure of fresh BC-PVP is found smoother than the fresh calcium phosphate filled hydrogel scaffolds. Additionally, it can be observed that the surface of fresh BC-PVP- $\beta$ -TCP/HA\_50:50 hydrogel scaffold is highly rough compared to other fresh calcium phosphate filled hydrogel scaffolds. On the other hand, the surface of the calcium phosphate filled hydrogel scaffolds after equilibrium swelling (i.e., after 330 min) is significantly rough due to the deposition of salts like NaCl sourced

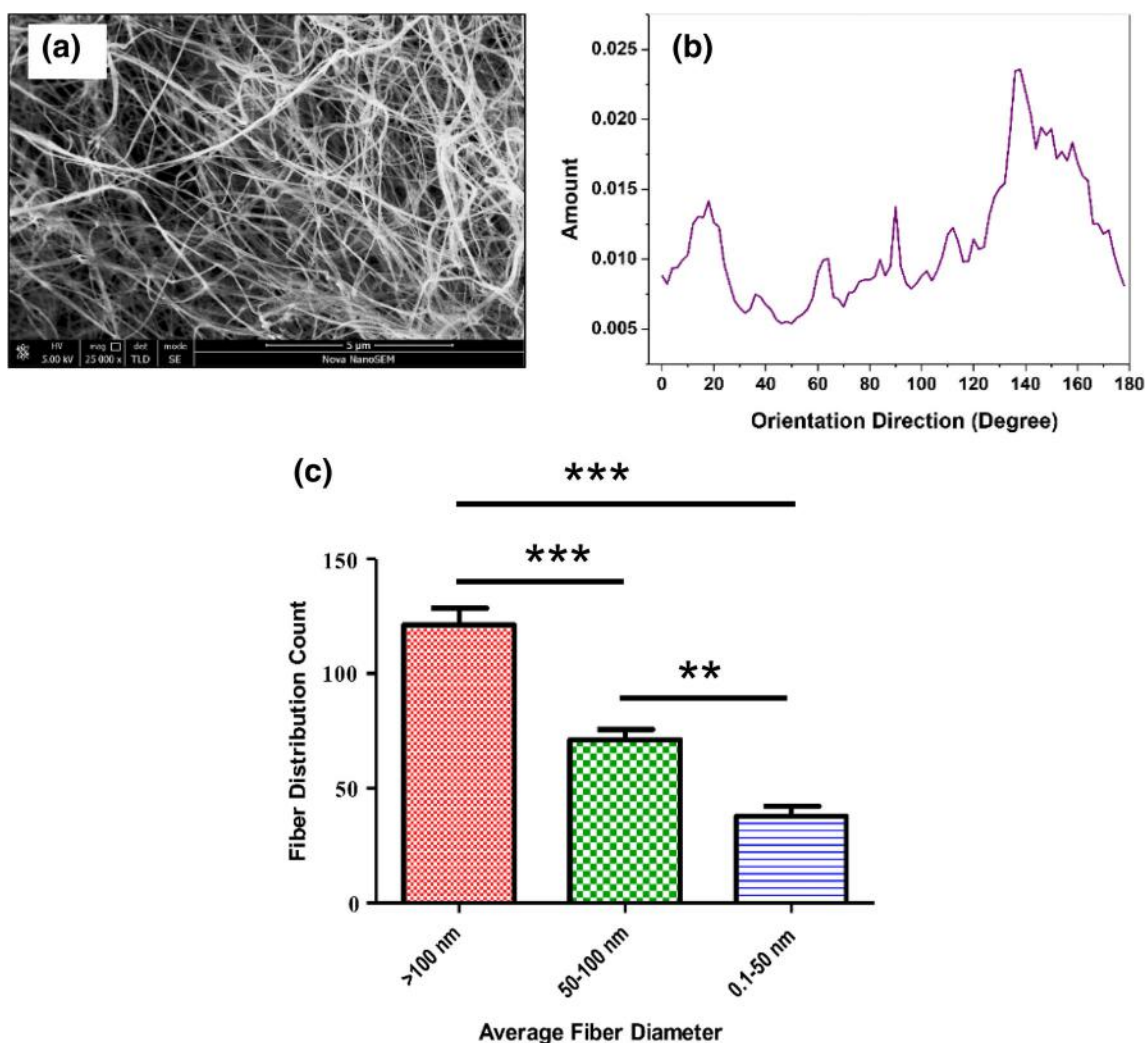


**Figure 2.** (a) Scanning electron microscopy (SEM) image of bacterial cellulose (BC). (b) Orientation direction of BC fiber in the produced BC. (c) Average BC fiber diameter versus fiber distribution count. Asterisk (\*\*\*) =  $P < 0.001$ ; \*\* =  $P < 0.01$ ) indicates the significant occurrence of fibers with a specific range of diameter. [Color figure can be viewed at [wileyonlinelibrary.com](http://wileyonlinelibrary.com)]

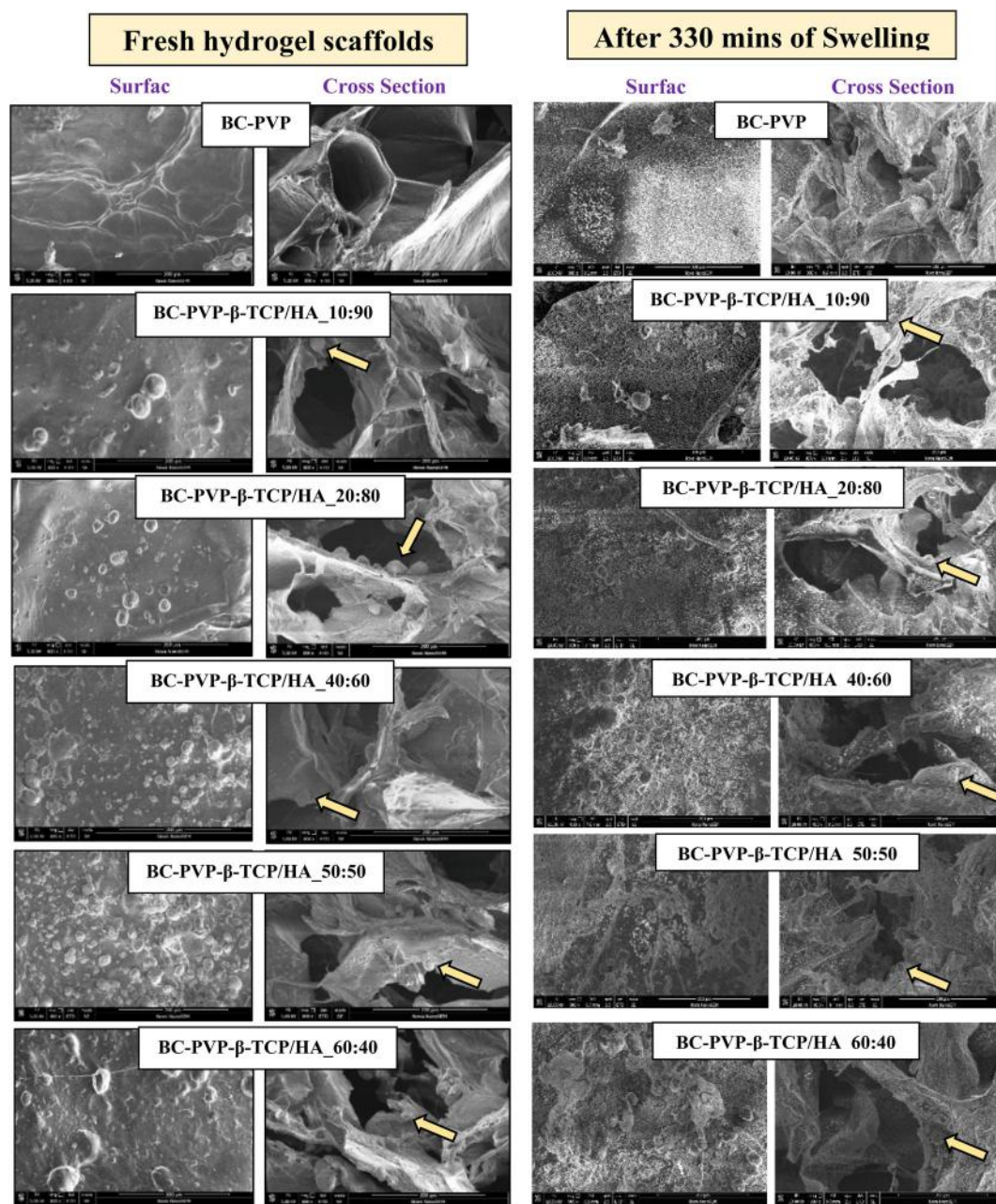


**Figure 3.** Scanning electron microscopy images of fresh and after swelled (after 330 min) calcium phosphate filled bacterial cellulose (BC)-based hydrogel scaffold: BC-PVP- $\beta$ -TCP/HA\_10:90, BC-PVP- $\beta$ -TCP/HA\_20:80, BC-PVP- $\beta$ -TCP/HA\_40:60, BC-PVP- $\beta$ -TCP/HA\_50:50, BC-PVP- $\beta$ -TCP/HA\_60:40; yellow arrows indicate the point of interaction of calcium phosphate and polymer phase. [Color figure can be viewed at [wileyonlinelibrary.com](http://wileyonlinelibrary.com)]

from the physiological saline solution. All the hydrogel scaffolds contain porous structures. The porous structures of the hydrogel can facilitate diffusion of water and other bioactive agents.<sup>48</sup> The morphology of the porous structures of fresh scaffolds is notable than after 330 min of swelling. A significant change in the porous structure influences the diffusion property of the material.<sup>58</sup> This diffusion property is also connected with the rheological behavior of polymer.<sup>59</sup>

The relationship between pore distribution and pore size of the fresh calcium phosphate filled BC-based scaffolds is also demonstrated in Figure 4. Tissue engineering scaffold with a pore

diameter of 100  $\mu\text{m}$  and above is an important factor in the context of cell-matrix and cell-cell interaction.<sup>60</sup> The porous structures ( $>100 \mu\text{m}$ ) are significant ( $P < 0.0001$  and  $P < 0.01$ ) in all the calcium phosphate filled BC-based hydrogel scaffolds, which can facilitate efficient cell adhesion to the scaffold.<sup>60</sup> Additionally, BC-PVP- $\beta$ -TCP/HA\_10:90, BC-PVP- $\beta$ -TCP/HA\_40:60, and BC-PVP- $\beta$ -TCP/HA\_50:50 also contain pores with a significant ( $P < 0.01$ ) size ranging between 50 and 100  $\mu\text{m}$ .

#### Rheological Study

Figure 5 depicts the viscoelastic property of before dry BC-based hydrogel scaffolds with different concentrations of calcium

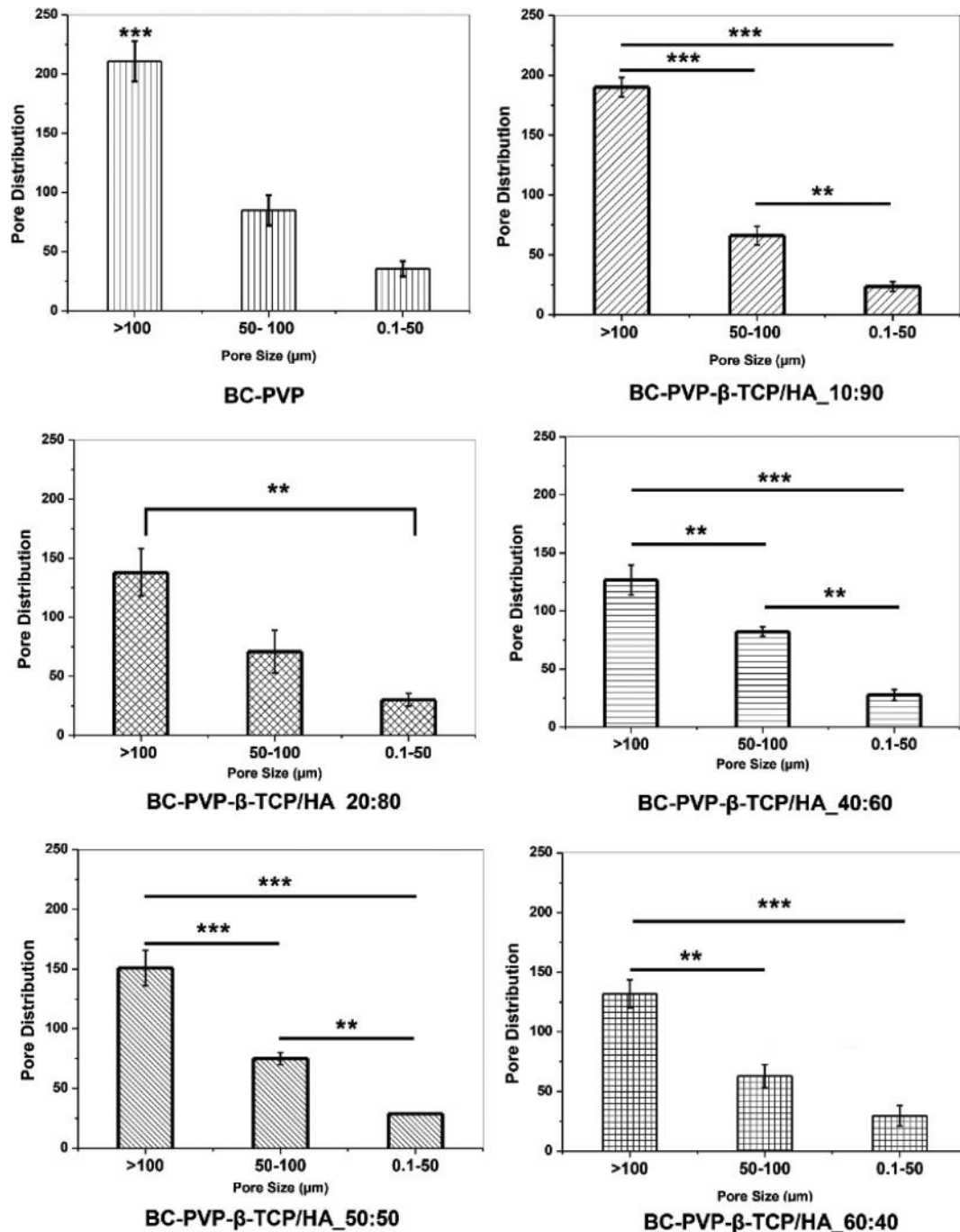


**Figure 4.** Relationship between pore size and pore distribution of calcium phosphate filled bacterial cellulose-based hydrogel scaffolds in fresh condition. Asterisk (\*\*\*) =  $P < 0.0001$ ; \*\* =  $P < 0.01$ ) indicates the significant difference of occurrence of a specific size of pore.

phosphate (BC-PVP-β-TCP/HA\_10:90, BC-PVP-β-TCP/HA\_20:80, BC-PVP-β-TCP/HA\_40:60, BC-PVP-β-TCP/HA\_50:50, BC-PVP-β-TCP/HA\_60:40). The properties are measured at room temperature (28 °C) and human internal body temperature (37 °C) to understand the rheological behavior of calcium phosphate filled BC-based hydrogel scaffolds. BC-PVP scaffold used as a control for both 28 and 37 °C. BC-PVP-β-TCP/HA\_20:80 considers as a reference sample for 28 °C.<sup>48</sup> From Figure 5(a), it can be seen that the storage modulus ( $G'$ ) of the different calcium phosphate filled

BC-based hydrogels have significantly higher than the loss modulus at both 28 and 37 °C, which in turn indicate their notable elastic property. Figure 5(a) also exhibits the higher storage modulus of the calcium phosphate containing hydrogel scaffolds at 28 °C which can be classified as follows: BC-PVP-β-TCP/HA\_20:80 > BC-PVP-β-TCP/HA\_10:90 > BC-PVP-β-TCP/HA\_50:50 > BC-PVP > BC-PVP-β-TCP/HA\_40:60, and BC-PVP-β-TCP/HA\_60:40. On the other hand, the  $G'$  of the aforementioned scaffolds at 37 °C exhibit the following pattern: BC-PVP-β-TCP/HA\_50:50 > BC-PVP-

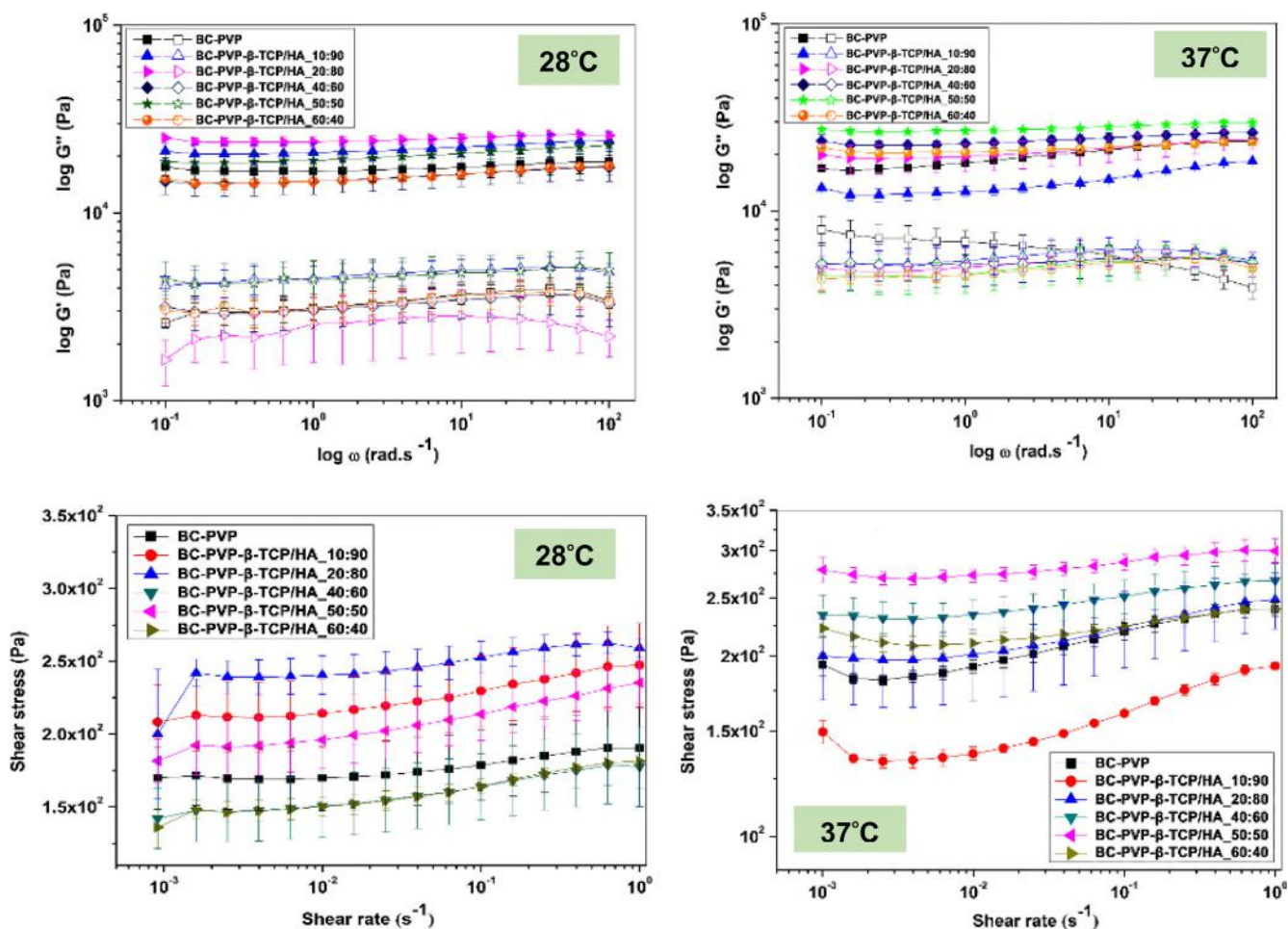


**Figure 5.** Viscoelastic property of calcium phosphate filled bacterial cellulose (BC)-based “before dry” hydrogel scaffolds at 28 and 37 °C at 1% strain amplitude and between 0.1 and 100  $\text{rad s}^{-1}$ ; (a) storage modulus (filled symbols) and loss modulus (open symbols); (b) shear stress versus shear rate of different concentrations containing calcium phosphate filled BC-based hydrogel scaffolds at 28 and 37 °C. [Color figure can be viewed at [wileyonlinelibrary.com](http://wileyonlinelibrary.com)]

$\beta$ -TCP/HA\_40:60 > BC-PVP- $\beta$ -TCP/HA\_60:40 > BC-PVP- $\beta$ -TCP/HA\_20:80 > BC-PVP > BC-PVP- $\beta$ -TCP/HA\_10:90. However, the overall trends of storage modulus at both temperatures (28 and 37 °C) are indicating that the scaffolds maintained crosslinked gel structure throughout the range of angular frequency. The significant storage modulus of the hydrogel scaffolds indicates their notable elastic property. The potential interactions between filler and polymer matrix of composite material influence the storage modulus.<sup>61</sup> The hydrogel scaffolds contain BC, PVP, PEG, agar as polymeric component, and calcium phosphate as rigid filler. The crosslinked polymeric matrix has its own viscoelastic property, where the calcium phosphate strengthens the rheological property of the scaffolds. The interactions between polymer chains and calcium phosphate in BC-PVP- $\beta$ -TCP/HA\_50:50 hydrogel scaffold at 37 °C facilitate its high storage modulus. The nature and placements of monomers of the polymers along with the filler concentration have also a significant effect on the viscosity at different temperatures.<sup>62</sup> The temperature can be the reason for the decrease of loss modulus of all BC-based hydrogel scaffolds at 37 and 28 °C. It is also observed that at 1% strain, the complex viscosity is decreasing with the increasing angular frequency, for all the BC-based hydrogel scaffolds both at 28 and 37 °C, respectively.

Additionally, the complex viscosity of all calcium phosphate filled hydrogel scaffold was found in decreasing trend with the increase of angular frequency, which indicates the nature of polymeric hydrogel.<sup>35</sup> This trend is also indicating the possible hydrodynamic effect of calcium phosphate fillers<sup>63</sup> inside the scaffolds.

The relationship between shear stress versus the shear rate of different calcium phosphate filled BC-based fresh hydrogel scaffolds at 28 and 37 °C is depicted in Figure 5(b). Here, BC-PVP is also used as a control scaffold. It can be seen that in both the temperatures, the shear stress of the scaffolds is showing an increasing trend with increasing shear rate. Interestingly, with the increase in temperature (from 28 to 37 °C) the shear stress values of BC-PVP- $\beta$ -TCP/HA\_20:80 hydrogel scaffolds are found to be decreased. On the other hand, the shear stress values of BC-PVP- $\beta$ -TCP/HA\_50:50, BC-PVP- $\beta$ -TCP/HA\_40:60, and BC-PVP- $\beta$ -TCP/HA\_60:40 hydrogel scaffolds remain higher at 37 °C. The temperature has a significant effect on the shear stress.<sup>64</sup> The increase and decrease of the shear stress values might reflect the effect of temperature on the structural composition of hydrogel composites. With the increasing shear rate, different particles can interact with each other by forces like Van der Waals force,<sup>65</sup>

which ultimately results in an increasing trend of shear stress with the increasing shear rate. This could be a plausible reason for the increasing trend of shear stress.

Figure 6 depicts the analysis of damping factor ( $\tan \delta$ ) of fresh calcium phosphate filled BC-based hydrogel scaffolds at human body temperature ( $37^\circ\text{C}$ ). The variation of  $\tan \delta$  was studied in four different angular frequencies ( $0.1\text{ rad s}^{-1}$ ,  $1\text{ rad s}^{-1}$ ,  $10\text{ rad s}^{-1}$ ,  $100\text{ rad s}^{-1}$ ) in 1% strain at  $37^\circ\text{C}$ . From the figure, it can be seen that the values of the damping factor of all the hydrogel scaffolds are less than 1 ( $\tan \delta < 1$ ) at  $37^\circ\text{C}$ , which indicate the maintenance of gel-like elastic behavior throughout the four different angular frequencies.<sup>66</sup> Filler concentration and its interaction with the polymers have the possible influence on the elastic and viscous properties.<sup>62</sup> At the angular frequencies (i.e.,  $0.1$ ,  $1$ ,  $10$ ,  $100\text{ rad s}^{-1}$ ) the  $\tan \delta$  of BC-PVP- $\beta$ -TCP/HA\_10:90 hydrogel scaffold remains less than 1, which reflects its overall gel-like elastic character. However, at  $1$ ,  $10$ , and  $100\text{ rad s}^{-1}$ , its  $\tan \delta$  value found higher than the other scaffolds. The presence of different fillers can also affect the flow behavior of the filled-in polymer system.<sup>62</sup> The concentration of  $\beta$ -TCP and HA of BC-PVP- $\beta$ -TCP/HA\_10:90 hydrogel might affect the viscous and elastic property of the afore-mentioned hydrogel. The differential loading of calcium phosphates (in the form

$\beta$ -TCP and HA) in the BC-based polymeric matrix facilitates the stress transfer phenomenon, which ensures the elastic strength of the scaffold.

As an implant, the hydrogel scaffold will immediately encounter different physiological parameters like temperature and pH after application in the body. In addition, the scaffold will show swelling over a period of time after interacting with water, blood, and other biological fluids. Thus, analysis of the rheological behavior of the “after swelled” (5 min) calcium phosphate filled hydrogel scaffold at  $37^\circ\text{C}$  is demonstrated in Figure 7. The effect of three specific angular frequencies in the low range:  $0.39\text{ rad s}^{-1}$ , mid-range:  $3.9\text{ rad s}^{-1}$ , and high range:  $39\text{ rad s}^{-1}$  on the viscoelastic property at  $37^\circ\text{C}$  are analyzed. It can be seen from Figure 7 (a) that the values of storage modulus ( $G'$ ) remain higher than the loss modulus ( $G''$ ) at  $37^\circ\text{C}$  throughout the study period for all the hydrogel scaffolds (BC-PVP, BC-PVP- $\beta$ -TCP/HA\_10:90, BC-PVP- $\beta$ -TCP/HA\_20:80, BC-PVP- $\beta$ -TCP/HA\_40:60, BC-PVP- $\beta$ -TCP/HA\_50:50, BC-PVP- $\beta$ -TCP/HA\_60:40), which indicates their significant elastic behavior. Specifically, the storage modulus of BC-PVP- $\beta$ -TCP/HA\_50:50 hydrogel scaffolds is found higher in  $0.39\text{ rad s}^{-1}$ ,  $3.9\text{ rad s}^{-1}$  at  $37^\circ\text{C}$  than the other hydrogel scaffolds. However, the elasticity of BC-PVP- $\beta$ -TCP/HA\_50:50 remains higher between 0 and 90 min at  $39\text{ rad s}^{-1}$ . On the other

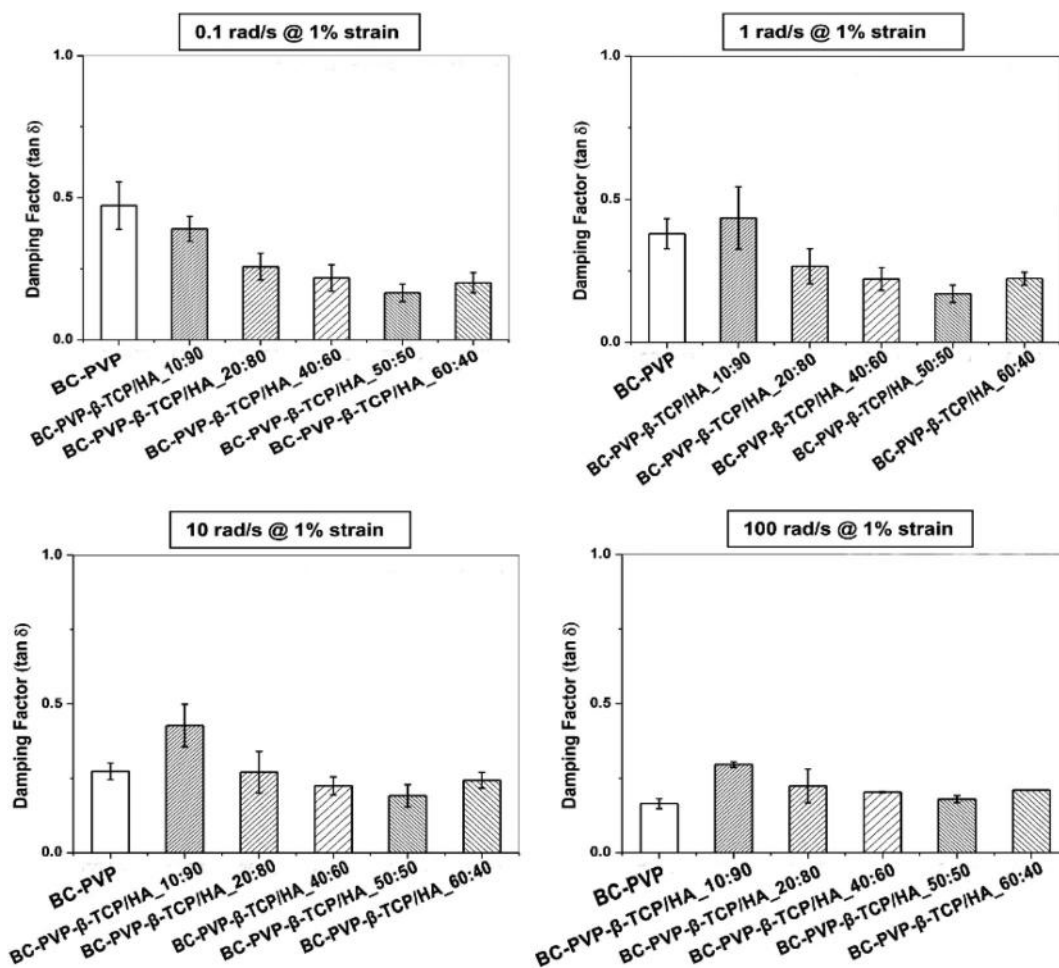
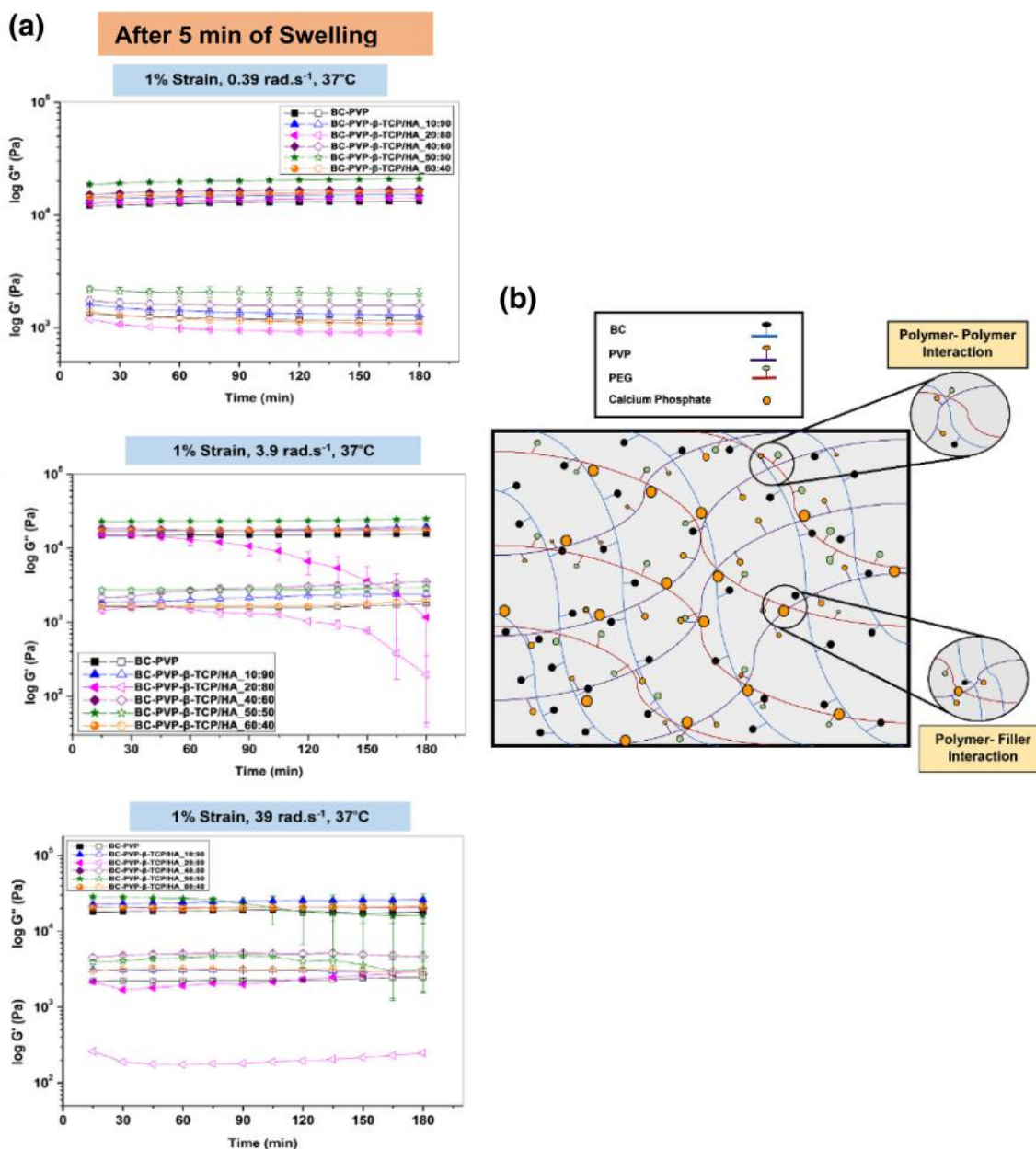


Figure 6. Damping factor ( $\tan \delta$ ) values of calcium phosphate filled bacterial cellulose-based hydrogel at different angular frequencies at  $37^\circ\text{C}$ .



**Figure 7.** (a) Rheological behavior of different calcium phosphate filled bacterial cellulose (BC)-based hydrogel scaffolds after 5 min of swelling at 37 °C in three different angular frequencies (0.39  $\text{rad}\cdot\text{s}^{-1}$ , 3.9  $\text{rad}\cdot\text{s}^{-1}$ , 39  $\text{rad}\cdot\text{s}^{-1}$ ), storage (filled symbols) and loss modulus (unfilled symbols); (b) Schematic diagram of plausible polymer–polymer and polymer–filler interactions inside the matrix of calcium phosphate filled BC-based hydrogel scaffolds. [Color figure can be viewed at [wileyonlinelibrary.com](http://wileyonlinelibrary.com)]

hand, the modulus of “after swelled” BC-PVP- $\beta$ -TCP/HA\_20:80 (after 5 min of swelling) scaffold has remained independent of angular frequency (i.e., 3.9  $\text{rad}\cdot\text{s}^{-1}$ ) up to below 60 min at 37 °C. However, both the  $G'$  and  $G''$  of “after swelled” BC-PVP- $\beta$ -TCP/HA\_20:80 scaffold started to decrease from 60 min. Additionally, the modulus ( $G'$  and  $G''$ ) of this scaffold has also remained lower than the other hydrogel scaffolds in 39  $\text{rad}\cdot\text{s}^{-1}$  at 37 °C. This behavior might result from either the rupture of the interface between the polymer and filler surface or the slipping phenomenon between polymer and filler.<sup>67,68</sup> Additionally, temperature (i.e., 37 °C) might also be a significant reason behind

this behavior. At a small angular frequency, the material behaves elastically,<sup>62</sup> which is evident from Figure 7(a), where the storage modulus remains significantly higher than the loss modulus. This indicates the dominance of the elastic behavior of the hydrogel scaffolds.

In the filled in polymer system, the ability of stress transfer of polymer to filler is an important aspect, which ensures the mechanical strength of the polymer composite. Here, the calcium phosphate (in the form of  $\beta$ -TCP/HA) is present as rigid inorganic filler in the calcium phosphate filled BC-based hydrogel

scaffolds. On the other hand, the hydrogel scaffolds also contain BC fibers which are also reinforcing the composite structure.<sup>62</sup> Both the inorganic filler and BC fibers, provide the mechanical strength to the hydrogel samples, whereas the hydrophilic polymers like PVP and PEG successfully accomplish the stress transfer to the filler substances, which ultimately reflects through the higher storage modulus of the samples. Interestingly, BC is a biopolymer which has high mechanical property.<sup>48</sup> Being a hydrophilic polymer, BC has the natural affinity to water; thus, gradual swelling of BC-based scaffolds have also a plausible effect on its mechanical property. On the other hand, BC is considered as a reinforcement fiber which provides an additional degree of mechanical strength to the scaffolds. The fiber structural anisotropy and fiber diameter are the two important factors for the rheological behavior of a composite.<sup>62</sup> As a natural fiber, BC has a significant structural anisotropy. Additionally, the diameters of the BC fibers are also different, which have a notable influence on the viscoelastic property of the materials.<sup>57</sup> These physiological factors of BC are responsible for the significant elastic behavior of the BC-based hydrogel scaffolds. Additionally, all the hydrogel scaffolds contain porous structures which can also influence the rheological property.<sup>55</sup> This can be reflected from the variation of the values of storage modulus of the different calcium phosphate filled BC-based hydrogel scaffolds in the same angular frequency range. The mechanical characteristics of composite materials depend also on the filler–filler interactions.<sup>69,70</sup> In the calcium phosphate filled BC-based hydrogel scaffolds, the calcium phosphate fillers interact between each other significantly along with the polymer chains. Both types of interactions (polymer–filler and filler–filler) influence the mechanical characteristics like elastic property of the calcium phosphate filled BC-based hydrogel scaffolds [Figure 7(b)]. As the filler, calcium phosphate like HA interacts notably with the BC.<sup>71</sup> The interaction between the polymer chains and calcium phosphate mainly involves ionic

bonds and hydrogen bonds.<sup>72</sup> The hydroxyl groups of polymer chains develop hydrogen bonds with the oxygen atom of phosphorous groups of calcium phosphate,<sup>73</sup> which facilitate the interaction of polymer chains and calcium phosphates. Additionally, the calcium phosphate particles have been found to be significantly adsorbed on the BC.<sup>74</sup> The irregular presence of calcium phosphate particles on the surface and porous structure [indicated with arrows in Figure 3] of the polymer phase from SEM study indicates the potential interaction of calcium phosphate and polymers.

Swelling study indicated the hydrogel scaffolds gradually swell and reach an equilibrium degree of swelling. As the hydrogel gradually swells, its volume also increases. Thus, the rheological behavior of swelled hydrogel scaffold at a higher swelling time and at equilibrium swelling condition will also be indicating the mechanical strength of the scaffolds and thereby confirms the efficiency of the scaffold material in the application site. Thus, for further analysis, the rheological study of three hydrogel scaffolds BC-PVP- $\beta$ -TCP/HA\_10:90, BC-PVP- $\beta$ -TCP/HA\_20:80, and BC-PVP- $\beta$ -TCP/HA\_50:50 is performed. These scaffolds are selected on the basis of their swelling behavior, which is as follows: BC-PVP- $\beta$ -TCP/HA\_50:50 > BC-PVP- $\beta$ -TCP/HA\_20:80 > BC-PVP- $\beta$ -TCP/HA\_10:90. BC-PVP scaffold has also kept here as a control. Figure 8(a,b) depicts the rheological characteristics in terms of storage and loss modulus of BC-PVP- $\beta$ -TCP/HA\_10:90, BC-PVP- $\beta$ -TCP/HA\_20:80, BC-PVP- $\beta$ -TCP/HA\_50:50 hydrogel scaffolds in 1% strain and 3.9 rad s<sup>-1</sup> at 37 °C. It is reported that materials behave elastically in fast deformations; however, in slow deformations, the materials behave liquid like.<sup>75</sup> Thus a mid-angular frequency, 3.9 rad s<sup>-1</sup> is selected for the study. It can be seen from the figure that, after 60 min of swelling and equilibrium swelling (i.e., 330 min), the trend of storage modulus has remained higher than the loss modulus for all the hydrogel

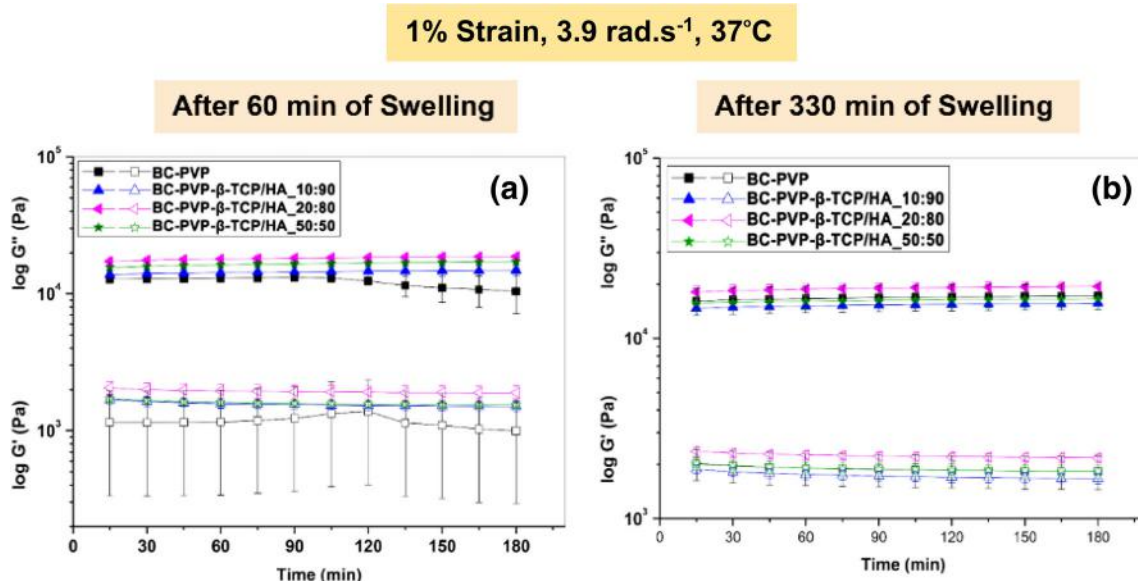


**Figure 8.** Viscoelastic behavior of calcium phosphate filled bacterial cellulose (BC)-based hydrogel scaffolds (i.e., BC-PVP- $\beta$ -TCP/HA\_10:90, BC-PVP- $\beta$ -TCP/HA\_20:80, BC-PVP- $\beta$ -TCP/HA\_50:50) after (a) 60 min and (b) after 330 min (equilibrium swelling). Storage (filled symbols) and loss modulus (open symbols). [Color figure can be viewed at [wileyonlinelibrary.com](http://wileyonlinelibrary.com)]



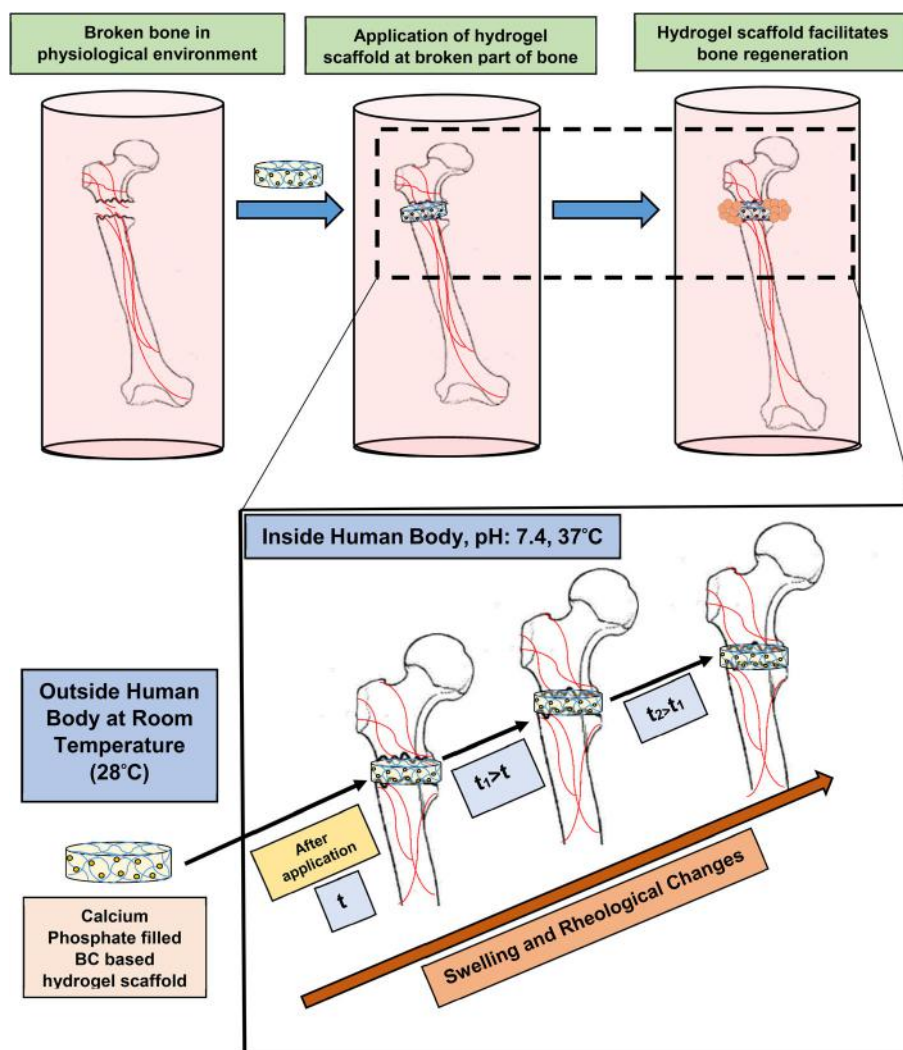


**Figure 9.** A thematic diagram representing about swelling and rheological characteristics of calcium phosphate filled bacterial cellulose-based hydrogel scaffolds in bone tissue engineering, where  $t$  = time of application and  $\odot$  = new bone cells grown around the hydrogel scaffold. [Color figure can be viewed at [wileyonlinelibrary.com](http://wileyonlinelibrary.com)]

samples. In this regard, it should be mentioned that, although all the hydrogel scaffolds are showing significant elastic property after 60 min of swelling and equilibrium swelling, however, the objective of this study is to find the better scaffold material with specific  $\beta$ -TCP and HA ratios. Thus, elastic property of the all studied hydrogel scaffolds was compared. The storage modulus is found to be the highest for BC-PVP- $\beta$ -TCP/HA\_20:80 in both after 60 min and after equilibrium swelled samples at 37 °C. The  $G'$  remained higher than  $G''$  for BC-PVP- $\beta$ -TCP/HA\_20:80 scaffold in 3.9 rad s<sup>-1</sup> at 37 °C after 60 min of swelling and also after equilibrium swelling (i.e., after 330 min). However, the trend of the storage modulus is observed to be notably different from the trend after 5 min of swelling. This difference in the trend of the modulus in 3.9 rad s<sup>-1</sup> at 37 °C after 60 min and after equilibrium swelling might be attributed from the significant polymer–filler, filler–filler interactions, and interaction between hydrophilic polymers with water molecules. The gradual swelling of the hydrogel scaffolds (from 5 min to 60 min and then to equilibrium swelling) develops a strong interaction

between BC fibers and water molecules.<sup>76,77</sup> This interaction further facilitates the intermolecular hydrogen bonds to develop amorphous and crystalline domains, which ultimately improves the strength of the BC and/or BC-based matrix.<sup>77,78</sup> This can be the reason behind the high storage modulus of the aforementioned hydrogel scaffolds; especially, BC-PVP- $\beta$ -TCP/HA\_20:80 after 60 min and after equilibrium swelling (i.e., after 330 min).

## CONCLUSIONS

This study focuses on the analysis of swelling characteristics and rheological behavior of calcium phosphate filled BC based hydrogel scaffolds: BC-PVP- $\beta$ -TCP/HA\_10:90, BC-PVP- $\beta$ -TCP/HA\_20:80, BC-PVP- $\beta$ -TCP/HA\_40:60, BC-PVP- $\beta$ -TCP/HA\_50:50, BC-PVP- $\beta$ -TCP/HA\_60:40. The surface structures of all the fresh calcium phosphate filled BC based hydrogel scaffolds are rough compared to the control (i.e., BC-PVP). However, the surface roughness of BC-PVP- $\beta$ -TCP/HA\_50:50 hydrogel scaffold is higher. Additionally, the SEM study revealed that internal

structure/morphology of hydrogel scaffolds comprises porous structures. From the swelling point of view, the highest degree of swelling exhibited in BC-PVP- $\beta$ -TCP/HA\_50:50 scaffold. All the fresh hydrogel scaffolds have found to be significantly elastic between 0.1 and 100 rad s<sup>-1</sup> and BC-PVP- $\beta$ -TCP/HA\_50:50 scaffold is found more elastic in 0.39 rad s<sup>-1</sup> and 3.9 rad s<sup>-1</sup> at 37 °C (after 5 min swelling). The elasticity of BC-PVP- $\beta$ -TCP/HA\_20:80 is also found notable after 60 min and at equilibrium swelling (i.e., after 330 min). Considering the swelling and rheological behavior of all the examined calcium phosphate filled BC-based hydrogel scaffolds, the BC-PVP- $\beta$ -TCP/HA\_20:80 and BC-PVP- $\beta$ -TCP/HA\_50:50 scaffolds exhibited their efficiency in regard to its applicability in bone tissue engineering. A thematic image about applicability of calcium filled hydrogel scaffold is depicted in Figure 9 for better understanding.

#### ACKNOWLEDGMENTS

This work is mainly supported by the Internal Grant Agency (Project No. IGA/CPS/2018/008), Tomas Bata University in Zlín, Czech Republic and Ministry of Education, Youth, and Sports of The Czech Republic—NPU Program I (LO1504). First author extends his sincere gratitude to Ing. Berenika Hausnerová, Tomas Bata University in Zlín for her kind suggestions regarding the rheological analysis.

#### CONFLICT OF INTEREST

The authors declare that there is no conflict of interest.

#### REFERENCES

- Mori, A. D.; Fernandez, M. P.; Blunn, G.; Tozzi, G.; Roldo, M. *Polymers*. **2018**, *10*(285), 1.
- Ager, J. W., III; Balooch, G.; Ritchie, R. Q. *J. Mater. Res.* **2006**, *21*(8), 451.
- Oryan, A.; Alidadi, S.; Moshiri, A. *Hard Tissue*. **2013**, *2*(2), 13.
- National Osteoporosis Foundation (NOF), 2018, USA. <https://www.nof.org/patients/what-is-osteoporosis/> (accessed February 10, 2018).
- Kroeze, R. J.; Helder, M. N.; Govaert, L. E.; Smit, T. H. *Materials*. **2009**, *2*, 833.
- Shen, F. H.; Samartzis, D.; An, H. S. *Spine J.* **2005**, *5*, 231S.
- Morgan, S. J.; Jeray, K. J.; Saliman, L. H.; Miller, H. J.; Williams, A. E.; Tanner, S. L.; Smith, W. R.; Broderick, J. S. *J. Bone Jt. Surg. Am.* **2006**, *88*, 2606.
- Iaquinta, M. R.; Mazzoni, E.; Manfrini, M.; D'Agostino, A.; Trevisiol, L.; Nocini, R.; Trombelli, L.; Barbanti-Brodano, G.; Martini, F.; Tognon, M. *Int. J. Mol. Sci.* **2019**, *20*, 2.
- Liu, M.; Zeng, X.; Ma, C.; Yi, H.; Ali, Z.; Mou, X.; Li, S.; Deng, Y.; He, N. *Bone Res.* **2017**, *5*, 17014.
- Sekuła, M.; Zuba-Surma, E. K. *IntechOpen*. **2018**, *2018*, 361. <https://doi.org/10.5772/intechopen.70122>.
- O'Brien, F. J. *Mater. Today*. **2011**, *14*(3), 88.
- Dhandayuthapani, B.; Yoshida, Y.; Maekawa, T.; Sakthi Kumar, D. *Int. J. Polym. Sci.* **2011**, *2011*, 19.
- Khan, F.; Tanaka, M. *Int. J. Mol. Sci.* **2018**, *19*(1), 17.
- Lee, E. J.; Kasper, K. F.; Mikos, A. G. *Ann. Biomed. Eng.* **2014**, *42*(2), 323.
- Shi, X.; Jing, Z.; Zhang, G. *J. Polym. Res.* **2018**, *25*(71), 3.
- Stratton, S.; Shelke, N. B.; Hoshino, K.; Rudraiah, S.; Kumbar, S. G. *Bioactive Mater.* **2016**, *1*(2), 93.
- Ghassemi, T.; Shahroodi, A.; Ebrahimzadeh, M. H.; Mousavian, A.; Movaffagh, J.; Moradi, A. *Arch. Bone Jt. Surg.* **2018**, *6*(2), 90.
- Zhu, J.; Merchant, R. E. *Expert Rev. Med. Devices*. **2011**, *8*(5), 607.
- Zarrintaj, P.; Manouchehri, S.; Ahmadi, Z.; Saeb, M. R.; Urbanska, A. M.; Kaplan, D. L.; Mozafari, M. *Carbohydr. Polym.* **2018**, *187*, 66.
- Demitri, C.; Raucci, M. G.; Giuri, A.; De Benedictis, V. M.; Giugliano, D.; Calcagnile, P.; Sannino, A.; Ambrosio, L. *J. Biomed. Mater. Res. A*. **2016**, *104*(3), 726.
- Rajwade, J. M.; Paknikar, K. M.; Kumbhar, J. V. *Appl. Microbiol. Biotechnol.* **2015**, *99*, 2491.
- Torgbo, S.; Sukyaia, P. *Appl. Mater. Today*. **2018**, *11*, 34.
- Qi, G. X.; Luo, M. T.; Huang, C.; Guo, H. J.; Chen, X. F.; Xiong, L.; Wang, B.; Lin, X. Q.; Peng, F.; Chen, X. D. *J. Appl. Polym. Sci.* **2017**, *45066*, 1.
- Basu, P.; Saha, N.; Alexandrova, R.; Andonova-Lilova, B.; Georgieva, M.; Miloshev, G.; Saha, P. *Int. J. Mol. Sci.* **2018**, *19*, 3980.
- Basu, P.; Saha, N.; Saha, P. *Int. J. Polym. Mater.* **2019**, *68*, 1.
- Roy, N.; Saha, N.; Kitano, T.; Saha, P. *J. Appl. Polym. Sci.* **2010**, *117*, 1703.
- El-Sherbiny, I. M.; Yacoub, M. H. *Global Cardiol. Sci. Pract.* **2013**, *2013*(3), 316.
- Rammensee, S.; Huemmerich, D.; Hermanson, K. D.; Scheibel, T.; Bausch, A. R. *Appl. Phys. A*. **2006**, *82*, 261.
- Chocholata, P.; Kulda, V.; Babuska, V. *Materials*. **2019**, *12*, 568.
- Kocen, R.; Gasik, M.; Gantar, A.; Novak, S. *Biomed. Mater.* **2017**, *12*, 025004.
- Liu, C.; Wei, Y.; Qiu, H.; Zhang, J.; Liu, C. *Polym. Compos.* **2015**, *36*, 47.
- Picout, D. R.; Ross-Murphy, S. B. *Sci. World J.* **2003**, *3*, 105.
- Jiao, Y.; Gyawali, D.; Stark, J. M.; Akcora, P.; Nair, P.; Tran, R. T.; Yang, J. *Soft Matter*. **2012**, *8*(5), 1499.
- Shah, R.; Vyroubal, R.; Fei, H.; Saha, N.; Kitano, T.; Saha, P. *AIP Conf. Proc.* **2015**, *1662*(040007), 1.
- Shah, R.; Saha, N.; Kitano, T.; Saha, P. *Appl. Rheol.* **2015**, *25*, 33979.
- Elango, J.; Zhang, J.; Bao, B.; Palaniyandi, K.; Wang, S.; Wu, W.; Robinson, J. S. *Int. J. Biol. Macromol.* **2016**, *91*, 51.

37. Mauro, N.; Chiellini, F.; Bartoli, C.; Gazzarri, M.; Laus, M.; Antonioli, D.; Griffiths, P.; Manfredi, A.; Ranucci, E.; Ferruti, P. *Tissue Eng. Regen. Med.* **2017**, *11*, 2164.
38. O'guz, O. D.; Ege, D. *Materials*. **2018**, *11*(604), 1.
39. Zuidema, J. M.; Rivet, C. J.; Gilbert, R. J.; Morrison, F. A. *J. Biomed. Mater. Res. Part B*. **2014**, *102B*, 1063.
40. Roy, N.; Saha, N.; Kitano, T.; Saha, P. *Carbohydr. Polym.* **2012**, *89*, 346.
41. Saha, N.; Shah, R.; Gupta, P.; Mandal, B. B.; Alexandrova, R.; Sikiric, M. D.; Saha, P. *Mater. Sci. Eng. C Mater. Biol. Appl.* **2018**, *95*, 440.
42. Yan, J.; Miao, Y.; Tan, H.; Zhou, T.; Ling, Z.; Chen, Y.; Xing, X.; Hu, X. *Mater. Sci. Eng. C*. **2016**, *63*, 274.
43. Bendtsen, S. T.; Quinnell, S. P.; Wei, M. *J. Biomed. Mater. Res. Part A*. **2017**, *105A*, 1457.
44. Dennis, S. C.; Deta, M. S.; Kieweg, S. L.; Berkland, C. J. *Langmuir*. **2018**, *30*, 3528.
45. Tommasi, G.; Perni, S.; Prokopovich, P. *Tissue Eng. Part A*. **2016**, *22*(11–12), 862.
46. Tabilo-Munizaga, G.; Sáenz-Hernández, C.; Herrera-Lavados, C. *Int. J. Food Sci. Technol.* **2018**, *53*, 1781.
47. Tang, X.; Qiao, X.; Sun, K. *Colloids Surf. A*. **2015**, *486*, 86.
48. Basu, P.; Saha, N.; Bandyopadhyay, S.; Saha, P. *AIP Conf. Proc.* **2017**, *1843*, 050008.
49. Alcantar, N. A.; Aydil, E. S.; Israelachvili, J. N. *J. Biomed. Mater. Res.* **2000**, *51*(3), 343.
50. Nayak, K. K.; Gupta, P. *Int. J. Biol. Macromol.* **2015**, *81*, 1.
51. Dusek, K.; Duskova-Smrckova, M.; Somvarsky, J. *Macromol. Symp.* **2015**, *358*, 120.
52. Sarikaya, B.; Murat Aydin, H. *Biomed. Res. Int.* **2015**, *2015*, 9.
53. Dan, Y.; Liu, O.; Liu, Y.; Zhang, Y. Y.; Li, S.; Feng, X.; Shao, Z.; Yang, C.; Yang, S. H.; Hong, J. *Nanoscale Res. Lett.* **2016**, *11*, 487.
54. Ganji, F.; Vasheghani-Farahani, S.; Vasheghani-Farahani, E. *Iran. Polym. J.* **2010**, *19*(5), 375.
55. Koponen, A. I.; Lauri, J.; Haavisto, S.; Fabritius, T. *Appl. Sci.* **2018**, *8*, 755.
56. Sheffield, C.; Meyers, K.; Johnson, E.; Rajachar, R. M. *Gels*. **2018**, *4*(51), 1.
57. Santos, S. F.; Teixeira, R. S.; Savastano Junior, H. In *Sustainable and Nonconventional Construction Materials using Inorganic Bonded Fiber Composites*; Savastano Junior, H.; Fiorelli, J.; Dos Santos, S. F., Eds., Woodhead Publishing: U.K., **2017**.
58. Elwinger, F.; Pourmand, P.; Furo, I. *J. Phys. Chem. C*. **2017**, *121*, 13757.
59. Carmella, C.; Ferrari, F.; Bonferoni, M. C.; Ronchi, M. *Boll. Chim. Farm.* **1989**, *128*, 298.
60. Bružauskaitė, I.; Bironaitė, D.; Bagdonas, E.; Bernotienė, E. *Cytotechnology*. **2016**, *68*(3), 355.
61. Thomas, P. C.; Jose, T. J.; George, G.; Thomas, S.; Joseph, K. *J. Compos. Mater.* **2014**, *48*(19), 2325.
62. Sheenoy, A. V. *Rheology of Filled Polymer Systems*; Elsevier: U.K., **1999**.
63. Ferreira, C. I.; Bianchi, O.; Oviedo, M. A. S.; Bof de Oliveira, R. V.; Mauler, R. S. *Polímeros*. **2013**, *23*(4), 456.
64. Lee, W. S.; Chen, T. H.; Lin, C. F.; Li, Z. Y. *Mater. Trans.* **2012**, *53*(3), 469.
65. Shukla, P.; Nandi, T.; Singh, R. P. *Orient. J. Chem.* **2017**, *33*(4), 1848.
66. Wuestenberg, T. *Cellulose and Cellulose Derivatives in the Food Industry: Fundamentals and Applications*; John Wiley & Sons: Weinheim, Germany, **2014**.
67. Chaudhry, A. U.; Mittal, V.; Matsko, N. B. In *Nanoscience & Nanotechnology*; Mittal, V., Ed., RSC Publishing: Cambridge, U.K., **2012**.
68. Cho, J. W.; Paul, D. R. *Polymer*. **2001**, *42*, 1083.
69. Ropers, S. *Bending Behavior of Thermoplastic Composite Sheets*; Springer: Germany, **2017**.
70. Huang, H. X.; Zhang, J. J. *J. Appl. Polym. Sci.* **2009**, *111*, 2806.
71. Turon, P.; Del Valle, L. J.; Alemán, C.; Puiggali, J. *Appl. Sci.* **2017**, *7*, 60.
72. Wei, Q.; Wang, Y.; Li, X.; Yang, M.; Chai, W.; Zhang, Y. *Front. Bioeng. Biotechnol.* **2016**, *4*, 01262.
73. Khripunov, A. K.; Baklagina, Y. G.; Sinyaev, V. A.; Shustikova, E. S.; Paramanov, B. A.; Romanov, D. P.; Smyslov, R. Y.; Tkachenko, A. A. *Glass Phys. Chem.* **2008**, *34*(2), 192.
74. Romanov, D. P.; Khripunov, A. K.; Baklagina, Y. G.; Severin, A. V.; Lukasheva, N. V.; Tolmachev, D. A.; Lavrent'ev, V. K. *Glass Phys. Chem.* **2014**, *40*(3), 367.
75. Vliet, T. V.; Luyten, H.; Walstra, P. In *Food Colloids and Polymers: Stability & Mechanical Properties*; Dickinson, E.; Walstra, P., Eds., Elsevier: U.K., **1993**.
76. Shen, X.; Shamshina, J. L.; Berton, P.; Gurauc, G.; Rogers, R. D. *Green Chem.* **2016**, *18*, 53.
77. Abayasinghe, N.K., Pererana, K.P.U., Thomas, C., Daly, A., Suresh, S., Burg, K., Harrison, G.M., Smith Jr D.W. In *Gels, Genes, Grafts and Giants: Festschrift on the Occasion of the 70th Birthday of Allan S. Hoffman*; Cooper S, Horbett T, Ratner M, Stayton P (ed); U.S. CRC Press, **2005**; p. 920.
78. Rebelo, A. R.; Archer, A. J.; Chen, X.; Liu, C.; Yang, G.; Liu, Y. *Sci. Technol. Adv. Mater.* **2018**, *19*(1), 203.

## PUBLICATION V

**Basu P. (50%), Saha N., Saha P. (2020)** “Viscoelastic behaviour of Calcium Phosphate Packed Bacterial Cellulose -Polyvinylpyrrolidone based Hydrogel Scaffolds at Human Fever Temperature”, *AIP conference proceedings of PPS Europe-Africa 2019 Regional Conference* (will be in Web of Science Indexed, Book Chapter), *Accepted for publication.*



AIP | Conference Proceedings

[proceedings.aip.org](http://proceedings.aip.org)



**POLYMER PROCESSING 4.0**

**Europe-Africa PPS2019**

November 18-21, Pretoria, South Africa

# Viscoelastic behavior of Calcium Phosphate Packed Bacterial Cellulose -Polyvinylpyrrolidone based Hydrogel Scaffolds at Human Fever Temperature

Probal Basu, Nabanita Saha\*, Oyunchimeg Zaandra and Petr Saha

*Centre of Polymer Systems, University Institute, Tomas Bata University in Zlin, Trida Tomase Bati 5678, 760 01 Zlín, Czech Republic*

\*Corresponding/reference author: nabanita@utb.cz

## Abstract

Calcium phosphate (CaP) packed bacterial cellulose (BC) and polyvinylpyrrolidone (PVP) based hydrogel scaffolds (BC-PVP-CaP) are being reported here considering its possible application in bone restoration. The primary focus of this work is to analyze the viscoelastic behavior of 'BC-PVP-CaP' hydrogel scaffolds at human fever temperature condition (39°C) in swelled state. In BC-PVP scaffolds, CaP [in the form of  $\beta$ -tricalcium phosphate ( $\beta$ -TCP) and hydroxyapatite (HA) is present as filler in different concentrations (i.e.  $\beta$ -TCP/HA\_20:80,  $\beta$ -TCP/HA\_40:60,  $\beta$ -TCP/HA\_50:50). The BC-PVP scaffold (without CaP) was marked as a control set for the evaluation of viscoelasticity of scaffolds. The BC-PVP-CaP\_50:50 hydrogel scaffold showed the highest degree of swelling at 39°C among the other BC-PVP-CaP scaffolds. However, the other hydrogel scaffolds were also showed notable viscoelasticity at 39°C. Experimental results confirmed that the CaP filled BC-PVP hydrogel scaffolds (BC-PVP-CaP\_20:80, BC-PVP-CaP\_40:60, BC-PVP-CaP\_50:50) exhibit a promising viscoelastic behavior at human fever temperature condition (39°C), can be endorsed for its potential application in bone repairing /bone restoration.

## INTRODUCTION

Bone is a fundamental unit of human musculoskeletal organ. Notable stressful physiological conditions lead to the unwanted bone fracture situation [1]. Aging along with a bone related disease also ameliorate the likeliness for bone fracture [2]. Among different well practiced methods, the bone autografting has been considered promising, due to its facilitation of fracture healing. However, this method also has some significant limitations [3]. Hence, a new approach is needed for the potential alternative to this method. In this context, a polymeric biomaterial can be efficient alternative approach to this problem. Hydrogel scaffold is a polymeric biomaterial which can retain significant amount of water [4]. It can be used in tissue engineering applications due to its similarity with the living tissue (in context of its water retaining capacity) [5]. Different polymer composites have been used as tissue engineering scaffolds. Synthetic polymers like poly (glycolic acid) [PGA], poly (lactic-co-glycolic) acid [PLGA] and natural polymers like chitosan, gelatin were being utilized [6]. Bacterial cellulose (BC) is biocompatible polymer which has significant mechanical property [5]. Different combinations of biomaterials were prepared with BC; where, the other components were either polymer or other bioactive agents e.g., BC/chitosan, BC/hydroxyapatite. Research indicated that calcium phosphate (CaP) [like hydroxyapatite (HA) and  $\beta$ -tricalcium phosphate ( $\beta$ -TCP)] can be used in bone tissue engineering application [6]. In our earlier work, we have prepared CaP packed BC-polyvinylpyrrolidone (PVP) based hydrogel scaffold, which has the necessary mechanical property and physiochemical property for utilization in bone tissue engineering [5]. The viscoelastic behavior of the CaP packed BC-PVP based hydrogel scaffold was also analyzed at normal human homeostatic temperature (37°C). However, the analysis of rheological performance of the scaffold material in altered physiological condition is important for the understanding its sustained efficiency. Thus, this study aims to analyze the rheological performance of CaP packed BC-PVP based hydrogel scaffolds in altered physiological condition (i.e. human fever temperature). The temperature plays a pivotal role in the maintenance of the viscoelastic property of the polymeric system. This work facilitates the understanding of the swelling and mechanical property (in the form of viscoelastic property) of CaP packed BC based hydrogel scaffolds in human fever temperature. According to the American College of Critical Care Medicine, and the Infectious Diseases Society of America, a human fever condition can be defined an elevation of the temperature of the human body at 38.3°C or higher [7]. This study focuses the rheological behavior of calcium phosphate filled BC based hydrogel scaffold at human fever temperature condition (39°C).

## EXPERIMENTATION

### Preparation of CaP packed BC-PVP based hydrogel scaffold

BC (holding 99% H<sub>2</sub>O) was synthesized in presence of basal synthetic Hestrin-Schramm (HS) nutritive medium (pH 7.0) using *Gluconacetobacter xylinus* CCM 3611<sup>T</sup> (syn. *Acetobacter xylinum*) at 30°C for 15 days. 100 mL bacteriological culture bottles were inoculated with 5 mL of H.S. medium containing  $96 \times 10^8$  cells/mL bacteria [bacteria counted at 550 nm wavelength with Grant-Bio McFarland Densitometer DEN-1B, Grant Instruments Ltd, UK]. The freshly prepared BC pellicle is treated with 0.5 N NaOH solution and then heated at 80°C for 1 hours to remove the possible contaminations from the BC pellicle. Thereafter, a homogenous suspension of BC (particle size: 159 nm [SD:  $\pm 11.33$ ]) from the obtained BC mat was prepared by grinding (12 minutes) the BC mat in distilled water. Hydrogel scaffolds were first developed by applying the BC (holding 99% water) with polyvinylpyrrolidone (PVP) [5]. 0.5 g BC and 0.5 g PVP were used in each composition. 1 g polyethylene glycol (PEG) was also used in all the solutions to reduce the risk of tissue damage and other significant cytotoxic effects. 2 g Agar was used as gelling agent and glycerin (1 mL) was used as a humectant. Additionally, calcium phosphate (CaP) was used in the form of  $\beta$ -TCP and HA and were applied (Table. 1) in the ratio of 20:80, 40:60 and 50:50 in the hydrogel scaffolds to produce the CaP packed BC based composite hydrogel scaffolds and henceforth will be termed as, “BC-PVP-CaP\_20:80”, “BC-PVP-CaP\_40:60”, “BC-PVP-CaP\_50:50”. BC-PVP hydrogel scaffold was used as base scaffolds (Table 1). All materials were used are reagent grade and majorly purchased from Sigma Aldrich.

**Table 1. CaP in BC-PVP based hydrogel scaffolds.**

Sample index	CaP (g)
	[ $\beta$ -TCP/HA]
BC-PVP	0.0/0.0
BC-PVP- CaP_20:80	0.2/0.8
BC-PVP- CaP_40:60	0.4/0.6
BC-PVP- CaP_50:50	0.5/0.5

The BC-PVP based hydrogel scaffolds were prepared following the solvent casting method, applying moist heat and pressure. 100 mL polymer solutions were prepared in 250 mL sealed glass bottles under 15 lbs (107 KPa) pressure and 120°C temperature for 20 minutes [4]. Two sets of polymer solutions were prepared; where one set was without CaP, and another set was with CaP ( $\beta$ -TCP/HA). 25 mL polymer solution from each sealed glass bottles was poured into 75 mm diameter petri-dishes and allowed to cool at room temperature (22-25°C). Finally, smooth, round shaped, off white color BC-PVP based scaffold without CaP (i.e. “BC-PVP”, Diameter: 75 mm; Thickness: 6.0-6.3 mm) and with calcium phosphate packed (i.e. “BC-PVP-CaP\_20:80”, “BC-PVP-CaP\_40:60”, “BC-PVP-CaP\_50:50”; Diameter: 75 mm; Thickness: 5.9-6.2 mm) hydrogel scaffolds were attained.

### Swelling analysis at human fever temperature (39 °C)

Practically, as an implant/scaffold material, the hydrogel scaffolds will be first become swelled after in contact with the biological fluids. Thus, the swelling analysis of CaP packed BC-PVP based hydrogel scaffolds (BC-PVP-CaP\_20:80”, “BC-PVP-CaP\_40:60”, “BC-PVP-CaP\_50:50) was performed with physiological saline solution (pH 7.40) at human fever temperature (39 °C). Circular sections (Diameter: 20 mm) of the hydrogel scaffolds were soaked for specific time intervals (5 min, 30 min, 60 min, 120 min, 180 min, 240 min, 300 min, 360 min). The absorptivity of the hydrogel scaffolds is measured by the degree of swelling which is defined by the following equation:

$$\text{Degree of swelling (\%)} = ((W_s - W_d) / W_d) \times 100$$

Where,  $W_s$  and  $W_d$  are weight of the swollen and dried hydrogel scaffold section.

### Study of viscoelastic behavior at human fever temperature (39 °C)

Thereafter, the viscoelastic property of the equilibrium swelled hydrogel scaffold samples (20 mm diameter) were studied and by using a modular compact rheometer testing device (Anton Paar, Austria) and “Rheoplus” software

package for data analysis. Dynamic frequency sweep analysis was conducted in the linear viscoelasticity region (LVR) at 1% strain amplitude. The rheological measurement was done in the oscillation mode with the angular frequency range from 0.1 to 100 rad.s<sup>-1</sup> at human fever temperature condition (39°C). The influence of angular frequency on storage ( $G'$ ) and loss ( $G''$ ) modulus and complex viscosity ( $\eta^*$ ) was calculated by the following equation:

$$\eta^* = [(G'/\omega)^2 + (G''/\omega)^2]^{1/2}$$

The tan  $\delta$  (damping factor) was also studied at specific angular frequencies (i.e. 0.1 rad.s<sup>-1</sup>, 1 rad.s<sup>-1</sup>, 10 rad.s<sup>-1</sup>, 100 rad.s<sup>-1</sup>.) intervals.

### Statistical Analysis

The data are presented as mean  $\pm$  standard error of the mean (SEM). Statistical differences between the studied samples were assessed using one-way analysis of variance (ANOVA) followed by Bonferonni's post-hoc test by using GraphPad Prism version 5.00 for Windows, GraphPad Software, San Diego California USA, www.graphpad.com.

## RESULT AND DISCUSSION

The CaP packed BC-PVP based hydrogel scaffolds (BC-PVP-CaP\_20:80", "BC-PVP-CaP\_40:60", "BC-PVP-CaP\_50:50) were prepared and their swelling and viscoelastic behavior were studied at human fever temperature (39 °C). BC-PVP (without CaP) scaffold is kept as control.

Fig. 1. demonstrates the degree of swelling of the CaP packed BC-PVP based hydrogel scaffolds i.e. "BC-PVP-CaP\_20:80", "BC-PVP-CaP\_40:60", "BC-PVP-CaP\_50:50" at human fever temperature (39°C). BC-PVP (without CaP) hydrogel scaffold used as control. It can be seen from the Fig. 1. that, BC-PVP (without CaP) is majorly showing highest degree swelling throughout the study period. On the other hand, BC-PVP-CaP\_50:50 hydrogel scaffolds is also showing the highest degree of swelling than BC-PVP-CaP\_20:80 and BC-PVP-CaP\_40:60. The hydrogel scaffolds reached to equilibrium swelling condition after 300 mins. After equilibrium swelling (i.e. 330 min), BC-PVP (without CaP) hydrogel scaffold is showing highest (P<0.0001) degree of swelling. On the hand, the degree of swelling of BC-PVP-CaP\_50:50 is also significant (P<0.0001). Additionally, the degree of swelling of BC-PVP-CaP\_40:60 hydrogel scaffold is also found higher (P<0.0001) than BC-PVP-CaP\_20:80 in equilibrium swelling condition.

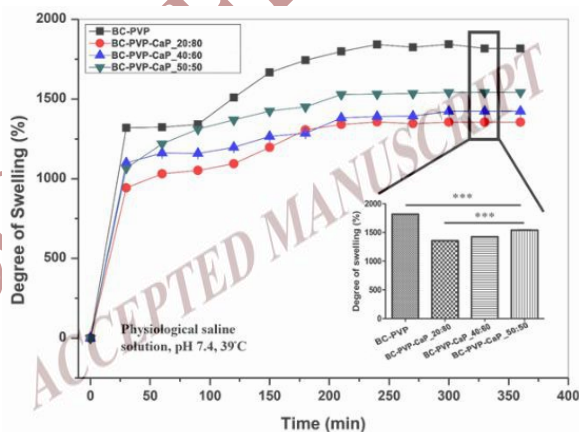


**FIGURE 1.** Degree of swelling of CaP packed BC-PVP based hydrogel scaffolds: BC-PVP-CaP\_20:80", "BC-PVP-CaP\_40:60", "BC-PVP-CaP\_50:50 at human fever temperature (39°C). Asterisk (\*\*\*) indicates level of significance (i.e. P <0.0001).

The CaP packed BC-PVP based hydrogel scaffolds have shown significant swelling ability at 39°C; especially, BC-PVP-CaP\_50:50 and BC-PVP-CaP\_40:60 hydrogel scaffolds has the highest swelling ability, which also indicate their significant macroporous internal structures [8].

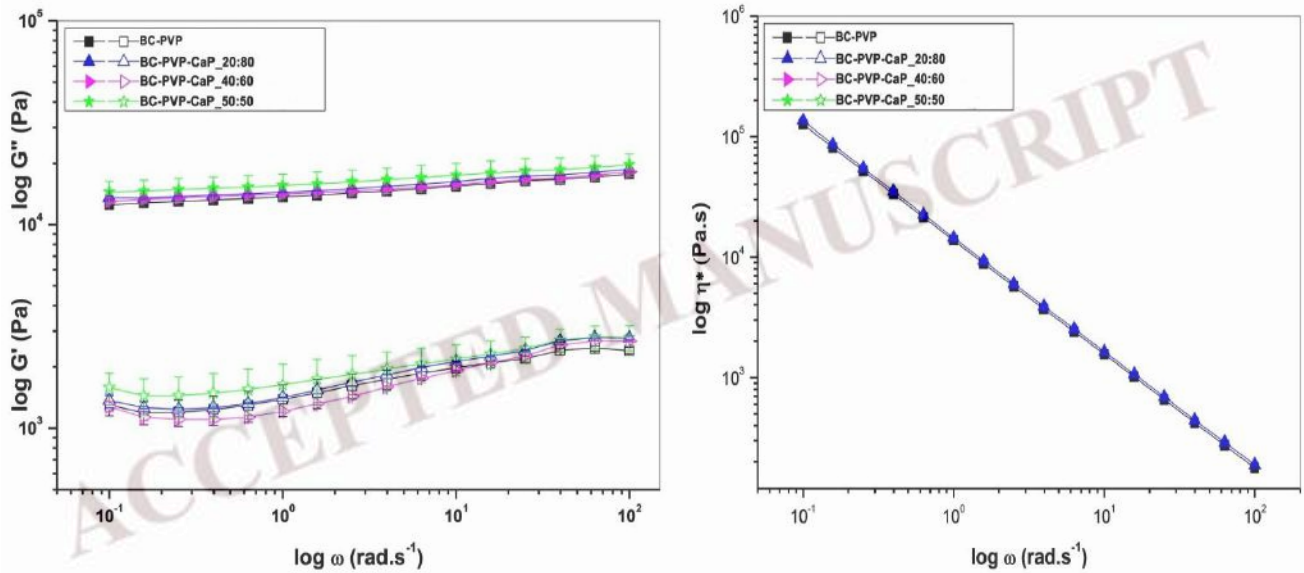
Fig. 2. represents the viscoelastic behavior of the CaP packed BC-PVP based hydrogel scaffolds i.e. BC-PVP-CaP\_20:80", "BC-PVP-CaP\_40:60", "BC-PVP-CaP\_50:50 at human fever temperature (39°C). It can be seen from

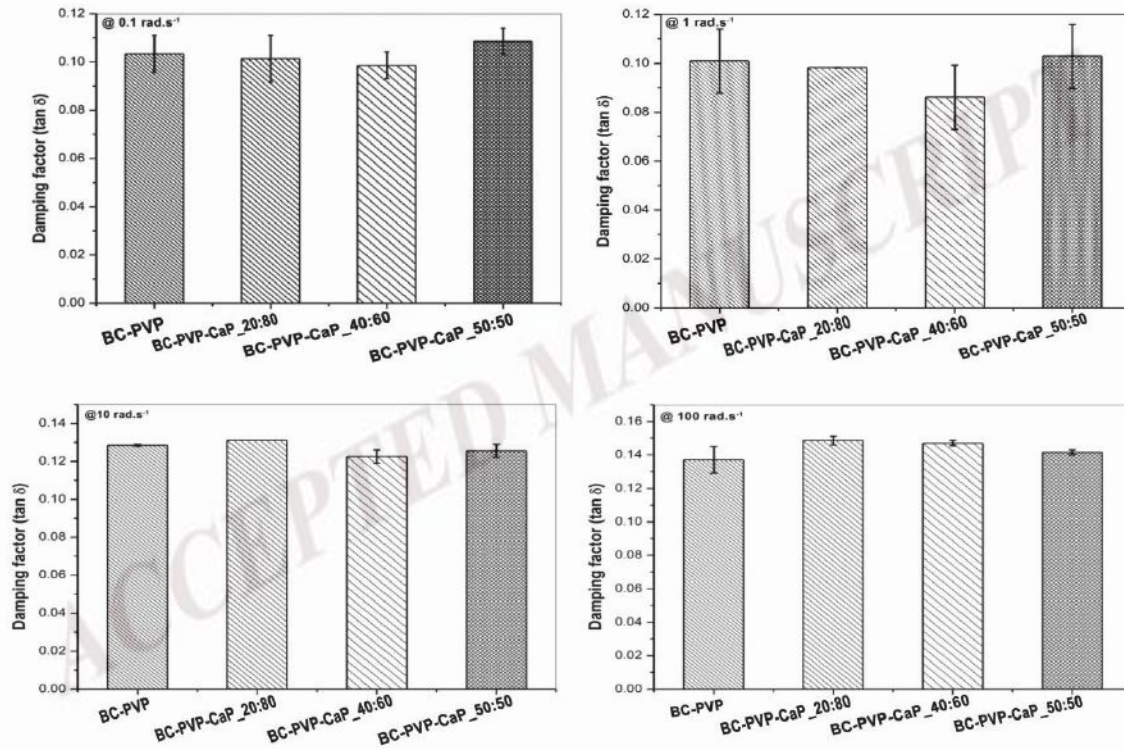


Fig. 2(a). that the storage ( $G'$ ) modulus of CaP packed BC-PVP based hydrogel scaffolds were higher than the loss ( $G''$ ) modulus, which indicates their significant rubbery consistency at 39°C throughout the angular frequency- 0.1-100  $\text{rad.s}^{-1}$ . BC-PVP (without CaP) scaffold was used as control. However, the storage modulus value of BC-PVP-CaP\_50:50 hydrogel scaffold is found higher at 39°C compared to other scaffolds. This indicates the notable mechanical strength of the BC-PVP-CaP\_50:50 hydrogel scaffold at 39°C. In general, the sustained plateau trend of storage modulus of all of the hydrogel scaffolds is also indicating cross-linked rigid gel like property. Interestingly, the overall trend of loss modulus of the hydrogel scaffolds throughout the angular frequency is increasing. This might be a plausible effect of the temperature.

The maintenance of the elastic nature at different angular frequency will indicate the integrity of the internal property and mechanical strength of the hydrogel scaffolds at fever temperature (39°C). Fig. 2(b). indicates the effect of angular frequency ( $\omega$ ) on complex viscosity ( $\eta^*$ ) of the CaP packed BC-PVP based hydrogel scaffolds. It can be observed that the complex viscosity values are decreasing with the increasing angular frequency at 1% strain amplitude, which indicates the significant elastic nature of the hydrogel scaffolds at 39°C.

Additionally, Fig. 2(c). shows the damping factor ( $\tan \delta$ ) values of CaP packed BC-PVP based hydrogel scaffolds at specific intervals of angular frequencies: 0.1  $\text{rad.s}^{-1}$ , 1  $\text{rad.s}^{-1}$ , 10  $\text{rad.s}^{-1}$ , 100  $\text{rad.s}^{-1}$ . It can be observed that the values of damping factor of all the hydrogel scaffolds are less than 1 ( $\tan \delta < 1$ ) at 39°C which indicates the maintenance of gel like elastic behavior throughout the four different angular frequencies in human fever temperature. This indicates that the CaP packed BC-PVP based hydrogel scaffolds maintain a notable mechanical property at altered physiological temperature i.e. human fever temperature.





**FIGURE 2.** Viscoelastic behavior of CaP packed BC-PVP based hydrogel scaffolds i.e. “BC-PVP-CaP\_20:80”, “BC-PVP-CaP\_40:60”, “BC-PVP-CaP\_50:50” at human fever temperature condition (39°C). (a) Storage ( $G'$ ) and Loss modulus ( $G''$ ); (b) Complex viscosity ( $\eta^*$ ); (c)  $\tan \delta$  values at angular frequencies:  $0.1 \text{ rad.s}^{-1}$ ,  $1 \text{ rad.s}^{-1}$ ,  $10 \text{ rad.s}^{-1}$ ,  $100 \text{ rad.s}^{-1}$ .

## CONCLUSION

This work focuses the viscoelastic behavior of equilibrium swelled CaP packed BC-PVP based hydrogel scaffolds i.e. BC-PVP-CaP\_20:80, BC-PVP-CaP\_40:60, BC-PVP-CaP\_50:50 at human fever temperature (39°C). The BC-PVP-CaP\_50:50 hydrogel demonstrated the highest degree of swelling at 39°C. The high swelling ability indicates the notable macro-porous structures of the scaffolds. On the other hand, it can be observed that, the BC-PVP-CaP\_20:80, BC-PVP-CaP\_40:60, BC-PVP-CaP\_50:50 scaffolds maintain a significant viscoelastic property at the human fever temperature condition. These observations further indicate the possibility of further study and utilization of the abovementioned scaffolds in bone bioengineering application.

## ACKNOWLEDGEMENTS

This work is supported by the Internal Grant Agency (Project No. IGA/CPS/2019/003), Tomas Bata University in Zlin, Czech Republic and Ministry of Education, Youth and Sports of The Czech Republic – NPU Program I (LO1504).

## REFERENCES

1. J.W. Ager III, G. Balooch, R.Q. Ritchie, *J. Mater. Res.* **21**(8), 451-454 (2006).
2. A. Oryan, S. Alidadi, A. Moshiri, *Hard tissue.* **2**(2), 13 (2013).
3. Shen, F.H., Samartzis, D., An, H.S. *Spine. J.* **5** (Suppl), 231S-239S (2005).
4. P. Basu, N. Saha, P. Saha, *Int J Polym Mater.* **68**:1-3, 134-144. (2018).
5. P. Basu, N. Saha, R. Alexandrova, B. Andonova-Lilova, M. Georgieva, G. Miloshev, P. Saha, *Int. J. Mol. Sci.* **19**, 3980 (2018).
6. E.J. Lee, K.F. Kasper, A.G. Mikos, *Ann Biomed Eng.* **42**(2), 323–337 (2014).
7. N.P. O’Grady, P.S. Barie, J.G. Bartlett, *Crit Care Med.* **36**:1330–49 (2008).
8. P. Basu, N.Saha, P. Saha, *J. Appl Polym Sci.* **136**, 48522 (2019).

## PUBLICATION VI

**Basu P. (50%), Saha N, Saha P. (2019)** “Calcium Phosphate Incorporated Bacterial Cellulose-Polyvinylpyrrolidone Based Hydrogel Scaffold: Structural Property and Cell Viability Study for Bone Regeneration Application”, *Polymers* [Web of Science Indexed, Q1 [Polymer Science], **J<sub>imp</sub>: 3.164**], 11(11), 1821. DOI:10.3390/polym11111821



*polymers*

an Open Access Journal by MDPI

**Polymers for Bone Tissue Engineering**



## Polymers for Bone Tissue Engineering

Guest Editor:

**Dr. Luis Rodríguez-Lorenzo**

CSIC - Instituto de Ciencia y  
Tecnología de Polimeros (ICTP),  
Madrid, Spain

[luis.rodriguez-lorenzo@  
ictp.csic.es](mailto:luis.rodriguez-lorenzo@ictp.csic.es)

Deadline for manuscript  
submissions:

**closed (29 February 2020)**

### Message from the Guest Editor

Dear Colleagues,

This Special Issue is dedicated to the different roles that polymers may play in bone regeneration. We would like to cover topics ranging from biodegradable natural-based polysaccharides (collagen, silk, alginate, chitosan, hyaluronic acid, etc.) and synthetic polyesters such as poly(lactic acid), PLA, poly(glycolic acid), PGA, poly(lactic-co-glycolide), PLGA, Poly(e-caprolactone), PCL, Polyhydroxyalkanoates, and PHA, to new chemical modifications including inorganic hybridation for improving biological interaction, and new roles and applications developed in the last few years that go from membranes for guided regeneration, antimicrobial membranes, drug and gen delivery particles or devices, thermoplastics for 3D printing, bioprinting, and any other aspect that involves macromolecules in the field of bone regeneration



Article

# Calcium Phosphate Incorporated Bacterial Cellulose-Polyvinylpyrrolidone Based Hydrogel Scaffold: Structural Property and Cell Viability Study for Bone Regeneration Application

Probal Basu <sup>1</sup> , Nabanita Saha <sup>1,\*</sup>, Radostina Alexandrova <sup>2</sup> and Petr Saha <sup>1</sup>

<sup>1</sup> Centre of Polymer Systems, University Institute, Tomas Bata University in Zlin, 760 01 Zlin, Czech Republic; probal@utb.cz (P.B.); saha@utb.cz (P.S.)

<sup>2</sup> Institute of Experimental Morphology, Pathology and Anthropology with Museum, Bulgarian Academy of Sciences, 1113 Sofia, Bulgaria; rialexandrova@hotmail.com

\* Correspondence: nabanita@utb.cz; Tel.: +420-57603-8156

Received: 12 September 2019; Accepted: 3 November 2019; Published: 6 November 2019



**Abstract:** This work focuses on the analysis of structural and functional properties of calcium phosphate (CaP) incorporated bacterial cellulose (BC)-polyvinylpyrrolidone (PVP) based hydrogel scaffolds referred to as “CaP/BC-PVP”. CaP is incorporated in the scaffolds in the form of hydroxyapatite (HA) and  $\beta$ -tricalcium phosphate ( $\beta$ -TCP) in different concentrations ( $\beta$ -TCP: HA ( $w/w$ ) = 20:80, 40:60, and 50:50). The scaffolds were characterized on the basis of porosity, thermal, biodegradation, mechanical, and cell viability/cytocompatibility properties. The structural properties of all the hydrogel scaffolds show significant porosity. The biodegradation of “CaP/BC-PVP” scaffold was evaluated following hydrolytic degradation. Weight loss profile, pH change, scanning electron microscopy (SEM), and Fourier Transform Infrared Spectroscopy (FTIR) study confirm the significant degradability of the scaffolds. It is observed that a 50:50\_CaP/BC-PVP scaffold has the highest degree of degradation. On the other hand, the compressive strengths of CaP/BC-PVP hydrogel scaffolds are found between 0.21 to 0.31 MPa, which is comparable with the human trabecular bone. The cell viability study is performed with a human osteosarcoma Saos-2 cell line, where significant cell viability is observed in all the hydrogel scaffolds. This indicated their ability to facilitate cell growth and cell proliferation. Considering all these substantial properties, CaP/BC-PVP hydrogel scaffolds can be suggested for detailed investigation in the context of bone regeneration application.

**Keywords:** bacterial cellulose; calcium phosphate; hydrogel scaffolds; degradation; mechanical property; bone regeneration

## 1. Introduction

Different traumatic and pathological phenomena can cause significant bone fractures [1–4]. Studies have indicated that more than 20 million individuals have been affected annually by the loss of bone due to trauma and other associated diseases [1,5]. The cost of bone defect repair in the European Union (EU) is currently estimated at about 40 billion Euros, and it is expected to increase by up to 25% by 2025 [1,6,7]. Additionally, the devices used for orthopedic trauma treatment had a market of 5.7 billion in 2013, and has been predicted to reach about 7.2% of the entire global market by 2020 [8]. The current bone fracture fixation treatments include the application of stainless steel, titanium, and titanium alloys [9]. However, these metallic implants are non-degradable and thus need to be surgically removed from the body [8,10]. In addition, the mechanical properties of the devices have also occasionally not matched with the human bone, which affects the normal load transfer

phenomenon from the implant to the healing bone [11]. Bone autografting has considered as the gold standard method, which facilitates the fracture healing through significant osteoconductivity and osteoinductivity [5]. However, the limitations of this method are also notable [11]. In this context, the application of polymeric biomaterials can be considered as a suitable alternative due to their composition, performance, and cost-effective production attributes [12].

Tissue engineering biomaterial has been devised using both natural and synthetic polymers [1,13]. Various synthetic polymers like polyethersulfone (PES), polycaprolactone (PCL), polyglycolide (PGA), poly (lactic-co-glycolic acid) (PLGA), poly ( $\alpha$ -lactic acid) (PLLA), poly (glycerol sebacate), and poly (propylene fumarate) were used in the development of biomaterials [1,14–22]. On the other hand, several natural polymers like collagen, chitosan, fibrin, silk, and fibroin have also been used [1,16–25]. Additionally, different polymer composites like hydroxyapatite (HA)-coated PLGA/poly ( $\alpha$ -lactic acid) (PLLA), HA/collagen/chitosan, HA/methacrylate-co-acryloyl-6-aminocaproic acid, and poly ( $\epsilon$ -caprolactone)/tricalcium phosphate (PCL/TCP) were also notably utilized in bone tissue engineering applications [1,16].

Cellulose has been considered as an excellent polymer due to its notable mechanical properties and crystallinity (60%–80%) [26]. Bacterial cellulose (BC) is a significant biodegradable biopolymer [27]. Significant biocompatibility makes this biomaterial important for application as tissue engineering scaffold [28]. Studies indicated that different composite materials with BC like calcium phosphate, BC/chitosan, BC/collagen, BC/agarose, and BC/poly (3-hydroxybutyrate) have been used in tissue engineering applications [29–32].

Material properties like porosity, degradation properties, mechanical properties, and biocompatibility are the important attributes of tissue engineering implantable devices [32] like polymeric hydrogels [12, 33–39]. A hydrogel is a polymeric structure which can retain a significant amount of water [40] and thus can be used notably in tissue engineering. Porosity and bio-degradability are important criteria for the applicability of polymeric tissue engineering scaffolds. Porosity of the polymeric scaffold will ensure that cell attachment occurs and facilitate significant vascularization inside the scaffold during regeneration [41]. On the other hand, the information regarding the ability of a scaffold material to disintegrate into its fundamental components after encountering with biological solution has provided the idea of the biodegradability of a material [42]. While the biodegradability of a tissue engineering scaffold promotes the development of an extracellular matrix [43], the controlled degradability is also an important aspect of a tissue engineering scaffold device [44]. Moreover, the cell viability and biocompatibility of the scaffold material indicates the cell's attachment, proliferation, and differentiation [45].

Polymeric PVP-CMC hydrogel was previously developed at our laboratory as a combination of synthetic polymers, polyvinylpyrrolidone (PVP), and carboxymethyl cellulose (CMC) [36,46]. The hydrogel was also found to be degradable [46]. Furthermore, in our previous work, the development of a hydrogel scaffold using BC and PVP was also reported [47]. Research indicated that the biphasic calcium phosphate (prepared in a combination of HA and  $\beta$ -TCP in different ratios after being sintered above 700 °C) were successfully utilized in bone tissue engineering application [48]. In our work, the osteogenic bioactive calcium phosphates (CaP): hydroxyapatite (HA) and  $\beta$ -tri calcium phosphate ( $\beta$ -TCP) [49] are simply combined with a BC-PVP polymeric matrix in different concentrations (i.e.,  $\beta$ -TCP:HA ( $w/w$ ) = 10:90, 20:80, 40:60, 50:50, and 60:40) to prepare a calcium phosphate (CaP) filled BC-PVP based hydrogel scaffold (i.e., CaP/BC-PVP). Our previous work indicated the swelling and rheological behavior of different CaP filled BC based hydrogel scaffolds, where the swelling and rheological properties were found to be promising for the samples with  $\beta$ -TCP:HA = 20:80, 40:60, and 50:50 [50].

Few studies have been reported so far where the structural and functional properties (like the cytocompatibility and cell proliferation ability) of polymeric tissue engineering scaffolds like hydrogel scaffolds have been analyzed simultaneously [33,34,51–55]. Additionally, there is little work where the structural properties and functional properties of CaP filled natural polymer, BC and synthetic

polymer, and a PVP based composite hydrogel scaffold were reported with the specific purpose of bone tissue regeneration. This article reports the structural and cell viability/cytocompatibility properties of CaP/BC-PVP hydrogel scaffolds. The test samples (20:80\_CaP/BC-PVP, 40:60\_CaP/BC-PVP, and 50:50\_CaP/BC-PVP) were chosen on the basis of their swelling and rheological properties, which were noticed in hydrogel scaffolds [50]. Structural properties like porosity, thermal and degradation characteristics, mechanical behavior and cell viability/cytocompatibility are reported in regard to their applicability for bone tissue engineering.

## 2. Experimental Section

### 2.1. Materials

Polyvinylpyrrolidone K30 (PVP K30; molecular weight: 40,000), polyethylene glycol 3000 (PEG; average molecular weight: 2700–3300), agar, and  $\beta$ -tri calcium phosphate ( $\beta$ -TCP; molecular weight: 310.18 g/mol) were supplied by Fluka, Buchs, Switzerland. Hydroxyapatite (HA; molecular weight: 502.31 g/mol) was obtained from Sigma Aldrich (St. Louis, MO, USA). Glycerin was obtained from Lach-Ner Ltd., Neratovice, Czech Republic.

Dulbecco's modified Eagle's medium (DMEM) and Fetal bovine serum (FBS) were obtained from Gibco-Invitrogen (Loughborough, Bishop Meadow Road, UK). Thiazolyl blue tetrazolium bromide (MTT), Dimethyl sulfoxide (DMSO) and Trypsin were obtained from AppliChem (Darmstadt, Germany). The antibiotics (Penicillin and Streptomycin) for cell cultures were from Lonza (Verviers, Belgium). Ethylenediaminetetraacetic acid (EDTA), and all other chemicals of the highest purity commercially available were purchased from local agents and distributors. All sterile plastic ware and syringe filters were from Orange Scientific (Braine-l0 Alleud, Belgium).

### 2.2. CaP/BC-PVP Hydrogel Preparation

#### 2.2.1. Microbial Synthesis and Preparation of Homogenous Suspension of BC

BC (holding 99% H<sub>2</sub>O) was synthesized in the presence of basal synthetic Hestrin-Schramm (HS) nutritive medium (pH 7.0) using *Gluconacetobacter xylinus* CCM 3611<sup>T</sup> (syn. *Acetobacter xylinum*) at 30°C for 15 days. 100 mL bacteriological culture bottles were inoculated with 5 mL of H.S. medium containing  $96 \times 10^8$  cells/mL bacteria (bacteria counted at 550 nm wavelength with Grant-Bio McFarland Densitometer DEN-1B, Grant Instruments Ltd., Shepreth, Royston, UK). The freshly prepared BC pellicle is treated with 0.5 N NaOH solution and then heated at 80 °C for 1 h to remove the possible contaminations from the BC pellicle. The newly produced BC pellicle was then treated with deionized water and the water was refreshed after 2 h of interval until the pH reached a neutral value. Thereafter, a homogenous suspension of BC (particle size: 159 nm (SD:  $\pm 11.33$ )) from the obtained BC mat was prepared by grinding (12 min) the BC mat in distilled water [12,31,50].

#### 2.2.2. Preparation of Hydrogel Scaffolds

"BC-PVP" hydrogel scaffold was prepared with BC (0.5 g,  $w/v \approx 50$  mL water based BC) suspension, where PVP (0.5 g,  $w/v$ ), PEG (1 g,  $w/v$ ), Agar (2 g,  $w/v$ ), and glycerin (1 mL,  $v/v$ ) were incorporated. The final volume of aqueous polymer solution was made to be 100 mL by adding additional distilled water [31,47].

The CaP filled BC-PVP based (CaP/BC-PVP) hydrogel scaffolds were prepared following the aforementioned composition with the addition of different amounts of CaP. The CaP was added into the "BC-PVP" polymer solution [47] in the form of  $\beta$ -TCP and HA, and incorporated in the following ratio:  $\beta$ -TCP: HA ( $w/w$ ) = 20:80, 40:60, and 50:50, to achieve the calcium phosphate containing polymer solutions.

Both the polymer solutions (with and without calcium phosphate) were then physically crosslinked by treating with moist heat and pressure. BC and PVP polymeric chains crosslinked together and

formed the hydrogel's network structure. Afterwards, 100 mL of polymer solution was treated in 250 mL sealed glass bottles under 15 lbs (107 KPa) of pressure and a temperature of 120 °C for 20 min [31,46]. Then, 25 mL of hot polymer solutions (from each sealed glass bottles) were poured into 75 mm diameter petri-dishes following the solvent casting method and allowed to cool at room temperature (22–25 °C) to obtain hydrogel scaffolds. Finally, smooth, round shaped, off white color hydrogel scaffolds were obtained. Here, while PEG and agar both had a role in the development of the polymeric hydrogel through cross-linking with base polymers like BC and PVP, the major role of PEG in calcium filled hydrogel scaffolds was to act as an agent which lowers the cellular cytotoxicity and reduces the tissue damage, while Agar acted as a notable gelling agent which maintains the hydrogel structure after solvent casting. Additionally, Glycerin acts as a humectant that retains the moisture content of the hydrogels to maintain its structural integrity [31].

The developed calcium filled BC-PVP based hydrogel scaffolds (Diameter: 75 mm; Thickness: 5.9–6.2 mm) are termed as “20:80\_CaP/BC-PVP” ( $\beta$ -TCP:HA = 20:80), “40:60\_CaP/BC-PVP” ( $\beta$ -TCP:HA = 40:60), and “50:50\_CaP/BC-PVP” ( $\beta$ -TCP:HA = 50:50), respectively (as mentioned in Table 1). BC-PVP based hydrogel scaffold (Diameter: 75 mm; Thickness: 6.0–6.3 mm) was marked as the control.

**Table 1.** Concentration (*w/w*) of CaP in BC-PVP based hydrogel scaffolds.

Sample Index	BC-PVP Solution (mL)	$\beta$ -TCP (g)	HA (g)
BC-PVP	100	0.0	0.0
20:80_CaP/BC-PVP	99	0.2	0.8
40:60_CaP/BC-PVP	99	0.4	0.6
50:50_CaP/BC-PVP	99	0.5	0.5

Finally, the BC-PVP and CaP/BC-PVP hydrogel scaffolds were freeze dried or lyophilized using Scanvac Cool Safe 110-4 PRO, Lyngø; lyophilizer at  $-80$  °C temperature and 0–5 kPa pressure, and then stored for further analysis. The thickness of freeze dried samples was as follows: BC-PVP (~5.91 mm) and CaP/BC-PVP (~4.70–5.03 mm).

### 2.3. Porosity and Void Fraction Study

The porosity of the freeze dried CaP/BC-PVP hydrogel scaffold samples was analyzed by the liquid displacement method. Three test samples ( $L = 10$  mm  $\times$   $B = 10$  mm  $\times$   $H = 1.5$ – $2.0$  mm = 150–200 mm<sup>3</sup>) for each were immersed into absolute ethanol for 48 h and examined carefully until they reached the saturation point [12]. The porosity of the samples was calculated by the following equation:

$$P = (W_2 - W_1)/\rho V_1 \quad (1)$$

where  $W_1$  and  $W_2$  are the weight of the hydrogel scaffolds before and after the immersion into absolute ethanol,  $V_1$  is the volume of the scaffolds before immersion into ethanol, and  $\rho$  is the constant of the density of ethanol. During the porosity study, the test sample “BC-PVP” was kept as the control and “20:80\_CaP/BC-PVP” was kept as the reference sample [12].

The void fraction of CaP/BC-PVP hydrogel scaffold were also determined by keeping the sample in ethanol [56]. Ethanol was selected as the solution because hydrogel is insoluble in ethanol [57]. The void fraction ( $F$ ) was determined by the following equation:

$$F = V_h/V_p \quad (2)$$

where  $V_h$  is the volume of the hydrogel and  $V_p$  is the total volume of the pores. The total volume of the pores was determined by the amount of ethanol absorbed into the polymeric hydrogel [58]. BC-PVP (without CaP) was kept as the control.



#### 2.4. Differential Scanning Calorimetry

Differential scanning calorimetry (DSC) of freeze dried samples of CaP filled BC based hydrogel scaffolds (20:80\_CaP/BC-PVP, 40:60\_CaP/BC-PVP, and 50:50\_CaP/BC-PVP) was performed to determine the thermal characteristics of the hydrogel scaffolds. 5–8 mg of the sample was taken. The DSC was measured with a differential scanning calorimeter (Mettler Toledo, Columbus, Ohio, USA) at a temperature range of  $-50$  to  $500$  °C in the presence of the nitrogen gas flow rate at 50 mL/min [59].

#### 2.5. Degradation Characterization

The degradability and the characteristics after degradation of the CaP/BC-PVP hydrogel scaffolds were measured through the following studies:

##### 2.5.1. Weight Loss Profile Study

Degradability of CaP/BC-PVP hydrogel scaffolds was analyzed on the basis of weight loss profile due to hydrolytic degradation. Sections ( $\Phi$  volume:  $628.32$ – $785.40$  mm<sup>3</sup>) of freeze dried hydrogel scaffolds were prepared for this study. The hydrolytic degradation experiment was performed through incubation of the sample sections in 25 mL of physiological saline solution (Ringer's solution; pH: 7.4) maintaining at  $37$  °C for 28 days (i.e., 4 weeks). The saline solution was changed weekly. The sample sections were removed from the solution at a specific time (i.e., after 7, 14, 21, or 28 days). The weight loss was also checked between 0–5 days (i.e., after 3 days) to understand the nature of the weight loss during the first week. They were then freeze dried after being washed by distilled water. The percentage of weight loss was evaluated according to the following equation [60]:

$$\text{Weight loss (\%)} = ((W_0 - W_t)/W_0) \times 100 \quad (3)$$

where  $W_0$  is the initial weight of the non-degraded freeze dried sample sections and  $W_t$  is the weight of the freeze dried biodegraded sample section at a specific time interval (i.e., 7, 14, 21, or 28 days), respectively.

##### 2.5.2. Gel Content Study

Changes in gel content of the hydrolytically degraded CaP/BC-PVP hydrogel samples were analyzed. The weights of the freeze dried hydrogel scaffolds were measured initially ( $W_0$ ) and after a specific time (7, 14, 21, or 28 days) ( $W_t$ ). The gel content of the scaffolds was measured through the following equation [61]:

$$\text{Gel content} = W_t/W_0 \times 100. \quad (4)$$

##### 2.5.3. Gel Density Study

The density of the freeze dried CaP/BC-PVP hydrogel scaffolds was studied at specific times (7, 14, 21, and 28 days) during the degradation study (in a physiological saline solution). The gel density  $\rho$  was determined by the following equation [62]:

$$\rho = W/\pi \times (d/2)^2 \times h \quad (5)$$

where  $W$  = weight of the scaffold,  $\pi = 3.14$ ,  $d$  = diameter of the samples, and  $h$  = thickness of the samples.

##### 2.5.4. pH Change and Calcium Release Study

The pH change of the medium (i.e., a physiological saline solution in which scaffolds were immersed) was also analyzed with a pH meter (Lovobond pH meter, Amesbury, UK). Additionally, the percentage of calcium released by the CaP/BC-PVP scaffolds (i.e., 20:80\_CaP/BC-PVP, 40:60\_CaP/BC-PVP, and 50:50\_CaP/BC-PVP) at specific times (i.e., 7, 14, 21, and 28 days) during

degradation was also studied. The percentage of calcium release was studied by X-ray fluorescence (ARL Quant X, Spectrometer, Thermo Scientific, Waltham, MA, USA) in the presence of helium atmosphere.

#### 2.5.5. Fourier Transform Infrared Spectroscopy (FTIR) Study

FTIR analysis was performed using fresh and hydrolytically degraded hydrogel scaffolds (over 7, 14, 21, or 28 days), which are calcium phosphate filled BC based hydrogel scaffolds designated as 20:80\_CaP/BC-PVP, 40:60\_CaP/BC-PVP, 50:50\_CaP/BC-PVP. In each case, the freeze dried sample was used for FTIR analysis and performed at room temperature (20–22 °C). A small amount of samples with flat surface were selected from each freeze dried hydrogel scaffolds. Three repeats of experiments were conducted. FTIR was performed at wave number 600–4000  $\text{cm}^{-1}$  with a uniform resolution of 2  $\text{cm}^{-1}$ . The ATR-FTIR analysis was conducted by using NICOLET 320 FTIR spectrophotometer with the “Omnic” software package.

#### 2.5.6. Energy Dispersive X-ray Fluorescence Study and Morphological Characterization by Scanning Electron Microscopy

The presence of calcium (Ca) and phosphate (P) in the CaP/BC-PVP scaffolds was determined by scanning electron microscope-energy dispersive X-ray fluorescence (EDX) study (SEM-EDX) with an accelerated voltage of 15 kV.

The morphological characterization of CaP/BC-PVP hydrogel scaffolds before being degraded (i.e., freshly prepared sample) and being after degraded was also performed. The samples were first lyophilized using Scanvac Cool Safe 110-4 PRO, Lyngø; lyophilizator at  $-80\text{ }^{\circ}\text{C}$  temperature and 0–5 kPa pressure. The cross-sectional structure of the fresh hydrogel scaffold and hydrolytically degraded scaffolds after 7, 14, and 21 days were then studied and compared by scanning electron microscopy (SEM) “NOVA nanoSEM” (FEI, Hillsboro, OR, USA), operating in the secondary electron imaging mode at an accelerating voltage of 5–20 kV. The pore size and pore distribution of the hydrolytically degraded CaP/BC-PVP scaffolds were investigated and analyzed by using ImageJ/Fiji software (Version J2, NIH, Bethesda, MD, USA).

### 2.6. Mechanical Property

Mechanical behavior of the fresh freeze dried CaP/BC-PVP scaffolds was analyzed in compression mode. “BC-PVP” was kept as the control and “20:80\_CaP/BC-PVP” was kept as the reference sample. Compressive strength of calcium phosphate filled BC based hydrogel scaffold was determined by using Testometric M350-5CT, England, UK at room temperature (20 °C) with a load cell having a full scale 300 kgf. Sections with 20 mm diameter and 2.5–3.5 mm thickness from freeze dried hydrogel samples were taken for the study. The study was done with a compression rate of 1  $\text{mm min}^{-1}$ .

### 2.7. Cell Proliferation and Cytocompatibility Study

#### 2.7.1. Cell Culture

Human osteosarcoma cell line and Saos-2 were used as model systems in our study. The cells were obtained from the cell culture collection of the Institute of Experimental Morphology, Pathology, and Anthropology Museum—Bulgarian Academy of Sciences (IEMPAM-BAS). The cell cultures were grown in DMEM medium supplemented with 10% FBS, 100 U/mL penicillin, and 100  $\mu\text{g/mL}$  streptomycin. The cultures were kept in a humidified incubator (Thermo Scientific, HEPA Class 100, Waltham, MA, USA) at 37 °C under 5%  $\text{CO}_2$  in air. For routine passages, the cells were detached using a mixture of 0.05% trypsin and 0.02% EDTA. The cell cultures were passaged 2–3 times per week (1:2 to 1:3 split). The experiments were performed during the exponential phase of cell growth.

### 2.7.2. Preparation of Test Samples for Cytocompatibility /Cell Viability/Proliferation Study

Three circular sections (volume:  $\Phi$  1.01–1.26 mm<sup>3</sup>) of each freeze dried sample (BC-PVP, 20:80\_CaP/BC-PVP, 40:60\_CaP/BC-PVP, and 50:50\_CaP/BC-PVP) were taken for this study. Circular sections were placed in the 48-well cell culture plate, treated with 50  $\mu$ L of 96% ethanol for 40 min at 30–32 °C until they were completely dried. Then, the prepared samples (BC-PVP, 20:80\_CaP/BC-PVP, 40:60\_CaP/BC-PVP, 50:50\_CaP/BC-PVP) were sterilized under the exposure of UV radiation for 80–90 min (surface sterilization) before use.

Indirect and direct experiments for cell proliferation/cytocompatibility study were performed to evaluate the influence of the materials (with and without calcium filled hydrogel scaffolds) on cell viability and proliferation. The number of test samples was 4 (BC-PVP, 20:80\_CaP/BC-PVP, 40:60\_CaP/BC-PVP, and 50:50\_CaP/BC-PVP) with 1 (Human osteosarcoma cell line; Saos-2) control, whereas the number of repeat experiments per condition was 8.

### 2.7.3. Indirect Experiments (IDE) for Cell Viability/Proliferation Study

For the cell viability/proliferation study, the Saos-2 cells were seeded in 96-well flat-bottomed microplates at a concentration of  $7.5 \times 10^3$  cells/well in fresh DMEM medium with 10% FBS and antibiotics. At the 24th hour, the culture medium from each well was removed and changed with 100  $\mu$ L DMEM containing hydrogel scaffolds extract (sample extracts, obtained after 1-, 3-, 5-, and 7-day incubation periods). The percent of viable cells was determined using an MTT (3-(4,5-Dimethylthiazol-2-yl)-2,5-diphenyltetrazolium bromide) test.

The MTT test was performed as described earlier [31]. Briefly, the cells were incubated for 3 h with MTT solution (0.3 mg MTT in 10 mL DMEM) at 37 °C under 5% CO<sub>2</sub> condition. The formed blue MTT formazan was extracted with a mixture of absolute ethanol and DMSO (1:1, *v/v*). The quantitative analysis was performed by absorbance measurements in an automated microplate reader (Tecan, Sunrise™, Grödig, Austria) at 540/620 nm.

### 2.7.4. Direct Experiments (DE) for Cytocompatibility Study

For cytocompatibility study, each material was placed in bottom of a 48 well cell culture plate on the drop (10  $\mu$ L) of FBS for 30 min at 30–32 °C in order to stick the sample to the surface of the well. Thereafter, 1 mL of DMEM (containing 10% FBS and antibiotics) was given to the wells (containing sterilized sample sections as well as empty wells that serve as controls).

The cells ( $5 \times 10^4$  cells/well) were seeded directly on the material sample placed on the bottom of a 48-well cell culture plate and incubated for 1, 3, 5, and 7 days in CO<sub>2</sub> incubator at 37 °C. The number and viability of the cells were determined before seeding using an automated cell counter and the trypan blue dye exclusion technique (zero time). The cell viability was found to be >95% in all experiments performed. At the start of the experiment the cell numbers were equal in all wells/ between all different samples, and they were cultured in equal conditions. Cells were grown in wells without materials, which served as controls. The effect of the materials on cell viability and proliferation was studied by MTT test. MTT concentration corresponded to the volume of the plate. Like those discussed in Section 2.7.3, the cells here were also incubated in MTT solution at 37 °C under a 5% CO<sub>2</sub> condition. The quantitative analysis was performed following the extraction of blue colored formazan.

## 3. Statistical Analysis

The data for void fraction, porosity, biodegradation study, and cell viability study are presented as the mean  $\pm$  standard error of the mean. The data of compressive strength is presented as mean  $\pm$  standard deviation of the mean. Statistical differences between control and treated groups, as well as between the studied samples were assessed using one-way analysis of variance (ANOVA) followed by a suitable post-hoc test (Dunnnett/Bonferonni) by using GraphPad Prism version 5.00 for Windows (San Diego, CA, USA) and MS Office 2010 (Redmond, WA, USA).

## 4. Results and Discussion

### 4.1. Void Fraction and Porosity

Figure 1a depicts the void fraction of CaP filled BC-PVP based hydrogel scaffolds (i.e., BC-PVP, 20:80\_CaP/BC-PVP, 40:60\_CaP/BC-PVP, and 50:50\_CaP/BC-PVP). BC-PVP (without CaP) scaffold was kept as the control. Void fraction indicates the water/solution uptake capability of the hydrogel scaffolds. Additionally, it provides information regarding the void volume of the scaffolds. It can be seen from Figure 1a that the void fraction of BC-PVP (without CaP) is notably higher ( $P < 0.0001$ ) than CaP/BC based scaffolds. In this study, CaPs ( $\beta$ -TCP/HA) are filler material, which interact with and occupy the spaces within the BC-PVP based scaffolds after application. The void fraction of 50:50\_CaP/BC-PVP hydrogel scaffold is significantly higher ( $P < 0.0001$ ) than 40:60\_CaP/BC-PVP and 20:80\_CaP/BC-PVP. This also indicates the higher water/solution uptake capacity of the 50:50\_CaP/BC-PVP scaffold. In the filled-in polymer system there are two major types of interaction observed: one is the filler-matrix interaction and the other is the filler-filler interaction. These types of interactions strengthen the hydrogel internal structure [63]. These interactions could have the ability to affect the porous structures of the scaffold since filler-matrix interaction influences the polymeric network structures. Thus, differential loading of filler material can potentially influence the porous structures of different CaP/BC-PVP based scaffolds. Figure 1b depicts the porosity of CaP filled BC-PVP based scaffolds. BC-PVP (without CaP) and 20:80\_CaP/BC-PVP scaffolds have been kept as the control. It can be seen from this figure that the porosity of CaP/BC-PVP scaffolds and BC-PVP (without CaP) was significantly different ( $P < 0.001$ ). Additionally, the porosity of the 50:50\_CaP/BC-PVP scaffold was notably higher ( $P < 0.0001$ ) than 40:60\_CaP/BC-PVP and 20:80\_CaP/BC-PVP. However, the porosity of the BC-PVP based hydrogel scaffold followed the following trend: BC-PVP > 50:50\_CaP/BC-PVP > 40:60\_CaP/BC-PVP > 20:80\_CaP/BC-PVP. Our study showed that the porosity of a material can be adjusted by changing the concentration of the structural composition/particles of that material [64]. The interaction of different concentrations of  $\beta$ -TCP and HA with the polymers present in the CaP/BC-PVP hydrogel scaffolds might be responsible for this trend.

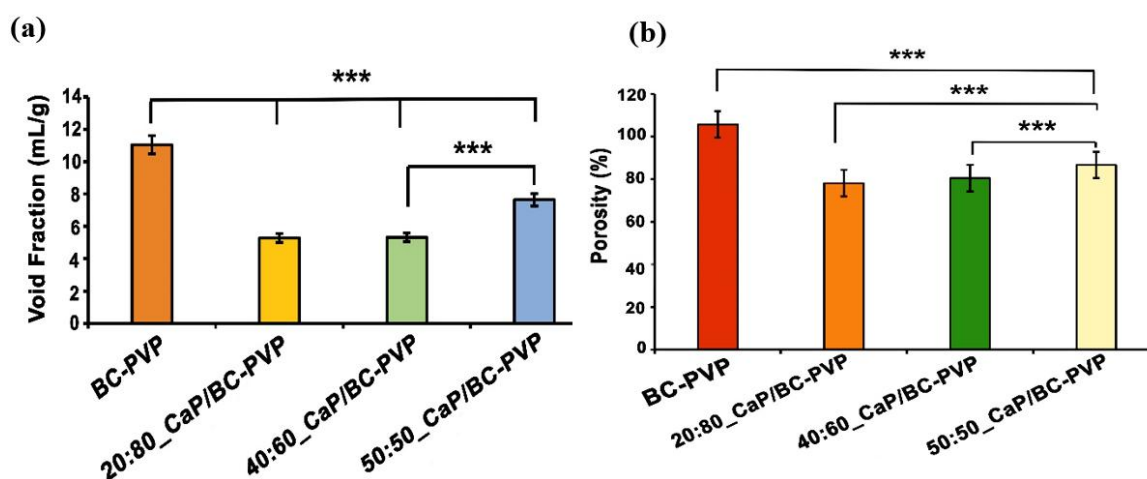


**Figure 1.** Void fraction (a) and Porosity (b) of calcium phosphate incorporated BC based hydrogel scaffolds (i.e., 20:80\_CaP/BC-PVP, 40:60\_CaP/BC-PVP, and 50:50\_CaP/BC-PVP). Asterisk (\*\*\*) indicates level of statistical significance. (Statistical analysis performed through mean  $\pm$  standard error of the mean and suitable post-hoc (Bonferonni test/Dunnet) test was performed followed by ANOVA). (Note: \*\*\* indicates the level of significance is explained by P value and thus written  $***P < 0.0001$ .)

### 4.2. Differential Scanning Calorimetry

Figure 2 represents the thermal characterization of CaP filled BC-PVP based hydrogel scaffolds (i.e., BC-PVP, 20:80\_CaP/BC-PVP, 40:60\_CaP/BC-PVP, 50:50\_CaP/BC-PVP) through differential scanning

calorimetry (DSC). BC-PVP (without CaP) scaffold was kept as the control. It can be seen from the figure that the DSC profiles of the hydrogel samples contained a notable endothermic peak between 50–100 °C, which occurred due to the moisture loss and which is typical for cellulose based materials [65]. This dehydration phenomenon can also be seen during a thermogravimetric analysis profile of the calcium filled hydrogel samples in our earlier study [12]. PVP polymer generally shows an endothermic peak near 100 °C, which corresponds to the moisture loss phenomenon [66]. Additionally, the endo peak occurring in the range 60–100 °C might be the melting temperature of PEG. Another endothermic event can also be observed near 250 °C, which might be due to melting of the crystalline region of cellulose [67]. The exothermic peak around 400 °C occurred due to the possible pyrolysis of cellulose. In CaP filled BC-PVP based hydrogel scaffold, the intensity of the peaks is less compared to BC-PVP (without CaP), but it indicates the significant interaction of calcium phosphate and the polymers. The intensity of the endothermic peaks gradually broadened from BC-PVP (without CaP) to 20:80\_CaP/BC-PVP, 40:60\_CaP/BC-PVP, 50:50\_CaP/BC-PVP. The intensity of the melting of the crystalline region had a decreasing trend from 50:50 to 20:80. This might be due to the differential ratio ( $w/w$ ) of CaP and its interaction with the polymers, particularly with BC. Many materials require a broad temperature range to melt [68]. The calcium phosphate melts at very high temperatures [69], and thus can be responsible for the different DSC thermogram to that of BC-PVP (without CaP).

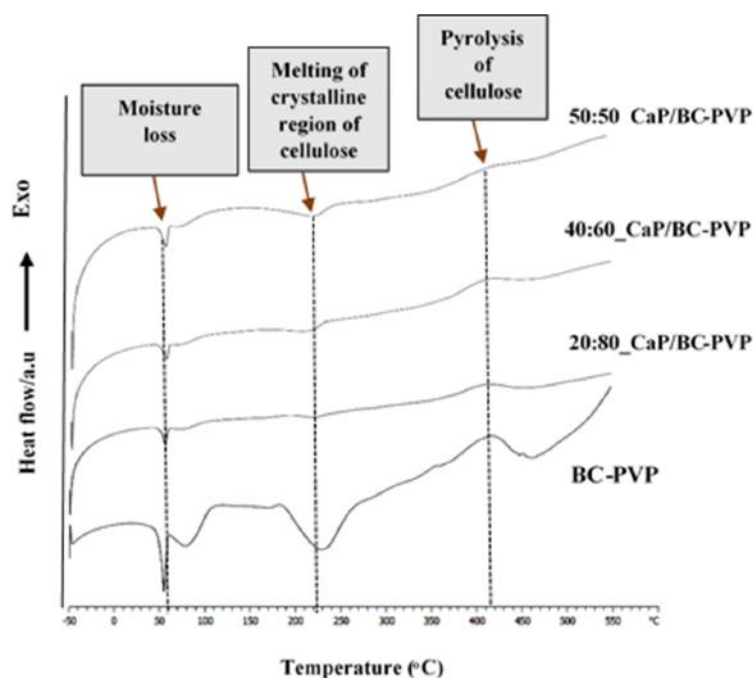


**Figure 2.** Thermal characterization of calcium phosphate incorporated BC based hydrogel scaffolds (i.e., 20:80\_CaP/BC-PVP, 40:60\_CaP/BC-PVP, 50:50\_CaP/BC-PVP) by DSC.

### 4.3. Hydrolytic Degradation Study

#### 4.3.1. Weight Loss Profile Study

Hydrolysis has been considered as one of the main degradation mechanisms which can occur inside the human body in the presence of the water from tissues. Research on hydrolytic degradation of biomaterials/tissue engineering scaffolds prepared with biodegradable polymers has been considered to be an important factor for biodegradation [39]. The degradation of cellulose based material is explained by the activity of cellulase enzyme. However, with the increase of time, the presence of significant cellulose amorphous structures in water based degradation medium indicates a notable chemical interaction and plausible breakdown of glycosidic bonds of cellulose [39,70,71]. Figure 3a represents the

hydrolytic degradation study of CaP filled BC-PVP based hydrogel scaffolds (i.e., 20:80\_CaP/BC-PVP, 40:60\_CaP/BC-PVP, and 50:50\_CaP/BC-PVP). BC-PVP (without CaP) scaffold was kept as a control. The figure indicates the weight loss (%) profile of CaP filled BC-PVP based hydrogel scaffolds is significant ( $P < 0.001, n=3$ ) after 7, 14, 21, and 28 days of hydrolytic degradation. It can be seen from the Figure 3a that, after 7 days in the physiological solution, the CaP/BC-PVP hydrogel scaffolds showed a marked 42%–52% weight loss. The weight loss between 0–5 days was also 30%–40%. However, after 14 days of hydrolytic degradation, a notable 48%–52% weight loss occurred. In particular, after 21 and 28 days, a significant weight loss was observed for 20:80\_CaP/BC-PVP. The hydrogel scaffolds contain hydrophilic polymers like BC and PVP, which are also biodegradable [47]. All the BC-PVP based polymeric hydrogel scaffolds could have undergone majorly bulk degradation and surface degradation, facilitated by hydrolysis. These changes would have influenced the weight loss of the hydrogel scaffolds [72]. During the degradation period, the hydrogel scaffolds absorbed the physiological solution and swelled up. In this process, the hydrolysis was facilitated by the diffusion of water inside the matrix, which finally led to bulk degradation of the scaffolds (Figure 3b) [72]. However, the balance between the hydrolysis and the swelling characteristics of the entire gels provides the idea of the bulk degradation phenomenon of the hydrogel scaffold material [73]. Previously, the void fraction study indicated the water uptake capacity of the CaP/BC-PVP hydrogel scaffolds and showed a comparable result with the weight loss (%) profile in hydrolytic degradation. The possible significant bulk degradation phenomenon led to the weight loss of the scaffolds. BC-PVP hydrogel scaffold (i.e., the control scaffold) showed a significant degradation ability ( $P < 0.0001$ ). On the other hand, 50:50\_CaP/BC-PVP hydrogel scaffold has shown a notable degradability ( $P < 0.0001$ ) compared to other CaP filled hydrogel scaffolds (i.e., 20:80\_CaP/BC-PVP and 40:60\_CaP/BC-PVP).

It should also be noted that a CaP like hydroxyapatite has insignificant solubility in water and other physiological saline media. It maintains its mechanical property in the medium. Research showed that the ceramic scaffolds with different HA/ $\beta$ -TCP compositions were non-degradable in water based media, even after 1 month [42,74]. In this study, different concentrations of HA/ $\beta$ -TCP containing BC-PVP based hydrogel scaffolds (i.e., 20:80\_CaP/BC-PVP, 40:60\_CaP/BC-PVP, and 50:50\_CaP/BC-PVP) have demonstrated the significant weight loss due to the hydrolytic degradation of the compositional polymers like BC and PVP. On the other hand, the poor interaction between polymer matrix and filler material could facilitate the degradation phenomenon [75,76]. The significant degradability of 50:50\_CaP/BC-PVP hydrogel scaffold might be due to its weak mechanical properties and poor filler-matrix interaction other than with the other calcium phosphate filled hydrogel scaffolds. However, in general, the CaP/BC-PVP hydrogel scaffolds demonstrated a notable degradability throughout the degradation period.

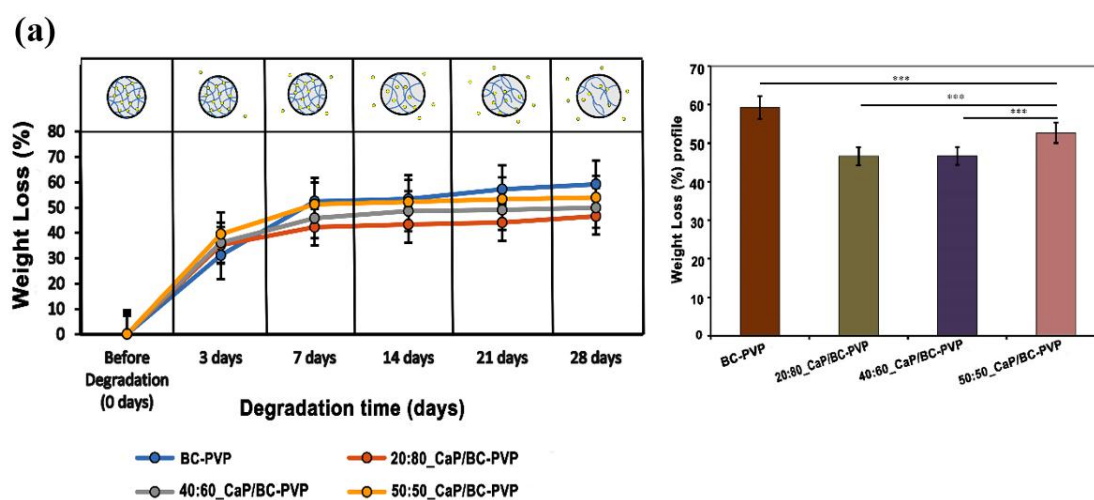
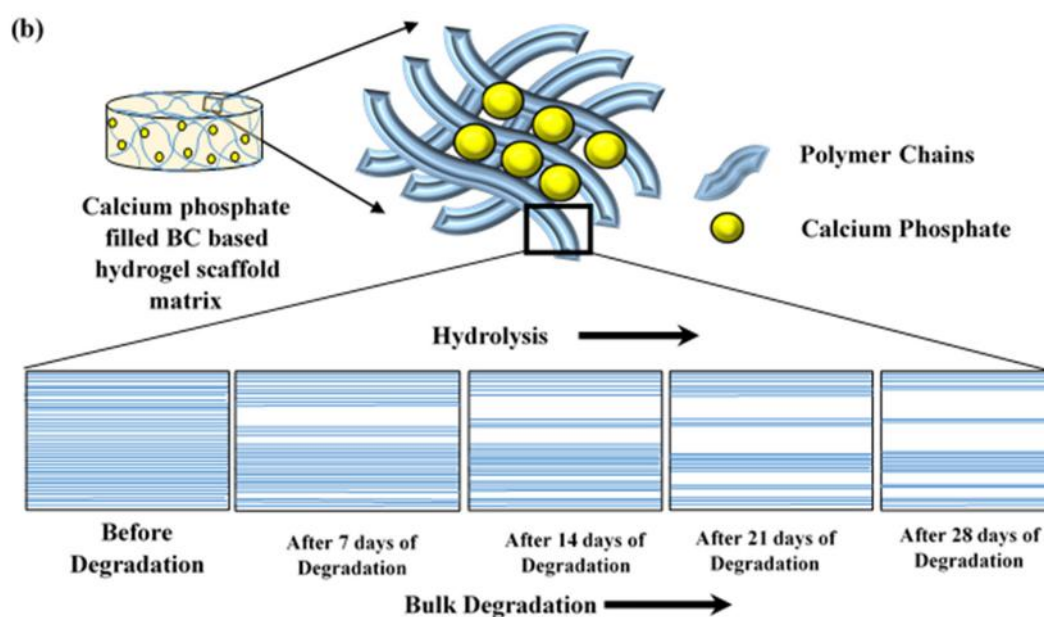


Figure 3. Cont.



**Figure 3.** Hydrolytic degradation study of calcium phosphate filled BC based hydrogel scaffolds (i.e., 20:80\_CaP/BC-PVP, 40:60\_CaP/BC-PVP, and 50:50\_CaP/BC-PVP). (a) Weight Loss (%) profiles of the scaffolds, Asterisks ( $***P < 0.0001$ ) indicate the level of significance, (Statistical analysis performed through mean  $\pm$  standard error of the mean and suitable post-hoc (Bonferonni test/Dunnet) test was performed followed by ANOVA). (b) Possible bulk degradation phenomenon of CaP filled BC based hydrogel scaffolds after 7, 14, 21, and 28 days of degradation [72].

#### 4.3.2. Gel Content Study

The degradation of the CaP/BC-PVP hydrogels was also indicated by the change in gel content of the hydrogel scaffolds, as shown in Figure 4a. It can be observed that the gel content of the CaP filled BC based hydrogel scaffolds (i.e., 20:80\_CaP/BC-PVP, 40:60\_CaP/BC-PVP, and 50:50\_CaP/BC-PVP) gradually decreases after hydrolytic degradation: Gel content before degradation > after 7 days > after 14 days > after 21 days > after 28 days. This might be led by the bulk degradation phenomenon caused by hydrolysis. Additionally, the change in gel content was notably seen after 28 days, which is also consistent with the weight loss profile of CaP/BC-PVP based hydrogel scaffolds.

#### 4.3.3. Gel Density Study

Gel density indicates the structural integrity of the gel [77]. The physical changes during the degradation period involve the change in gel density [42]. Figure 4b represents the change in gel density of the CaP/BC-PVP hydrogel scaffolds due to degradation. It can be seen from the figure that the hydrogel density gradually declined with the degradation time, with the trend being gel density before degradation > after 7 days > after 14 days > after 21 days > after 28 days. This declining trend of the hydrogel density provides the necessary information of the notable gel structure which could be obtained from the bulk degradation events facilitated by significant hydrolysis [42]. On the other hand, an increasing trend of gel density before the degradation stage from BC-PVP (without CaP) to 50:50\_CaP/BC-PVP hydrogel scaffold can be observed, which might be caused by the presence of different concentrations of CaP ( $\beta$ -TCP/HA) loading.

#### 4.3.4. pH Change and Calcium Release Study

A degradation phenomenon facilitates the physiochemical changes of the studied material, which involve the expected change of pH in the surrounding medium, facilitated by the local change of the concentration of the ions [42,78]. Figure 4c depicts the change in pH of the medium of the CaP filled BC based hydrogel scaffolds after 7, 14, 21, and 28 days of hydrolytic degradation. It can be seen

that the pH of the mediums of 20:80\_CaP/BC-PVP, 40:60\_CaP/BC-PVP, and 50:50\_CaP/BC-PVP were in decreasing order from before the degradation state (i.e., 0 days) to after 7 days of degradation, in general. However, the trend of decrease of the pH value of BC-PVP hydrogel scaffold (i.e., control) medium was the following: Before degradation > 7 days > 14 days > 21 days > 28 days. Nevertheless, the general decrease in the pH indicates the occurrence of hydrolysis inside the hydrogel structure [79], which could facilitate the bulk degradation phenomenon of the BC-PVP based scaffolds. Research demonstrated that the development of an oligomeric hydrolysis product like a carboxylic or acidic group could accelerate the decrease in the local pH, which in turn facilitates the degradation phenomenon [72]. This can be a plausible reason behind the sudden decrease in pH in the environment after 7 days of hydrolytic degradation. On the other hand, the pH values of the medium containing CaP/BC-PVP hydrogel scaffolds (20:80\_CaP/BC-PVP, 40:60\_CaP/BC-PVP, and 50:50\_CaP/BC-PVP) are also in an increasing trend between 7 days and 28 days of hydrolytic degradation. Studies showed that the local increase of calcium ion could elevate the pH of the environment [80]. These increased values of pH of the CaP/BC-PVP hydrogel scaffold containing medium might be caused by the notable calcium release due to erosion and degradation of the CaP filled scaffolds.

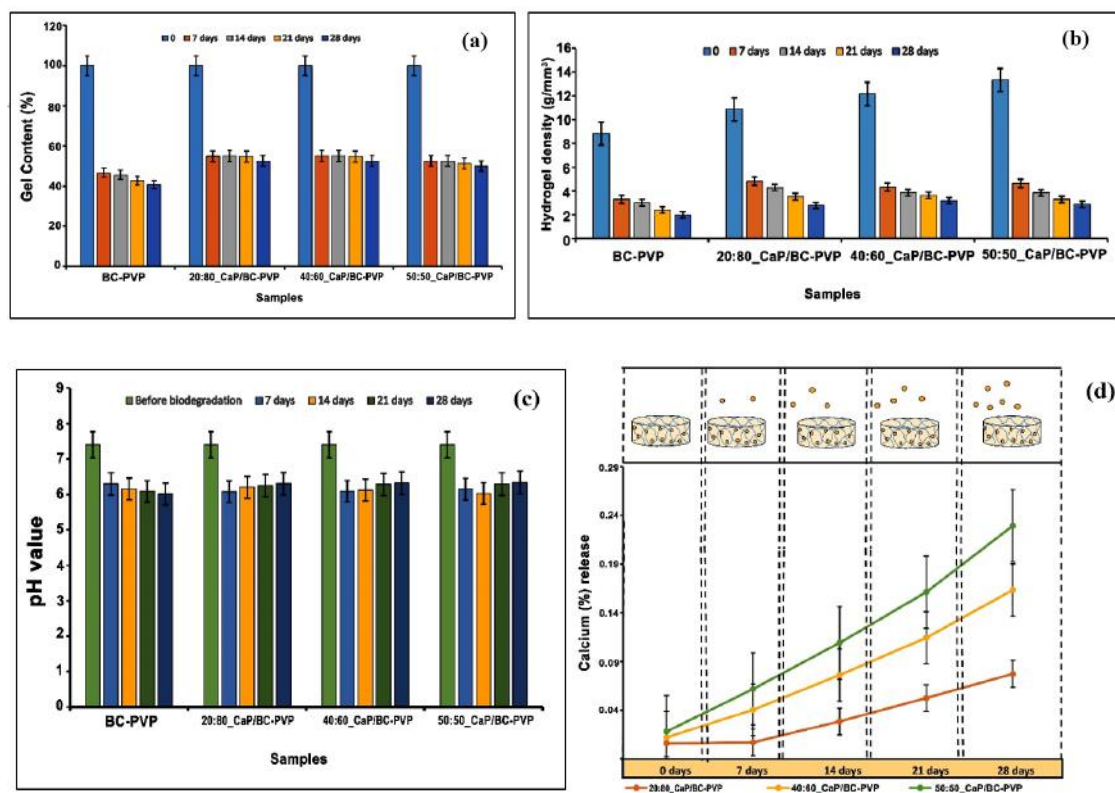


**Figure 4.** Gel content (%) histogram (a) and (b) Hydrogel density profile before and after 7, 14, 21, and 28 days of hydrolytic degradation analysis; pH change (c) and calcium release (%) profile (d) in the medium after 7, 14, 21, and 28 days of hydrolysis degradation analysis of calcium phosphate incorporated BC based hydrogel scaffolds (i.e., BC-PVP, 20:80\_CaP/BC-PVP, 40:60\_CaP/BC-PVP, and 50:50\_CaP/BC-PVP).

Ion exchange within the study material and in the solution can result in the gradual breakdown of the structural network, which subsequently facilitates the degradation phenomenon [42]. Figure 4d represents the release profile (%) of calcium ion from the CaP filled BC based hydrogel scaffolds to the medium after 7, 14, 21, and 28 days of hydrolytic degradation. The leaching out of the filler material could also explain the degradation phenomenon of the scaffolds [81]. The release of calcium ion into the medium can be thus related with the elevated pH from 7 days to 28 days within the mediums of CaP/BC-PVP hydrogel scaffolds (Figure 4c). Interestingly, the calcium ion release profile from



50:50\_CaP/BC-PVP hydrogel scaffold after 7, 14, 21, and 28 days of hydrolytic degradation was found to be higher than the 20:80\_CaP/BC-PVP and 40:60\_CaP/BC-PVP hydrogel scaffolds. The significant calcium release from 50:50\_CaP/BC-PVP might facilitated the notable degradation of this scaffold; which is also comparable with the weight loss profile of 50:50\_CaP/BC-PVP (Figure 3a).

#### 4.3.5. Fourier Transform Infrared Spectroscopy (FTIR) Study

Figure 5 depicts the FTIR analysis of CaP/BC-PVP hydrogel scaffolds (i.e., 20:80\_CaP/BC-PVP, 40:60\_CaP/BC-PVP, and 50:50\_CaP/BC-PVP) before degradation and after 7, 14, 21, and 28 days of degradation. Here the data is given in the range of 800–2600  $\text{cm}^{-1}$ , as all the significant peaks and bands were revealed in this zone. BC-PVP (without CaP) was also used here as the control. The FTIR spectra provides information of the characteristic bond vibrations. It can be seen from the figure that at 1106  $\text{cm}^{-1}$ , there is a peak that corresponds to C–O stretching of glucose [82]. Additionally, the peaks at 1279 and 1342  $\text{cm}^{-1}$  correspond to the C–H stretching and C–H<sub>2</sub> deformation vibration of cellulose [83]. These peaks confirm the presence of the biopolymer, BC. On the other hand, the peaks at 1290 and 1657  $\text{cm}^{-1}$  correspond to the C=O stretching and C–N bond vibration, which are the signature peaks of the synthetic polymer, PVP [12,77]. In addition, the peak at 1030–1043  $\text{cm}^{-1}$  indicates the presence of PO<sub>4</sub> of the CaP filled BC based hydrogel scaffolds [84]. This peak represents the presence of CaP in the hydrogel scaffold materials. CaP is a filler material which interacts with the polymer chains of the hydrogel scaffolds. As a filler, it also influences the mechanical property and at the same time it also has a role in chemical characteristics of the material. The significance presence of the CaP in the hydrogel scaffolds supports the fact that the CaP/BC-PVP based hydrogel scaffolds has the necessary ability to interact with the bone specific cells and can thereby initiate or facilitate cell proliferation.

Research indicated that the degradation time for calcium phosphate is very long [85]. This study was done for 28 days and this period is not enough for the complete degradation of calcium phosphate.

The effect of hydrolytic degradation on the CaP/BC-PVP hydrogel scaffolds can also be visualized in the Figure 5. The signature peaks of the components of the hydrogel scaffolds are in decreasing order along with increasing degradation times (i.e., before degradation > after 7 days of degradation > after 14 days of degradation > after 21 days of degradation > after 28 days of degradation). Interestingly, FTIR peak intensity is influenced by the degradation phenomenon. Degradation causes the generation of ions and compounds, which affects the peak intensity of functional groups. Thus, FTIR qualitative analysis of hydrolytic degradation is performed and shown here (Figure 6). Two signature wavenumbers of the main/major polymers BC and PVP were selected and the absorbance peaks were compared with the degradation time (i.e., after 7, 14, 21, and 28 days of degradation). The 1279 and 1342  $\text{cm}^{-1}$  wavenumbers were selected for BC, while 1290 and 1657  $\text{cm}^{-1}$  wavenumbers were selected for PVP. Figure 6 represents the relationship between absorbance values of the aforementioned wavenumbers and degradation time. It can be seen that a clear decreasing trend of the absorbance peaks and values occurred, which is indicated by the trend line in Figure 6. The decreasing trend of the absorbance values indicates the degradation phenomenon of the major polymeric components BC and PVP of the hydrogel scaffolds.

#### 4.3.6. Energy Dispersive X-ray Fluorescence Study and Morphological Characterization

Figure 7a represents the elemental analysis through an energy dispersive X-ray (EDX) study of CaP filled BC based hydrogel scaffolds (20:80\_CaP/BC-PVP, 40:60\_CaP/BC-PVP, and 50:50\_CaP/BC-PVP). From the EDX spectra, it can be seen that the calcium (Ca) and phosphorous (P) are present in the CaP filled BC based hydrogel scaffolds. However, only BC-PVP hydrogel scaffold showed no Ca and P.

From the weight loss study, it was observed that the significant degradation had occurred after up to 21 days of hydrolytic degradation. Thus the morphological analysis was done after 7, 12, and 21 days of degradation. Figure 7b represents the morphology of the cross sectional structures of CaP/BC-PVP hydrogel scaffolds (20:80\_CaP/BC-PVP, 40:60\_CaP/BC-PVP, and 50:50\_CaP/BC-PVP) before degradation and after 7, 14, and 21 days of hydrolytic degradation. A BC-PVP (without CaP) scaffold was also

kept as a control. The surface structures of all CaP filled hydrogels were rough and contained much fewer notable changes during this period, and thus are not discussed further here. However, the cross-sectional structures demonstrated significant changes and are thus provided here. It can be seen from the figure that all the hydrogel scaffolds contained porous structures. The morphology of the pores between before degradation and after degradation was significant. The degraded hydrogel scaffold contained irregular pore morphologies [86]. The change in pore morphology was significant between before degradation condition and after 21 days of degradation. This might be due to a loss of interaction between the polymer chains, which causes an altered pore structure. In particular, the change in morphologies of the pores of 40:60\_CaP/BC-PVP, 50:50\_CaP/BC-PVP, and 20:80\_CaP/BC-PVP hydrogel scaffolds are significant from before degradation to after 21 days of degradation. The loss of interaction between the polymer chains may create an possible overlapping (of the polymer phase) between each other, which can affect the morphology of the pores. Additionally, the degradation can result in the change in the matrix properties [87], which influences the morphology of the pores. The porosity and pore size have a significant relationship with the degradation rate [88]. Figure 7c indicates that the change in average pore sizes of the pores which are categorized as:  $>100\ \mu\text{m}$ , between  $50\text{--}100\ \mu\text{m}$ , and  $< 50\ \mu\text{m}$  pores. It can be seen that the average pore size of all the pores of CaP filled BC-PVP based hydrogel scaffolds (20:80\_CaP/BC-PVP, 40:60\_CaP/BC-PVP, 50:50\_CaP/BC-PVP) are in an increasing trend with the degradation time as follows: Before degradation  $<$  After 7 days of degradation  $<$  After 14 days of degradation  $<$  After 21 days of degradation. The degradation time influences the the pore sizes in the polymer systems [89]. The hydrolytic degradation decreases the interaction of the polymer-polymer and polymer-CaP, which ultimately causes the larger pore sizes.

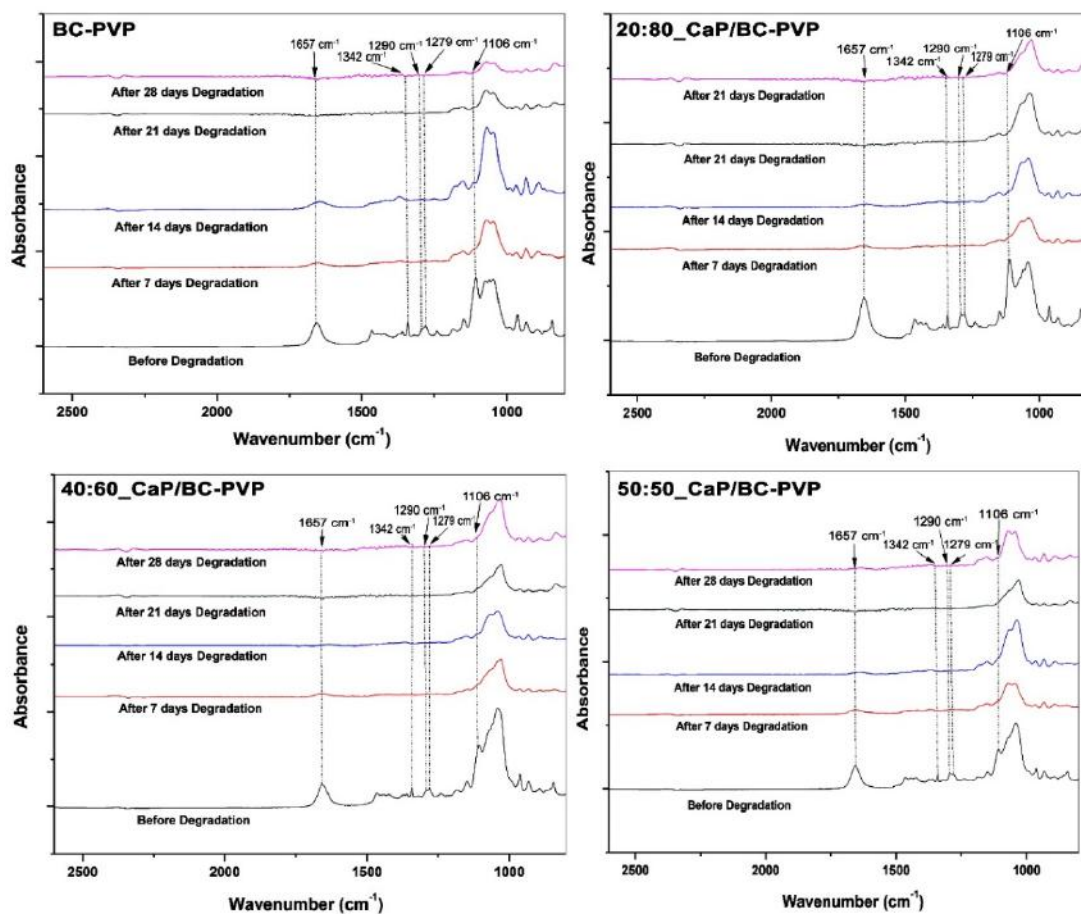


**Figure 5.** FTIR analysis of calcium phosphate incorporated BC based hydrogel scaffolds (i.e., 20:80\_CaP/BC-PVP, 40:60\_CaP/BC-PVP, 50:50\_CaP/BC-PVP) before and after hydrolytic degradation.

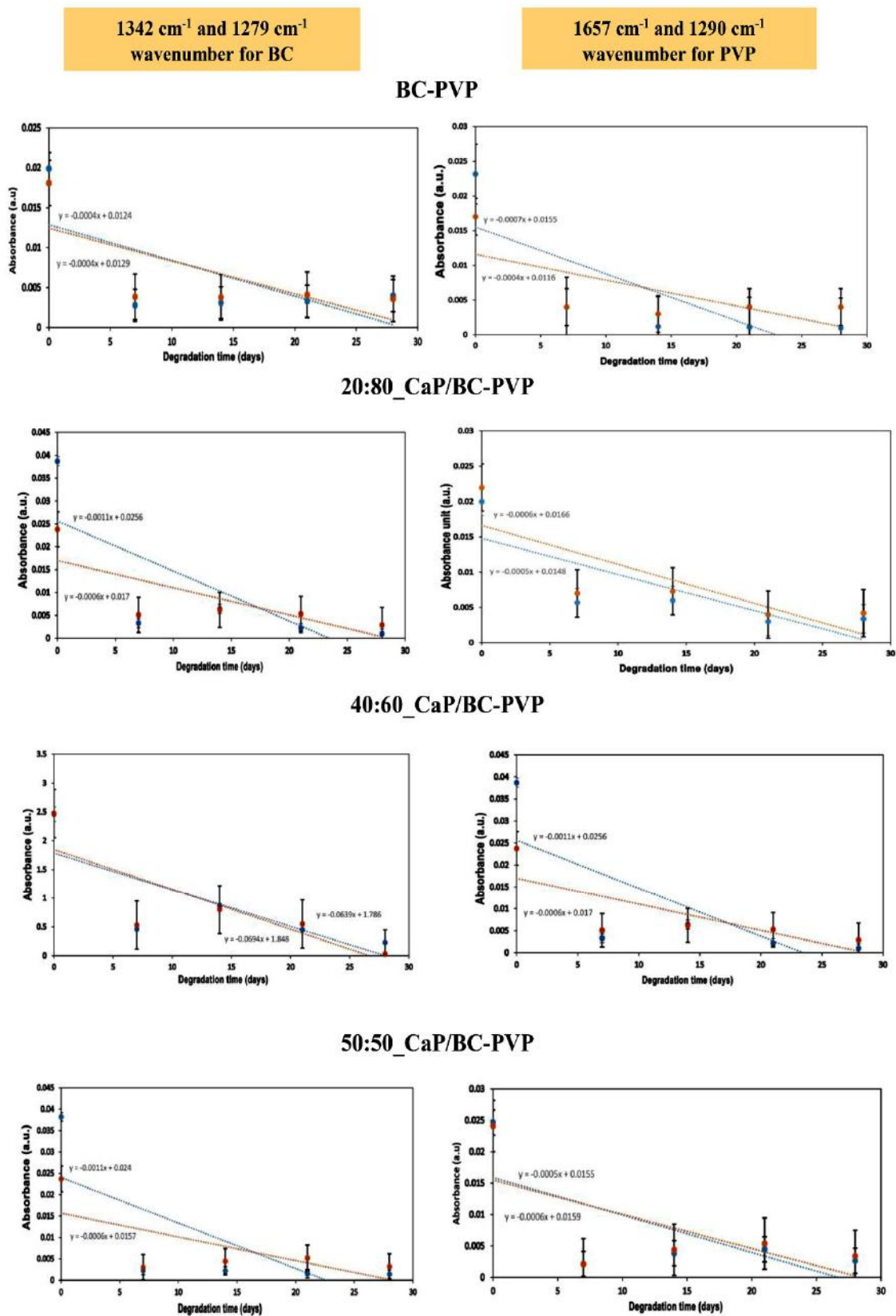


Figure 6. Relationship between the absorbance value of 1342, 1279, 1657, and 1290  $\text{cm}^{-1}$  wavenumbers and hydrolytic degradation time obtained by FTIR. Trend lines showing a decreasing trend (7, 14, 21, and 28 days).

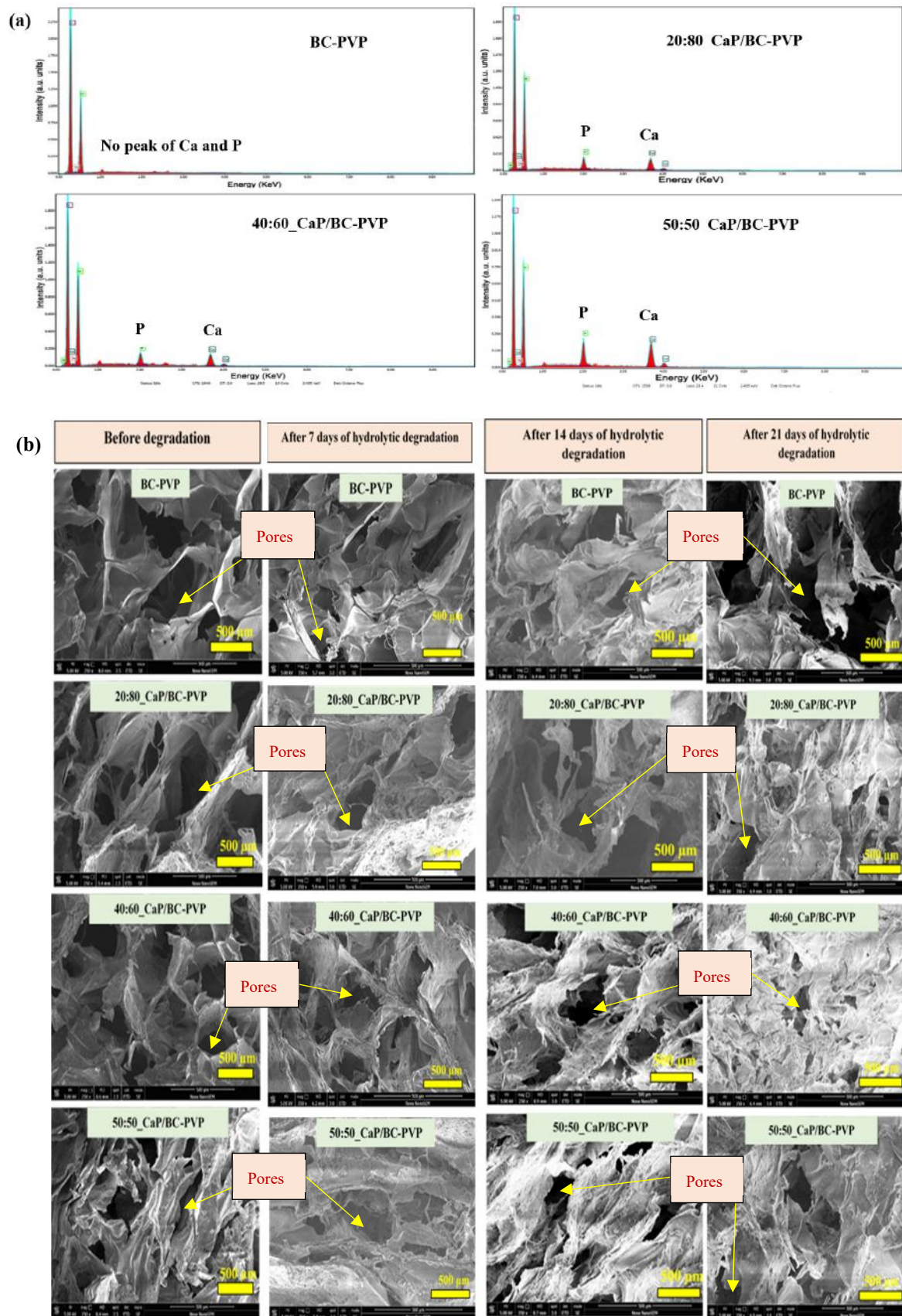
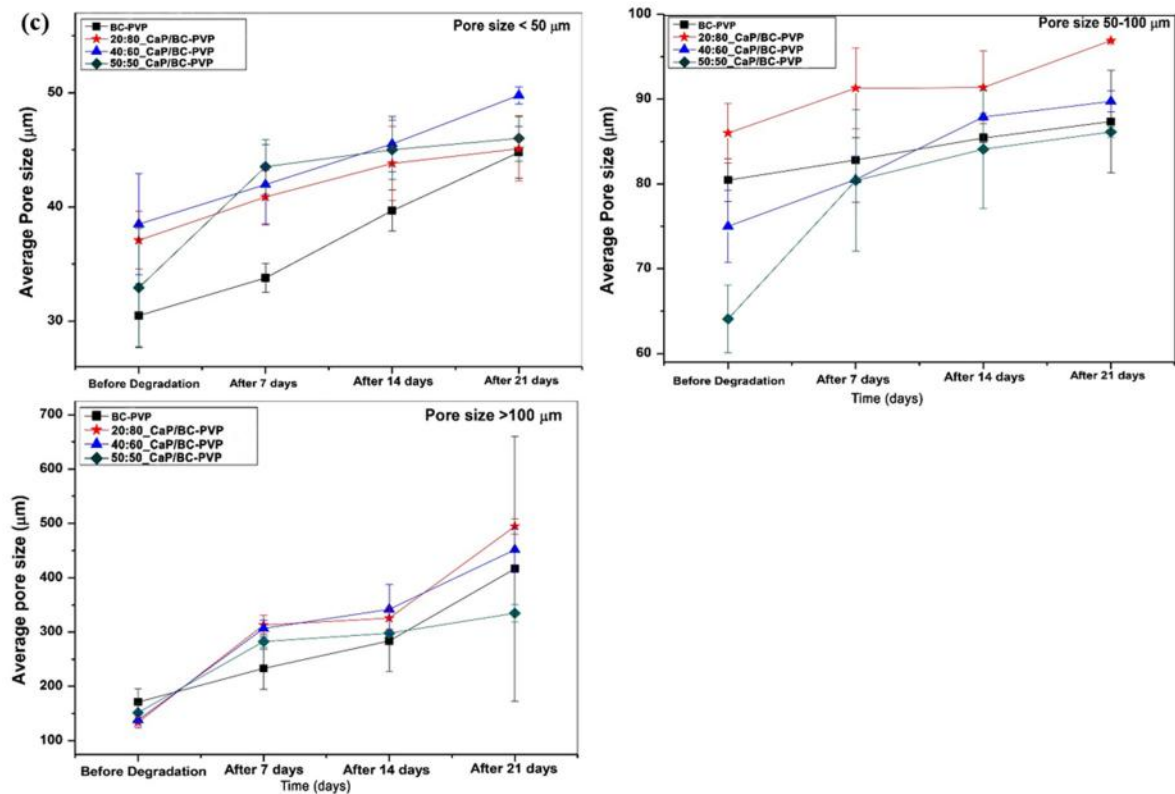


Figure 7. Cont.



**Figure 7.** CaP/BC-PVP hydrogel scaffolds (a) SEM-EDX of CaP/BC-PVP hydrogel scaffolds indicates the presence of Ca and P in the scaffolds; (b) SEM morphology of cross-sectional structure after hydrolytic degradation; (c) relationship average pore size (pores > 100 μm, pores between 50–100 μm, and pores < 50 μm) with hydrolytic degradation times.

#### 4.4. Mechanical Property Analysis

The mechanical characteristics of fresh/before degraded freeze dried CaP filled BC-PVP based hydrogel scaffolds are represented in Table 2. “BC-PVP” was kept as the control and “20:80\_CaP/BC-PVP” was kept as the reference sample. Earlier research reported that the compressive strength of human cancellous bone ranged between 0.22 and 10.44 MPa [90,91]. It can be seen from Table 2 that the compressive strength of all the BC-PVP based hydrogel scaffolds is comparable with the human trabecular or cancellous bone. Interestingly, the compressive strength of all the BC-PVP based hydrogel scaffolds can be categorized as follows: 20:80\_CaP/BC-PVP > 40:60\_CaP/BC-PVP > 50:50\_CaP/BC-PVP > BC-PVP. A varying concentration of fillers can influence the mechanical property of the composite [45,91]. The variation of the compressive strength of CaP filled BC based hydrogel scaffolds can be the result of varying degree of polymer-filler interaction in the hydrogel composite system. The compressive strength values are given here as mean ± standard deviation (S.D).

**Table 2.** The compressive strength of BC based hydrogel scaffolds.

BC-PVP Based Hydrogel Scaffolds		Compressive Strength (MPa)
BC-PVP based scaffold without CaP	BC-PVP	0.21 ± 0.02
	20:80_CaP/BC-PVP	0.31 ± 0.01
BC-PVP based scaffold with CaP	40:60_CaP/BC-PVP	0.25 ± 0.04
	50:50_CaP/BC-PVP	0.24 ± 0.08

#### 4.5. Cell Viability and Cytocompatibility Study

Figure 8 indicates the cell viability/cytocompatibility property of CaP filled BC-PVP based hydrogel scaffolds (20:80\_CaP/BC-PVP, 40:60\_CaP/BC-PVP, 50:50\_CaP/BC-PVP). It can be seen from Figure 8 that there is significant growth of cells both in DE and IDE. The cell viability of BC-PVP (without CaP) remains notable throughout 7 days in IDE. However, in DE, a sudden decrease can be seen in the percentage of growth of BC-PVP scaffold in 3 days compared to 1, 5, and 7 days of incubation. On the other hand, a gradual increase from 1 to 5 days of Saos-2 cell viability can be seen in IDE and DE for 50:50\_CaP/BC-PVP. Additionally, a notable increase of cell viability can also be seen from 1 to 5 days for 40:60\_CaP/BC-PVP and 20:80\_CaP/BC-PVP in IDE. The cell viability was found to be more significant ( $P < 0.0001$ ) for 40:60\_CaP/BC-PVP and 20:80\_CaP/BC-PVP than for 50:50\_CaP/BC-PVP after 1 day of incubation at IDE. Interestingly, after 1 day of incubation, the cell viability of BC-PVP (without CaP) was found to be more significant than CaP filled hydrogels in IDE. On the other hand, the cell proliferation has found prominent ( $***P < 0.0001$  and  $**P < 0.001$ ) for 20:80\_CaP/BC-PVP after 1 day of incubation in DE. This might be result from the stimulatory effect of CaP filled BC based hydrogel scaffolds. The appropriate mechanical property and calcium induced stimulatory effect might activate the cell signaling for proliferation of Saos-2 cells after 1 day of incubation [31,45]. In DE, the cell viability is also significant ( $P < 0.05$ ) for 20:80\_CaP/BC-PVP than 40:60\_CaP/BC-PVP. Additionally, significant cell viability was also found for 50:50\_CaP/BC-PVP ( $P < 0.05$ ) after 5 days of incubation in DE. In this context, it should be mentioned that human Saos-2 exhibits similar characteristics to those of human osteoblast cell lines. The presence of the calcium phosphate in the medium can be notably recognized by the Saos-2. This might be the reason for the significant cell viability seen both in IDE and in DE from 1 day of incubation. Additionally, the presence of significant calcium concentration in the medium allows them to maintain proliferation signaling, which is evident from the significant cell proliferation/viability of the scaffold during 7 days of incubation. Interestingly, the BC-PVP (without CaP) scaffold shows significant cell viability in both IDE and DE. It is known that porosity and pore geometry is one of the most important factors for cell viability [45]. BC-PVP scaffold i.e., control scaffold is a significant porous scaffold [12] and is devoid of any CaP, which helps the bone specific Saos-2 cells to grow. However, from Figure 8b, it is also evident that more significant cell growth is seen after 1 day of incubation with the CaP/BC-PVP scaffolds than for the BC-PVP (without CaP) scaffold. Nevertheless, the cell proliferation for all hydrogel scaffolds is found to be promising after the 1st, 3rd, 5th, and 7th day of incubation when compared to the control, both in indirect experiment (IDE) and direct experiment (DE).

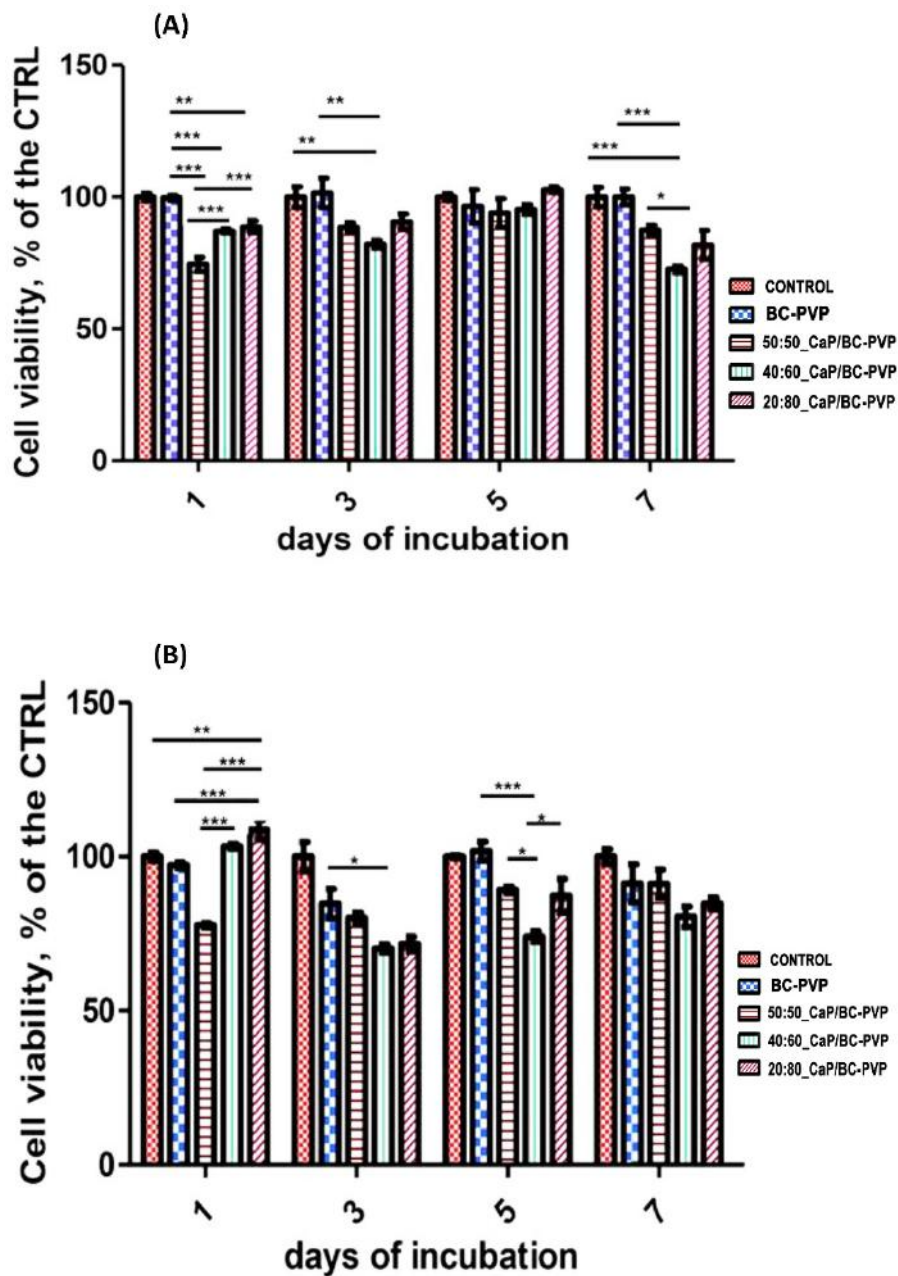


**Figure 8.** Direct and indirect cell viability for CaP/BC-PVP hydrogel scaffold with Saos-2. (A) Indirect experiment (IDE) and (B) direct experiment (DE). The asterisks indicate the level of significance (\*\* $P < 0.0001$ , \*\* $P < 0.001$ , \* $P < 0.05$ ) in cell viability/proliferation.

## 5. Conclusions

This study focuses on the analysis of structural and functional properties of calcium phosphate (CaP) which incorporated bacterial cellulose (BC)-polyvinylpyrrolidone (PVP) (i.e., 20:80\_CaP/BC-PVP, 40:60\_CaP/BC-PVP, 50:50\_CaP/BC-PVP) based hydrogel scaffolds. The evaluation of the properties of scaffolds was performed on the basis of porosity, degradability, thermal, and mechanical properties, and cell viability/cytocompatibility. The porosity of all the CaP filled BC-PVP based hydrogel scaffolds was found to be nearly 80% which is significant. DSC indicates the thermal characterization of the hydrogel scaffolds. Moreover, the weight loss profile through hydrolytic degradation confirms the significant degradability of the calcium phosphate which incorporated hydrogel scaffolds. It was determined that 50:50\_CaP/BC-PVP hydrogel scaffold has the highest degree of weight loss compared

to the other scaffolds. The degradation behavior was also indicated by the gel content, density studies, FTIR study, and SEM study. SEM study portrays the notable structural morphology of pores of the hydrogel scaffolds. In addition, it can be observed that average pore sizes are gradually increased with the period of hydrolytic degradation (i.e., 7, 14, and 21 days). On the other hand, compressive strengths of the hydrogel scaffolds were found to be comparable (0.21–0.31 MPa) with the human cancellous bones. In addition, significant cell viability and proliferation can be found with all the BC-PVP based hydrogel scaffolds during between 1 day and 7 days of incubation, which confirms the cytocompatibility of the CaP filled BC based hydrogel scaffolds. Thus, it can be notably concluded that the calcium phosphate incorporated polymeric hydrogel scaffolds (CaP/BC-PVP) can be utilized in bone tissue engineering applications. Further intensive in vivo investigation is recommended in animal models before their application in bone regeneration.

**Author Contributions:** Conceptualization, P.B.; Data curation, P.B., R.A., Investigation, P.B.; Supervision, N.S. and P.S.; Writing—original draft, P.B.; Writing—review and editing, P.B., N.S.

**Funding:** This work is mainly supported by the Ministry of Education, Youth and Sports of The Czech Republic – NPU Program I (LO1504) and the work was performed on the basis of a granted project of Internal Grant Agency (Project No. IGA/CPS/2019/003), Tomas Bata University in Zlin, Czech Republic. The authors would like to thank Boyka Andonova-Lilova (IEMPAM-BAS) for her sincere and kind help in this cytocompatibility study.

**Conflicts of Interest:** The authors declare no conflicts of interests.

## References

1. Iaquinta, M.R.; Mazzoni, E.; Manfrini, M.; D’Agostino, A.; Trevisiol, L.; Nocini, R.; Trombelli, L.; Barbanti-Brodano, G.; Martini, F.; Tognon, M. Innovative Biomaterials for Bone Regrowth. *Int. J. Mol. Sci.* **2019**, *20*, 618. [[CrossRef](#)] [[PubMed](#)]
2. Chauvin-Kimoff, L.; Allard-Dansereau, C.; Colbourne, M. The medical assessment of fractures in suspected child maltreatment: Infants and young children with skeletal injury. *Paediatr. Child Health* **2018**, *23*, 156–160. [[CrossRef](#)] [[PubMed](#)]
3. Cohen, H.; Kugel, C.; May, H.; Medlej, B.; Stein, D.; Slon, V.; Hershkovitz, I.; Brosh, T. The impact velocity and bone fracture pattern: Forensic perspective. *Forensic Sci. Int.* **2016**, *266*, 54–62. [[CrossRef](#)] [[PubMed](#)]
4. Rabie, A.B.; Wong, R.W.; Hagg, U. Composite autogenous bone and demineralized bone matrices used to repair defects in the parietal bone of rabbits. *Br. J. Oral. Maxillofac. Surg.* **2000**, *38*, 565–570. [[CrossRef](#)] [[PubMed](#)]
5. Habibovic, P. Strategic Directions in Osteoinduction and Biomimetics. *Tissue Eng. Part A* **2017**, *23*, 1295–1296. [[CrossRef](#)]
6. Hernlund, E.; Svedbom, A.; Ivergard, M.; Compston, J.; Cooper, C.; Stenmark, J.; McCloskey, E.V.; Jonsson, B.; Kanis, J.A. Osteoporosis in the European Union: Medical management, epidemiology and economic burden. A report prepared in collaboration with the International Osteoporosis Foundation (IOF) and the European Federation of Pharmaceutical Industry Associations (EFPIA). *Arch. Osteoporos.* **2013**, *8*, 136. [[CrossRef](#)]
7. Oral, A.; Kucukdeveci, A.A.; Varela, E.; Ilieva, E.M.; Valero, R.; Berteanu, M.; Christodoulou, N. Osteoporosis. The role of physical and rehabilitation medicine physicians. The European perspective based on the best evidence. A paper by the UEMS-PRM Section Professional Practice Committee. *Eur. J. Phys. Rehabil. Med.* **2013**, *49*, 565–577.
8. Tian, L.; Tang, N.; Ngai, T.; Wu, C.; Ruan, Y.; Huang, L.; Qin, L. Hybrid fracture fixation systems developed for orthopaedic applications: A general review. *J. Orthop. Transl.* **2018**, *16*, 1–13. [[CrossRef](#)]
9. Siallagan, S.F.; Silalahi, M.; Boediono, A.; Estuningsih, S.; Noviana, D. A Wearable Iron-Based Implant as an Intramedullary Nail in Tibial Shaft Fracture of Sheep. *Int. J. Biomater.* **2019**, *2019*, 1–10. [[CrossRef](#)]
10. Christensen, F.B.; Dalstra, M.; Sejling, F.; Overgaard, S.; Bunger, C. Titanium-alloy enhances bone-pedicle screw fixation: Mechanical and histomorphometrical results of titanium-alloy versus stainless steel. *Eur. Spine J.* **2000**, *9*, 97–103. [[CrossRef](#)]
11. Sheikh, Z.; Najeeb, S.; Khurshid, Z.; Verma, V.; Rashid, H.; Glogauer, M. Biodegradable Materials for Bone Repair and Tissue Engineering Applications. *Materials* **2015**, *8*, 5744–5794. [[CrossRef](#)] [[PubMed](#)]



12. Basu, P.; Saha, N.; Saha, P. Inorganic calcium filled bacterial cellulose based hydrogel scaffold: Novel biomaterial for bone tissue regeneration. *Int. J. Polym. Mater.* **2019**, *68*, 134–144. [[CrossRef](#)]
13. Ratner, B.D. *Biomaterials Science: An Introduction to Materials in Medicine*; Academic Press: Cambridge, MA, USA, 2004.
14. Liu, X.; Miller II, A.L.; Park, S.; George, M.N.; Waletzki, B.E.; Xu, H.; Terzic, A.; Lu, L. Two-Dimensional Black Phosphorus and Graphene Oxide Nanosheets Synergistically Enhance Cell Proliferation and Osteogenesis on 3D Printed Scaffolds. *ACS Appl. Mater. Interfaces* **2019**, *11*, 23558–23572. [[CrossRef](#)] [[PubMed](#)]
15. Kankala, R.K.; Xu, X.-M.; Liu, C.-G.; Chen, A.-Z.; Wang, S.-B. 3D-Printing of Microfibrous Porous Scaffolds Based on Hybrid Approaches for Bone Tissue Engineering. *Polymers* **2018**, *10*, 807. [[CrossRef](#)] [[PubMed](#)]
16. Winkler, T.; Sass, F.A.; Duda, G.N.; Schmidt-Bleek, K. A review of biomaterials in bone defect healing, remaining shortcomings and future opportunities for bone tissue engineering: The unsolved challenge. *Bone Jt. Res.* **2018**, *7*, 232–243. [[CrossRef](#)] [[PubMed](#)]
17. Harris, J.J.; Lu, S.; Gabriele, P. Commercial challenges in developing biomaterials for medical device development. *Polym. Int.* **2018**, *67*, 969–974. [[CrossRef](#)]
18. Jeon, O.H.; Panicker, L.M.; Lu, Q.; Chae, J.J.; Feldman, R.A.; Elisseef, J.H. Human iPSC-derived osteoblasts and osteoclasts together promote bone regeneration in 3D biomaterials. *Sci. Rep.* **2016**, *6*, 26761. [[CrossRef](#)]
19. Puppi, D.; Migone, C.; Grassi, L.; Piroso, A.; Maisetta, G.; Batoni, G.; Chiellini, F. Integrated three-dimensional fiber/hydrogel biphasic scaffolds for periodontal bone tissue engineering. *Polym. Int.* **2016**, *65*, 631–640. [[CrossRef](#)]
20. Ardeshiryajimi, A.; Dinarvand, P.; Seyedjafari, E.; Langroudi, L.; Adegani, F.J.; Soleimani, M. Enhanced reconstruction of rat calvarial defects achieved by plasma-treated electrospun scaffolds and induced pluripotent stem cells. *Cell Tissue Res.* **2013**, *354*, 849–860. [[CrossRef](#)]
21. Jin, G.Z.; Kim, T.H.; Kim, J.H.; Won, J.E.; Yoo, S.Y.; Choi, S.J.; Hyun, J.K.; Kim, H.W. Bone tissue engineering of induced pluripotent stem cells cultured with macrochanneled polymer scaffold. *J. Biomed. Mater. Res. A* **2013**, *101*, 1283–1291. [[CrossRef](#)]
22. Levi, B.; Hyun, J.S.; Montoro, D.T.; Lo, D.D.; Chan, C.K.; Hu, S.; Sun, N.; Lee, M.; Grova, M.; Connolly, A.J.; et al. In vivo directed differentiation of pluripotent stem cells for skeletal regeneration. *Proc. Natl. Acad. Sci. USA* **2012**, *109*, 20379–20384. [[CrossRef](#)] [[PubMed](#)]
23. Duan, X.; Tu, Q.; Zhang, J.; Ye, J.; Sommer, C.; Mostoslavsky, G.; Kaplan, D.; Yang, P.; Chen, J. Application of induced pluripotent stem (iPS) cells in periodontal tissue regeneration. *J. Cell. Physiol.* **2011**, *226*, 150–157. [[CrossRef](#)] [[PubMed](#)]
24. Ko, J.Y.; Park, S.; Im, G.I. Osteogenesis from human induced pluripotent stem cells: An in vitro and in vivo comparison with mesenchymal stem cells. *Stem Cells Dev.* **2014**, *23*, 1788–1797. [[CrossRef](#)] [[PubMed](#)]
25. Ye, J.H.; Xu, Y.J.; Gao, J.; Yan, S.G.; Zhao, J.; Tu, Q.; Zhang, J.; Duan, X.J.; Sommer, C.A.; Mostoslavsky, G.; et al. Critical-size calvarial bone defects healing in a mouse model with silk scaffolds and SATB2-modified iPSCs. *Biomaterials* **2011**, *32*, 5065–5076. [[CrossRef](#)] [[PubMed](#)]
26. Cheng, D.; Zhang, X.; Wang, S.; Liu, L. Effect on Mechanical and Thermal Properties of Random Copolymer Polypropylene/Microcrystalline Cellulose Composites Using T-ZnOw as an Additive. *Adv. Polym. Technol.* **2019**, *2019*, 1–16. [[CrossRef](#)]
27. Schröpfer, S.B.; Bottene, M.K.; Bianchin, L.; Robinson, L.C.; de Lima, V.; Jahno, V.D.; da Silva Barud, H.; Ribeiro, S.J. Biodegradation evaluation of bacterial cellulose, vegetable cellulose and poly (3-hydroxybutyrate) in soil. *Polímeros* **2015**, *25*, 154–160. [[CrossRef](#)]
28. Qi, G.X.; Luo, M.T.; Huang, C.; Guo, H.J.; Chen, X.F.; Xiong, L.; Wang, B.; Lin, X.Q.; Peng, F.; Chen, X.D. Comparison of bacterial cellulose production by *Gluconacetobacter xylinus* on bagasse acid and enzymatic hydrolysates. *J. Appl. Polym. Sci.* **2017**, *134*, 45066. [[CrossRef](#)]
29. Torgbo, S.; Sukyaia, P. Bacterial cellulose-based scaffold materials for bone tissue engineering. *Appl. Mater. Today* **2018**, *11*, 34–49. [[CrossRef](#)]
30. Pirsá, S.; Shamusi, T.; Kia, E.M. Smart films based on bacterial cellulose nanofibers modified by conductive polypyrrole and zinc oxide nanoparticles. *J. Appl. Polym. Sci.* **2018**, *135*, 46617. [[CrossRef](#)]
31. Basu, P.; Saha, N.; Alexandrova, R.; Andonova-Lilova, B.; Georgieva, M.; Miloshev, G.; Saha, P. Biocompatibility and Biological Efficiency of Inorganic Calcium Filled Bacterial Cellulose Based Hydrogel Scaffolds for Bone Bioengineering. *Int. J. Mol. Sci.* **2018**, *19*, 3980. [[CrossRef](#)]

32. Fan, X.; Zhang, T.; Zhao, Z.; Ren, H.; Zhang, Q.; Yan, Y.; Lv, G. Preparation and characterization of bacterial cellulose microfiber/goat bone apatite composites for bone repair. *J. Appl. Polym. Sci.* **2013**, *129*, 595–603. [[CrossRef](#)]
33. Wang, Y.; Xue, Y.; Wang, J.; Zhu, Y.; Zhu, Y.; Zhang, X.; Liao, J.; Li, X.; Wu, X.; Qin, Y.-X.; et al. A Composite Hydrogel with High Mechanical Strength, Fluorescence, and Degradable Behavior for Bone Tissue Engineering. *Polymers* **2019**, *11*, 1112. [[CrossRef](#)] [[PubMed](#)]
34. Ozcelik, B.; Palmer, J.; Ladewig, K.; Facal Marina, P.; Stevens, G.W.; Abberton, K.; Morrison, W.A.; Blencowe, A.; Qiao, G.G. Biocompatible Porous Polyester-Ether Hydrogel Scaffolds with Cross-Linker Mediated Biodegradation and Mechanical Properties for Tissue Augmentation. *Polymers* **2018**, *10*, 179. [[CrossRef](#)] [[PubMed](#)]
35. De Mori, A.; Peña Fernández, M.; Blunn, G.; Tozzi, G.; Roldo, M. 3D Printing and Electrospinning of Composite Hydrogels for Cartilage and Bone Tissue Engineering. *Polymers* **2018**, *10*, 285. [[CrossRef](#)] [[PubMed](#)]
36. Saha, N.; Shah, R.; Gupta, P.; Mandal, B.B.; Alexandrova, R.; Sikiric, M.D.; Saha, P. PVP-CMC hydrogel: An excellent bioinspired and biocompatible scaffold for osseointegration. *Mater. Sci. Eng. C Mater. Biol. Appl.* **2019**, *95*, 440–449. [[CrossRef](#)] [[PubMed](#)]
37. Kocen, R.; Gasik, M.; Gantar, A.; Novak, S. Viscoelastic behaviour of hydrogel-based composites for tissue engineering under mechanical load. *Biomed. Mater.* **2017**, *12*, 025004. [[CrossRef](#)] [[PubMed](#)]
38. Racine, L.; Texier, I.; Auzély-Velty, R. Chitosan-based hydrogels: Recent design concepts to tailor properties and functions. *Polym. Int.* **2017**, *66*, 981–998. [[CrossRef](#)]
39. Lyu, S.P.; Untereker, D. Degradability of Polymers for Implantable Biomedical Devices. *Int. J. Mol. Sci.* **2009**, *10*, 4033–4065. [[CrossRef](#)]
40. Lodhi, B.A.; Hussain, M.A.; Sher, M.; Haseeb, M.T.; Ashraf, M.U.; Hussain, S.Z.; Hussain, I.; Bukhari, S.N.A. Polysaccharide-Based Superporous, Superabsorbent, and Stimuli Responsive Hydrogel from Sweet Basil: A Novel Material for Sustained Drug Release. *Adv. Polym. Technol.* **2019**, *2019*, 1–11. [[CrossRef](#)]
41. Janoušková, O. Synthetic Polymer Scaffolds for Soft Tissue Engineering. *Physiother. Res.* **2018**, *67*, S3335–S3348. [[CrossRef](#)]
42. Goudouri, O.M.; Balasubramanian, P.; Boccaccini, A.R. Characterizing the degradation behavior of bioceramic scaffolds. In *Characterisation and Design of Tissue Scaffolds*; Tomlins, P., Ed.; Woodhead Publishing Series in Biomaterials; Elsevier: Amsterdam, The Netherlands, 2016; Chapter 6; pp. 127–147.
43. O'Brien, F.J. Biomaterials & scaffolds for tissue engineering. *Mater. Today* **2011**, *14*, 88–95.
44. Kumar, P.T.S.; Srinivasan, S.; Lakshmanan, V.K.; Tamura, H.; Nair, S.V.; Jayakumar, R.  $\beta$ -Chitin hydrogel/nano hydroxyapatite composite scaffolds for tissue engineering applications. *Carbohydr. Polym.* **2011**, *85*, 584–591. [[CrossRef](#)]
45. Will, J.; Detsch, R.; Boccaccini, A.R. Characterization of Biomaterials. In *Structural and Biological Characterization of Scaffolds*; Bandyopadhyay, A., Bose, S., Eds.; Academic Press: Cambridge, MA, USA, 2013; Chapter 7.1; pp. 299–310.
46. Roy, N.; Saha, N.; Kitano, T.; Saha, P. Biodegradation of PVP–CMC hydrogel film: A useful food packaging material. *Carbohydr. Polym.* **2012**, *89*, 346–353. [[CrossRef](#)] [[PubMed](#)]
47. Shah, R.; Vyroubal, R.; Fei, H.; Saha, N.; Kitano, T.; Saha, P. Preparation of bacterial cellulose based hydrogels and their viscoelastic behavior. *AIP Conf. Proc.* **2015**, *1662*, 1–7.
48. LeGeros, R.Z.; Lin, S.; Rohanizadeh, R.; Mijares, D.; LeGeros, J.P. Biophasic calcium phosphate bioceramics: Preparation, properties and application. *J. Mater. Sci. Mater. Med.* **2003**, *14*, 201–209. [[CrossRef](#)]
49. Akaraonye, E.; Filip, J.; Safarikova, M.; Salih, V.; Keshavarz, T.; Knowles, J.C.; Roy, I. Composite scaffolds for cartilage tissue engineering based on natural polymers of bacterial origin, thermoplastic poly(3-hydroxybutyrate) and micro-fibrillated bacterial cellulose. *Polym. Int.* **2016**, *65*, 780–791. [[CrossRef](#)]
50. Basu, P.; Saha, N.; Saha, P. Swelling and rheological study of calcium phosphate filled bacterial cellulose based hydrogel scaffold. *J. Appl. Polym. Sci.* **2019**, *136*, 48522. [[CrossRef](#)]
51. Lin, F.; Zheng, R.; Chen, J.; Su, W.; Dong, B.; Lin, C.; Huang, B.; Lu, B. Microfibrillated cellulose enhancement to mechanical and conductive properties of biocompatible hydrogels. *Carbohydr. Polym.* **2019**, *205*, 244–254. [[CrossRef](#)]

52. Kumar, A.; Zhang, Y.; Terracciano, A.; Zhao, X.; Su, T.-L.; Kalyon, D.M.; Katebifar, S.; Kumbar, S.G.; Yu, X. Load-bearing biodegradable polycaprolactone-poly (lactic-co-glycolic acid)- beta tri-calcium phosphate scaffolds for bone tissue regeneration. *Polym. Adv. Technol.* **2019**, *30*, 1189–1197. [[CrossRef](#)]
53. Porter, J.R.; Henson, A.; Popat, K.C. Biodegradable poly (epsilon-caprolactone) nanowires for bone tissue engineering applications. *Biomaterials* **2009**, *30*, 780–788. [[CrossRef](#)]
54. Wu, L.; Ding, J. In vitro degradation of three-dimensional porous poly (D, L-lactide-co-glycolide) scaffolds for tissue engineering. *Biomaterials* **2004**, *25*, 5821–5830. [[CrossRef](#)] [[PubMed](#)]
55. Bouhadir, K.H.; Lee, K.Y.; Alsberg, E.; Damm, K.L.; Anderson, K.W.; Mooney, D.J. Degradation of partially oxidized alginate and its potential application for tissue engineering. *Biotechnol. Prog.* **2001**, *17*, 945–950. [[CrossRef](#)] [[PubMed](#)]
56. Gupta, N.V.; Shivakumar, H.G. Investigation of swelling and mechanical properties of pH-sensitive superporous hydrogel composite. *Iran. J. Pharm. Res.* **2012**, *11*, 481–493. [[PubMed](#)]
57. Maswal, M.; Chat, O.A.; Dar, A.A. Rheological characterization of multi component hydrogel based on carboxymethyl cellulose: Insight into its encapsulation capacity and release kinetics towards ibuprofen. *Colloid Polym. Sci.* **2015**, *293*, 1723–1735. [[CrossRef](#)]
58. Köse, G.T.; Kenar, H.; Hasirci, N.; Hasirci, V. Macroporous poly (3-hydroxybutyrate-co-3-hydroxyvalerate) matrices for bone tissue engineering. *Biomaterials* **2003**, *24*, 1949–1958. [[CrossRef](#)]
59. Mohite, B.V.; Patil, S.V. Physical, structural, mechanical and thermal characterization of bacterial cellulose by *G. hansenii* NCIM 2529. *Carbohydr. Polym.* **2014**, *106*, 132–141. [[CrossRef](#)]
60. Ferfera-Harrar, H.; Aouaz, N.; Dairi, N. Environmental-sensitive chitosan-g-polyacrylamide/ carboxymethylcellulose superabsorbent composites for wastewater purification I: Synthesis and properties. *Polym. Bull.* **2016**, *73*, 815–840. [[CrossRef](#)]
61. Sun, S.; Cao, H.; Su, H.; Tan, T. Preparation and characterization of novel injectable in situ cross-linked hydrogel. *Polym. Bull.* **2009**, *62*, 699–711. [[CrossRef](#)]
62. Mao, J.S.; Zhao, L.G.; Yin, Y.J.; Yao, K.D. Structure and properties of bilayer chitosan–gelatin scaffolds. *Biomaterials* **2003**, *24*, 1067–1074. [[CrossRef](#)]
63. Sheenoy, A.V. *Rheology of Filled Polymer Systems*; Elsevier: Amsterdam, The Netherlands, 1999.
64. Annabi, N.; Nichol, J.W.; Zhong, X.; Ji, C.; Koshy, S.; Khademhosseini, A.; Dehghani, F. Controlling the porosity and microarchitecture of hydrogels for tissue engineering. *Tissue Eng. Part B Rev.* **2010**, *16*, 371–383. [[CrossRef](#)]
65. Pandit, V.; Pai, R.S.; Devi, K.; Suresh, S. In vitro-in vivo evaluation of fast-dissolving tablets containing solid dispersion of pioglitazone hydrochloride. *J. Adv. Pharm. Technol. Res.* **2012**, *3*, 160–170. [[PubMed](#)]
66. Maghraby, G.M.; Ghanem, S.F. Preparation and Evaluation of Rapidly Dissolving Tablets of Raloxifene Hydrochloride by Ternary System Formation. *Int. J. Pharm. Pharm. Sci.* **2016**, *8*, 127–136.
67. Oliveira, R.L.; Vieira, J.G.; Barud, H.S.; Assunção, R.M.N.; Filho, G.R.; Ribeiro, S.J.L.; Messadeqq, Y. Synthesis and Characterization of Methylcellulose Produced from Bacterial Cellulose under Heterogeneous Condition. *J. Braz. Chem. Soc.* **2015**, *26*, 1861–1870. [[CrossRef](#)]
68. Gabbott, P. *Principles and Applications of Thermal Analysis*; Blackwell Publishing: Hoboken, NJ, USA, 2008; p. 464.
69. Matraszek, A.; Radomska, E. The revised phase diagram of the Ca<sub>3</sub>(PO<sub>4</sub>)<sub>2</sub>–YPO<sub>4</sub> system. The temperature and concentration range of solid-solution phase fields. *J. Therm. Anal. Calorim.* **2014**, *117*, 101. [[CrossRef](#)]
70. Klemm, D.; Ahrem, H.; Kramer, F.; Fried, W.; Wippermann, J.; Kinne, R.W. Bacterial Nanocellulose Hydrogels Designed as Bioartificial Medical Implants. In *Bacterial NanoCellulose a Sophisticated Multifunctional Material*; Gama, M., Gatenholm, P., Klemm, D., Eds.; CRC Press: Boca Raton, FL, USA, 2012; Chapter 9; pp. 175–196.
71. Ghassemi, T.; Shahroodi, A.; Ebrahimzadeh, M.H.; Mousavian, A.; Movaffagh, J.; Moradi, A. Current Concepts in Scaffolding for Bone Tissue Engineering. *Arch. Bone Jt. Surg.* **2018**, *6*, 90–99. [[PubMed](#)]
72. Gajjar, C.R.; King, M.W. Degradation Process. In *Resorbable Fiber-Forming Polymers for Biotextile Applications, Briefs in Materials*; Gajjar, C.R., King, M.W., Eds.; Springer: Berlin, Germany, 2014.
73. Akagi, Y.; Goshio, S.; Anraku, Y.; Sakuma, I. Control of Degradation Properties of Polymer Gel. In Proceedings of the ECS Meeting Abstract (Abstract MA2018-03 88), Poster Paper Presented at First International Conference on 4D Materials and Systems, Yonezawa, Japan, 26–30 August 2018.

74. Houmard, M.; Fu, Q.; Genet, M.; Saiz, E.; Tomsia, A.P. On the structural, mechanical, and biodegradation properties of HA/ $\beta$ -TCP robocast scaffolds. *J. Biomed. Mater. Res. B Appl. Biomater.* **2013**, *101*, 1233–1242. [[CrossRef](#)]
75. Sala, G. Composite degradation due to fluid absorption. *Compos. Part B* **2000**, *31*, 357–373. [[CrossRef](#)]
76. Ratner, B.D.; Hoffman, A.S.; Schoen, F.J.; Lemons, J.E. *Biomaterials Science: An Introduction to Materials in Medicine*, 3rd ed.; Academic Press: Cambridge, MA, USA, 2012.
77. Yacob, N.; Hashim, K. Morphological effect on swelling behaviour of hydrogel. *AIP Conf. Proc.* **2014**, *1584*, 153.
78. Nie, L.; Suo, J.; Zou, P.; Feng, S. Preparation and properties of biphasic calcium phosphate scaffolds multiply coated with HA/PLLA nanocomposites for bone tissue engineering applications. *J. Nanomater.* **2012**, *2012*, 1–11. [[CrossRef](#)]
79. Kumar, A.; Sinha, J. Chapter 8 Electrochemical Transistors for Applications in Chemical and Biological Sensing. In *Organic Semiconductors in Sensor Applications*; Bernards, D.A., Owens, R.M., Malliaras, G.G., Eds.; Springer Series in Materials Science; Springer: Berlin, Germany, 2008; Volume 107, pp. 245–261.
80. Grover, C.; Shetty, N. Evaluation of calcium ion release and change in pH on combining calcium hydroxide with different vehicles. *Contemp. Clin. Dent.* **2014**, *5*, 434–439. [[CrossRef](#)]
81. Feng, J.; Zhang, Q.; Tu, Z.; Tu, W.; Wan, Z.; Pan, M.; Zhang, H. Degradation of silicone rubbers with different hardness in various aqueous solutions. *Polym. Degrad. Stabil.* **2014**, *109*, 122–128. [[CrossRef](#)]
82. Bartošová, A.; Soldán, M.; Sirotiak, M.; Blinová, L.; Michalíková, A. Application of Ftir-Atr Spectroscopy for Determination of Glucose in Hydrolysates of Selected Starches. *J. Slovak Univ. Technol.* **2013**, *21*, 116–121. [[CrossRef](#)]
83. Fengyan, L.; Fu, H. Effect of Alkaline Degumming on Structure and Properties of Lotus Fibers at Different Growth Period. *J. Eng. Fibers Fabr.* **2015**, *10*, 135–139.
84. Mróz, W.; Bombalska, A.; Budne, B.; Burdyska, S.; Jedynski, M.; Prokopiuk, A.; Menaszek, E.; Scisłowska-Czarnecka, A.; Niedzielska, A.; Niedzielski, K. Comparative study of hydroxyapatite and octacalcium phosphate coatings deposited on metallic implants by PLD method. *Appl. Phys. A* **2010**, *101*, 713–716. [[CrossRef](#)]
85. Chen, Q.Z.; Boccaccini, A.R. Bioactive Materials and scaffolds for Tissue Engineering. In *Encyclopedia of Biomaterials and Biomedical Engineering*, 2nd ed.; Wnek, G.E., Bowlin, G.L., Eds.; CRC Press: Boca Raton, FL, USA, 2008; pp. 142–151.
86. Deshmukh, M.; Singh, Y.; Gunaseelan, S.; Gao, D.; Stein, S.; Sinko, P.J. Biodegradable poly (ethylene glycol) hydrogels based on a self-elimination degradation mechanism. *Biomaterials* **2010**, *31*, 6675–6684. [[CrossRef](#)] [[PubMed](#)]
87. Rodel, M.; Meiningner, S.; Groll, J.; Gbureck, U. Bioceramics as drug delivery systems. In *Fundamental Biomaterials: Ceramics*; Thomas, S., Balakrishnan, P., Sreekala, M.S., Eds.; Woodhead Publishing Series in Biomaterials; Woodhead Publishing: Cambridge, UK, 2018; Chapter 7; pp. 153–194.
88. Odelius, K.; Höglund, A.; Kumar, S.; Hakkarainen, M.; Ghosh, A.K.; Bhatnagar, N.; Albertsson, A.-C. Porosity and Pore Size Regulate the Degradation Product Profile of Polylactide. *Biomacromolecules* **2011**, *12*, 1250–1258. [[CrossRef](#)]
89. Chiu, Y.C.; Kocagöz, S.; Larson, J.C.; Brey, E.M. Evaluation of Physical and Mechanical Properties of Porous Poly (Ethylene Glycol)-co-(L-Lactic Acid) Hydrogels during Degradation. *PLoS ONE* **2013**, *8*, e60728. [[CrossRef](#)]
90. Gerhardt, L.-C.; Boccaccini, A.R. Bioactive Glass and Glass-Ceramic Scaffolds for Bone Tissue Engineering. *Materials* **2010**, *3*, 3867–3910. [[CrossRef](#)]
91. Misch, C.E.; Zhimin, Q.; Bidez, M.W.J. Mechanical properties of trabecular bone in the human mandible: Implications for dental implant treatment planning and surgical placement. *J. Oral. Maxillofac. Surg.* **1999**, *57*, 700–706. [[CrossRef](#)]



## **PUBLICATION VII**

**Basu P. (50%),** Saha N., Alexandrova R., Andonova-Lilova, B., Saha, P. “*In vitro* efficiency of calcium phosphate incorporated bacterial cellulose based hydrogel scaffold for bone regeneration”, *Manuscript is in preparation and will be submitted to an impact factor journal.*

## Curriculum Vitae

Name:	Probal Basu
Date of birth:	26 <sup>th</sup> September, 1989
Place of birth:	Kolkata, West Bengal, India
Permanent address:	6B Barendrakrishna Bhattacharjee Lane, Kolkata-700014
Affiliation:	Polymer centre, Faculty of Technology, Tomas Bata University in Zlin, Nám. T. G. Masaryka 5555, 760 01 Zlín
Telephone:	(+420) 776643451
E-mail:	<a href="mailto:probal@utb.cz">probal@utb.cz</a>
Education:	<p><i>2016 – to date</i> Tomas Bata University in Zlin, Center of Polymer Systems (Faculty of Technology), Ph.D. studies in Chemistry and Materials Technology, Specialization: <i>Technology of Macromolecular Compounds</i></p> <p><i>2010 – 2012</i> Presidency College, University of Calcutta, Kolkata, West Bengal, India. Master of Science degree in Zoology.</p> <p><i>2007 – 2010</i> Asutosh College, University of Calcutta, Kolkata, West Bengal, India, Bachelor of Science in Zoology.</p>

## **Exposure of Other Laboratory and Training School Attended in Abroad:**

1. **Short Term Scientific Mission (STSM) visit, supported by** European Cooperation of Science and Technology (COST) NEWGEN MP1301 (European Union), 15<sup>th</sup> June-15<sup>th</sup> July, 2017 for working at Institute of Experimental Morphology, Pathology and Anthropology with Museum-Bulgarian Academy of Sciences (IEMPAM-BAS), Sofia, Bulgaria.
2. **Training School “Non Living Materials meet living Biology”**, 9<sup>th</sup> - 12<sup>th</sup> May, 2017 at Patras, Greece. Organized by European Ceramic Society (ECerS) and COST MP1301 “NEWGEN”.

## **Projects:**

- *IGA/CPS/2017/003* Preparation and characterization of a Bacterial cellulose (BC) based hydrogel with enhanced mechanical and bio-adhesive property. (**Co-investigator**)
- *IGA/CPS/2018/008* Bacterial Cellulose based Bioactive and Functional Biomaterials: Preparation and Characterization (**Principal Investigator**)
- *IGA/CPS/2019/003* Calcium phosphate filled bacterial cellulose based hydrogel scaffolds. (**Principal Investigator**)

## **List of publications**

1. **Basu P.**, Saha N., Saha P. (2020) Viscoelastic behavior of Calcium Phosphate Packed Bacterial Cellulose -Polyvinylpyrrolidone based Hydrogel Scaffolds at Human Fever Temperature, *AIP conference proceedings* related to *Europe-Africa PPS2019 conference*, November 18-21, Pretoria, South Africa, *Accepted for publication*.
2. **Basu P**, Saha N & Saha P. (2020) Swelling and rheological study of calcium phosphate filled bacterial cellulose-based hydrogel scaffold, *J. Appl. Polym. Sci*, 137, 48522.

3. **Basu P**, Saha N, Saha P. (2019) Calcium Phosphate Incorporated Bacterial Cellulose-Polyvinylpyrrolidone Based Hydrogel Scaffold: Structural Property and Cell Viability Study for Bone Regeneration Application, *Polymers*, 11(11), 1821.
4. **Basu P**, Saha N & Saha P. (2019) Inorganic calcium filled bacterial cellulose based hydrogel scaffold: novel biomaterial for bone tissue regeneration, *Int J Polym Mater*, 68:1-3, 134-144.
5. **Basu P**, Saha N, Alexandrova R, Andonova-Lilova B, Georgieva M, Miloshev G, Saha P. (2018) Biocompatibility and Biological Efficiency of Inorganic Calcium Filled Bacterial Cellulose Based Hydrogel Scaffolds for Bone Bioengineering, *Int. J. Mol. Sci.* **19**(12): 3980.
6. Bhattacharya S and **Basu P**. Chapter 13, Microorganisms in the management of mosquito vectors: a sustainable eco-friendly approach. In *Microbial Control of Vector-Borne Diseases*: edited by Tyagi B.K. and Dhanasekaran D, CRC Press (Francis & Taylor), USA, **2018**.
7. Bhattacharya S and **Basu P**. Chapter 17, Ecology and biology of *Culex quinquefasciatus* Say, 1823 in two physiographically different ecosystems with special reference to human lymphatic filariasis in West Bengal, India. In Tyagi BK (Eds) *Lymphatic Filariasis - Epidemiology, Treatment and Prevention- The Indian Perspective*, India; Springer, Singapore, **2018**.
8. **Basu P**, Saha N, Bandyopadhyay S, Saha P. (2017) Rheological Performance of Bacterial Cellulose based non-mineralized and mineralized hydrogel scaffolds, *AIP Conf. Proc.* **1843**, 050008-1–050008-7.DOI: 10.1063/1.4983000
9. Bhattacharya S and **Basu P**. (2016) The Southern House Mosquito, *Culex quinquefasciatus*: profile of a smart vector. *J. Entomol. Zool. Stud.* 2016; **4**(2): 73-81.
10. **Basu P** and Bhattacharya S. (2016) A new dimension in the dengue epidemiology with special reference to the genetic diversity of the virus: A review, *Int. J. of Fauna and Biol. Studies.* **3**(3): 29-41.



11. Bhattacharya S., Chaudhuri P., Mandal A.K., Majumder S., **Basu P (2014)** Reappearance of *Anopheles sunaicus* at Sundarban coastal area, West Bengal, India: *J. Appl. Biosci.*, **40**(1): 58-59.
12. Bhattacharya S and **Basu P. (2014)** Japanese encephalitis virus (JEV) infection in different vertebrates and its epidemiological significance: a review. *Int. J. of Fauna and Biol. Studies.* **1** (6):32-37.
13. **Basu P** and Bhattacharya S. (2014) Perspectives of antiviral RNA interference (RNAi) pathway of insects with special reference to mosquito in the context of dengue infection: a review, *Int. J. of Mosquito Research.* **1** (3): 74-81.
14. **Basu P.**, Shrivastava D.K., Bhattacharya. S., (2012) Incidence of Malaria in relation to ABO Blood Groups in Kolkata, India, *J. Appl. Biosci.*, **38** (2): 211-212.
15. Chakrabarty A., Bhattacharya. S., **Basu P. (2012)** Medically Important Arthropods in a Housing Complex and Its Surroundings in South Kolkata, West Bengal”, *Proceedings of the 6th Conference on Medical Arthropodology* (CRME, ICMR India); Editor: B. K. Tyagi; P: 36-47.

## ● Conferences/seminar/workshop Attended

1. **Basu P**, Saha N, Saha P (2019) Biomechanical property of calcium phosphate filled bacterial cellulose based hydrogel scaffolds, 25th Congress of the European Society of Biomechanics (ESB-2019), July 7th- 10th, 2019, Vienna, Austria. Abst Pap. P. 562 (ISBN: 978-3-903024-96-0).
2. **Basu P**, Saha N, Saha P (2019) Calcium filled bacterial cellulose based composite hydrogel for bone tissue engineering: Optical microscopy and bone marker analysis, 35th International Conference of the Polymer Processing Society (PPS-35), May 26-30, 2019, Çeşme-İzmir, Turkey.
3. **Basu P**, Saha N, and Saha P (2018) Inorganic Calcium filled Bacterial Cellulose based Scaffold for Bone Regeneration, 4<sup>th</sup> International Conference on Biomedical Polymers & Polymeric Biomaterials, 15<sup>th</sup> July – 18<sup>th</sup> July 2018, Krakow, Poland, Abst Pap. P. 05 (ISBN: 978-83-65955-10-4).

4. **Basu P**, Saha N, and Saha P (2017) Calcium Phosphate loaded bioadhesive biopolymer based hydrogel scaffold: a novel biomaterial for bone tissue engineering, Proceedings of Eight Workshop on “Experimental Models and Methods in Biomedical Research”, 14-16<sup>th</sup> June-2017, IEMPAM-BAS, Sofia, Bulgaria. ISSN: 1314-9091.
5. **Basu P**, Saha N, and Saha P. (2017) Rheological Performance of Bacterial Cellulose based non-mineralized and mineralized hydrogel scaffolds, Novel Trends in Rheology VII, 26<sup>th</sup>- 27<sup>th</sup> July-2017, Tomas Bata University in Zlin, Czech Republic.
6. **Basu P**, Saha N, Saha P (2017) Calcium phosphate filled bacterial cellulose based hydrogel scaffolds for dental and orthopaedic application, European Cooperation of Science and Technology (COST) NEWGEN MP1301 (European Union) Workshop and WG Meeting (Cluj-Napoca, Romania) on Biomaterials for Dental and Orthopaedic applications, Abst. Pap. P. 10.
7. **Basu P**, Saha N, Saha P (2016) Functional Significance of Three Dimensional Hydrogel Scaffolds in Bone Tissue Engineering – A Review, European Cooperation of Science and Technology (COST) NEWGEN MP1301 (European Union), Workshop and WG Meeting (Zlin, Czech Republic) on Hydrogel/ Biomineralized Biomaterial for Bone Tissue Regeneration, Abst. Pap. P. 22 (ISBN: 978-80-7454-623-5).
8. Bhattacharya S and **Basu P** (2014). Non-Human Vertebrate Hosts of Japanese encephalitis Virus, Abst. Pap. Brain Storming Conference on Emerging New Epidemiological Dimensions of Japanese Encephalitis (JE) and other Acute Encephalitis Syndromes (AES), Madurai, India. P.67.
9. **Basu P.**, Mandal A.K., Majumder S., Mukherjee D., Acharyya D., Bhattacharya S., (2014) Mosquito Vector Diversity in Kolkata, *International Conference on Entomology* (February 21-23, 2014) Organized by Department of Zoology & Environmental Sciences; Punjabi University, Patiala, Punjab, India.
10. Mandal A.K., **Basu P**, Shrivastava D.K., Naskar R., Majumdar S., Bhattacharya S. (2013) Mosquito faunastic survey around a bird sanctuary in West Bengal, *XII International Conference On Vector and Vector Borne Diseases; Challenges in 21<sup>st</sup> Century: Their Global Impacts and Strategic Management*; organized by Department of Zoology, Mohanlal Sukhadia University, Udaipur Rajasthan and National Academy of Vector Borne Disease, Bhubaneswar.

11. **Basu P.**, Saha T., Roy Chowdhury N., Mukherjee D., Bhattacharya S. (2013) Mosquito borne disease diversity in West Bengal State, India *XII International Conference On Vector and Vector Borne Diseases; Challenges in 21<sup>st</sup> Century: Their Global Impacts and Strategic Management*; organized by Department of Zoology, Mohanlal Sukhadia University, Udaipur Rajasthan and National Academy of Vector Borne Disease, Bhubaneswar.

## List of Awards/Scholarship

1. **ITC Conference Grant (CA-15216-1480)** for participating *25<sup>th</sup> Congress of the European Society of Biomechanics (ESB-2019)*, July 7th-10th, **2019**, Vienna, Austria
2. Awarded **Third Position** in Power-point presentation and English language contest in “*Show off/ Zeig Dich*” competition, 18<sup>th</sup> April, **2018** at Faculty of Humanities, Tomas Bata University in Zlin, Czech Republic.
3. **Short Term Scientific Mission (STSM) Fellowship, COST Action NEWGEN MP1301**, 15<sup>th</sup> June-15<sup>th</sup> July, **2017** for working at IEMPAM-BAS, Sofia, Bulgaria.
4. Awarded **First Position** in Poster Presentation Contest at Training School “*Non Living Materials meet living Biology*”, 9<sup>th</sup> –12<sup>th</sup> May, **2017** at Patras, Greece. Organized by European Ceramic Society (ECerS) and COST Action NEWGEN MP1301.

## Professional Experience

1. **Research Assistant, August, 2012 - August, 2016:** Virus research and vector borne diseases research at Graduate Department of Zoology, Asutosh College (University of Calcutta) Kolkata, India.
2. **Guest Faculty, from September, 2013 - March, 2015:** Department of Zoology, Asutosh College (University of Calcutta), Kolkata-700026, West Bengal, India.

Tomas Bata University in Zlín  
Faculty of Technology  
Polymer Centre  
Zlín, September, 2020